Not only is water the source of all life, but it is also essential for economic, social, and environmental development. Global water usage has increased sixfold over the last 100 years and continues to grow. The United Nations has produced the 2030 Agenda, which has been adopted worldwide, with the Sustainable Development Goal to "guarantee the availability of water and its sustainable management and sanitation". In this context, nature-based solutions can provide alternatives for wastewater treatment. An example of this is constructed wetlands.

Microbial electrochemistry is an emerging discipline devoted to study the interaction between microorganisms and electrically conductive materials. The most applied version is represented by Microbial Electrochemical Technologies (METs). These systems take advantage of the mechanism of extracellular electron transfer (EET). EET allows electroactive bacteria to convert chemical energy, stored in water pollutants, into electrical current. One of the most impactful MET applications is the METland®. This MET-based solution constitutes the integration of electro-conductive granular material in constructed wetlands to effectively outperform their bioremediation.

METlands are an environmentally friendly solution that minimize operation and maintenance costs, allowing effective wastewater treatment in decentralized locations. This thesis explores the technology and science that underpins those METland® in order to understand and optimize their electrobioremediation capacity.

PhD in Hydrology and Water Resource Management

Amanda Prado de Nicolás

Exploring METland Technology

Treating wastewater by integrating electromicrobiology into Nature-based Solutions

2021

Exploring METland Technology

Treating wastewater by integrating electromicrobiology into Nature-based Solutions

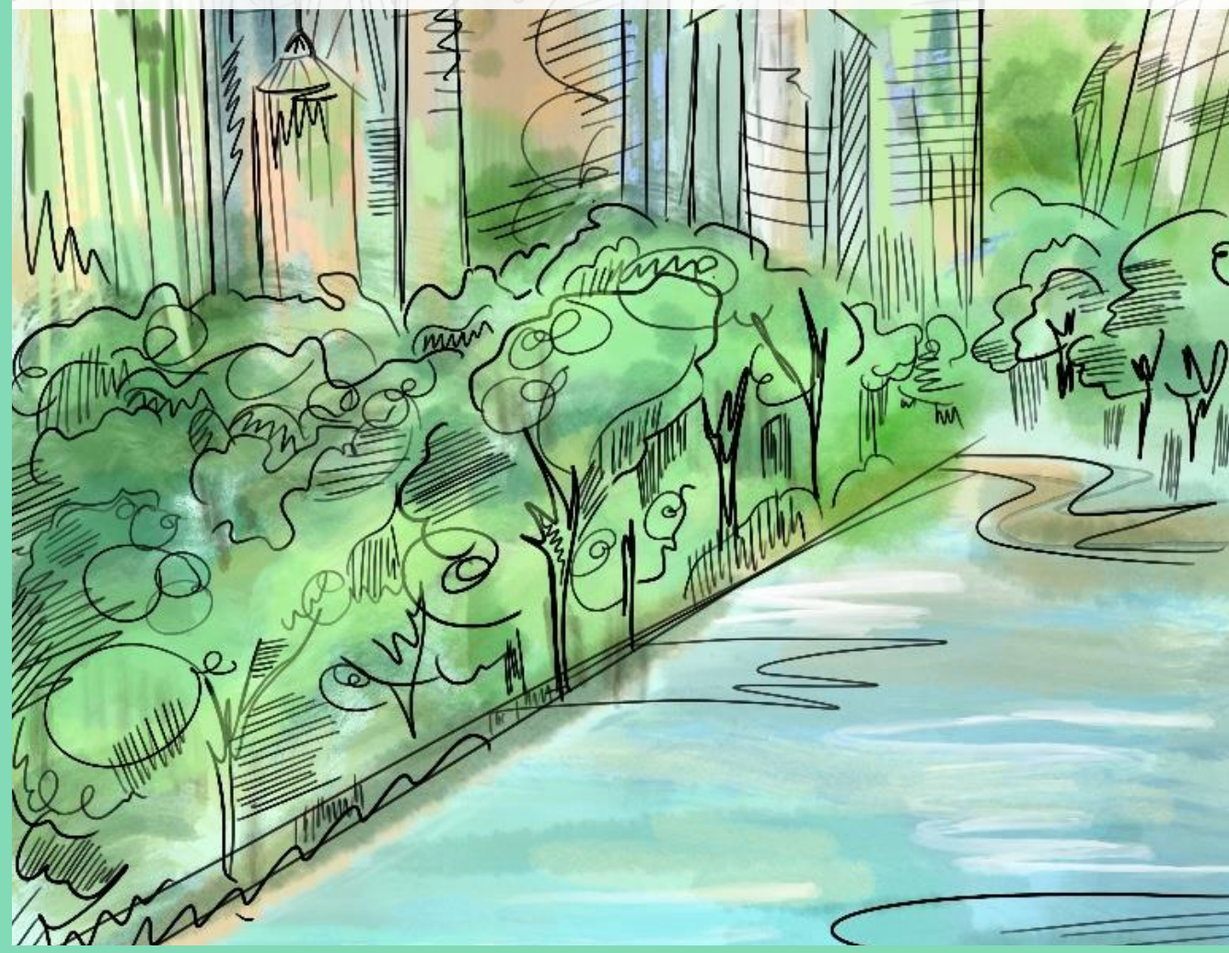

Universidad de Alcalá

Amanda Prado de Nicolás

Ph.D. Thesis
2021

Escuela de Postgrado de la Universidad de Alcalá
Programa de Doctorado en Hidrología y Gestión de los Recursos Hídricos

TESIS DOCTORAL

Exploring METland® technology:
treating wastewater by integrating electromicrobiology into Nature-based Solutions

Memoria presentada para optar al título de Doctor por Universidad de Alcalá por:

Amanda Prado de Nicolás

Dirigida por:

Dr. Abraham Esteve Núñez

Departamento de Química Analítica, Química Física e Ingeniería Química

Universidad de Alcalá, 2021

“I don´t believe in magic,

I believe in hard work”

Richie McCaw

A todas ellas

Table of Contents

Summary 7
Resumen 11

CHAPTER 1: INTRODUCTION, OBJECTIVES AND RESEARCH FRAMEWORK

Introduction 19
1.1 Nature-based solutions (NbS) 19
1.1.1 Origins of nature-based solutions 20
1.1.2 Operational parameters for nature-based solutions 22
1.1.3 Nature-based solutions for climate change mitigation 22
1.1.4 Nature-based solutions for water management 23
1.2 Wastewater treatment 24
1.2.1 The water problem: shortages in the future 24
1.2.2 Types and pollutants in wastewater 25
Types of wastewater 25
Wastewater pollutants 27
1.2.3 Wastewater treatment in small urban communities 31
1.2.4 Constructed wetlands as a wastewater treatment system 35
Types of constructed wetlands 37
Treatment processes and microbial communities 39
1.3 Microbial Electrochemistry: Fundaments 43
1.3.1 The origins of microbial electrochemistry 43
Electroactive Bacteria (EAB) 43
Geobacter as model bacteria 45
1.3.2 Microbial Extracellular Electron Transfer (EET) mechanism 48
Direct Extracellular Electron Transfer 48
Mediated Extracellular Electron Transfer 51
1.3.3 Electrochemical methods for the study of EET 51
Cyclic Voltammetry (CV) 52
Chronoamperometry (CA) 54
1.3.4 Microbial Electrochemical Technologies (METs):

configurations and processes. 54
Microbial Fuel Cells (MFCs) 54
Microbial Electrolysis Cells (MECs) 57
Microbial Electrochemical Snorkel. 59
1.3.5 Microbial electrochemical pollutants removal 60
Microbial electrochemical organic matter removal 61
Microbial electrochemical nutrients removal. 62
1.3.6 Integration of MET technology in constructed wetlands 63
Constructed Wetlands–Microbial Fuel Cell (CW–MFC) 64
METland® technology 65
1.3.7 Full-scale MET-based wastewater treatment systems 66
1.4 References. 69

Objectives And Thesis Outline. 80

Research Framework. 83

CHAPTER 2: WITHIN A BIOELECTROCHEMICALLY-ASSISTED CONSTRUCTED WETLAND (METLAND®): GIVING INSIGHTS ON WW TREATMENT THROUGH THE ANALYSIS OF MATERIALS, PERFORMANCE AND ELECTROACTIVE COMMUNITIES

2.1 Abstract. 91
2.2 Introduction 92
2.3 Materials and methods. 95
2.3.1 Biofilters construction and bed materials 95
2.3.2 Characterization of Bed materials 96
2.3.3 Biofilter operation and water quality analysis 97
2.3.4 Electrochemical measurements 98
2.3.4.1 Electric potentials profiles with depth 98
2.3.4.2 Cyclic voltammetry of single granules 98
2.3.5 Microbial communities and data analysis 99
2.3.5.1 16S Metagenomic Sequencing 99
2.3.5.2 Scanning electron microscopy SEM 99
2.3.6 Statistical analysis 100

2.4 Results and discussion. 100
2.4.1 Characterization of bed materials: physico-chemical properties. 101
2.4.2 Performance of the bioelectrochemically-assisted treatment: what, how and who 104
2.4.2.1 Removal of organic pollutants. 104
2.4.2.2 Removal of nitrogen 106
2.4.2.3 Performance in planted and non-planted biofilters 109
2.4.3 Electrochemical characterization of bed in lab-scale METlands® 109
2.4.3.1 Electric potentials depth profiles. 109
2.4.3.2 Cyclic voltammetry of single granules 112
2.4.4 *Geobacter* as key actor in electrochemical syntrophies. 114
2.5 Conclusions. 116
2.6 References 116
2.7. Supplementary Information. 125

CHAPTER 3: ELECTROACTIVE BIOCHAR OUTPERFORMS HIGHLY CONDUCTIVE CARBON MATERIALS FOR BIODEGRADING POLLUTANTS BY ENHANCING MICROBIAL EXTRACELLULAR ELECTRON TRANSFER

3.1 Abstract. 141
3.2 Introduction 142
3.3 Materials and methods 145
3.3.1 Bed materials. 145
3.3.2 Characterization of bed materials. 145
3.3.3 Design and construction of biofilters. 147
3.3.4 Operation of the biofilters 148
3.3.5 Physical, chemical and statistical analyses 149
3.4 Results and discussion 149
3.4.1 Characterization of biofilter materials: physico-chemical properties, electroconductivity and EET 149
3.4.2 Biofilters performance for treating wastewater using different electroconductive bed materials 153
3.4.2.1 Biofilter performance for treating synthetic wastewater 155

3.4.2.2 Biofilter performance for treating real wastewater 157
3.4.2.3 Biofilter performance for treating urban real wastewater using polarized beds. 158
3.4.3 Giving insight into the extracellular electron transfer to electroconductive carbon materials 163
3.4.4 Characterization of the bed materials after microbial colonization. . . 167
3.4.5 Electroconductive biochar: a sustainable material for constructing microbial electrochemical systems. 170
3.5 Conclusions. 172
3.6 Reference 172
3.7. Supplementary Information. 177

SIMULTANEOUS CHARACTERIZATION OF POROUS AND NON-POROUS ELECTRODES IN MICROBIAL ELECTROCHEMICAL SYSTEMS

3.8 Abstract. 182
3.9 Method details. 183
3.10 Method validation 188
Strategies for avoiding corrosion in wiring: a CV diagnosis. 188
Wires and connections. 189
Method for perform a multielectrode analysis using one potentiostat 193
3.11 References. 195

CHAPTER 4: NOVEL BIOELECTROCHEMICAL STRATEGIES FOR DOMESTICATING THE ELECTRON FLOW IN CONSTRUCTED WETLANDS

4.1 Abstract. 201
4.2 Introduction. 202
4.3 Materials and methods. 206
4.3.1 Construction of the e-sink device 206
4.3.2 Biofilters construction and operation 206
4.3.3 Sampling and laboratory analysis 207
4.3.4 Electric potential measurements 208
3.4.5 Statistical analysis 209
4.4 Results and discussion. 209

4.4.1 Electric potential profiles and electron currents. 209
4.4.2 Pollutants removal rates and electron flux. 217
4.5 Conclusions. 220
4.6 Reference. 221
4.7. Supplementary Information. 225

CHAPTER 5: REAL CASE STUDY: FROM LAB-SCALE TO FULL-SCALE OF A METLAND FOR PIGGERY WASTEWATER TREATMENT

5.1 Abstract. 233
5.2 Introduction. 234
5.3 Materials and methods 237
5.3.1 Site description and manure wastewater sampling. 237
5.3.2 Lab-sale bioelectrochemically-assisted manure wastewater treatment system: design and operating parameters. 237
5.3.3 Physical, chemical and statistical analyses. 238
5.4 Results and discussion. 238
5.4.1 Validation of the lab-scale bioelectrochemically-assisted manure wastewater treatment system. 239
5.4.2 Full-scale bioelectrochemically-assisted manure wastewater treatment system. 243
5.5 Conclusions. 245
5.6 Reference. 245

CHAPTER 6: GENERAL DISCUSSION, CONCLUSIONS AND FUTURE WORK

6.1 General discussion. 253
6.2 Final conclusions 265
6.3 Recommendations and future work. 266
6.3 References. 228

Annex 265
List of figures 267
List of supplementary figures. 270
List of tables. 273

List of supplementary tables 274
Abbreviations 275

CHAPTER 1:

INTRODUCTION, OBJECTIVES AND RESEARCH FRAMEWORK

CHAPTER 1

CHAPTER 1

Introduction

1.1 Nature-based solutions

The term nature-based solutions (NbS) were coined in the European Union and is an umbrella term for different approaches that use nature to improve urban sustainability, like green infrastructure, green space, restoring rivers, ecosystem services, and ecosystem-based adaptation. For the European Commission, nature-based solutions are defined as: *"solutions that are inspired and supported by nature, which are cost-effective, simultaneously provide environmental, social and economic benefits and help build resilience. Such solutions bring more, and more diverse, nature and natural features and processes into cities, landscapes and seascapes, through locally adapted, resource-efficient and systemic interventions".* For the International Union for the Conservation of Nature, a non-governmental organization that promotes nature conservation, nature-based solutions are: *"actions to protect, sustainably manage, and restore natural or modified ecosystems, that address societal challenges effectively and adaptively, simultaneously providing human well-being and biodiversity benefits".* While these two definitions vary, both see that nature-based solutions seek to use the properties of nature to address societal challenges (Faivre et al., 2017).

It is now widely recognized that human activities have reached a level that could result in abrupt and, in some cases, irreversible environmental changes detrimental to human development. Societies face increasing challenges such as climate change, jeopardized food security and water resource provision, and enhanced disaster risk. In the face of climate change and increasing environmental pressures, sustainable development has become a strategic issue for cities in Europe and around the world. No longer a "nice to have" addition to development as usual, sustainability is now central to the response to climate change and in enabling growth, security and social well-being. This new framework is focused on the integration of nature-based solutions in the built environment (Fig. 1.1). In contrast to conventional urban development solutions, nature-based actions offer simultaneously a wide range of

sustainability benefits. As most towns and cities have limited spaces for green planting more research is needed to understand the specific urban ecosystem service benefits to justify their maintenance and expansion. Integration of green and grey infrastructures is key for nature-based urban solutions (Eggermont et al., 2015; Faivre et al., 2017).

Figure 1.1. Nature-based Solutions as an umbrella term for ecosystem-related approaches.

1.1.1 Origins of nature-based solutions

Although the term nature-based solutions were recently coined, as early as the 1970s the idea of environmental or ecosystem services began to establish itself in the modern scientific literature. By the 1990s it was generally realized that a more systematic approach was required to document and understand this relationship between people and nature. The 2005 Millennium Ecosystem Assessment, itself a product of this growing awareness, provided a strong evidence base for subsequent policies to promote the conservation, restoration, and sustainable management of ecosystems while also taking into account the increasing demands placed on ecosystem services (Millenium Ecosystem Assessment, 2005). A few years later, during the late 2000s, the term Nature-

Based Solutions emerged, marking a subtle yet important shift in perspective: not only were people the passive beneficiaries of nature's benefits, but they could also proactively protect, manage or restore natural ecosystems as a purposeful and significant contribution to addressing major societal challenges. The emergence of the NbS concept in environmental sciences and nature conservation contexts came as international organizations, such as IUCN and the World Bank, searched for solutions to work with ecosystems rather than relying on conventional engineering interventions, to adapt to and mitigate climate change effects, while improving sustainable livelihoods and protecting natural ecosystems and biodiversity (Mittermeier et al., 2008).

On 06 May 2019, the most comprehensive global assessment on the state of biodiversity to date reconfirmed how natures unprecedented decline is a global emergency on par with climate change (Osojnik, n.d. IPBES, 2019). As a result of that assessment, the EU took its boldest action to fight planetary degradation. To reach the new 2030 Sustainable Development Goals (SDGs) is required a significant increase in eco-system-based mitigation. The EU and its Member States are committed to achieving the SDGs by 2030, including targets on climate action and protecting life on land and at sea. The implementation of these goals is highly interdependent, not least as climate change is a direct negative driver of ecosystem change with important knock-on effects on human well-being (Osojnik, n.d. IPBES, 2019). The degradation of land and marine ecosystems worldwide already undermines the well-being of at least 3.2 billion people and costs about 10% of the annual global GDP in the loss of ecosystem services.

The 2030 global and EU commitments for sustainable development, climate action and biodiversity all point to the urgent need for ecosystem restoration. NbS at different scales can provide cost-effective, win-win solutions by providing employment, and multiple public health and wellbeing benefits (Faivre et al., 2017; Walters et al., 2016).

1.1.2 Operational parameters for nature-based solutions

Although the operational parameters for NbS have not been officially detailed today, many works coincide with the need to define a robust operational framework and standard that can be used to assess any NbS intervention. There has been some work already undertaken in the identification of these candidate parameters, being the ones listed below (Walters et al., 2016):

- Ecological complexity. This parameter supports interventions that would maintain or promote complexity at different ecological scales.
- Long-term stability. This parameter would support interventions that can persist over many years.
- The scale of ecological organization. This parameter would support implementation at a scale that helps mediate the upstream and downstream relationships, dependencies and benefits.
- Direct societal benefits. This parameter would support the delivery of an attributable and substantial stream of direct societal benefits.
- Adaptive governance. This parameter would ensure that the NbS intervention and the ecosystems on which it depends are supported by institutional and decision-making arrangements that can be flexible enough to adapt over time, to meet the changing needs of the people who manage and rely on these ecosystems.

1.1.3 Nature-based solutions for climate change mitigation

Climate change is one of the most pressing challenges confronting humanity today. Depending on how the worlds ecosystems are managed, they can either contribute to the problem or provide effective Nature-based Solutions for climate change mitigation and adaptation.

First, NbS in the form of ecosystem-based mitigation can prevent the degradation and loss of natural ecosystems. Deforestation and forest degradation, for example, release an estimated 4.4 Gt of CO_2 per year into the atmosphere (Matthews and Van Noordwijk, 2014), or around 12% of anthropogenic CO_2 emissions (Pachauri and Reisinger, 2008). Avoidance of these emissions, through better conservation and land management actions, is

a powerful intervention that can make a significant contribution towards global mitigation efforts.

Second, natural and modified ecosystems can also make contributions in combating climate change through their function as a natural carbon sink by absorbing and sequestering CO_2 emissions. Conservation, restoration, and sustainable management of forests, wetlands, and oceans thus play a critical role in the healthy functioning of the carbon cycle and the balanced regulation of the planets climate (Eggermont et al., 2015).

Finally, in addition to providing these direct mitigation benefits, NbS can also help vulnerable communities, especially those who depend on natural resources, to better adapt and become more resilient to the adverse effects of climate change (Walters et al., 2016).

1.1.5 Nature-based solutions for water management

Growing urban populations around the world are causing rising demand for water. Concurrently, changing climate is increasing extreme events in cities, from drought to floods, with severe social and economic consequences. New demands on solutions for water security are emerging in a global context where about four billion people (60 percent of the world's population) live in regions with a state of near-permanent water stress. One in four large cities already faces water stress, and water demand is projected to increase 55% by 2050. Also, water stress is exacerbated by pollution; some 80-90% of all wastewater in developing countries is discharged directly into surface water bodies, creating severe risks for human health (Corcoran, 2010). Applying NbS by harnessing the water-related services of natural infrastructure, such as forests, wetlands, and floodplains will help combat the risk of the water crisis, particularly in the face of future climate stresses (DiFrancesco et al., 2015).

1.2 Wastewater treatment

1.2.1 The water problem: shortages in the future

Water is at the core of sustainable development and is critical for socio-economic development, energy and food production, healthy ecosystems and for human survival itself. In these first decades of the 21st century, the availability and sustainability of water resources face great threats. Thus, in many areas, water resources are being affected by the climatic evolution of the planet, characterized by important alterations in the distribution, duration and intensity of rainfall, and a generalized rise in temperature. The occurrence of these phenomena is generating serious negative impacts on water resources. These include sharp declines in net water reserves, as well as degradation and loss of quality. If the climatic effects are added to the other great threats that look over water resources, which are the increase in demand and the deterioration of water quality due to pollution and overexploitation -which can be especially critical in some areas of the world-, we are in a water emergency situation. It is urgent and essential that we approach the challenge of managing water resources from a holistic approach, making correct use of all available tools.

If we put figures to the aforementioned, according to the United Nations, water consumption has doubled in the last 50 years, 2600 million people lack access to basic sanitation, which represents 40% of the world's population, and 497 million people in cities depend on shared sanitation, a figure that has doubled since 1990. But it doesn't stop there. The WHO affirms that the water source must be located no more than 1,000 meters from the home and, however, millions of people in the world must walk up to 6 hours a day to collect water for domestic use. In addition, according to the UNDP (United Nations Development Programme) (Klingebiel and Hildebrand, 2010), the cost of water should not exceed 3% of the income of the family unit, but the reality is that poor countries pay up to 50 times more for a litter of water than their richer neighbors, because they have to buy the water from private sellers. Looking ahead, there isn't a much more hopeful outlook. Current statistics from the United Nations World Water Development Report 2018 indicate that global water

demand has been estimated at around 4,600 km^3/year and is projected to increase between 20% and 30% (from 5500 to 6000 km^3/year) by 2050 (Boretti and Rosa, 2019). The same report indicates that global water use has increased six times in the last 100 years (Gain et al., 2016) and continues to grow steadily at a rate of approximately 1% per year. Much of this growth can be attributed to a combination of population growth, economic development and shifting consumption patterns. Agriculture currently accounts for 69% of global water withdrawals, which are mainly used for irrigation but also include water used for livestock and aquaculture. Industry (including energy and power generation) accounts for 19%, while municipalities are responsible for the remaining 12%.

That is why water has been included in the Sustainable Development Goals (SDGs) or Global Goals. SDGs are a collection of 17 interlinked global goals designed to be a "blueprint to achieve a better and more sustainable future for all" (Assembly, 2017). The SDGs were set up in 2015 by the United Nations General Assembly and are intended to be achieved by the year 2030. The Goal related to water is the 6 and is: Ensure availability and sustainable management of water and sanitation for all. The targets cover all aspects of both the water cycle and sanitation systems, and their achievement is designed to contribute to progress across a range of other SDGs, most notably on health, education, economics and the environment.

1.2.2 Types and pollutants in wastewater

FAO defines wastewater as: Water that has no immediate value for the purpose for which it was used or for the purpose for which it was produced due to its quality, quantity or when it is available. However, one user's wastewater can serve as a supply for another user elsewhere. Cooling water is not considered wastewater.

Types of wastewaters

It is important to know the different types of wastewaters to carry out the correct treatment (Fig. 1.2). The different types of wastewaters are included in the European Directive 91/271 CEE. In this regulation, three types of wastewaters

are distinguished according to their origin. Types of wastewaters (Barrimi et al., 2013):

Domestic wastewater: This class of wastewater are originated in homes and is essentially produced by human metabolism and by activities carried out in the domestic environment. These, in addition, can be subdivided into:

- Black Waters: they are characterized by being waters that are transported from urine and the toilet.
- Gray Waters: they are characterized by being soapy waters that can contain fats, coming from the shower, tub, sink, dishwasher, laundry room and washing machine.

Urban wastewater: these waters are characterized by being liquid waste from an urban conglomerate, of which it has domestic and industrial activities, transported by a sewage network.

Industrial wastewater: within this type of wastewater are all those that have been discharged from a place for commercial or industrial purposes.

- Industrial liquid waste: these waters are characterized by coming from different industrial processes; therefore, their composition varies according to the type of industrial process and even for the same industrial process, likewise its different characteristics can be determined in different industries.
- Agricultural wastewater: these waters are characterized by being those that come from surface runoff from agricultural areas and are characterized by the presence of pesticides, salts and a high content of suspended solids.

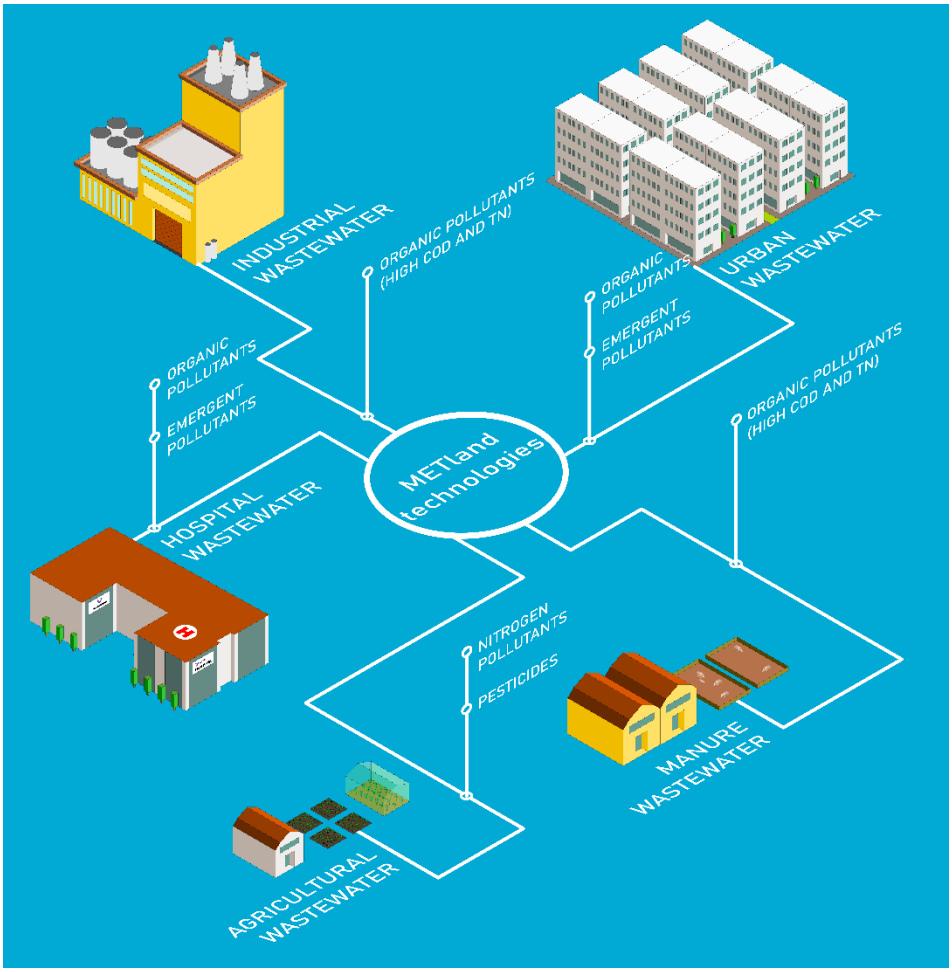

Figure 1.2. Types of wastewaters that can be treated in a METland.

Wastewater pollutants

The composition of wastewater often shows a wide range of variation between different types of water and is defined by the amount of the physical, chemical and biological components present in it. Classically they have been grouped in this way (Wetlands et al., 2013):

Physical: The physical components of wastewater are color, odor, solids, and temperature.

- Increase or decrease in temperature, from industrial activities that use water as a coolant. In reservoirs, the water that comes from the turbines to the river has a lower temperature. If the water

temperature rises, the amount of dissolved oxygen decreases, which can affect the development of some species.

- Radioactive particles. From nuclear power plant cooling circuits and radioactive waste.
- Solid particles in suspension. They can be of different sizes, from macro- to micro- pollutants.

Chemicals: They include organic and inorganic compounds dissolved or dispersed in water.

- Inorganic pollutants: inorganic pollutants are various products dissolved or dispersed in water that come from domestic, agricultural and industrial discharges or soil erosion. The main ones are chlorides, sulfates, nitrates and carbonates. Also, acidic and alkaline wastes and toxic gases are dissolved in water such as oxides of sulfur, nitrogen, ammonia, chlorine and hydrogen sulfide. A high part of the inorganic fraction is in soluble form, although the insoluble part in suspended particles form is also significant. Due to their environmental impact, soluble species are more relevant since are more mobile and their toxic scope is higher. Among the inorganic pollutants in water, the following can be highlighted:
  - Nitrogen ions. Found in the form of NO_3^-, NO_2^-, NH_4^+ and organic N. Nitrites and ammonia are very unstable and tend to oxidize to nitrate. An excessive load of nitrogenous nutrients in basins sloping to lakes or reservoirs can cause eutrophication of the same, or in rivers with the possible incidence of groundwater. They are generally indicators of agricultural pollution.
  - Cyanide ions. Their presence in water always indicates industrial-type contamination, usually coming from electroplating, blast furnaces and coking plants. Its toxicity is very high.

- Sulfate ions. Pollution by these ions is mainly due to the contribution of rain (acid rain) and causes acidification of the aquatic environment, causing serious alterations to its life.
- Heavy metals. Although many of the metallic elements are necessary for the development of living organisms, when they exceed a certain concentration, they can be harmful. Many of these elements have an affinity for sulfur, thereby attacking the bonds that make up this element in enzymes, causing it to be immobilized. Others, such as cadmium, copper, or lead (in ionic form) form stable complexes with amino and carboxylic groups, hindering transport processes through cell walls. Heavy metals are a major global problem. This problem is related to its persistence in the environment, and the consequent accumulation factor.

▪ Organic pollutants: an organic compound refers to a wide group of chemical compounds that have in common the fact that carbon is always involved in their composition. They are the compounds of carbon, although carbon itself must be excepted in its different forms, its oxides, carbonic acid and its salts, carbides, cyanides and some other carbon compounds that are completely inorganic. Organic pollutants are also compounds dissolved or dispersed in water that come from household, agricultural, industrial wastes, and from soil erosion. They are human and animal waste, from slaughterhouses, from food processing for humans and animals, various industrial chemicals of natural origin such as oils, fats, tars and dyes, and various synthetic chemicals such as paints, herbicides and insecticides. Organic pollutants consume dissolved oxygen in the water and affect aquatic life.

- Pesticides are worth highlighting among the organic pollutants. These are agents that fight organisms that attack food and other essential materials for human beings, for which they have a phytosanitary, livestock, domestic, environmental use, in the

food industry and even in personal hygiene. Many of them have a synthetic origin are hardly biodegradable by microorganisms, if we also take into account their wide toxicity with organisms, we will realize the importance of their control.

Biological: among the main biological pollutants in water we find different pathogens, such as bacteria, viruses, protozoa and parasites that come into contact with water and that come mostly from organic waste.

- Viruses are among the most important and potentially most hazardous pollutants in wastewater. They are more resistant to treatment, more infectious, more difficult to detect, and require smaller doses to cause infections.
- For bacteria, they are the most common microbial pollutants in wastewater. They cause a wide range of infections, such as diarrhea, dysentery, skin and tissue infections.

In recent years, the development of new and more sensitive analysis methods has made it possible to detect the presence of other contaminants, potentially dangerous, globally known as emerging. Emerging pollutants are defined as previously unknown or unrecognized pollutants whose presence in the environment is not necessarily new, but concern about its possible consequences. Another peculiarity of these compounds is that, due to their high production and consumption, and the consequent continuous introduction of them into the environment, they do not need to be persistent to cause negative effects (Petrovic M et al., 2003). The list of emerging contaminants includes a wide variety of everyday products with both industrial and domestic applications. Some examples are detergents, pesticides, drugs, or microplastics.

Several parameters are used to measure contamination (Table 1). The most common are (Kadlec and Wallace, 2009):

- COD (Chemical Oxygen Demand) and BOD_5 (Biochemical Oxygen Demand after five days): quantify the amount of matter organic present in wastewater, measured in the form of mg O_2/l. These

parameters are a measure of the impact that the discharge on the oxygen levels of the receiving channel.

- Suspended Solids (SS): quantifies the impact of solids in the receiving channel, whose accumulation gives rise to turbidity and sludge formation.
- Total Nitrogen (NT) and Total Phosphorus (PT): the measure of nutrients responsible for eutrophication (excessive growth of algae and other plants) of the receiving channel.

Table 1.1 parameters are used to measure contamination

	Parameter	Optimal values for life	Effects on aquatic ecosystems	Sources
General condictions	Temperature	< 30 °C	Increased metabolic rate Toxic potentiation	Deforestation Refrigeration Reservoirs
	pH	6 - 8	Acidification	Acid rain Mines Industry
	Suspended solids	< 50 mg/L	Low light penetration Mechanics Clogging	Deforestation Mines Grave Industrial agriculture
	Salts	< 1 ‰	Internal osmotic pressure	Salt mines Water softeners
Organic matter	Oxygen	> 5 mg/L	Low oxygen BOD increase Toxic potentiation Eutrophication	Leaves trees Urban Industrial Slurry
	BOD	< 5 mg/L		
	COD	< 30 mg/L		
Nutrients	Phosphorus	< 0.02 mg/L	Eutrophication Excessive algae growth	Urban Industrial Slurry Diffuse sources
	Nitrogen	< 10 mg/L		
Toxics	Metals	< µg/L	Lethal / Sublethal Bioaccumulation Eliminate competition / predators	Industrial Passive coatings, paints Pest control
	Pesticides			
	Organic micropollutants			
	Solvents			

1.2.3 Wastewater treatment in small urban communities

On many occasions, urban wastewater discharges exceed the dilution and self-purification capacity of the channels and receiving media, which leads to a progressive deterioration of their quality, and makes the subsequent reuse of the water impossible.

Regardless of the origin and characteristics of urban wastewater, it must be properly treated before its discharge or reuse, to (Barrimi et al., 2013):

- Protect the ecological status of the receiving environments (reservoirs, rivers, ravines, aquifers, sea, etc.) from the bulk of organic pollution from urban wastewater.
- Avoid risks to the public health of the population.
- Produce effluents with physical, chemical and microbiological characteristics suitable for reuse.

The treatment of wastewater generated in small towns continues to be a pending issue, the solution of which has been postponed over time, by prioritizing (logically) the purification of discharges generated in large and medium-sized cities. When talking about small-scale wastewater treatment, it is necessary to emphasize two concepts, in line with Directive 91/271 / EEC (Rosa Huertas et al., 2012):

- We are not talking about towns, but about urban agglomerations, understanding by urban agglomeration: the area whose population and/or economic activities present sufficient concentration for the collection and conduction of urban wastewater to a treatment facility for said water or a final discharge point.
- The population to be treated is not counted according to the number of its inhabitants, but rather its equivalent inhabitants, which makes it possible to consider the biodegradable industrial load that will enter the treatment station.

Regarding what we understand by small urban agglomeration, it has been agreed to establish the limit at 2,000 equivalent inhabitants, below which the aforementioned Directive requires that an adequate treatment be applied to wastewater. Once these premises have been established, it is necessary to take into account that the treatment of wastewater from small agglomerations presents a series of conditioning factors, both technical (strong daily and seasonal fluctuations in the flows and loads to be treated), and economic (not benefiting from the advantages of economies of scale), which make it necessary

to implement specific treatment solutions that adapt to these conditions (Barrimi et al., 2013; Rosa Huertas et al., 2012; Wetlands et al., 2013). As a result of this idiosyncrasy, the following criteria when selecting the type of technology to apply in small urban agglomerations are recommended:

- Adequate for technical and economic resources: technologies that require simple maintenance. Minimum implementation and operating costs, regardless of energy consumption, electromechanical elements and chemical reagents as much as possible. Simplicity in the management of sludge generated in purification.
- Robust systems: treatment systems must be robust, capable of self-regulating effectively over a wide range of flow rates and loads to obtain an effluent of sufficient quality.
- Environmental integration: the facilities must be adapted to the environment with the highest environmental integration, even seeking to provide the added value from an educational, tourist, or recreational nature point of view.

Actually, for the treatment of urban wastewater in small towns Conventional and Non-Conventional Technologies installations are used. The reality confirms that the two types of technologies are valid to purify the generated discharges, but the reality also shows that, in a small population, due to the aforementioned characteristics, priority should be given to the chosen technology robust and low cost of operation and maintenance. The processes that intervene in non-conventional technologies include many of those that are applied in conventional treatments (sedimentation, filtration, adsorption, chemical precipitation, ion exchange, biological degradation), together with processes typical of natural treatments (photosynthesis, photooxidation, assimilation by plants) but unlike conventional technologies, in which processes take place sequentially in tanks and reactors, in non-conventional technologies is operated at natural speed (without energy input), developing the processes in a single reactor-system and the energy savings are offset by a greater need for surface area. However, when installing this type of technology, it must be taken

into account that its "simplicity" of operation and maintenance does not imply "simplicity" of design, which unfortunately and on many occasions, has been wrongly assimilated. Not enough attention has been paid to the sizing phase of the treatment system or the subsequent construction stage. These deficiencies have been reflected in numerous facilities in which the expected performance is not achieved (Barrimi et al., 2013; Kadlec and Wallace, 2009; Rosa Huertas et al., 2012; Wetlands et al., 2013).

Below, each of the different technologies, both conventional and non-conventional, that are currently in use to treat urban wastewater generated in small towns are presented in detail.

- Non-Conventional Technologies:
  - Those that resort to the use of soil as a purifying element.
    Subsurface application systems: filter ditches, filter beds.
    Intermittent buried sand filters.
    Surface application systems: green filters.
  - Those that simulate the conditions of natural wetlands: Constructed wetlands, in their different forms: free flow and subsurface flow.
  - Those that imitate the natural purification processes that occur in rivers and lakes: lagoons.
  - Those that are based on the filtration of the water to be treated through a natural carbon: peat filters.
- Technologies that present intermediate characteristics between Non-Conventional and Conventional Technologies:
  - Bacterial beds.
  - Rotating biological contactors.
- Conventional Technologies:
  - Prolonged aerations.

In all the systems mentioned above, the elimination of pollutants is carried out in an orderly and sequential way through different stages, which,

applied in succession, provide an increasing degree of treatment of the water (Barrimi et al., 2013; Díaz et al., 2014)

- Pre-treatment: prior separation of as many contaminants as possible that by nature or size can cause problems later (coarse solids, sand and floating).
- Primary treatment: the main objective is the elimination of settleable and floating solids.
- Secondary treatment: in this case the objective is the elimination of the biodegradable organic matter dissolved or in colloidal form, as well as the rest of the solids and part of the nutrients present in the water.
- Tertiary treatment: allows obtaining higher quality effluents, to be discharged in areas with more demanding requirements. Generally, the elimination of nutrients and pathogens is sought.

1.2.4 Constructed wetlands as a wastewater treatment system

Wetlands have properties that make them unique among the major ecosystem groups on Earth. Ample water is important for most forms of biological productivity, and wetland plants are adapted to take advantage of this abundant supply of water while overcoming the periodic shortage of other essential chemical elements, such as oxygen. Because of this, wetlands are among the most biologically productive ecosystems on the planet. As such, they are frequently inhabited by jungle-like growths of plants and are home to a multitude of animals including mammals, birds, reptiles, amphibians, and fish that are uncommon in other ecosystems. In addition, because wetlands have a higher rate of biological activity than most ecosystems, they can transform many of the common pollutants that occur in conventional wastewaters into harmless by-products or essential nutrients that can be used for additional biological productivity. These transformations are accomplished by the wetlands land area, with its inherent natural environmental energies of sun, wind, soil, plants, and animals. These pollutant transformations can be obtained for a relatively low cost. Wetlands are one of

the least expensive treatment systems to operate and maintain (Kadlec and Wallace, 2009; Koottatep and Polprasert, 1997; Truu et al., 2009).

We can define Constructed Wetlands (CW) as purification systems in which the previously mentioned pollutant elimination processes are reproduced. The artificial character of this type of wetlands is defined by the following peculiarities:

- The confinement of the wetland is built mechanically and is waterproofed to avoid losses of water to the subsoil.
- The use of substrates different from the original soil for the rooting of the plants.
- The selection of the type of plants that will colonize the wetland.

Constructed Wetlands technology thus acts as a complex ecosystem. The purification of wastewater takes place by circulating it through these constructed wetlands, in which physical, chemical and biological processes take place, which reduces the pollutants present. The main elements that participate in the process are the following (Dotro et al., 2017a; Truu et al., 2009; Villaseñor et al., 2013):

- The water to be treated, which circulates through the filtering substrate and/or the vegetation.
- The substrate or bed material, which has the purpose of supporting the vegetation and allowing the microbial population fixation (in the form of biofilm), which will participate in most of the purification processes.
- The aquatic plants, which provide a surface for the formation of bacterial films, facilitate the filtration and adsorption of the constituents of the wastewater, contribute to the oxygenation of the substrate and the elimination of nutrients. In addition, the vegetation contributes significantly to the landscape integration of these treatment devices.

Types of constructed wetlands

Modern constructed wetlands are man-made systems that have been designed to emphasize specific characteristics of wetland ecosystems for improved treatment capacity. Constructed wetlands can be constructed in a variety of hydrologic modes. At the current stage of technology development, three types of wetlands are in widespread use (Dotro et al., 2017b; Kadlec and Wallace, 2009; Vymazal and Kröpfelová, 2015):

- Free water surface (FWS) wetlands, have areas of open water and are similar in appearance to natural marshes.
- Horizontal subsurface flow (HSSF) wetlands, which typically employ a gravel bed planted with wetland vegetation. The water, kept below the surface of the bed, flows horizontally from the inlet to the outlet.
- Vertical flow (VF) wetlands distribute water across the surface of a sand or gravel bed planted with wetland vegetation. The water is treated as it percolates through the plant root zone and bed material.

Free water surface (FWS) wetlands. The water to be treated flows freely over the surface of the substrate where the plants are rooted, circulating their stems and leaves, so it is directly exposed to the atmosphere (Fig. 1.3). These wetlands are made up of ponds or channels with emergent vegetation and shallow water levels (less than 0.4 m). To a certain extent, these systems can be considered as a variety of classic lagoons, with the aforementioned differences in terms of the lower depth of the water surface and the existence of rooted vegetation at the bottom (Kadlec and Wallace, 2009).

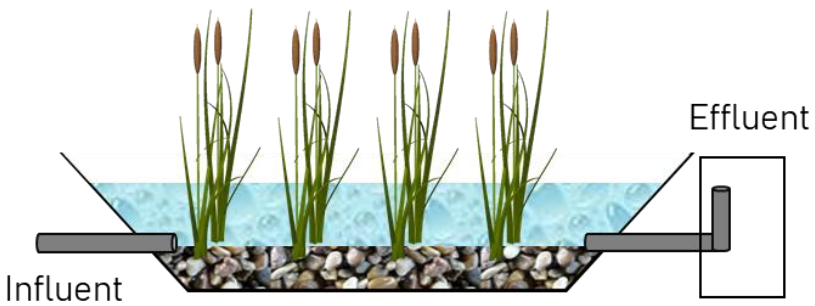

Figure 1.3. Basic elements of a free water surface constructed wetland.

Horizontal subsurface flow (HSSF) wetlands. consist of gravel or soil beds planted with wetland vegetation. They are typically designed to treat primary effluent before either soil dispersal or surface water discharge. The wastewater is intended to stay beneath the surface of the bed and flows in and around the roots and rhizomes of the plants and the bacteria biofilm growth around the bed material (Fig. 1.4). Because the water is not exposed during the treatment process, the risk associated with human or wildlife exposure to pathogenic organisms is minimized. Properly operated HSSF wetlands do not provide suitable habitats for mosquitoes. HSSF wetland systems are generally more expensive than FWS wetlands, although maintenance costs remain low compared to alternatives. They are commonly used for secondary treatment for single-family homes or small cluster systems, or small. However, there are many other applications to treat wastewaters from the industry (Kadlec and Wallace, 2009).

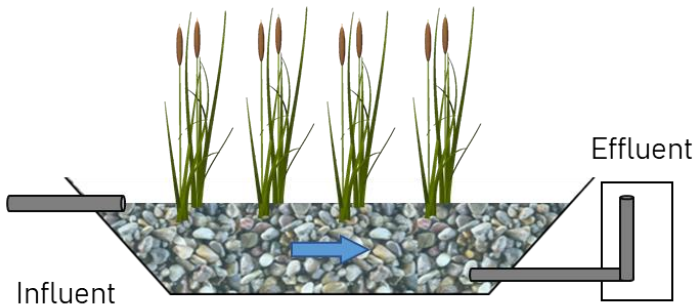

Figure 1.4. Schematic horizontal subsurface flow constructed wetland.

Vertical flow (VF) wetlands. The water supply is carried out intermittently, for which it generally resorts to the use of pumps (commanded by timers or level buoys) or, when the topography allows it, to controlled discharge siphons. Recently, to distribute the water over the filtration surface, pipes are used that are supported by pivots distributed over the entire surface, with a feeding point every 25-30 m^2 of wetland surface. The waters circulate vertically through a filtering substrate of sand-gravel, of the order of 1 m thick, in which the vegetation is fixed. At the bottom of these wetlands, a drainage network allows the collection of treated effluents. A set of conduits are connected to this drainage network, which protrudes from the layer of aggregates, to increase the

oxygenation of the filtering substrate by natural ventilation (chimney effect). The contribution of oxygen by the roots of the plants, in this type of wetlands, is small compared to the contributions through the alternating periods of flooding and drying and the ventilation system (Table 1.2) (Ortega et al., 2010).

Table 1.2. Treatment performance values in subsurface slow constructed wetlands (From Ortega *et al.* 2010).

Parameter	Vertical CW		Horizontal CW	
	% Removal	Effluent (mg/L)	% Removal	Effluent (mg/L)
SS	90-95	13-25	90-95	13-25
BOD_5	90-95	15-25	85-90	15-30
COD	80-90	60-120	80-90	60-120
NH_4-N	60-70	9-12	20-25	22-24
TN	60-70	15-20	20-30	35-40
TP	20-30	7-8	20-30	7-8

Treatment processes and microbial communities

- Suspended solids

Wetland systems have long hydraulic residence times, generally several days or longer. Consequently, virtually all settleable and floatable solids of wastewater origins are removed. The major processes responsible for the removal of settleable suspended solids are sedimentation and filtration. Non-settling/colloidal solids are removed, at least partially, by bacteria growth (which results in the settling of some colloidal solids and the microbial decay of others) and collisions with the adsorption to other solids (plants, pond bottom, suspended solids).

In all types of constructed wetlands, most of the solids of wastewater origin are filtered out and settled within the first few meters beyond the inlet zone. The accumulation of trapped suspended solids is a major threat to the good performance of some systems, especially those with the subsurface flow, which can be clogged with suspended solids. In many systems, however, the majority of settleable solids are removed in a mechanical pre-treatment unit (e.g. sedimentation or Imhoff tanks) before the wastewater is discharged to the actual wetland system (Dotro et al., 2017b; Kadlec and Wallace, 2009).

- Removal of organic matter

Organics compounds are degraded aerobically as well as anaerobically. The oxygen required for aerobic degradation is supplied directly from the atmosphere by diffusion or oxygen leakage from the macrophyte roots into the rhizosphere. The uptake of organic matter by the macrophytes is negligible compared to biological degradation.

Aerobic degradation of soluble organics matter is governed by the aerobic heterotrophic bacteria according to the following reactions (Eq. 1):

$$(CH_2O) + O_2 \rightarrow CO_2 + H_2O \qquad \text{(Eq. 1)}$$

The autotrophic group of bacteria which degrades organic compounds containing nitrogen under aerobic conditions is called nitrifying bacteria, the process is called ammonification and will be. discussed later. Both groups consume organics but the faster metabolic rate of the heterotrophs means that they are mainly responsible for the reduction in the BOD of the system. Insufficient supply of oxygen to this group will greatly reduce the performance of aerobic biological oxidation, however, if the oxygen supply is not limited, aerobic degradation will be governed by the amount ·of active organic matter available to the organisms.

Anaerobic degradation is a multistep process that occurs within constructed wetlands in the absence of dissolved oxygen. The process can be carried out by either facultative or obligate anaerobic heterotrophic bacteria. In the first step the primary end-products of fermentation are fatty acids such as acetic (Eq. 2), butyric, and lactic (Eq. 3) acids, alcohols (Eq. 4) and the gases CO_2 and H_2 (Vymazal 1995):

$$C_6H_{12}O_6 \rightarrow 3\ CH_3COOH + H_2 \qquad \text{(Eq. 2)}$$

$$C_6H_{12}O_6 \rightarrow 2\ CH_3CHOHCOOH \text{ (lactic acid)} \qquad \text{(Eq. 3)}$$

$$C_6H_{12}O_6 \rightarrow 2\ CO_2 + 2\ CH_3CH_2OH \text{ (ethanol)} \qquad \text{(Eq. 4)}$$

Acetic acid is the primary acid formed in most flooded soils and sediments. Strictly anaerobic sulfate-reducing (Eq. 5) and methane-forming bacteria then utilize the end-products of fermentation and, in fact, depending on the complex community of fermentative bacteria to supply substrate for their

metabolic activities. Both groups play an important role in organic matter decomposition and carbon cycling in wetlands:

$$CH_3OOH + H_2SO_4 \rightarrow 2\ CO_2 + 2\ H_2O + H_2S \quad \text{(Eq. 5)}$$

Anaerobic degradation of organic compounds is much slower than aerobic degradation. However, when oxygen is limiting at high organic loadings, anaerobic degradation will predominate.

- Nitrogen removal

The removal mechanisms for nitrogen in constructed wetlands are manifold and include volatilization, ammonification, nitrification/denitrification, plant uptake and matrix adsorption. Numerous studies have proven that the major removal mechanism in most constructed wetlands is microbial nitrification/denitrification. In systems with free-floating macrophytes, ammonia volatilization can significantly contribute to nitrogen reduction (Dotro et al., 2017b; Vymazal et al., 1998).

Ammonification: (mineralization) is the process where organic N is converted into inorganic N. Mineralization rates are fastest in the oxygenated zone and decrease as mineralization switches from aerobic to facultative anaerobic and obligate anaerobic microflora. The rate of ammonification in wetlands is dependent on temperature, pH value, C/N ratio of the residue, available nutrients in the system, and soil conditions such as texture and structure.

Nitrification: is usually defined as the biological oxidation of ammonium to nitrate with nitrite as an intermediate in the reaction sequence. Nitrification is a chemoautotrophic process. The nitrifying bacteria derive energy from the oxidation of ammonia and/or nitrite and carbon dioxide is used as a carbon source for the synthesis of new cells. These organisms require O_2 during ammonium oxidation to nitrite and nitrite oxidation to nitrate (Eqs. 6, 7, 8). Oxidation of ammonium to nitrate is a two-step process:

$$NH_4^+ + 1.5\ O_2 \rightarrow NO_2^- + 2H^+ + H_2O \quad \text{(Eq. 6)}$$

$$NO_2^- + 0.5\ O_2 \rightarrow NO_3^- \quad \text{(Eq. 7)}$$

$$NH_4^+ + 2\ O_2 \rightarrow NO_3^- + 2\ H^+ + H_2O \quad \text{(Eq. 8)}$$

The first step, the oxidation of ammonium to nitrite, is executed by strictly chemolithotrophic (strictly aerobic) bacteria which are entirely dependent on the oxidation of ammonia for the generation of energy for growth. In soil, species belonging to the genera *Nitrosospira*.

The second step in the process of nitrification, the oxidation of nitrite to nitrate, is performed by facultative chemolithotrophic bacteria which can also use organic compounds, in addition to nitrite, for the generation of energy for growth.

Denitrification: the first anoxic oxidation process to occur after oxygen depletion is the reduction of nitrate to molecular nitrogen or nitrogen gases. From a biochemical viewpoint, denitrification is a bacterial process in which nitrogen oxides (in ionic and gaseous forms) serve as terminal electron acceptors for respiratory electron transport. Electrons are carried from an electron-donating substrate (usually, but not exclusively, organic compounds) through several carrier systems to a more oxidized N form. The resultant free energy is conserved in ATP, following phosphorylation, and is used by the denitrifying organisms to support respiration. Denitrification is illustrated by the following equation (Eq. 9) :

$$6\,(CH_2O) + 4\,NO_3^- \rightarrow 6\,CO_2 + 2\,N_2 + 6\,H_2O \qquad \text{(Eq. 9)}$$

This reaction is irreversible and occurs in the presence of available organic substrate only under anaerobic or anoxic conditions (Eh = +350 to +100 mV), where nitrogen is used as an electron acceptor in place of oxygen.

The denitrifying ability has been demonstrated in 17 genera of bacteria. Most denitrifying bacteria are chemoheterotrophs. They obtain energy solely through chemical reactions and use organic compounds as electron donors and as a source of cellular carbon. The genera *Bacillus, Micrococcus* and *Pseudomonas* are probably the most important in soils, *Pseudomonas, Aeromonas* and *Vibrio* in the aquatic environment.

- Phosphorous removal

Phosphorous in wastewater is in the form of organic phosphorous and inorganic orthophosphate (Vymazal et al., 1998). Between 10 and 20% is assimilated in microbial biomass. Three are the main processes to remove phosphorous in CWs:

- Direct absorption by plants: plants adsorb much less phosphorous than nitrogen.
- Adsorption on the particles: in can be released under certain environmental conditions, especially by changes in redox potential.
- Physicochemical precipitation, using reactions of phosphorous with iron, aluminum and calcium of the wastewater, resulting in insoluble phosphates.

Phosphorous removal in CWs is approximately from 20 to 30%. This percentage can be improved by filtering specific substrates, i.e. containing iron. It has been observed that the retention of phosphorous decreases over time.

1.3 Microbial Electrochemistry: Fundaments

1.3.1 The origins of microbial electrochemistry

Microbial electrochemistry deals with the interactions between microorganisms and electronic devices and with the novel electrical properties of microorganisms. Diversity of microorganisms can donate electrons to, or accept electrons from, electrodes without the addition of artificial electron shuttles. However, the mechanisms for microbe-electrode electron exchange have been seriously studied in only a few microorganisms. Electroactive bacteria (EAB) have several potential practical applications, but additional basic research will be necessary for rational optimization (Schröder et al., 2015a).

Electroactive Bacteria (EAB)

The idea of electroactive bacteria is not a new one: experimental data were first reported in 1911 by Potter (Potter, 1911) who demonstrated current production by both yeast and bacteria. Several other efforts were reported by several workers in the mid-20th century, but as with the earlier experiments, the current production was very low, and any potential applications as power

sources were not taken seriously. In recent years, the situation has begun to change. In 1988, two papers appeared nearly simultaneously, describing two different bacteria that were capable of growth on solid metal (iron or manganese) oxides as terminal electron acceptors (TEA) (Bücking et al., 2013; Lovley et al., 1998). One of these ultimately named *Shewanella* (Myers, C.R. and Myers, 1992) was a facultative aerobe, isolated from the oxic/anoxic interface of Oneida Lake, N.Y., where it was responsible for the rapid rates of manganese reduction seen in the lake, and shown to be able to catalyze rapid metal oxide reduction in the laboratory and to grow with solid manganese oxide as the sole electron acceptor. The other, ultimately named *Geobacter*, was an oxygen-sensitive delta proteobacteria that was isolated from deep sediments of the Potomac River, N.Y., where it was catalyzing the rapid reduction of iron oxides (Lovley and Phillips, 1988). For almost 30 years, these two very different microbes have served as the model organisms for mechanistic studies of a process now referred to as extracellular electron transport or EET.

This interaction between microorganisms and electrodes as their electron acceptor is based on one of the oldest respiratory processes on earth. Ferric iron was and still is a very abundant potential electron acceptor (Lovley and Phillips, 1988). Nevertheless, the dissimilatory (respiratory) reduction of iron necessitates certain adaptations by microorganisms because iron occurs in soil sediments in the form of insoluble minerals such as ferrihydrite and hematite. Hence, the reduction of ferric iron is dependent on the evolution of an extended respiratory chain to the cell surface. Usually, the activity of enzymes is highly specific and follows the lock and key principle. In the case of ferric iron respiration, evolution has been selected for rather unspecific terminal reductases that can reduce a broad range of solid-phase electron acceptors if they have a redox potential that sustains the electron transfer process. This ability is necessary because environmental ferric iron minerals have an uncountable number of different shapes, which makes a specific lock–key interaction unsuitable. The redox potential of the electron acceptor determines the electron transfer rate. Using electrodes as electron acceptors offers the ability to steer the respiratory rate and thereby the overall metabolic activity of

electrode-attached organisms. The two common routes of extracellular electron transfer, occur either via direct contact between the electron acceptor and redox-active enzymes on the cell surface or via the use of endogenously produced shuttling substances (Harnisch and Holtmann, 2019).

The clear advantage of exploiting electroactive communities is that electrodes can boost microbial metabolism in anaerobic systems that are typically electron acceptor limited. Electroconductive material may represent an inexhaustible source of electron acceptors, hosting the additional advantage of providing a more easily modulated redox potential compared to standard, low-reducing redox species that generally drive these systems (Fig. 1.5) (Kato, 2015; Kato et al., 2012).

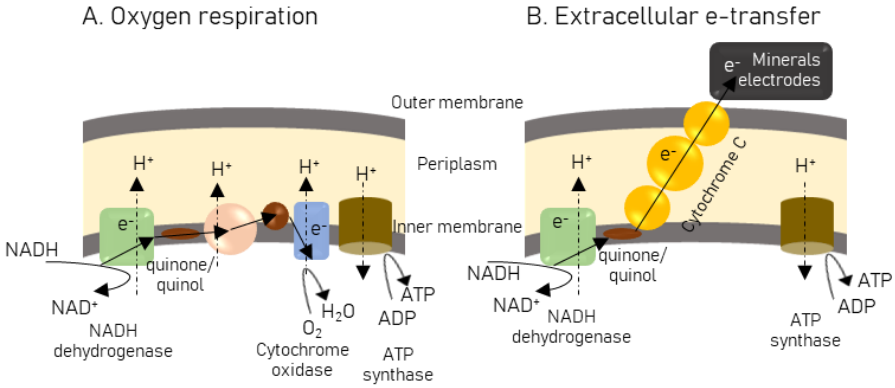

Figure 1.5. Schematic diagrams of respiration: (A) electron transfer to a soluble compound (as oxygen) and (B) microbial extracellular electron transfer. From (Kalo *et al.* 2012).

Geobacter as model bacteria

Geobacter species are in the family Geobacteraceae, which is within the domain Bacteria, phylum Proteobacteria, class Deltaproteobacteria. All Geobacter isolates are Gram-negative rods and can use a diversity of electron acceptors to support anaerobic growth, and there is evidence that *G. sulfurreducens* can grow via oxygen reduction at low oxygen tensions (Lin et al., 2004). Soluble electron acceptors that can be reduced intracellularly include nitrate, fumarate, and chlorinated compounds. Family Geobacteraceae is one of the best-studied groups of microorganisms capable of extracellular electron

exchange reactions, oxidizing acetate with the reduction of Fe(III). The two most heavily studied Geobacter species have been *G. metallireducens* and *G. sulfurreducens. G. metallireducens* was the first *Geobacter* species recovered in pure culture (Lovley, 2012; Lovley and Phillips, 1988).

The hallmark physiological capability of Geobacter species is their ability to couple the oxidation of organic compounds to the reduction of Fe (III), which allows Geobacter species to fill key niches in the anaerobic microbial food chain of sedimentary environments such as aquatic sediments, wetlands, rice paddies, and subsurface environments in which Fe(III) reduction is an important terminal electron-accepting process (Lovley, 1987, 1991, 1993, 1995, 2000). Other factors such as the "remarkably low" maintenance energy requirement of Geobacter species may also be an important factor in their success in subsurface environments (Lin et al., 2009).

Electron transfer to minerals and electrodes necessitates direct contact between the cells and the electron acceptor because the microorganisms do not produce an endogenous mediator for indirect/mediated electron transfer (Nevin and Lovley, 2002; Straub and Schink, 2003). Some of the factors that play a role in direct extracellular electron transfer are the cytochromes. C-type cytochromes are the key players in this process (Aklujkar et al., 2013; Butler et al., 2010; Holmes et al., 2006; Mehta et al., 2005), as can be judged by their abundance and diversity (Aklujkar et al., 2009; Butler et al., 2010). The genome of *G. sulfurreducens* encodes for more than 100 c-type cytochromes. Among these, 65 homologs have been identified within the genome of the closely related strain *G. metallireducens* (Aklujkar et al., 2009). A well-conserved c-type cytochrome in *Geobacter* species is PpcA. This triheme periplasmic cytochrome (Butler et al., 2010) is localized to the periplasm of the cell and predicted to transfer electrons from the cytoplasmic membrane to the outer membrane by heme groups that are oriented in parallel or perpendicular to each other (Morgado et al., 2010). For the inner membrane, there is evidence for at least two transfer pathways of electrons into the periplasm. The multiheme c-type cytochrome ImcH is required for respiration to extracellular electron acceptors with high redox potentials, whereas CbcL, an inner membrane protein, is chosen

for the reduction of acceptors with redox potentials lower than -0.1 V (Zacharoff et al., 2016).

The universal ability of all Geobacter species to oxidize acetate with Fe (III) serving as the sole electron-acceptor points to their key ecological/ biogeochemical role in wetlands, soils and sediments. Acetate is the key extracellular intermediate in the anaerobic degradation of organic matter (Lovley and Chapelle, 1995). Although there are some Fe(III)-reducing microorganisms that can completely oxidize fermentable organic compounds, such as sugars and amino acids (Lovley et al., 2004), they do not appear to be competitive with fermentative microorganisms. For example, in sediments in which Fe(III) reduction was the predominant terminal electron- accepting process, glucose was metabolized to acetate and other minor fermentation acids (Lovley and Phillips, 1988). Therefore, the mineralization of organic matter can only take place if there are Fe(III) reducers capable of coupling the oxidation of acetate to the reduction of Fe(III).

After Fe(III) reduction, electron transfer to electrodes is probably the most studied form of respiration in Geobacter species (Lovley, 2008, 2006; Lovley et al., 2011; Nevin et al., 2014). All Geobacter species that have been evaluated have the capacity for electron transfer to electrodes. Geobacter or closely related species are frequently the most abundant microorganisms that colonize electrodes from mixed species inocula or natural communities, especially under strictly anaerobic conditions. Frequently, the *Geobacter* species enriched are most closely related to *G. sulfurreducens,* which is consistent with the finding that *G. sulfurreducens* strains produce the highest current densities of any known pure cultures and accomplish this with very high (>90%) coulombic efficiencies (Nevin et al., 2008). This is expected to give them a competitive advantage in colonizing electrodes. A wide diversity of conductive materials are appropriate electrode surfaces for Geobacter species. Solid graphite is the most commonly employed (Bond and Lovley, 2003). but other graphite/carbon materials, carbon cloth, gold, steel, platinum and diversity of conductive polymers are also effective.

1.3.2 Microbial Extracellular Electron Transfer (EET) mechanism

Many anaerobes can only transfer electrons to soluble compounds such as nitrate or sulfate that can diffuse across the cell membrane, but electroactive bacteria are distinguished from these anaerobes by their ability to directly transport electrons outside of the cell, through a mechanism currently known as extracellular electron transfer (EET). EET is defined as the microbial metabolic process that enables electron transfer between microbial cells and extra-cellular solid materials and is a type of microbial respiration. Respiration converts redox potential differences between the oxidation and reduction of chemical compounds into a bio-available form of energy, generally ATP. In the respiration process, electrons derived from the oxidation of electron donors (as acetate, lactate, hydrogen, methane, ammonia, sulfides, etc.) are transferred to electron acceptors, that can be in the form of soluble oxidized compounds (as oxygen, carbon dioxide, nitrate or sulfate), insoluble forms (as humic acids) or solids (as minerals or electrodes). Through EET, microorganisms can transfer the electrons to the outer surface of the cell to reduce an extracellular solid terminal electron acceptor (Lovley, 2008). When microorganisms interact with conductive solid surfaces, electron transfer is thought to happen through several possible mechanisms (Fig. 1.6).

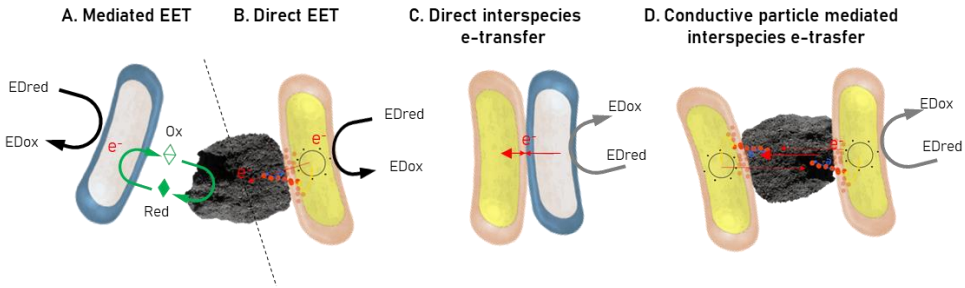

Figure 1.6. A. MEET via secondary metabolites B. DEET to electrodes via membrane bound cytochromes. C. Direct Interspecies electrons transfer (DIET). D. Conductive-particles mediates interspecies electron transfer (CIET).

Direct Extracellular Electron Transfer

DEET requires physical contact between the microorganism and the electrode, usually attached forming a biofilm on the electrode surface (Fig. 1.6). This mechanism involves transmembrane redox-active proteins as c-type

cytochromes (Allen et al., 2009; Busalmen and Esteve-Núñez, 2017). The DEET via outer membrane cytochromes requires the physical contact of the bacterial cell to the electrode, with the consequence that only bacteria in the first monolayer at the anode surface are electrochemically active. This causes a limitation of the catalysis by the maximum cell density in this bacterial monolayer. However, it has been demonstrated that some species have developed nanowires or pili to reach and utilize distant insoluble electron acceptors or to interconnect inners layers in the biofilm. This kind of strategy has been observed for *Geobacter* and *Shewanella* species (Gorby et al., 2006; Reguera et al., 2005).

Another example of DEET is when a cell uses another cell as TEA. Electrical contacts documented to date include electrically conductive pili, as well as conductive iron minerals and conductive carbon moieties such as activated carbon and biochar. To clearly distinguish between conductive mineral mediated and direct cell contact authors (Rotaru et al., 2021; Shrestha and Rotaru, 2014) have subcategorized the pili mediated electron transfer, as direct interspecies electron transfer (DIET) and the conductive mineral mediated as conductive particle-mediated Interspecies electron transfer (CIET).

DIET was first described in *G. metallireducens* and *G. sulfurreducens* co-cultures, growing in a defined minimal medium with ethanol as electron donor and fumarate as electron acceptor (Summers et al., 2010). The mechanism for DIET in *Geobacter* co-cultures were intensely studied during the past few years, combining phenotypic, genetic, transcriptomics, proteomics analysis (Shrestha et al., 2009; Shrestha and Rotaru, 2014; Summers et al., 2010). The absence of H2/formate mediated electron transfer in the co-culture was best shown by the ability of *G. metallireducens* to generate successful syntrophic co-cultures with a double mutant of *G. sulfurreducens* (*_hybL_fdnG*) incapable of H_2 or formate uptake (Liu et al., 2012; Rotaru et al., 2021). Furthermore, DIET is seemingly capable to produce successful co-cultures in the absence of acetate transfer as supportive mechanism of electron exchange as revealed in a recent study in co-cultures of *G. metallireducens* with a strain of *G. sulfurreducens* depleted in acetate utilization capacity, a citrate synthase mutant (*_gltA*) (Lovley et al., 2011).

This study revealed that DIET alone is sufficient for energy conservation in syntrophic co-cultures.

The need to produce biological conductive molecular networks can be averted by the addition of conductive minerals (Chen et al., 2014; Liu et al., 2012). CIET could take place via non-biological conductive networks of semi-conductive minerals like nano-magnetite (Chen et al., 2014; Kato et al., 2012), granulated activated carbon (GAC) (Liu et al., 2012), or biochar (Chen et al., 2014) in the absence of molecular conduits. For example, electrically conductive magnetite nano-particles facilitate CIET from *G. sulfurreducens* to *Thiobacillus denitrificans*, accomplishing acetate oxidation coupled to nitrate reduction (Kato et al., 2012). Conductive minerals are often present in natural environments (Canfield, 1989; Kappler and Straub, 2005; Morse and Cornwell, 1987), and their absence during laboratory incubations severely impacts species distribution and survival (Kato et al., 2019; Rotaru et al., 2019, 2018). CIET is more straightforward to investigate than DIET. This is because we can use conductive minerals to specifically enrich CIET-partners from environmental communities where partners may rely on conductive minerals to interact with each other (Aulenta et al., 2021; Rotaru et al., 2021). Under such enrichment conditions, non-syntrophic species fade out. For example, a *Geobacter-Methanosarcina* consortium from Baltic Sea sediments required the presence of conductive materials (iron-oxides or activated carbon) to carry out syntrophic acetate oxidation (Rotaru et al., 2018). Without conductive minerals, syntrophic acetate oxidation ceased, and both groups went extinct.

Microbial extracellular electron transfer, either in form of DIET (Direct Interspecies Electron Transfer) or CIET (Conductive-particle-mediated Interspecies Electron Transfer) is currently a trending topic in the environmental biotechnology field (Aulenta et al., 2014; Rotaru et al., 2021). Thus, such kinds of syntrophies have a key role in engineering applications for treating brewery wastewater in anaerobic digestors (Zhuang et al., 2019) or microbial electrochemical fluidized bed reactors (Kato and Igarashi, 2019; Tejedor-Sanz et al., 2017).

Mediated Extracellular Electron Transfer

Mediated Electron-Transfer (MEET) occurs through low-molecular compounds, referred to as electron mediators, which act as the electron carriers between microbial cells and solid materials. Electron mediators are chemical compounds that facilitate the transfer of electrons to and from bacteria, these may include sulfur compounds, humic substances (Lovley et al., 1999, 1996, 1998; Newman and Kolter, 2000) and flavins (Brutinel and Gralnick, 2012; Marsili et al., 2008; Von Canstein et al., 2008).

Some microorganisms can naturally synthesize and excrete endogenous redox-active molecules that function as electron mediators, such as flavins or phenazine compounds. Bacteria that rely on these compounds for extracellular electron transfer include *Shewanella* (Gorby et al., 2006; Logan and Regan, 2006; Marsili et al., 2008), *Lactococcus* (Korneel et al., 2004), *and Pseudomonas* (Pham et al., 2008).

Likewise, these mediators can be external agents, artificially added to the media or present in natural environments as humic substances. Humic substances are ubiquitous (Lovley et al., 1996). The humic substance analog, anthraquinone disulphonate (AQDS) serves as an electron shuttle between *G. metallireducens* and *G. sulfurreducens* (Liu et al., 2012), or between *G. metallireducens* and *W. succinogenes* (Lovley et al., 1999).

1.3.3 Electrochemical methods for the study of EET

Microbial electrochemistry deals with the interactions between microorganisms and electronic devices and with the electrical properties of microorganisms. Diversity of microorganisms can donate electrons to, or accept electrons from, electrodes without the addition of artificial electron shuttles. However, the mechanisms for microbe-electrode electron exchange have been seriously studied in only a few microorganisms. Interfacing microbial, enzymatic, and electrochemical transformations have led to the new field of microbial electrochemistry. Electrochemical reactions take place at the electrode/solution interface and, in the case of electroactive microbial biofilms, at the interface between the biofilm and the electrode surface. Microbial biofilms are far more complex than inorganic electrocatalytic moieties, and so

consequently the number of steps involved in their bioelectrochemical reactions increases dramatically (Schröder et al., 2015b).

For the electrochemical studies to be described here, a potentiostat controlled three-electrode system is required. A potentiostat is an electronic amplifier that controls the potential drop between the working electrode (WE) and the electrolyte solution, it hosts a reference electrode (RE) as a sensing component and a counter electrode (CE) for balancing the current flow. The working electrode (WE) is the electrode where the reaction of study takes place; its potential is controlled versus the reference electrode in a three-electrode system. The reference electrode (RE) is a non-polarizable (stable) electrode with a fixed potential that sets or measures the potential of the WE. And the counter electrode (CE) is the electrode that allows the reaction at the WE accompanying it with a respective reverse reaction (Biofilms, 2012; Schröder et al., 2015a).

Cyclic Voltammetry (CV)

One of the most important and most widespread applied electrochemical techniques is cyclic voltammetry (CV). Cyclic voltammetry is a powerful technique for the study of the extracellular electron transfer of electroactive microbial biofilms. This electrochemical analysis consists of the registration of the current production while a potential sweep is performed along with a potential window. It is common to initiate the CV in an initial potential (Ei) from where the sweep can be done towards either positive potentials (anodic sweep, oxidation reactions take place) or negative potentials (cathodic sweep, reduction reactions take place). Once, the extreme potential of the window is reached, the sweep is inverted until reaching the other extreme potential. Depending on the necessities of the assay, the cycle can be repeated *n* times. The speed of the sweep is known as scan rate and is equivalent to the potential variation per unit of time. The scan rate allows obtaining information about the speed of the reactions that occur on the WE. A CV (Current (I) vs. potential (E)) of a reversible system is shown in figure 1.7. In the anodic sweep, no current flow is observed until the potential approaches the standard potential of the redox pair (E_0). Then,

the current increases due to an oxidation reaction. As the potential continues to increase, the concentration of the species to be oxidized at the surface of the electrode begins to drop. When the potential reached is higher than the E_0 and the concentration of the species is almost zero, the current is at its maximum since the mass transport is at its highest rate. When the potential increases and the species is consumed, the current eventually drops. The highest current corresponds to a potential known as peak potential (Ep) and the maximum current is called Peak Current (Ip). When the extreme potential chosen is reached, the sweep is inverted. The shape of the inverse curve (cathodic) depends on the potential at which the sweep was inverted. If the extreme potential chosen is higher than the peak potential, the shape of the inverse curve is the same as the anodic sweep (Bard et al., 2001.).

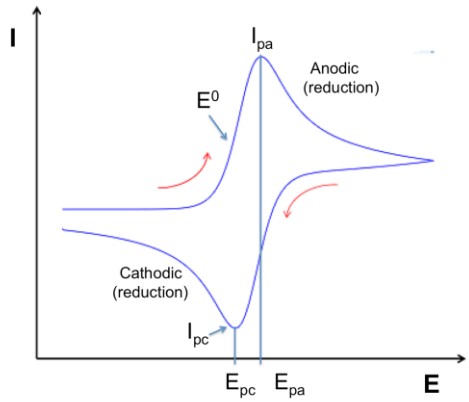

Figure 1.7. Cyclic voltammetry where Epa: anodic peak potential; Epc: cathodic peak potential; Ipa: anodic peak current; Ipc: cathodic peak current; E0: standard potential.

Useful thermodynamic information, as well as qualitative information on the nature of the electron-transfer process, can be extracted from CV experiments, including 1) formal potentials of redox species, 2) the reversibility of redox species and its dependency on the scan rate, 3) studying the influence of the mass transfer, 4) elucidating which redox couples are responsible for the development of turnover currents, i.e. the identification of the bioelectrocatalytically active sites, and 5) distinguishing between adsorbed and diffusive natures of the mediators.

Chronoamperometry (CA)

Chronoamperometry (CA) is another electrochemical tool where the working electrode acquires a constant potential and the resulting current from the biological extracellular oxidation or reduction of a compound on the surface of the working electrode is recorded as a function of time. The applied potential depends on the experimental goal. When the objective is oxidizing compounds, the polarization potential must be more positive than the OCP for the working electrode. In contrast, the polarization potential must be more negative when the goal is promoting the reduction at the working electrode (Babauta et al., 2012).

1.3.4 Microbial Electrochemical Technologies (METs): configurations and processes

Microbial Electrochemical Technologies (MET) can be derived as technologies or applications that utilize the electrochemical interaction of microbes and electrodes. In the great majority, these interactions involve extracellular electron transfer (Schröder et al., 2015b).

Microbial Fuel Cells (MFCs)

The MFC is a device which converts chemical energy to electrical energy during substrate oxidation by microorganisms so-called electroactive (Allen and Bennetto, 1993; Park and Zeikus, 2000). The schematic representation of the two-chambered MFC functionality is presented in figure 1.8. An anode and a cathode are each placed in aqueous solutions in two chambers separated by a proton exchange membrane (PEM). Microbes in the anode chamber oxidize fuel (electron donor) generating electrons and protons. The current generation is due to the nature of microorganisms, as they transfer electrons from a reduced electron donor to an electron acceptor at a higher electrochemical potential. Anode respiring bacteria (ARB) in an anode biofilm carry out an oxidation half-reaction of organic matter, producing electrons from renewable biomass, including wastes, and producing one proton for every electron (Torres et al., 2008). Carbon dioxide is eventually produced as an oxidation product. Electrons

are transferred to the cathode through the external circuit, powering the external device, and protons are transferred internally through the membrane. Electrons and protons are consumed on the cathode, reducing oxygen to water and generating electricity. In addition, bacteria can consume electrons at the cathode with the reduction of electrochemically positive electron acceptors such as nitrate, perchlorate, or metals (Clauwaert et al., 2007; Gregory et al., 2004; Gregory and Lovley, 2005; Thrash et al., 2007).

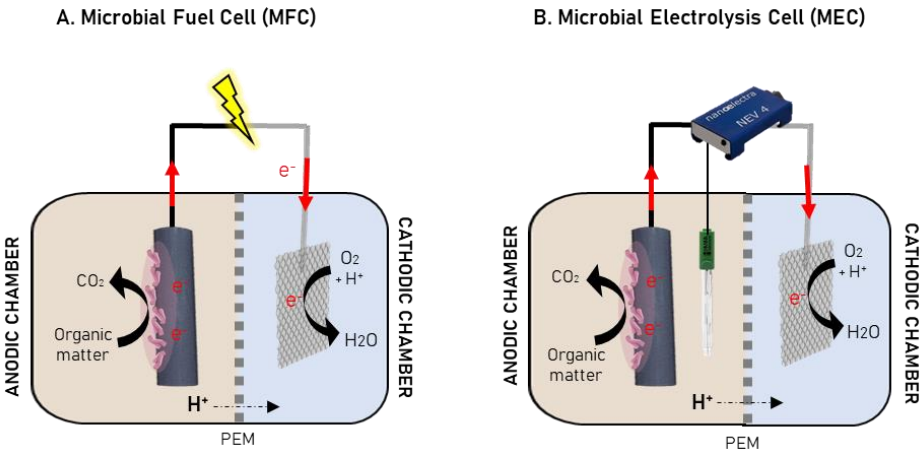

Figure 1.8. Schematic representation of microbial fuel cell working principle.

The main characteristic of MFC devices is the production of electricity coupled to biodegradation of soluble organic matter. However, the power output reached so far, make industrial applications still not available. Due to this limitation, the electricity stored in rechargeable devices as capacitors (Bruno et al., 2018; Franks and Nevin, 2010) has been suggested. On the other hand, promising performances on the laboratory scale have presented the MFCs as a suitable option for applications like bioremediation or even biosensing (see below). The most important applications of MFC configuration are:

Microbial desalination cells (MDCs). The basic principle of MDCs is to utilize the potential gradient generated across the anode and cathode to drive desalination in situ. Compare to other METs, MDCs have a third chamber for desalination by inserting an anion exchange membrane (AEM) and a cation exchange membrane (CEM) in between the anode and cathode chambers (Fig.

1.9). When electroactive bacteria in the anode chamber oxidize organic substrates and produce electrons and protons, the anions (e.g., Cl^-) from the salty water in the middle chamber migrate to the anode and the cations (e.g., Na^+) are drawn to the cathode for charge balance, thus the middle chamber solution is desalinated (Luo et al., 2012; Morel et al., 2012). MDC became of great interest because it can be used as a stand-alone technology for simultaneously removing organics and salt with no energy consumption (Ramirez-Moreno et al., 2021; Ramírez-Moreno et al., 2019).

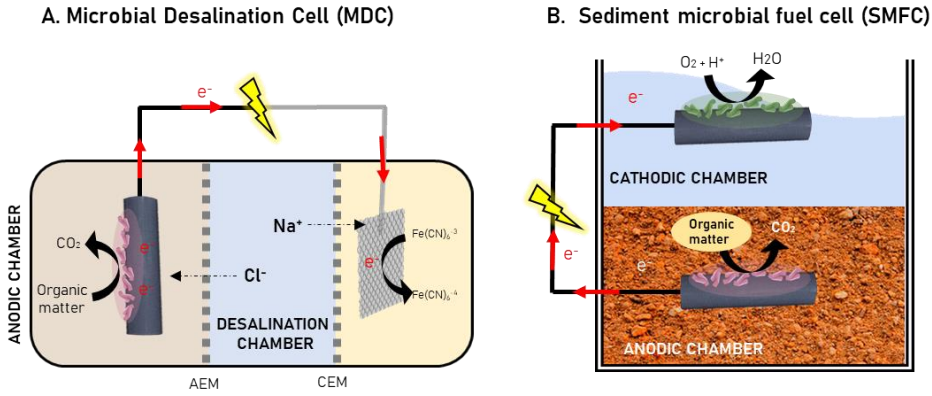

Figure 1.9. A) Schematic of a typical Microbial Desalination Cell (MDC) of 3 cameras, without external power supply. B) Schematic of a Sediment microbial fuel cell (SMFC).

Sediment microbial fuel cells (SMFCs) for harvesting energy from sediments and soil. SMFCs are variants of MFCs that are placed in ecological water bodies. The anode is placed in the sediment and connected through an electrical circuit to a cathode in the overlaying water layer. The energy is obtained through several reactions like either the electrochemical oxidation of microbially produced reductants like humic acids, Fe_2^+, S_2^- or the microbial oxidation of organics. Most of the SMFCs described so far have been installed in marine sediments, like the described before of Reimers et al. (Reimers et al., 2001). Other variations of SMFC have been located in freshwater natural environments like rice crop soils, where the plant exudates provide a source of organic substrates for the SMFC or changing the soil physical properties by stimulating colloid formation via the addition of silica (agricultural reagent) (Domínguez-Garay et al., 2018; Rodrigo Quejigo et al., 2018).

Biosensors. in this case, unlike other MET applications, the technology has been miniaturized. In comparison to conventional MFCs, miniaturized-METs allow obtaining significantly shorter start-up times and rapid electrical response (Estevez-Canales et al., 2015b, 2015a). One of the most feasible applications for the downscaled METs are biosensors based on electrochemical detection, as they can perform in situ analysis with high accuracy and stability. In wastewater technologies, biosensors have been successfully developed for measuring the biological oxygen demand (BOD) (Angelidaki et al., 2011), acetate (Estevez-Canales et al., 2015a), glucose (Kumlanghan et al., 2007), pH (Uria et al., 2016) as well as toxic compounds (Dávila et al., 2011).

Microbial Electrolysis Cells (MECs)

Microbial electrolysis cell (MEC) are devices where electrical power is used to enhance the potential difference between the anode and the cathode, either to enable or increase the rate of the electrode reactions. The energy can be provided by a power source or a potentiostat depending on the selected mode of operation: galvanostatic mode (current flow is fixed) or at potentiostatic mode (the potential difference between two electrodes is fixed). In galvanostatic mode, only two electrodes are needed; however, for poisoning an electrode under a selected potential value potential (working electrode) then a third electrode, so-called reference, is necessary. The other electrode is called counter or auxiliary electrode and its potential is dependent upon the current flow circulating through the system. This configuration allows control of the anodic or cathodic reactions, which is crucial for the study of the microbial-electrode interaction(Rosenbaum et al., 2010; Schröder et al., 2015b). When the anode potential is controlled in a 3-electrode configuration, the organic matter oxidation is being performed at this working electrode. In other cases, the potential is fixed at the cathode to solve the energy requirements and remove contaminants present in waters by reducing reactions such as SO_4 from groundwater, and N from low COD effluents. In addition, simpler systems have been developed to allow scaling-up and implementation in wastewater

treatment plants (Lu and Ren, 2016). The most important applications of MEC configuration are:

The microbial electrochemical fluidized bed reactor (ME-FBR) (Tejedor-Sanz et al., 2017). The ME-FBR has been developed to i) maximize the superficial area of the electrode available for electroactive microorganisms and ii) to improve the kinetics of the catalysis by employing an environment with favourable mixing properties. These systems have been used to treat real wastewater and studies report that the ME-FBR was able to remove up to 95% of the COD in brewery effluent (Tejedor-Sanz et al., 2018).

Microbial electroremediating cells (MERCs). Bioremediation is a relatively efficient and cost-effective technology for treating polluted soils, yet it finds limitations in the bacteria respiration process. MERCs consist of a variety of bioelectrochemical devices that aim to overcome bacterial electron acceptor limitation and maximize metabolic activity to enhance the biodegradation of a pollutant in the environment (Rodrigo Quejigo et al., 2018).

In microbial electrosynthesis cells (MES), the electroactive bacteria use the electrons derived from the cathode to reduce carbon dioxide and other chemicals into a variety of organic compounds. In general, acetogenic bacteria use hydrogen as the electron donor and CO_2 as a carbon source. However, it was found that a cathode could also serve as an electron source for producing organic acids for acetogenic species (Nevin et al., 2011). Methanogens can also accept electrons directly from cathodes (Clauwaert et al., 2008) to produce hydrogen, which can be further converted to methane in an external anaerobic digester. Microbial electrosynthesis is probably the most emerging area in microbial electrochemical research.

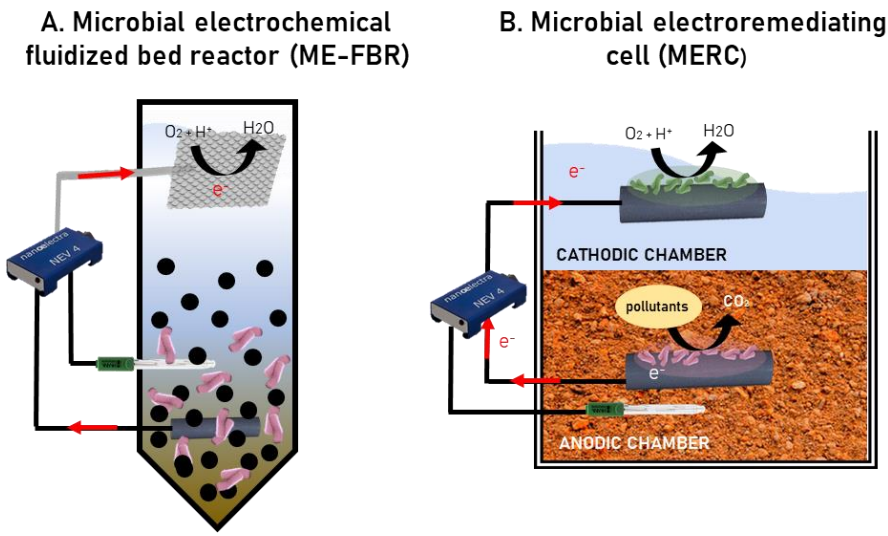

Figure 1.10 A) Schematic of a typical Microbial electrochemichal fluidized bed reactor (ME-FBR). B) Schematic of a Microbial electroremediating cell (MERC).

Microbial Electrochemical Snorkel

If the ultimate goal is no longer to produce current but only to maximize the oxidation of organic matter, the system does not require complex electrochemical reactors with membranes or any other type of separators. The system can be simplified to two connected electrodes, or even a single piece of conductive material, a short-circuited MFC as illustrated in figure 1.10. The result is a basic device that the authors propose calling a microbial electrochemical snorkel (MES) because it works exactly like a snorkel that allows the anode respiring bacteria to transfer to oxygen the electrons produced by their metabolism (Erable et al., 2010). Unlike MFCs, an MES does not divert energy to produce electricity but it ensures maximum efficiency for the oxidation of organic matter.

Technically, the snorkel concept can simply consist of the following (Fig. 1.10): (i) a conductive material acting as an anode, which must be colonized by an EAB, (ii) a conductive material acting as the cathode, that ensures electron removal to the final electron acceptor and allows bacteria snorkeling to oxygen for example. The same scheme can be applied to final electron acceptors, other than oxygen, eg nitrates, nitrites, sulfates, and thiosulfates. The cathodic

reaction can be abiotic, or also benefit from the development of an EAB (biocathode) (Hoareau et al., 2019; Viggi et al., 2015).

The main application of this configuration is the oxidation of organic matter in wastewater treatment (Ramirez 2018). For it, the standard design for constructed wetland has been recently altered by the integration of biocompatible electroconductive materials typically used in METs. The new-born technology can be considered a bioelectrochemical-assisted constructed wetland also named as METland® (Aguirre-Sierra et al., 2016). This technology will be fully described in section 1.3.6.

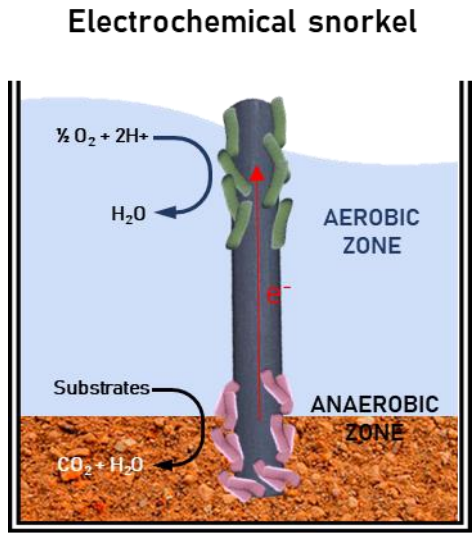

Figure 1.11. Microbial electrochemical snorkel (MES) concept.

1.3.5 Microbial electrochemical pollutants removal

In a bioremediation context, many oxidized and reduced species require removal which opens up opportunities for METs (Fig. 1.11). In the following section, we highlight some of the key studied electricity-driven processes for pollutant removal.

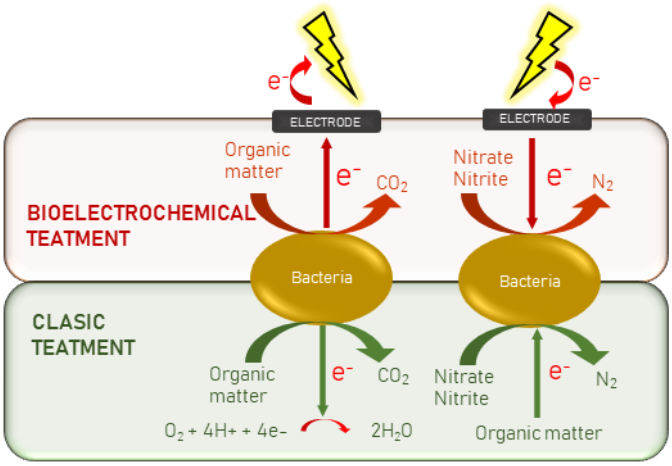

Figure 1.12. Bioelectrochemical nitrogen and organic matter removal process in wastewater.

Microbial electrochemical organic matter removal

Electroactive bacteria can use organic and inorganic simple molecules to obtain energy in anaerobic conditions: acetate, ethanol, glucose, hydrogen gas, etc (Coppi, 2005). If more complex substrates are present in the wastewater, then the electrogenic metabolism needs a partner that breaks these compounds into more simple molecules (Ren et al., 2007). When real wastewaters are treated, the electrochemical performance is importantly decreased compared to using synthetic water with easier biodegradable substrates. This is due to the low degradation rates of complex organic matter and the appearance of competing processes as methanogenesis. The performance of the treatment depends highly on the wastewater composition.

From the very beginning in the METs field, the bioelectrochemical treatment of domestic wastewaters has been the center of attention of researchers (Min and Logan, 2004; Rozendal et al., 2008). The potential advantages derived from using an electrogenic metabolism instead of an aerobic one, which has traditionally been used in urban wastewater treatment plants (WWTPs), have been the main stimulating factor. However, currently, a wide range of wastewaters have been successfully treated by METs: brewery effluents (Dong et al., 2015; Wang et al., 2008; Yu et al., 2015), cheese industry

wastewaters (Kelly and He, 2014), palm oil mill effluents (Baranitharan et al., 2015), wine lees (Cercado-Quezada et al., 2010), yogurt waste (Cercado-Quezada et al., 2010), swine wastewaters, (Lim et al., 2012; Min et al., 2005), rice mill effluents (Behera et al., 2010).

The performance of the treatment depends highly on the wastewater composition. It has been observed that COD can be removed at higher removal rates when organic matter concentration is high, but it results in decreasing coulombic efficiencies. This is due to the stimulation of other microbial processes such as fermentation and methanogenesis (Freguia et al., 2009; Kim et al., 2007).

The materials used for the anodes are commonly carbon-based materials such as carbon and graphite due to their stability when microbial cultures are grown on them and to their relatively low cost. Larger surface areas provide more space for microbial attachment, which results in higher electron transfer and reaction rates per volume of treated wastewater.

Microbial electrochemical nutrients removal

- Nitrogen

The disadvantage of the conventional nitrification/denitrification reaction is that it requires considerable amounts of energy because the wastewater needs to be aerated to supply oxygen for the conversion of ammonium to nitrate. Additionally, electrons in the form of COD must be supplied for denitrification (Arredondo et al., 2015).

Ammonium removal by MFC has focused on two different strategies: MFC ammonium nitrification under aerobic conditions in the cathode (Virdis et al., 2010) or, given that ammonia can be diffused from anode to cathode through the cation exchange membrane; it can be stripped with a suitable gas and subsequently absorbed (Desloover et al., 2012; Puig et al., 2012). Anodic oxidation of ammonium to nitrite has been reported by few authors (He et al., 2009; Zhan et al., 2014; Zhu et al., 2016) in two-chamber MECs. Furthermore, it has been reported Anammox process to be enhanced by previous bioelectrochemical oxidation of ammonia to nitrate (Zhu et al., 2016).

In conventional WWT systems, the organic matter available in the wastewater is typically used as an electron donor during denitrification. In contrast, METs can be a potential alternative for removing nitrate from wastewater with low organic matter content, even from groundwater (Pous et al., 2014; Tong et al., 2013). In METs, the cathode can serve as an electron source for heterotrophic or autotrophic electroactive microorganisms to reduce the nitrate. The electrons provided by a biocathode can either come from acetate oxidation in a bioanode or from the abiotic electrochemical oxidation of other compounds such as water (Pous et al., 2014; Virdis et al., 2010). Given that in a MEC a flow of electrons can be supplied to the electrodes, denitrification could be controlled without adding organic matter and better results could be reached.

Different reactor designs have been tested for performing a complete nitrogen removal treatment. For instance, nitrification can be accomplished in a separate chamber, transforming the ammonium to nitrite or nitrate, while denitrification can be carried out in the cathode, as previously described by Virdis et al. (Virdis et al., 2008). Other studies have investigated the simultaneous aerobic nitrification/bioelectrochemical denitrification in the same chamber (Sayess et al., 2013; Virdis et al., 2010).

1.3.6 Integration of MET technology in constructed wetlands

The requirements of new environmental legislation on municipal and industrial wastewater effluents have driven researchers to find more efficient technologies for wastewater treatment that minimize both the energy demand and the final waste while reusing the by-products generated. In this regard, some research lines are focused on alternative forms of microbial metabolisms (e.g. anammox (Mulder et al., 1995) and microbial electrochemistry (Lovley, 2006) while others try to optimize the already existing configurations. One of the most widespread configurations of METs today for wastewater treatment is CW-MFC and METland® (Fig. 1.12).

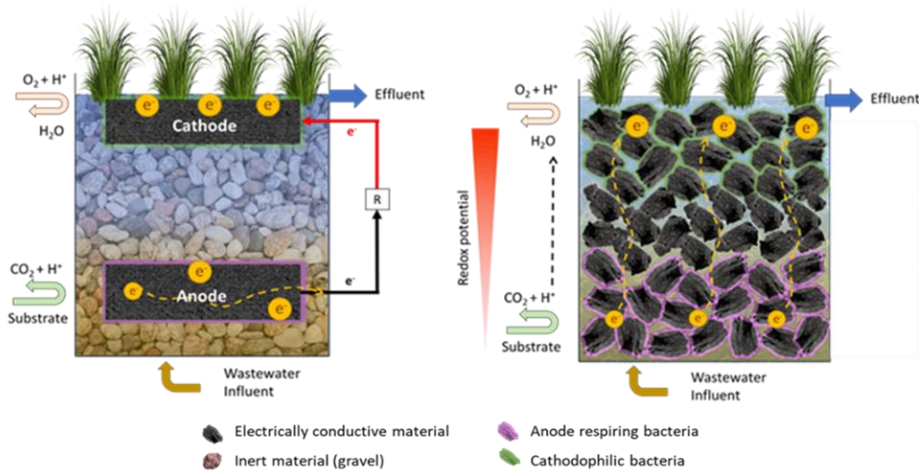

Figure 1.13. The integration of microbial electrochemical technologies (MET) in constructed wetlands (CW): left) microbial fuel cell (MFC) in CW; right) snorkel, a single electrode-based configuration under short circuit with no resistors (METland®).

Constructed Wetlands–Microbial Fuel Cell (CW–MFC)

The presence of redox gradients along a CW depth profile with anaerobic zones at the bottom and anoxic/aerobic zones at the top led to the exploration of the possibility of combining them with MET (Corbella et al., 2014). Similar to a conventional MFC, a CW–MFC includes the installation of an anode located at the bottom in the anaerobic zone and a cathode located at the top in the anoxic/aerobic zone. On the anodic zone, the metabolic activity of electroactive bacteria allows the consumption of organic compounds, releasing electrons that are transferred to the anode. From the anode, the electrons flow along an external circuit to the cathode, where they can be used in the reduction of O2 or NO3. To complete the charge balance, some configurations incorporate an ion separator, others simply allow them to flow in the bulk fluid (Reimers et al., 2001). Likewise, in conventional MET for wastewater treatment with CW–MFC systems it is intended to achieve a treatment performance at least as good as in conventional CW, but with the added value of harvesting energy derived from EAB metabolic activity and their interaction with the electrodes installed in the set-up (Ramírez-Vargas et al., 2018) A typical setup of CW–MFC is presented in figure 1.12.

METland® technology

The so-called METland® is a MET-based application that integrates the use of electro-conductive granular material in constructed wetlands to effectively perform bioremediation in diverse contexts (Wang et al., 2020). Originally, METland® was designed to operate under flooded conditions and short-circuit modes as "snorkel" electrodes (Aguirre-Sierra et al., 2016). The natural redox gradient between the bottom of the system and the naturally oxygenated surface greatly enhanced microbial oxidative metabolism for removing organic pollutants (Aguirre-Sierra et al., 2016; Ramírez-vargas et al., 2019). To explain the inner workings of a METland®, it is necessary to delve into the electron flow along the bed. Full-scale METland® units have been constructed with different electroconductive granular materials like electroconductive coke (Aguirre-Sierra et al., 2016) or more sustainable materials like electroconductive biochar (ec-biochar) obtained after wood pyrolysis at high temperature (Prado et al., 2019). Although most of the MET-based applications are classically operated under anoxic conditions to avoid oxygen competition with anodic reactions, METland® has been recently proved to be effective even under down-flow aerated mode (Aguirre-Sierra et al., 2020). Electroactive bacteria from the genus *Geobacter* have been found to outcompete in such redox mixed environments and, interestingly, such aerobic conditions favoured nitrification so METland® can be operated to remove COD as well as nutrients (Aguirre-Sierra et al., 2020). Indeed, last generation of METland® was operated under hybrid operation combining aerated aerobic downflow with the anoxic flooded mode to clean up 25 m^3/day urban wastewater in less than 0.5 m^2 per person equivalent (www.imetland.eu). METland® is especially effective for removing recalcitrant pollutants like pharmaceuticals present in urban wastewater. As reported by a recent study, seven pharmaceutical compounds (sulfamethoxazole, paraxanthine, carbamazepine, caffeine, ampyrone, atenolol, and naproxen) in emerging contaminants were removed over 95% in a METland® flooded configuration (Pun et al., 2019).

1.3.7 Full-scale MET-based wastewater treatment

During the last 5 years, a number of successful activities have demonstrated that METland® can operate at a number of different conditions. From a constructive point of we can differentiate two kinds of configurations for the technology: constructed METland® and modular METland®, all design and commercialize by METfilter, a spinoff company from Bioe Group.

Constructed METland® follow the classical construction methodology from constructed wetland systems. However, the low cell yield from electroactive bacteria allow to use deeper heights for bed since clogging risk is lower than in gravel-bed systems. Examples of such constructed METland® were implemented in Spain, Denmark, Argentina and Mexico as part of the iMETLAND project funded by EU H2020 program.

Constructed METland® constructed in Spain and Denmark were devoted to treat real urban wastewater generated by ca. 200 people at 80 m^2. Moreover, the systems constructed in American land were treating the wastewater generated in a University Building on Campus. Constructed METLand® have been successfully evaluated regarding sustainability after Life Cycle Analysis (Peñacoba-Antona et al., 2021), outperforming classical systems in performance per footprint (ca. 0.4m2/pe).

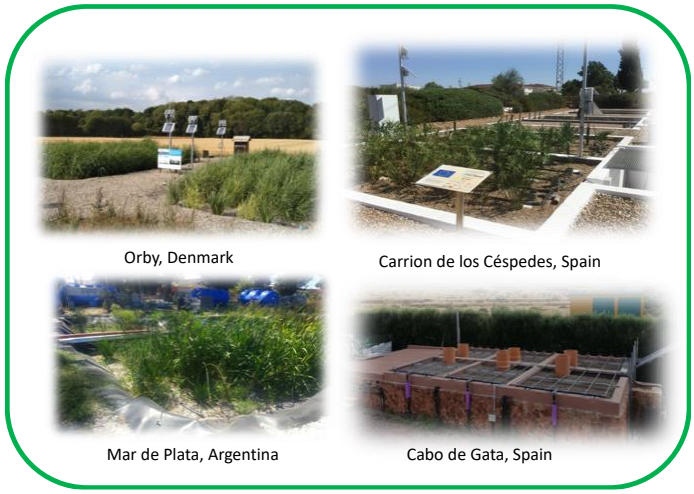

Figure 1.14. Constructed METland® implemented at different internal locations.

In contrast with constructed configurations, modular METland® systems are constructed in polyester tanks and, could be ship-containerized to allow easy transportability overseas or using conventional terrestrial vehicles. In contrast with other classical systems that require civil engineering or legal permits, modular METland® allow a direct implementation where the customer needs it, saving relevant costs in civil construction. Any single unit of modular METland® can treat water generated by cad. 100-200 people in a camping site, hotel, or small communities. These modular systems can operate in the range of 0.1 m2/pe, outperforming standard cw by 20-fold. As the units have been designed to fit inside shipping containers, they can be 3D-grown into larger structures because all ship containers are robust, made-of-steel, and have identical dimensions. Due to the modular design, additional construction is as easy as stacking more units. Thus, we the treatment capacity can be easily based on direct replication of the modular unit.

Table 1.3. Summary of those Research and Innovation actions leading to METland® solution from TRL1 to TRL9.

	History	Technological features
TRL 1-3 (2010-2015)	Funded by national program. **Proof of concept** tested with real urban ww at lab scale or small out-door assays	2m^3/day (12-15 people) Anaerobic operation showing limitations for nutrient removal. Bed made of graphite
TRL 4-6 (2016-2018)	**Pilot scale** funded by **H2020** (www.imetland.eu). Tested in Spain and Denmark with real urban wastewater.	H2020 validation: 20 m^3/day (200 people) MVP validations 20 m^3/day (200 people) Aerobic/anaerobic operation showing efficient nutrient removal. Bed made of a mixed of ec-coke & ec-biochar.
TRL 8-9 (2016-2021)	**Full scale** **MVP** qualified as successful technology after testing in real environment by a prestigious Public Water Company	Customer validation: 25 m^3/day (200 people) 100 m^3/day (100 people)

Figure 1.14. Reconstruction of the implementation of a full-scale METland® in a green city

1.4 References

Aguirre-Sierra, A., Bacchetti-De Gregoris, T., Berná, A., Salas, J.J., Aragón, C., Esteve-Núñez, A., 2016. Microbial electrochemical systems outperform fixed-bed biofilters in cleaning up urban wastewater. Environ. Sci. Water Res. Technol. 2, 984–993. https://doi.org/10.1039/C6EW00172F

Aguirre-Sierra, A., Bacchetti-De Gregoris, T., Salas, J.J., De Deus, A., Esteve-Núñez, A., 2020. A new concept in constructed wetlands: Assessment of aerobic electroconductive biofilters. Environ. Sci. Water Res. Technol. 6, 1312–1323. https://doi.org/10.1039/c9ew00696f

Aklujkar, M., Coppi, M. V, Leang, C., Kim, B.C., Chavan, M.A., Perpetua, L.A., Giloteaux, L., Liu, A., Holmes, D.E., 2013. Proteins involved in electron transfer to Fe (III) and Mn (IV) oxides by Geobacter sulfurreducens and Geobacter uraniireducens. Microbiology 159, 515–535.

Aklujkar, M., Krushkal, J., DiBartolo, G., Lapidus, A., Land, M.L., Lovley, D.R., 2009. The genome sequence of Geobacter metallireducens: features of metabolism, physiology and regulation common and dissimilar to Geobacter sulfurreducens. BMC Microbiol. 9, 1–22.

Allen, J.W.A., Sawyer, E.B., Ginger, M.L., Barker, P.D., Ferguson, S.J., 2009. Variant *c* -type cytochromes as probes of the substrate specificity of the *E. coli* cytochrome *c* maturation (Ccm) apparatus. Biochem. J. 419, 177–186. https://doi.org/10.1042/BJ20081999

Allen, R.M., Bennetto, H.P., 1993. Microbial fuel-cells. Appl. Biochem. Biotechnol. 39, 27–40.

Angelidaki, I., Karakashev, D., Batstone, D.J., Plugge, C.M., Stams, A.J.M., 2011. Biomethanation and its potential. Methods Enzymol. 494, 327–351.

Arredondo, M.R., Kuntke, P., Jeremiasse, A.W., Sleutels, T., Buisman, C.J.N., Ter Heijne, A., 2015. Bioelectrochemical systems for nitrogen removal and recovery from wastewater. Environ. Sci. Water Res. Technol. 1, 22–33.

Assembly, G., 2017. Resolution adopted by the General Assembly on 6 July 2017. A/RES/71/313.

Aulenta, F., Fazi, S., Majone, M., Rossetti, S., 2014. Electrically conductive magnetite particles enhance the kinetics and steer the composition of anaerobic TCE-dechlorinating cultures. Process Biochem. 49, 2235–2240.

Aulenta, F., Tucci, M., Cruz Viggi, C., Dolfing, J., Head, I.M., Rotaru, A., 2021. An underappreciated DIET for anaerobic petroleum hydrocarbon-degrading microbial communities. Microb. Biotechnol. 14, 2–7.

Babauta, J., Renslow, R., Lewandowski, Z., Beyenal, H., 2012. Electrochemically active biofilms: facts and fiction. A review. Biofouling 28, 789–812.

Baranitharan, E., Khan, M.R., Prasad, D.M.R., Teo, W.F.A., Tan, G.Y.A., Jose, R., 2015. Effect of biofilm formation on the performance of microbial fuel cell for the treatment of palm oil mill effluent. Bioprocess Biosyst. Eng. 38, 15–24.

Bard, A.J., Faulkner, L.R., Swain, E., Robey, C., n.d. Fundamentals and Applications.

Barrimi, M., Aalouane, R., Aarab, C., Hafidi, H., Baybay, H., Soughi, M., Tachfouti, N.,

Nejjari, C., Mernissi, F.Z., Rammouz, I., McKenzie, R.B., 2013. Guía sobre tratamientos de aguas residuales urbanas para pequeños núcleos de población, Encephale.

Behera, M., Jana, P.S., More, T.T., Ghangrekar, M.M., 2010. Rice mill wastewater treatment in microbial fuel cells fabricated using proton exchange membrane and earthen pot at different pH. Bioelectrochemistry 79, 228–233.

Biofilms, M., 2012. A Basic Tutorial on Cyclic Voltammetry for the Investigation of Electroactive 466–475. https://doi.org/10.1002/asia.201100740

Bond, D.R., Lovley, D.R., 2003. Electricity Production by. Microbiology 69, 1548–1555. https://doi.org/10.1128/AEM.69.3.1548

Boretti, A., Rosa, L., 2019. Reassessing the projections of the World Water Development Report. npj Clean Water 2, 15. https://doi.org/10.1038/s41545-019-0039-9

Bruno, L.B., Jothinathan, D., Rajkumar, M., 2018. Microbial fuel cells: fundamentals, types, significance and limitations, in: Microbial Fuel Cell Technology for Bioelectricity. Springer, pp. 23–48.

Brutinel, E.D., Gralnick, J.A., 2012. Shuttling happens: soluble flavin mediators of extracellular electron transfer in Shewanella. Appl. Microbiol. Biotechnol. 93, 41–48.

Bücking, C., Schicklberger, M., Gescher, J., 2013. The Biochemistry of Dissimilatory Ferric Iron and Manganese Reduction in Shewanella oneidensis, in: Microbial Metal Respiration: From Geochemistry to Potential Applications. pp. 49–82. https://doi.org/10.1007/978-3-642-32867-1

Busalmen, J.P., Esteve-Núñez, A., 2017. C - Type Cytochromes Wire Electricity - Producing Bacteria to Electrodes C-Type Cytochromes Wire Electricity-Producing Bacteria to Electrodes ** 4952–4955. https://doi.org/10.1002/ange.200801310

Butler, J.E., Young, N.D., Lovley, D.R., 2010. Evolution of electron transfer out of the cell: comparative genomics of six Geobacter genomes. BMC Genomics 11, 1–12.

Canfield, D.E., 1989. Reactive iron in marine sediments. Geochim. Cosmochim. Acta 53, 619–632.

Cercado-Quezada, B., Delia, M.-L., Bergel, A., 2010. Testing various food-industry wastes for electricity production in microbial fuel cell. Bioresour. Technol. 101, 2748–2754.

Chen, S., Rotaru, A.E., Shrestha, P.M., Malvankar, N.S., Liu, F., Fan, W., Nevin, K.P., Lovley, D.R., 2014. Promoting interspecies electron transfer with biochar. Sci. Rep. 4. https://doi.org/10.1038/srep05019

Clauwaert, P., Aelterman, P., De Schamphelaire, L., Carballa, M., Rabaey, K., Verstraete, W., 2008. Minimizing losses in bio-electrochemical systems: the road to applications. Appl. Microbiol. Biotechnol. 79, 901–913.

Clauwaert, P., Rabaey, K., Aelterman, P., De Schamphelaire, L., Pham, T.H., Boeckx, P., Boon, N., Verstraete, W., 2007. Biological denitrification in microbial fuel cells. Environ. Sci. Technol. 41, 3354–3360.

Coppi, M. V, 2005. The hydrogenases of Geobacter sulfurreducens: a comparative genomic perspective. Microbiology 151, 1239–1254.

Corbella, C., Garfí, M., Puigagut, J., 2014. Science of the Total Environment Vertical redox

pro fi les in treatment wetlands as function of hydraulic regime and macrophytes presence : Surveying the optimal scenario for microbial fuel cell implementation. Sci. Total Environ. 470–471, 754–758. https://doi.org/10.1016/j.scitotenv.2013.09.068

Corcoran, E., 2010. Sick water?: the central role of wastewater management in sustainable development: a rapid response assessment. UNEP/Earthprint.

Dávila, D., Esquivel, J.P., Sabate, N., Mas, J., 2011. Silicon-based microfabricated microbial fuel cell toxicity sensor. Biosens. Bioelectron. 26, 2426–2430.

Desloover, J., Vlaeminck, S.E., Clauwaert, P., Verstraete, W., Boon, N., 2012. Strategies to mitigate N2O emissions from biological nitrogen removal systems. Curr. Opin. Biotechnol. 23, 474–482.

Díaz, S., Estevan, M.G., González, A.M., 2014. Aprendiendo metabolismo microbiano en una EDAR (Estación Depuradora de Aguas Residuales). Reduca 7, 15–32.

DiFrancesco, K., Gartner, T., Ozment, S., Association, I.W., 2015. Natural infrastructure in the nexus. IUCN.

Domínguez-Garay, A., Quejigo, J.R., Dörfler, U., Schroll, R., Esteve-Núñez, A., 2018. Bioelectroventing: an electrochemical-assisted bioremediation strategy for cleaning-up atrazine-polluted soils. Microb. Biotechnol. 11, 50–62. https://doi.org/10.1111/1751-7915.12687

Dong, Y., Qu, Y., He, W., Du, Y., Liu, J., Han, X., Feng, Y., 2015. A 90-liter stackable baffled microbial fuel cell for brewery wastewater treatment based on energy self-sufficient mode. Bioresour. Technol. 195, 66–72.

Dotro, G., Langergraber, G., Molle, P., Nivala, J., Puigagut, J., Stein, O., Von Sperling, M., 2017a. Treatment wetlands. IWA publishing.

Dotro, G., Molle, P., Nivala, J., Puigagut, J., Stein, O., 2017b. Treatment Wetlands. First. ed. IWA Publishing, London.

Eggermont, H., Balian, E., Azevedo, J.M.N., Beumer, V., Brodin, T., Claudet, J., Fady, B., Grube, M., Keune, H., Lamarque, P., Reuter, K., Smith, M., Van Ham, C., Weisser, W.W., Le Roux, X., 2015. Nature-based solutions: New influence for environmental management and research in Europe. Gaia 24, 243–248. https://doi.org/10.14512/gaia.24.4.9

Erable, B., Duţeanua, N.M., Ghangrekar, M.M., Dumas, C., Scott, K., 2010. Application of electro-active biofilms. Biofouling 26, 57–71. https://doi.org/10.1080/08927010903161281

Estevez-Canales, M., Berná, A., Borjas, Z., Esteve-Núñez, A., 2015a. Screen-printed electrodes: new tools for developing microbial electrochemistry at microscale level. Energies 8, 13211–13221.

Estevez-Canales, M., Kuzume, A., Borjas, Z., Füeg, M., Lovley, D., Wandlowski, T., Esteve-Núñez, A., 2015b. A severe reduction in the cytochrome C content of Geobacter sulfurreducens eliminates its capacity for extracellular electron transfer. Environ. Microbiol. Rep. 7, n/a-n/a. https://doi.org/10.1111/1758-2229.12230

Faivre, N., Fritz, M., Freitas, T., de Boissezon, B., Vandewoestijne, S., 2017. Nature-Based Solutions in the EU: Innovating with nature to address social, economic and environmental challenges. Environ. Res. 159, 509–518. https://doi.org/10.1016/j.envres.2017.08.032

Franks, A.E., Nevin, K.P., 2010. Microbial fuel cells, a current review. Energies 3, 899–919.

Freguia, S., Masuda, M., Tsujimura, S., Kano, K., 2009. Lactococcus lactis catalyses electricity generation at microbial fuel cell anodes via excretion of a soluble quinone. Bioelectrochemistry 76, 14–18.

Gain, A.K., Giupponi, C., Wada, Y., 2016. Measuring global water security towards sustainable development goals. Environ. Res. Lett. 11, 124015.

Gorby, Y.A., Yanina, S., McLean, J.S., Rosso, K.M., Moyles, D., Dohnalkova, A., Beveridge, T.J., Chang, I.S., Kim, B.H., Kim, K.S., 2006. Electrically conductive bacterial nanowires produced by Shewanella oneidensis strain MR-1 and other microorganisms. Proc. Natl. Acad. Sci. 103, 11358–11363.

Gregory, K.B., Bond, D.R., Lovley, D.R., 2004. Graphite electrodes as electron donors for anaerobic respiration. Environ. Microbiol. 6, 596–604.

Gregory, K.B., Lovley, D.R., 2005. Remediation and recovery of uranium from contaminated subsurface environments with electrodes. Environ. Sci. Technol. 39, 8943–8947.

Harnisch, F., Holtmann, D., 2019. Bioelectrosynthesis. Springer. https://doi.org/https://doi.org/10.1007/978-3-030-03299-9

He, Z., Kan, J., Wang, Y., Huang, Y., Mansfeld, F., Nealson, K.H., 2009. Electricity production coupled to ammonium in a microbial fuel cell. Environ. Sci. Technol. 43, 3391–3397.

Hoareau, M., Erable, B., Bergel, A., 2019. Microbial electrochemical snorkels (MESs): A budding technology for multiple applications. A mini review. Electrochem. commun. 104, 106473. https://doi.org/10.1016/j.elecom.2019.05.022

Holmes, D.E., Chaudhuri, S.K., Nevin, K.P., Mehta, T., Methé, B.A., Liu, A., Ward, J.E., Woodard, T.L., Webster, J., Lovley, D.R., 2006. Microarray and genetic analysis of electron transfer to electrodes in Geobacter sulfurreducens. Environ. Microbiol. 8, 1805–1815.

Kadlec, R., Wallace, S., 2009. Ttreatment wetlands, in: Vasa. p. 1048.

Kappler, A., Straub, K.L., 2005. Geomicrobiological cycling of iron. Rev. Mineral. Geochemistry 59, 85–108.

Kato, S., 2015. Biotechnological Aspects of Microbial Extracellular Electron Transfer. Microbes Environ. 30, 133–139. https://doi.org/10.1264/jsme2.ME15028

Kato, S., Hashimoto, K., Watanabe, K., 2012. Microbial interspecies electron transfer via electric currents through conductive minerals. Proc. Natl. Acad. Sci. 109, 10042–10046. https://doi.org/10.1073/pnas.1117592109

Kato, S., Igarashi, K., 2019. Enhancement of methanogenesis by electric syntrophy with biogenic iron-sulfide minerals. Microbiologyopen 8, e00647.

Kato, S., Wada, K., Kitagawa, W., Mayumi, D., Ikarashi, M., Sone, T., Asano, K., Kamagata, Y., 2019. Conductive iron oxides promote methanogenic acetate degradation by microbial communities in a high-temperature petroleum reservoir. Microbes Environ. ME18140.

Kelly, P.T., He, Z., 2014. Nutrients removal and recovery in bioelectrochemical systems:

a review. Bioresour. Technol. 153, 351–360.

Kim, J.R., Jung, S.H., Regan, J.M., Logan, B.E., 2007. Electricity generation and microbial community analysis of alcohol powered microbial fuel cells. Bioresour. Technol. 98, 2568–2577. https://doi.org/10.1016/j.biortech.2006.09.036

Klingebiel, S., Hildebrand, M., 2010. UNDP–United Nations Development Programme, in: A Concise Encyclopedia of the United Nations. Brill Nijhoff, pp. 706–711.

Koottatep, T., Polprasert, C., 1997. Role of plant uptake on nitrogen removal in constructed wetlands located in the tropics. Water Sci. Technol. 36, 1 LP – 8.

Korneel, R., Nico, B., D., S.S., Marc, V., Willy, V., 2004. Biofuel Cells Select for Microbial Consortia That Self-Mediate Electron Transfer. Appl. Environ. Microbiol. 70, 5373–5382. https://doi.org/10.1128/AEM.70.9.5373-5382.2004

Kumlanghan, A., Liu, J., Thavarungkul, P., Kanatharana, P., Mattiasson, B., 2007. Microbial fuel cell-based biosensor for fast analysis of biodegradable organic matter. Biosens. Bioelectron. 22, 2939–2944.

Lim, S.J., Park, W., Kim, T.-H., Shin, I.H., 2012. Swine wastewater treatment using a unique sequence of ion exchange membranes and bioelectrochemical system. Bioresour. Technol. 118, 163–169.

Lin, W.C., Coppi, M. V, Lovley, D.R., 2004. Geobacter sulfurreducens Can Grow with Oxygen as a Terminal Electron Acceptor. Appl. Environ. Microbiol. 70, 2525–2528.

Liu, F., Rotaru, A.-E., Shrestha, P.M., Malvankar, N.S., Nevin, K.P., Lovley, D.R., 2012. Promoting direct interspecies electron transfer with activated carbon. Energy Environ. Sci. 5, 8982. https://doi.org/10.1039/c2ee22459c

Logan, B.E., Regan, J.M., 2006. Electricity-producing bacterial communities in microbial fuel cells. TRENDS Microbiol. 14, 512–518.

Lovley, D.R., 2012. Electromicrobiology. Annu. Rev. Microbiol. 66, 391–409. https://doi.org/10.1146/annurev-micro-092611-150104

Lovley, D.R., 2008. Extracellular electron transfer: Wires, capacitors, iron lungs, and more. Geobiology 6, 225–231. https://doi.org/10.1111/j.1472-4669.2008.00148.x

Lovley, D.R., 2006. Bug juice: harvesting electricity with microorganisms. Nat. Rev. Microbiol. 4, 497–508. https://doi.org/10.1038/nrmicro1442

Lovley, D.R., Chapelle, F.H., 1995. Deep subsurface microbial processes. Rev. Geophys. 33, 365–381.

Lovley, D.R., Coates, J.D., Blunt-Harris, E.L., Phillips, E.J.P., Woodward, J.C., 1996. Humic substances as electron acceptors for microbial respiration. Nature. https://doi.org/10.1038/382445a0

Lovley, D.R., Fraga, J.L., Coates, J.D., Blunt-Harris, E.L., 1999. Humics as an electron donor for anaerobic respiration. Environ. Microbiol. 1, 89–98.

Lovley, D.R., Holmes, D.E., Nevin, K.P., 2004. Dissimilatory fe (iii) and mn (iv) reduction. Adv. Microb. Physiol. 49, 219–286.

Lovley, D.R., Phillips, E.J.P., 1988. Novel mode of microbial energy metabolism: organic carbon oxidation coupled to dissimilatory reduction of iron or manganese. Appl. Environ. Microbiol. 54, 1472.

Lovley, D.R., Ueki, T., Zhang, T., Malvankar, N.S., Shrestha, P.M., Flanagan, K.A., Aklujkar, M., Butler, J.E., Giloteaux, L., Rotaru, A.-E., Holmes, D.E., Franks, A.E., Orellana, R., Risso, C., Nevin, K.P., 2011. Geobacter: The Microbe Electric's Physiology, Ecology, and Practical Applications, 1st ed, Advances in Microbial Physiology. Elsevier Ltd. https://doi.org/10.1016/B978-0-12-387661-4.00004-5

Lovley, D R, Fraga, J L, Blunt-Harris, E L, Hayes, L A, Phillips, E J P, Coates, J D, Lovley, Derek R, Fraga, Jocelyn L, Blunt-Harris, Elizabeth L, Hayes, Lory A, Phillips, Elizabeth J P, Coates, John D, 1998. Humic Substances as a Mediator for Microbially Catalyzed Metal Reduction Huminstoffe als Vermittler bei der mikrobiell katalysierten Metallreduktion. Acta Hydrochim. hydrobiol 26.

Lu, L., Ren, Z.J., 2016. Microbial electrolysis cells for waste biorefinery: A state of the art review. Bioresour. Technol. 215, 254–264.

Luo, H., Xu, P., Roane, T.M., Jenkins, P.E., Ren, Z., 2012. Microbial desalination cells for improved performance in wastewater treatment, electricity production, and desalination. Bioresour. Technol. 105, 60–66.

Marsili, E., Baron, D.B., Shikhare, I.D., Coursolle, D., Gralnick, J.A., Bond, D.R., 2008. Shewanella secretes flavins that mediate extracellular electron transfer. Proc. Natl. Acad. Sci. 105, 3968–3973.

Matthews, R.B., Van Noordwijk, M., 2014. From euphoria to reality on efforts to reduce emissions from deforestation and forest degradation (REDD+). Mitig. Adapt. Strateg. Glob. Chang. 19, 615–620.

Mehta, T., Coppi, M. V, Childers, S.E., Lovley, D.R., 2005. Outer membrane c-type cytochromes required for Fe (III) and Mn (IV) oxide reduction in Geobacter sulfurreducens. Appl. Environ. Microbiol. 71, 8634.

Millennium Ecosystem Assessment, 2005. Ecosystems and human well-being: Biodiversity synthesis. Washington, D. C.: World Resources Institute (WRI).

Min, B., Kim, J., Oh, S., Regan, J.M., Logan, B.E., 2005. Electricity generation from swine wastewater using microbial fuel cells. Water Res. 39, 4961–8. https://doi.org/10.1016/j.watres.2005.09.039

Min, B., Logan, B.E., 2004. Continuous electricity generation from domestic wastewater and organic substrates in a flat plate microbial fuel cell. Environ. Sci. Technol. 38, 5809–5814.

Mittermeier, R.A., Totten, M., Ledwith Pennypacker, L., Boltz, F., Prickett, G., Mittermeier, C.G., Rodriguez, C.M., Brooks, T., Hannah, L., Vitale, B., 2008. A climate for life: Meeting the global challenge.

Morel, A., Zuo, K., Xia, X., Wei, J., Luo, X., Liang, P., Huang, X., 2012. Microbial desalination cells packed with ion-exchange resin to enhance water desalination rate. Bioresour. Technol. 118, 43–48.

Morgado, L., Saraiva, I.H., Louro, R.O., Salgueiro, C.A., 2010. Orientation of the axial ligands and magnetic properties of the hemes in the triheme ferricytochrome PpcA from G. sulfurreducens determined by paramagnetic NMR. FEBS Lett. 584, 3442–3445.

Morse, J.W., Cornwell, J.C., 1987. Analysis and distribution of iron sulfide minerals in recent anoxic marine sediments. Mar. Chem. 22, 55–69.

Mulder, A., Van de Graaf, A.A., Robertson, L.A., Kuenen, J.G., 1995. Anaerobic ammonium oxidation discovered in a denitrifying fluidized bed reactor. FEMS Microbiol. Ecol. 16, 177–183.

Myers, C.R., Myers, J.M., 1992. Localization of cytochromes to the outer membrane of anaerobically grown Shewanella putrefaciens. MR-1. J. Bacteriol. 174, 3429–3438.

Nevin, K., Izbicki, J., Snoeyenbos-West, O., Lovley, D., 2014. Shifting microbial respiration patterns in soils and sediments with benthic snorkels, in: ISME 2014 - The Power of the Small. International Symposium on Microbial Ecology. Copenhaguen, p. 25.

Nevin, K., Richter, H., Covalla, S.F., Johnson, J.P., Woodard, T.L., Orloff, A.L., Jia, H., Zhang, M., Lovley, D.R., 2008. Power output and columbic efficiencies from biofilms of Geobacter sulfurreducens comparable to mixed community microbial fuel cells. Environ. Microbiol. 10, 2505–2514. https://doi.org/10.1111/j.1462-2920.2008.01675.x

Nevin, K.P., Hensley, S.A., Franks, A.E., Summers, Z.M., Ou, J., Woodard, T.L., Snoeyenbos-West, O.L., Lovley, D.R., 2011. Electrosynthesis of organic compounds from carbon dioxide is catalyzed by a diversity of acetogenic microorganisms. Appl. Environ. Microbiol. 77, 2882.

Nevin, K.P., Lovley, D.R., 2002. Mechanisms for Fe (III) oxide reduction in sedimentary environments. Geomicrobiol. J. 19, 141–159.

Newman, D.K., Kolter, R., 2000. A role for excreted quinones in extracellular electron transfer. Nature 405, 94–97.

Ortega, E., Ferrer, Y., Sala, J.., Aragón, C., Real, Á., 2010. Manual para la implantación de sistemas de depuración en pequeñas poblaciones.

Osojnik, I.G., n.d. REGIONAL ASSESSMENT REPORT ON BIODIVERSITY AND ECOSYSTEM SERVICES FOR EUROPE AND CENTRAL ASIA.

Pachauri, R.K., Reisinger, A., 2008. Climate change 2007. Synthesis report. Contribution of Working Groups I, II and III to the fourth assessment report.

Park, D.H., Zeikus, J.G., 2000. Electricity generation in microbial fuel cells using neutral red as an electronophore. Appl. Environ. Microbiol. 66, 1292.

Peñacoba-Antona, L., Gómez-Delgado, M., Esteve-Núñez, A., 2021. Multi-criteria evaluation and sensitivity analysis for the optimal location of constructed wetlands (METland) at oceanic and Mediterranean locations. Int. J. Environ. Res. Public Health.

Pham, T.H., Boon, N., Aelterman, P., Clauwaert, P., De Schamphelaire, L., Vanhaecke, L., De Maeyer, K., Höfte, M., Verstraete, W., Rabaey, K., 2008. Metabolites produced by Pseudomonas sp. enable a Gram-positive bacterium to achieve extracellular electron transfer. Appl. Microbiol. Biotechnol. 77, 1119–1129. https://doi.org/10.1007/s00253-007-1248-6

Potter, M.., 1911. Electrical effects accompanying the decomposition of organic compounds. Proc. R. Soc. Lond. B 84, 260–276. https://doi.org/10.1098/rspb.1911.0073

Pous, N., Koch, C., Colprim, J., Puig, S., Harnisch, F., 2014. Extracellular electron transfer of biocathodes: Revealing the potentials for nitrate and nitrite reduction of denitrifying microbiomes dominated by Thiobacillus sp. Electrochem. commun. 49,

93–97.

Prado, A., Berenguer, R., Esteve-Núñez, A., 2019. Electroactive biochar outperforms highly conductive carbon materials for biodegrading pollutants by enhancing microbial extracellular electron transfer. Carbon N. Y. 146. https://doi.org/10.1016/j.carbon.2019.02.038

Puig, S., Coma, M., Desloover, J., Boon, N., Colprim, J., Balaguer, M.D., 2012. Autotrophic denitrification in microbial fuel cells treating low ionic strength waters. Environ. Sci. Technol. 46, 2309–2315.

Pun, Á., Boltes, K., Letón, P., Esteve-nuñez, A., 2019. Bioresource Technology Reports Detoxification of wastewater containing pharmaceuticals using horizontal flow bioelectrochemical filter. Bioresour. Technol. Reports 7, 100296. https://doi.org/10.1016/j.biteb.2019.100296

Ramirez-Moreno, M., Esteve-Núñez, A., Ortiz, J.M., 2021. Desalination of Brackish Water Using a Microbial Desalination Cell: analysis of the electrochemical behaviour. Electrochim. Acta 138570.

Ramírez-Moreno, M., Rodenas, P., Aliaguilla, M., Bosch-Jimenez, P., Borràs, E., Zamora, P., Monsalvo, V., Rogalla, F., Ortiz, J.M., Esteve-Núñez, A., 2019. Comparative performance of Microbial Desalination Cells using air diffusion and liquid cathode reactions: study of the salt removal and desalination efficiency. Front. Energy Res. 7, 135.

Ramírez-vargas, C.A., Arias, C.A., Carvalho, P., Zhang, L., Esteve-núñez, A., Brix, H., 2019. Science of the Total Environment Electroactive bio fi lm-based constructed wetland (EABB-CW): A mesocosm-scale test of an innovative setup for wastewater treatment. Sci. Total Environ. 659, 796–806. https://doi.org/10.1016/j.scitotenv.2018.12.432

Ramírez-Vargas, C.A., Prado, A., Arias, C.A., Carvalho, P.N., Esteve-Núñez, A., Brix, H., 2018. Microbial electrochemical technologies for wastewater treatment: Principles and evolution from microbial fuel cells to bioelectrochemical-based constructed wetlands. Water (Switzerland) 10. https://doi.org/10.3390/w10091128

Reguera, G., McCarthy, K.D., Mehta, T., Nicoll, J.S., Tuominen, M.T., Lovley, D.R., 2005. Extracellular electron transfer via microbial nanowires. Nature 435, 1098–1101.

Reimers, C.E., Tender, L.M., Fertig, S., Wang, W., 2001. Harvesting energy from the marine sediment– water interface. Environ. Sci. Technol. 35, 192–195.

Ren, Y.-X., Nakano, K., Nomura, M., Chiba, N., Nishimura, O., 2007. Effects of bacterial activity on estrogen removal in nitrifying activated sludge. Water Res. 41, 3089–3096.

Rodrigo Quejigo, J., Domínguez-Garay, A., Dörfler, U., Schroll, R., Esteve-Núñez, A., 2018. Anodic shifting of the microbial community profile to enhance oxidative metabolism in soil. Soil Biol. Biochem. 116, 131–138. https://doi.org/10.1016/j.soilbio.2017.09.012

Rosa Huertas, Marcos, C., Ibarguren, N., Ordás, S., 2012. GUÍA PRÁCTICA para la depuración de aguas residuales en pequeñas poblaciones.

Rosenbaum, M., Agler, M.T., Fornero, J.J., Venkataraman, A., Angenent, L.T., 2010. Integrating BES in the wastewater and sludge treatment line, in: Bioelectrochemical Systems: From Extracellular Electron Transfer to

Biotechnological Application. pp. 393–408.

Rotaru, A.-E., Calabrese, F., Stryhanyuk, H., Musat, F., Shrestha, P.M., Weber, H.S., Snoeyenbos-West, O.L.O., Hall, P.O.J., Richnow, H.H., Musat, N., 2018. Conductive particles enable syntrophic acetate oxidation between Geobacter and Methanosarcina from coastal sediments. MBio 9.

Rotaru, A.-E., Posth, N.R., Loscher, C.R., Miracle, M.R., Vicente, E., Cox, R.P., Thompson, J., Poulton, S.W., Thamdrup, B., 2019. Interspecies interactions mediated by conductive minerals in the sediments of the Iron rich Meromictic Lake La Cruz, Spain. Limnetica 38, 21–40.

Rotaru, A.E., Yee, M.O., Musat, F., 2021. Microbes trading electricity in consortia of environmental and biotechnological significance. Curr. Opin. Biotechnol. 67, 119–129. https://doi.org/10.1016/j.copbio.2021.01.014

Rozendal, R.A., Hamelers, H.V.M., Rabaey, K., Keller, J., Buisman, C.J.N., 2008. Towards practical implementation of bioelectrochemical wastewater treatment. Trends Biotechnol. 26, 450–459.

Sayess, R.R., Saikaly, P.E., El-Fadel, M., Li, D., Semerjian, L., 2013. Reactor performance in terms of COD and nitrogen removal and bacterial community structure of a three-stage rotating bioelectrochemical contactor. Water Res. 47, 881–894.

Schröder, U., Harnisch, F., Angenent, L.T., 2015a. Microbial electrochemistry and technology: terminology and classification. Energy Environ. Sci. 8, 513–519. https://doi.org/10.1039/C4EE03359K

Schröder, U., Harnisch, F., Angenent, L.T., 2015b. Microbial electrochemistry and technology: Terminology and classification. Energy Environ. Sci. 8, 513–519. https://doi.org/10.1039/c4ee03359k

Shrestha, J., Rich, J.J., Ehrenfeld, J.G., Jaffe, P.R., 2009. Oxidation of ammonium to nitrite under iron-reducing conditions in wetland soils: Laboratory, field demonstrations, and push-pull rate determination. Soil Sci. 174, 156–164. https://doi.org/10.1097/SS.0b013e3181988fbf

Shrestha, P.M., Rotaru, A.-E., 2014. Plugging in or going wireless: strategies for interspecies electron transfer . Front. Microbiol. .

Straub, K.L., Schink, B., 2003. Evaluation of electron-shuttling compounds in microbial ferric iron reduction. FEMS Microbiol. Lett. 220, 229–233.

Summers, Z.M., Fogarty, H.E., Leang, C., Franks, A.E., Malvankar, N.S., Lovley, D.R., 2010. Direct exchange of electrons within aggregates of an evolved syntrophic coculture of anaerobic bacteria. Science (80-.). 330, 1413–1415.

Tejedor-Sanz, S., Fernández-Labrador, P., Hart, S., Torres, C.I., Esteve-Núñez, A., 2018. Geobacter Dominates the Inner Layers of a Stratified Biofilm on a Fluidized Anode During Brewery Wastewater Treatment . Front. Microbiol. .

Tejedor-Sanz, S., Quejigo, J.R., Berná, A., Esteve-Núñez, A., 2017. The Planktonic Relationship Between Fluid-Like Electrodes and Bacteria: Wiring in Motion. ChemSusChem 10, 693–700. https://doi.org/10.1002/cssc.201601329

Thrash, J.C., Van Trump, J.I., Weber, K.A., Miller, E., Achenbach, L.A., Coates, J.D., 2007. Electrochemical stimulation of microbial perchlorate reduction. Environ. Sci. Technol. 41, 1740–1746.

Tong, S., Zhang, B., Feng, C., Zhao, Y., Chen, N., Hao, C., Pu, J., Zhao, L., 2013. Characteristics of heterotrophic/biofilm-electrode autotrophic denitrification for nitrate removal from groundwater. Bioresour. Technol. 148, 121–127.

Torres, C.I., Kato Marcus, A., Rittmann, B.E., 2008. Proton transport inside the biofilm limits electrical current generation by anode-respiring bacteria. Biotechnol. Bioeng. 100, 872–881.

Truu, M., Juhanson, J., Truu, J., 2009. Microbial biomass, activity and community composition in constructed wetlands. Sci. Total Environ. 407, 3958–3971. https://doi.org/10.1016/j.scitotenv.2008.11.036

Uria, N., Abramova, N., Bratov, A., Muñoz-Pascual, F.-X., Baldrich, E., 2016. Miniaturized metal oxide pH sensors for bacteria detection. Talanta 147, 364–369.

Viggi, C.C., Presta, E., Bellagamba, M., Kaciulis, S., Balijepalli, S.K., Zanaroli, G., Papini, M.P., Rossetti, S., Aulenta, F., 2015. The "Oil-Spill Snorkel": An innovative bioelectrochemical approach to accelerate hydrocarbons biodegradation in marine sediments. Front. Microbiol. 6, 1–11. https://doi.org/10.3389/fmicb.2015.00881

Villaseñor, J., Capilla, P., Rodrigo, M.A., Cañizares, P., Fernández, F.J., 2013. Operation of a horizontal subsurface flow constructed wetland - Microbial fuel cell treating wastewater under different organic loading rates. Water Res. 47, 6731–6738. https://doi.org/10.1016/j.watres.2013.09.005

Virdis, B., Rabaey, K., Rozendal, R.A., Yuan, Z., Keller, J., 2010. Simultaneous nitrification, denitrification and carbon removal in microbial fuel cells. Water Res. 44, 2970–2980.

Virdis, B., Rabaey, K., Yuan, Z., Keller, J., 2008. Microbial fuel cells for simultaneous carbon and nitrogen removal. Water Res. 42, 3013–3024.

Von Canstein, H., Ogawa, J., Shimizu, S., Lloyd, J.R., 2008. Secretion of flavins by Shewanella species and their role in extracellular electron transfer. Appl. Environ. Microbiol. 74, 615.

Vymazal, J., Brix, H., Cooper, P.F., Haberl, R., Perfler, R., Laber, J., 1998. Removal mechanisms and types of constructed wetlands, in: Constructed Wetlands for Wastewater Treatment in Europe. Backhuys Publishers, Leiden, The Netherlands, pp. 17–66.

Vymazal, J., Kröpfelová, L., 2015. Wastewater Treatment in Constructed Wetlands with Horizontal Sub-Surface Flow, CEUR Workshop Proceedings. https://doi.org/10.1017/CBO9781107415324.004

Walters, G., Janzen, C., Maginnis, S., 2016. Nature-based solutions to address global societal challenges, Nature-based solutions to address global societal challenges. https://doi.org/10.2305/iucn.ch.2016.13.en

Wang, X., Aulenta, F., Puig, S., Esteve-Núñez, A., He, Y., Mu, Y., Rabaey, K., 2020. Microbial electrochemistry for bioremediation. Environ. Sci. Ecotechnology 1, 100013. https://doi.org/10.1016/j.ese.2020.100013

Wang, X., Feng, Y.J., Lee, H., 2008. Electricity production from beer brewery wastewater using single chamber microbial fuel cell. Water Sci. Technol. 57, 1117–1121.

Wetlands, C., Ornamental, W., Removal, F.O.R., Organic, O.F., Sewage, C.I.N., 2013. Para El

Tratamiento De Materia Orgánica Y Nutrientes Contenidos En Aguas Servidas * for Removal of Organic Matter and Nutrients 22, 33–46.

Yu, J., Park, Y., Kim, B., Lee, T., 2015. Power densities and microbial communities of brewery wastewater-fed microbial fuel cells according to the initial substrates. Bioprocess Biosyst. Eng. 38, 85–92.

Zacharoff, L., Chan, C.H., Bond, D.R., 2016. Reduction of low potential electron acceptors requires the CbcL inner membrane cytochrome of Geobacter sulfurreducens. Bioelectrochemistry 107, 7–13.

Zhan, G., Zhang, L., Tao, Y., Wang, Y., Zhu, X., Li, D., 2014. Anodic ammonia oxidation to nitrogen gas catalyzed by mixed biofilms in bioelectrochemical systems. Electrochim. Acta 135, 345–350.

Zhu, T., Zhang, Y., Bu, G., Quan, X., Liu, Y., 2016. Producing nitrite from anodic ammonia oxidation to accelerate anammox in a bioelectrochemical system with a given anode potential. Chem. Eng. J. 291, 184–191.

Zhuang, L., Tang, Z., Ma, J., Yu, Z., Wang, Y., Tang, J., 2019. Enhanced anaerobic biodegradation of benzoate under sulfate-reducing conditions with conductive iron-oxides in sediment of Pearl River Estuary. Front. Microbiol. 10, 374.

Objectives and Thesis Outline

The present thesis aims to evaluate the performance of METland, a new born technology that integrate Microbial Electrochemical Technologies (METs) in the standard constructed wetlands (CW). The challenge of this hybrid technology is to overcome some of the technological, economical and performance bottlenecks for the challenge of wastewater treatment. Thus, the following specific objectives and outlines were proposed:

1. To study the differences between a constructed wetland and a METland in terms of operation and performance and to determine the effect of each of its elements: vegetation, microorganisms and bed material.

This objective has been developed through **Chapter 2:** *Within a bioelectrochemically-assisted constructed wetland (METland®): giving insights on wastewater treatment through the analysis of materials, performance and electroactive communities.* In this context, different biofilters were built to assess the impact of four different bed materials, gravel (inert material) and three types of carbonaceous materials. Furthermore, we have studied the impact of vegetation on the treatment efficiency, together with the analysis of bacterial communities. In this chapter, we present the use of electroconductive carbon-based materials for the construction of biofilters like METland® as an strategy to stimulate the electroactive microbial communities.

2. To assess the potential capability of the electroconductive carbon materials to promote extracellular electron transfer (EET) and to understand how the material determines the flux of electrons inside the METland bed.

This objective has been addressed in **Chapter 3**: *Electroactive biochar outperforms highly conductive carbon materials for biodegrading pollutants by enhancing microbial extracellular electron transfer.* Our goal was to evaluate the performance of different electroconductive carbon materials (graphite, coke, biochar) for supporting microbial EET while removing pollutants from wastewater. Indeed, we made a deep physical-chemical analysis of materials.

Moreover, we correlated the electrochemical response of such materials with the removal of pollutants.

3. To develop a methodology for simultaneous electrochemical control and measurement of the microbial response on different electrode materials under the same physicochemical and biological conditions.

This objective was developed in **Chapter 3**: *Simultaneous characterization of porous and non-porous electrodes in microbial electrochemical systems*. We studied the possibility of adapting two of the main electrochemical techniques, cyclic voltammetry and chronoamperometry, to our microbiological tests. In addition, we propose several strategies to avoid corrosion in the electrode connections.

4. To explore a novel electrochemical strategy to accelerate the microbial metabolism and, consequently, improve METland® efficiency without energy consumption.

This objective was developed in **Chapter 4**: *Novel bioelectrochemical strategies for domesticating the electron flow in constructed wetlands.* Our goal was to evaluate the performance of a new electron sink (e-sink) device. The e-sink device was integrated inside the biofilter bed and it was operated using different electron acceptors with high redox potentials.

5. To operate a real scale METland system treating livestock wastewater

This objective was developed in **Chapter 5**: *A METland® real case for treating manure wastewater: from lab-scale to full-scale.* A lab-scale system based on METland technology was designed and evaluated for its water pollutants removal efficiency. Finally, we transferred this model from lab-scale to full-scale, implementing a real system to treat livestock wastewater produced in Animal Nutrition Institute (Zaidín Experimental Station (EEZ) - CSIC).

Chapters 2 to **Chapter 5** of this thesis pursue to achieve scientific objectives and correspond to material published or submitted to peer-review international journals prior to PhD defence. **Chapter 1** is introductory and describes a general framework for this thesis. Finally, **Chapter 6** presents a general discussion, conclusions and future outlook. The researching activities described in chapter 4 were performed in collaboration with the Biosciences Department, Area of Aquatic Biology at Aarhus University (Denmark) under the supervision of Dr. Carlos A. Arias.

Research Framework

University of Alcalá awarded the author a PhD fellowship funded by the Formación de Personal Investigador (FPI) programme.

The present PhD thesis was developed within the frame of three research projects, completely or partially focused on applying METland technology for treating wastewaters.

The first one, iMETland, *A new generation of Microbial Electrochemical Wetland for effective decentralised wastewater treatment,* (2015-2018). Was a project funded through the European Union's Horizon 2020 research and innovation programme (grant agreement No. 642190). The consortium was was coordinated by IMDEA Water and it was composed by 11 partners from 4 different EU member states and two associated countries (Argentina and Mexico): Foundation CENTA, Aqua-Consult Ingenieros, PWC and Piroeco Bioenergy (Spain); Aston University (United Kingdom); Aarhus Universitet and Kilian Water (Denmark); the European research media center, youris.com (Belgium); INTEMA (Argentina) and IMTA (México). The iMETland project aims at unleashing the small community economies potential through innovative wastewater treatments technologies, creating a virtuous circle connecting water, energy, ICT, land resources and safeguarding the environment. Some of the results presented in this thesis (Chapter 3 and 4) were obtained during the course of iMETland (www.imetland.eu).

The second project, MET4HOME, *Microbial electrochemical strategies oriented to a sustainable and decentralized urban waste water reuse*, was funded by the Spanish Ministry of Science, Innovation and Universities (CTM2015-71520-C2-1-R). The initiative aimed to take advantage of the metabolism of the electroactive bacteria to change the paradigm of decentralized water purification through the design, construction and validation

of a compact prototype designed to clean-up and disinfect the water generated by an isolated dwelling, allowing its reuse for irrigation, sanitary tanks, etc. Some of the results of this thesis were associated to this project.

Last, the author participated as well in the ELECTRA Project, *Electricity Driven Low Energy and Chemical Input Technology for Accelerated Bioremediation,* (2019-2022). An EU-China initiative funded by the Horizon 2020 Framework Programme of the European Union (GA 826244). The ELECTRA consortium consists of 22 partners from 6 European countries (BE, GR, IT, DE, HU, ES), 1 associated country (CH) and China. The ELECTRA project is a 4-year Research Innovation Action consisting of one EC- funded consortium working closely together with a NSFC (Natural Science Foundation of China)-funded Chinese consortium. The ELECTRA consortium aims to jointly develop and test highly innovative electrobioremediation technologies; first at laboratory scale, and then under environmentally relevant conditions in both China and Europe. The field in which this thesis has contributed is in the treatment of water contaminated with nutrients with METLand technology (Chapter 2 and 5) (www.electra.site).

Another result of this thesis (Chapter 4) is the contribution to a patent application:

- International Patent application under PCT program. Authors: Esteve-Núñez A., PradoA., Berná A., Esteve R., Dominguez A. *App number*: PCT/ES2017/070160.

During the PhD thesis development, the author made numerous national and international scientific visits.

Within the framework of national scientific visits, the author was at CENTA (Foundation Center of New Water Technologies, Seville, Spain), coordinated by Dr. Juan José Salas, to validate different METs applications on a pilot scale.
In addition, the author supervised the construction of the bioelectrochemically-assisted manure wastewater treatment system at the Animal Nutrition Institute (Zaidín Experimental Station (EEZ) -CSIC) (Granada, Spain).

Within the framework of the European project iMETland, in 2018, the author was a visiting scientist for 3 months in the group of Dr. Carlos A. Arias at the Biosciences Department, Area of Aquatic Biology from Aarhus University (Denmark). During this period, the author collaborated in studies devoted to measure electron flow through electric potential at different depth profiles. Such experiments are fully included in Chapter 4.

Within the framework of the European project ELECTRA, in 2019, the author was a visiting scientist in the group of Dr. Matthias Kästner at the Department Environmental Biotechnology from Helmholtz Centre for Environmental Research – UFZ, Leipzig (Germany). During this period the author participated in the construction of METland systems at laboratory scale in order to evaluate the removal of micropollutants in wastewater.

CHAPTER 2:

WITHIN A BIOELECTROCHEMICALLY-ASSISTED CONSTRUCTED WETLAND (METLAND®)

This section has been redrafted after:

Amanda Prado de Nicolás[a,b] , Raúl Berenguer[c], Abraham Esteve-Núñez[a,b,d]. 2021. *Within a bioelectrochemically-assisted constructed wetland (METland®): giving insights on wastewater treatment through the analysis of materials, performance and electroactive communities*. Submitted to Chemical Engineering Journal.

[a] Department of Analytical Chemistry, Physical Chemistry and Chemical Engineering, University of Alcalá, Alcalá de Henares, Spain
[b] IMDEA Water Institute, Alcalá de Henares, Madrid, Spain
[c] Instituto Universitario de Materiales, Departamento Química Física, Universidad de Alicante, Alicante, Spain
[d] METfilter, Carrión de los Céspedes, Spain

Within a bioelectrochemically-assisted constructed wetland (METland®): giving insights on wastewater treatment through the analysis of materials, performance and electroactive communities

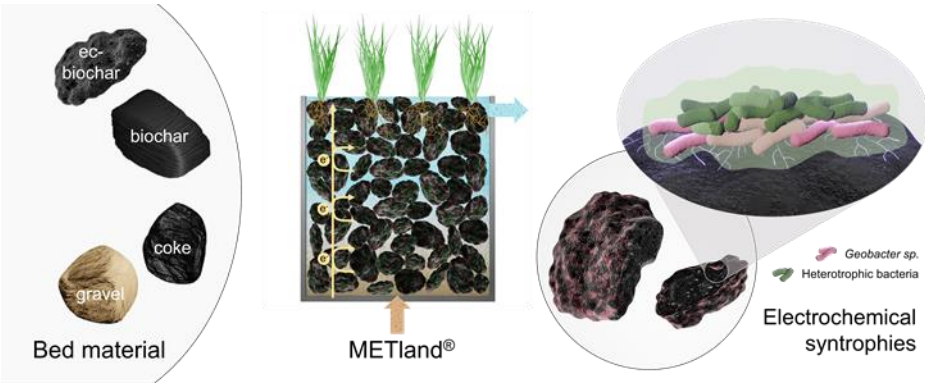

2.1. Abstract

METland® technology consists of a bioengineering strategy for treating wastewater by integrating microbial electrochemical concepts into constructed wetland systems to enhance pollutants removal. In this context, we have constructed planted (*Iris sibirica)* biofilters to assess the impact of four different bed materials (electroconductive coke, electroconductive biochar, non-electroconductive biochar and gravel) on (i) wastewater treatment efficiency (COD and nitrogen removal), (ii) bioelectrochemical response, and (iii) role of microbial communities. Electroconductive materials outperformed non-conductive ones allowing removal rates as high as 175-180 g COD/bed-m^3 day capable to support footprint as low 0.6 m^2/pe. In contrast, the highest nitrogen removal rates were achieved with non-conductive biochar in presence of plants (80 %) regardless the anoxic conditions of the assay. This was confirmed by the presence of annamox bacteria like Planctomycetes. Furthermore, the presence of a marked electric potential profile along the bed height in electroconductive materials together with redox pairs (cyclic voltammetry analysis) demonstrated an effective electron flow from bottom to uppermost layers of the bed (geoconductor mechanism). In electroconductive biochar, such effective conductivity-based model co-exists with a geobattery mechanism due to

presence of electroactive phenolic and carbonyl/quinone groups and/or microporosity. Microbial biodiversity analysis revealed the impact of plants just at the upper layers of the biofilters where roots and *Rhizobium* predominate. Bacteria from genus *Clostridium* were dominant in gravel inert material; in contrast, bacteria from genus *Geobacter* and *Trichococcus* outcompete the rest of communities for an effective colonization of carbonaceous beds, suggesting their main role as part of the electrosyntrophies mechanism after METland®.

Key words: Microbial electrochemistry; constructed wetland; Metland®; electroactive bacteria; wastewater treatment; electroconductive biochar.

2.2. Introduction

Nature-based solutions (NBSs) are technologies that rely on naturally occurring processes and simultaneously provide environmental, social and economic benefits. Indeed, they are a real solution to worldwide challenges like mitigating the deterioration of water resources caused by ineffective wastewater treatment (Faivre et al., 2017). Constructed wetlands (CWs) are a common example of NBS that mimic natural wetland to passively treat wastewater. Many CWs use substrates to support microorganisms and plants that can remove contamination from the water being treated (Brix, 1994). This environmentally friendly technology has been widely implemented throughout the world due to its simple mode of operation, low cost, and high efficiency treating various types of wastewater (Brix et al., 2007; Vymazal, 2008). However, compared to conventional biological technologies, CWs have a large footprint of land required and limitations for pollutants removal (Kadlec and Wallace, 2009).Thus, there is a pressing need for exploring strategies to intensify pollutants removal in CWs.

To overcome this limitation, the integration of microbial electrochemical technologies (MET) with CWs represents a promising approach (Ramírez-Vargas et al., 2019). METs are based on the ability of electroactive bacteria (EAB) to exchange electrons with electrically conductive materials (Esteve-Núñez et al., 2011). The EAB can oxidize organic pollutants present in wastewater that would be otherwise slowly degradable in conventional CWs because they

transfer excess electrons to an electrically conductive bed materials so electron acceptor limitation is minimized (Wang et al., 2020). The most widespread way to incorporate METs into CWs aim to harvest electrical energy from organic pollutants through the so-called microbial fuel cells (CW-MFCs) (Ramírez-Vargas et al., 2018). This strategy has shown success at lab scale for harvesting energy from complex wastewater (Corbella et al., 2015; Doherty et al., 2015b; Xu et al., 2018; Yadav et al., 2012); however, power generation higher than mW range seems difficult due to internal resistance between the electrodes, which increases linearly with the size and distance (Corbella and Puigagut, 2015; Doherty et al., 2015a; Tang et al., 2019).

An alternative strategy to overcome the scaling limitations to merge MET and CW has recently generated a hybrid technology known as METland® (Aguirre-Sierra et al., 2016). This new-born concept requires a complete replacement of the conventional bed material (gravel and sand) with an electrically conductive material, a never-ending source of terminal electron acceptor to support the microbial catabolism of pollutants (Prado et al., 2019). Originally, METland® was designed to operate under flooded conditions and short-circuit modes as snorkel electrodes (Aguirre-Sierra et al., 2016; Erable et al., 2011). The natural redox gradient between the bottom of the electroconductive bed and the naturally oxygenated surface greatly enhanced microbial oxidative metabolism (Prado et al., 2020). The existence of such electron flow along the METland® bed was demonstrated by measuring the profile of electric potential along distances larger than 40 cm (Prado et al., 2020; Ramírez-Vargas et al., 2019) and, interestingly, such electron flow can also be controlled by integrating artificial devices so-called e-sinks [20] . Full scale METlands® using large electroconductive carbonaceous-based biofilters, have been implemented in diverse geographic regions while achieving COD removal efficiencies of 90% (iMETland European H2020 project.). Furthermore, they are proved to be environmentally sustainable after LCA analysis (Peñacoba-Antona et al., 2021).

Conventional CWs include vegetation, mainly for absorbing nutrients, excreting oxygen into the rhizosphere, providing a surface for bacterial

attachment, and supporting microbial community biodiversity, as well as preventing the substrate clogging (Koottatep and Polprasert, 1997; Zhang et al., 2018). However, the plants contribution in METland® regarding nutrient removal exist but it is low in comparison with the microbial role due to the high loading rate (ca. 15 gN/m^2day) used to feed such bioelectrochemical systems (Aguirre-Sierra, 2017). In bioelectrochemical-assisted constructed wetlands like METland®, the electrically conductive carbonaceous material provides a competitive advantage for EABs (Prado et al., 2019; Ramírez-vargas et al., 2019) to efficiently interact with the bed material. These interactions promote the accepting and/or donating of electrons by creating electrochemical syntrophies (Rotaru et al., 2021) between bacteria which stimulate their metabolic activity allowing for increased removal rates.

Efficient extracellular electrons transfer (EET) is key for co-metabolic partnerships. There are two main pathways for EET. First, EET mediated by the conductive bed material itself (Conductive-particle-mediated Interspecies Electron Transfer/CIET) where the conductive particle acts as a vector for EET. The second is the direct exchange of electrons between microbes or Direct Interspecies Electron Transfer (DIET) (Rotaru et al., 2021). The model electrogenic microorganism *Geobacter sulfurreducens* plays a key role in this electron transfer. It acts as a conduit between the heterotrophs that oxidize organic compounds and the electroconductive bed (Tejedor-Sanz et al., 2018). Here, material properties play a key role in the bacteria-material electron transfer (Prado et al., 2019). It is thought that the electrically conductivity of the material may be crucial for effective electron transfer what has been referred to as "geoconductor" mechanism (Sun et al., 2017). Carbon-based materials that present oxygen surface groups may act like-quinones (Yuan et al., 2017) allowing these materials to store electrons (on carbon basal plans or chemical bonds). These electrons may be reversibly exchanged in biogeochemical processes, furthermore these mechanisms have been associated with geocapacitor and geobattery behaviours (Prado et al., 2019; Pun et al., 2019).

This work aims to understand the complex functioning of a METland® and identify the key factors that determine the systems efficiency for wastewater

treatment. We explored the impact of the physicochemical properties of the conductive material on wastewater treatment efficiency. Finally, we explored how these properties, in combination with plants from *Iris sibirica genus,* affected the development of bacterial communities, specifically the role that *Geobacter* may play as a key electroactive bacterial genus in the performance of this solution.

2.3. Materials and Methods

2.3.1 Biofilters construction and bed materials

Every biofilter consisted of a 2.2 L polyvinylchloride (PVC) cylinder (diameter: 90 mm, height: 35 cm) with an up-flow feed. One perforated pipe for sampling was placed inside every biofilter. The lower side of every cylinder was drilled (4 cm diameter hole) in order to sample the bed granules from the bottom layer. Every hole was sealed with a butyl septum. Biofilters were filled with abiotic materials as previously described and dead volume was approximately 50% of the total volume.

Four couples of biofilters were built (Fig. 2.1). Each couple of biofilters was hosting the following materials: electroconductive coke (ecC), electroconductive biochar (ecB), non-electroconductive biochar (ncB) and gravel (G) as inert control, all supplied with same granulometry (1.5 – 3.0 cm) by METfilter SL. (Table S2.1).

Four biofilter made of all different materials were planted with *Iris sibirica* freshly harvested from the Botanical Garden from University of Alcalá, (Alcalá de Henares, Spain). In a first step, the plants were acclimatized to wastewater in a full-scale METland® (10 m^2) at IMDEA Water facilities. The wetland plants, with one rhizome density per unit, were rinsed three times with tap water before being transplanted to the biofilter of the current study. Their roots shown lengths of 7.5 ± 0.8 cm and plants had stems with an average length of 27.0 ± 2.4 cm.

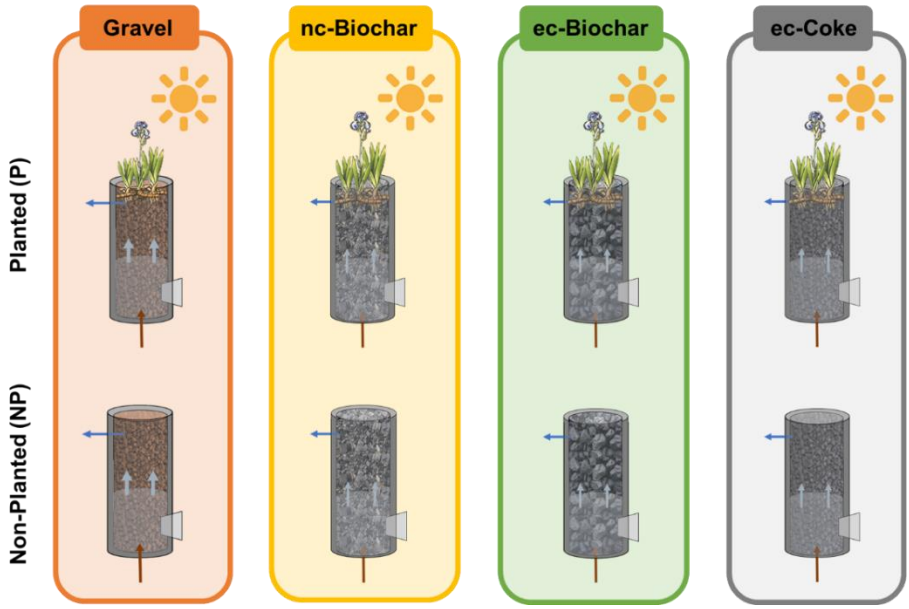

Figure 2.1. Scheme of electrochemically-assisted biofilters made of four materials: (gravel, nc-biochar, ec-biochar and ec-coke) operating up-flow in absence or presence of plants.

2.3.2 Characterization of Bed materials

Electrical conductivity measurements were carried out by using a Lucas Lab resistivity equipment with four probes in-line (Miccoli et al., 2015). The samples were dried under vacuum for 24 h and shaped into pellets of 0.013 m diameter by applying a pressure of 7.4·108 Pa. The porous texture was characterized by N_2 adsorption/desorption at 196 °C and by CO_2 adsorption at 0 °C (in the case of microporous samples), using a Quadrasorb-Kr/MP (Quantrachrome Corporation) equipment. Samples were previously outgassed for 6 h at 150 °C under vacuum. The specific surface area (S_{BET}) and the micropore volume ($V_{DR}(N_2)$) were calculated from the N_2 adsorption-desorption isotherms by using the BET and Dubinin-Radushkevich equations, respectively (Rios-Del Toro et al., 2018). The mesopore volume (V_{mes}) was calculated as the difference between total pore volume ($V_{0.995}$, volume at relative pressure of 0.995) and micropore volume (Rios-Del Toro et al., 2018). The narrow micropore volume ($V_{DR}(CO_2)$) and the narrow micropore surface area ($A_{DR}(CO_2)$) were estimated for

both types of biochar by applying the Dubinin-Radushkevich equation to the CO_2 adsorption isotherm (Rios-Del Toro et al., 2018). The pore volume and dimensions were further characterized by Hg intrusion-extrusion porosimetry, with a PoreMaster 60-GT porosimeter (Quantachrome Instruments) using a pressure range from 6.84 to 408330 kPa. The Washburn equation was utilized to relate the applied pressure with the pore diameter (Lowell et al., 2012).

The amount and nature of surface oxygen groups present on the carbon materials were studied by temperature-programmed desorption (TPD) experiments in a simultaneous TGA/DSC 2 equipment (Mettler-Toledo) coupled to a mass spectrometer (ThermoStar GSD 301 T, Pfeiffer Vacuum). In these experiments, around 20 mg of the carbon sample were heated up to 1000 °C at 20 °C/min under a He flow rate of 100 mL/min. Upon heating, surface oxygen groups on carbon materials decompose producing CO and CO_2 at different temperatures as a function of their thermal stability (Figueiredo et al., 1999). The quantification of the evolved CO and CO_2 groups was done by using a calcium oxalate monohydrate calibration and considering the CO disproportionation.

2.3.3 Biofilter operation and water quality analysis

The biofilters were housed indoor with constant temperature of 27°C and 12 hours of lighting with full spectrum led lamp (from 380nm to 800nm) for indoor plants.

The eight systems were operated in parallel to study the influence of several elements, including bed material and plants. Systems were fed with urban wastewater (860 mg/L COD, 65 mg/L NH_4^+ and no NO_3^-). The biofilter were operated in a continuous up-flow mode with an HRT of 2 days, using a peristaltic pump (Watson-Marlow®).

The start-up period lasted 10 days, then steady state conditions were reached in all systems. The study of water contaminants, including COD and N species, was carried out during both the start-up and steady state periods. To evaluate the quality of the water, samples of the influent and effluent were taken from all systems every three days. The COD was analyzed following a standard method (APHA/AWWA/WEF, 2012) and NH_4^+ and NO_3^- were monitored by ion

chromatography using a Metrohm 930 Compact Ion Chromatograph Flex. Removal efficiencies were calculated as percentage of the inlets. Removal rates were obtained from the inlet-outlet difference as COD grams per cubic meter of bed material per day.

In addition, oxygen concentration profiles were made in-situ, measured with a fiberoptic oxygen meter (FireSting O_2, Pyro-science) along the entire depth of the systems, taking measurements every 5 cm.

2.3.4 Electrochemical measurements

2.3.4.1 Electric potentials profiles with depth

To measure the electric potential (EP) two reference electrodes shielded silver/silver chloride were used (Prado et al., 2019). These reference electrodes are more insensitive to redox-active compounds than the liquid ones. One reference electrode was placed in the upper layer of the biofilter below the surface of the water. Both electrodes were connected to a digital voltmeter. The difference of the potential between both reference electrodes was measured along depth every three centimeters in all the systems. These profiles were performed in each of the eight systems at time 0 (abiotic conditions) during the start-up period (10 days) and in the steady state (20 days), all of them with wastewater as electrolyte. The overlying water signal value was used as a reference potential to normalized all the profiles. This value was subtracted from all the values in the profile. The results are a normalized electric potential depth profile.

2.3.4.2 Cyclic voltammetry of single granules

The microbial electrochemical response was studied by cyclic voltammetry (CV) in a single chamber cell. Single granule CVs were performed in the upper and lower location of every biofilter. From each, three independent granules (considered as replicas) of ca. 1 cm^2 were selected from upper and lower environment of every biofilter. A butyl septum sealing the lower part of the system was used to access the lowermost bed. Furthermore, every granule was perforated and hooked by a non-conductive thread so they could be easily

identified and selected during the course of the experiment. Actually, granules were back to the biofilter after CV analysis. Such procedure allows bacterial biofilm to grow during the course of the assay.

To perform the CV, the granules were hooked by a gold wire in order to make electrical contact and behave as a reliable working electrode (A. Prado et al., 2020). The CV experiments were carried out in a conventional three-electrodes single chamber at 10 mV/s in a potential range between -0.6 V and 0.6 V (*vs.* Ag/AgCl). A HANNA HI-5311 glass body Ag/AgCl (sat.) electrode with ceramic junction was used as reference electrode, whereas a 2x3 cm Ti/Pt mesh, attached to a copper wire protected by heat shrink tubing, acted as a counter electrode. All the electrodes were immersed in anaerobic phosphate buffer 100mM deoxygenated with N_2 and acetate 10mM. Three CVs were performed to each of the chosen granules over time: t0 (abiotic conditions), t10 days (start-up period) and t20 days (steady state).

2.3.5 Microbial communities and data analysis

2.3.5.1 16S Metagenomic Sequencing

To identify the microbial diversity and composition in different biofilter and locations, a sample of bed granules (15ml) was taken from top and bottom sections in every biofilter. The samples were stored at -20°C before DNA extraction. The DNA extraction, PCR amplification, and high-throughput sequencing were performed by external service for genomic analysis (Institute of Biotechnology and Biomedicine, UAB, Barcelona).

The V3-V4 region of the 16Sr DNA bacterial gene was amplified by a polymerase chain reaction (PCR) using the 338F/806R primers. The protocols of which were set according to Klindworth et al. (Klindworth et al., 2013). A high-throughput sequencing analysis was conducted using Illumina- MiSeq from Servei de Genòmica i Bioinformàtica (Barcelona, Spain).

2.3.5.2 Scanning electron microscopy SEM

For scanning electron microscopy (SEM) analysis, granules with biofilms were taken from each reactor, upper and bottom sections of every biofilter (16

samples in total). Granules were fixed in 5% (v/v) glutaraldehyde in 0.2 M sodium cacodylate pH7.2 for 60 min. Granules were then washed twice with 0.2 M sodium cacodylate pH7.2 for 10 min. The fixed granules were dehydrated in ethanol series (sequentially in 25%, 50%, 70%, 90% and 100% ethanol for 10 min each), acetone 100% 10 min and substituted with anhydrous acetone for 12 h in refrigerator. The fixed granules were dried with a critical-point drier using liquid CO_2 and coated with gold for 2 min (E1030, Hitachi, Spain) at 100 V and 100 mA. The coated granules were examined with an SEM (model DSM 950, Zeiss) at 3.5 kV.

2.3.6 Statistical analysis

Removal efficiencies were calculated as a percentage of the total inlet concentration of pollutants. Removal rates were obtained from the inlet-outlet difference as grams per cubic meter of bed per day. The error bars in the bar graphs represent the standard error of the mean. The values include in the bar graphs correspond to the average value of the measurements taken at each operation period (start-up and steady state). In order to validate the true effect of the bed materials under each operation condition, statistical procedures were conducted with these 3 measurements using R software and R-commander package (Fox, 2005).

The alpha diversity index, including Shannon and Simpson diversity index, ACE and Chao1 estimation and the dendrogram and PCoA graphs, were provided by the Servei de Genòmica i Bioinformàtica (Barcelona, Spain).

2.4 Results and discussion

Nature-based solutions, like constructed wetlands, are a sustainable technology for treating urban wastewater where bed material is a matter of current research. Actually, the use of electroconductive material for making the biofiltering bed led to large enhancement in microbial biodegradation of organic pollutants as shown by recent studies (Aguirre-Sierra et al., 2020; Prado et al., 2020; Prado et al., 2019). In this context, we aimed to explore the impact of the bed material and plants from genus *Iris sibirica* regarding: i) treatment efficiency

(COD and nitrogen removal), ii) microbial diversity and iii) bioelectrochemical response.

2.4.1 Characterization of biofilter materials: physico-chemical properties

The textural, structural and chemical properties of the bed materials play a key role on the microbial activity and/or colonization, so the four materials: gravel, ec-coke, ec-biochar and nc-biochar were characterized. The features of the gravel and ec-coke were previously reported (Prado et al., 2019). Essentially, the siliceous material did no present electrical conductivity and a very smooth surface without micro- (diameter (d) < 2 nm), meso- (2 < d < 50 nm) or macro-pores (d > 50 nm). On the contrary, the ec-coke exhibited a high conductivity of ~10.4 S/cm (Fig. 2.2A) and a remarkable rough morphology (Fig. 2.2B) which accounts for a porosity of 37 % (Fig. 2.2C), as deduced from Hg intrusion curves (Fig. S2.2). Besides, this material stands out for its poor surface chemistry, with a low content of oxygen functionalities (Fig. 2.2E), and the lack of micropores (Fig. 2.2C) and mesopores (see TPD curves and N2 adsorption-desorption isotherms in Fig. S2.3 and S2.4, respectively).

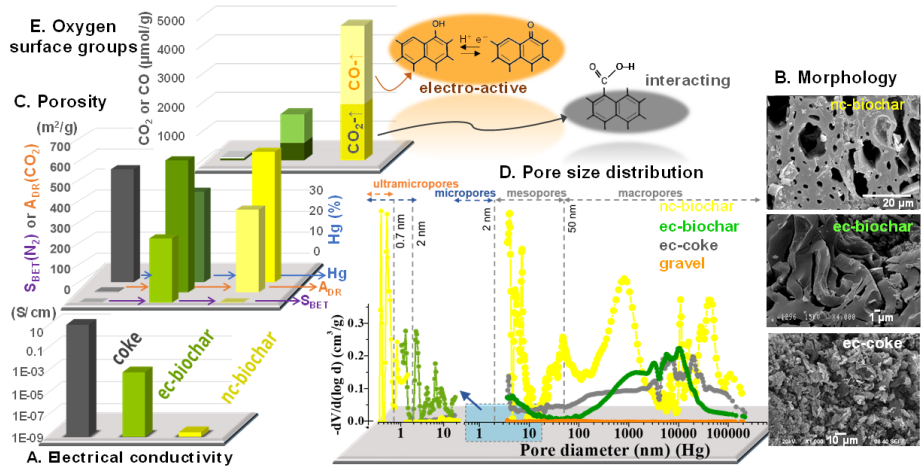

Figure 2.2. Main physico-chemical properties of the carbonaceous biofilter materials, including the electrical conductivity (A); morphology (SEM images, B); porosity (BET and $A_{DR}(CO_2)$ specific surface areas and % porosity in C); pore size distribution (D); oyxgen surface groups (CO_2-like and CO-like evolving groups from TPD in E).

Regarding the two types of biochars, the main distinguishing feature was their electrical conductivity (Fig. 2.2A). The conductive one (ec-biochar) showed a conductivity of 0.6 mS/cm, which was 5 orders of magnitude larger than the one measured for non-conductive biochar ($2.6E10^{-6}$ mS/cm), but much lower (ca. 18000 times) compared to that of the ec-coke (~10.4 S/cm). These differences were attributed to their different graphitic microstructures (Fig. S2.5) that, in fact, may arise from their distinct precursors and preparation conditions.

On the other hand, both type of biochar displayed exclusive textural and chemical properties. First, the biochar samples exhibited more uniform pores than the others materials used as bed (Fig. 2.2 B), typical of vascular and cellular systems of the vegetal precursors (Prado et al., 2019). Particularly, the ec-biochar presented distorted slit-like pores (Fig. 2.2B), but quite a similar percentage of macroporosity (about 40 % in Fig. 2.2C) and pore size distribution (between 0.1 and 40 μm, in Fig. 2.2D) compared to the ec-coke. For the nc-biochar, well-defined cylindrical channels of variable size were observed (Fig. 2.2B). In this sense, the defined peaks in the pore size distribution of this material (Fig. 2.2D) reflected the uniformity of its pore structure, revealing also the existence of smaller pores of less than 100 nm. Accordingly, the % of porosity in the nc-biochar was considerably larger than that for the other tested carbon materials (ca. 54 % in Fig. 2.2C).

Second, both biochars exhibited a well-developed microporosity, and especially narrow microporosity (as deduced from $A_{CO2} > S_{BET}$), which was larger in the case of the ec-biochar (Fig. 2.2C). In this sense, it should be stressed that the micropores of the nc-biochar were so narrow that they were inaccessible to N_2 gas probe (see N_2 adsorption-desorption isotherm in Fig. S2.4). By contrast, the ec-biochar showed a combination of both narrower and wider micropores (large S_{BET} and A_{CO2} values in Fig. 2C). Particularly, the volume of ultramicropores (d < 0.7 nm) in the ec-biochar and nc-biochar were 0.226 and 0.169 cm^3/g, giving rise to specific surface areas ($A_{DR}(CO_2)$) of 625 and 395 m^2/g, respectively (Fig. 2.2C).

Third, the concentration of oxygen surface groups in the biochar materials (between 2200-6600 μmol O/g) was remarkably larger compared to ec-coke (Fig. 2.2E). In this case, however, the largest amount of these functionalities corresponded to the nc-biochar. Besides, the figure distinguishes between both the CO_2- and CO-evolving groups. Deconvolution of TPD profiles (Fig. S2.3) (Lemus-Yegres et al., 2007) indicated that carboxylic-like functionalities stand out among the CO_2-evolving groups, while phenolic and carbonyl/quinone ones clearly prevail among the CO-evolving ones. The former could participate in the interaction with the bacteria proteins and/or biomolecules, whereas the last groups have been associated to electron transfer processes with electroactive bacteria (Prado et al., 2019).

To study the growth of biofilms in the different granules, their surface was explored by scanning electron microscope (SEM). As shown in Fig. S2.6, granules from the top and bottom layer of each system (planted and unplanted) were taken after 20 days of operation. At the top of the four planted beds, roots were clearly visible. These structures served as support for bacterial growth and had a positive effect on the microbial community, promoting greater morphological and species diversity. Furthermore, filamentous species, like phylum Actinobacteria, were very present on the surface of the granules of both biochar-based beds (Fig. S2.13). Furthermore, in the upper granules of the non-planted systems a high morphological diversity was observed, while no filamentous species were present in the gravel pebbles. This density and diversity of species can be attributed to the presence of aerophilic or microaerophilic species (Fig. S2.14). In the granules of the bottom layers, differences were only found between materials, and not due to the effect of the plant. The SEM micrographs of the gravel granules showed a biofilm that was visually less dense. As for the granules of carbonaceous materials, biofilms developed as a compact and homogeneous layer of cells, which even penetrated through the channels presented in the biochar-based materials.

2.4.2 Performance of the bioelectrochemically-assisted treatment: what, how and who

The impact of the bed material was evaluated by measuring the COD and nitrogen removal efficiency in combination with the microbial biodiversity associated to the process. In addition, the growth of the plants was monitored to evaluate their role in the different bed materials. All biofilters were independently operated up-flow with urban real wastewater under continuous mode. Two stages were analysed separately: the start-up period (days 0-10) and the steady-state (day 10-20).

2.4.2.1 Removal of organic pollutants

The bioremediation of the organic pollutants present in urban wastewater was monitored through the evolution of COD values. Thus, some dependence between the electroconductivity of the material and bioremediation was observed from the very beginning of the assay during the start-up period (Fig. 2.3). Once steady-state was reached, METland® treatments led to removal rates as high as 175-180gCOD/m^3day, outperforming gravel biofilter by 80 %. Such material-mediated bioremediation generated effluents with COD values in a range as low as 70-80 mg/l, in contrast with effluents from gravel biofilter that were poorly cleaned-up (300-400 mg/l) under same TRH of two days (Fig. 2.3). In terms of performance, electroconductive bed (either ec-coke or ec-biochar) exhibited the best response, followed by the nc-biochar that still outperformed the gravel by 50-60 % (Table S2.2). If all that WWT performance data are translated into the context of constructed wetlands (CW) we can anticipate our anaerobic electroconductive biofilters would accept a hydraulic loading rate as high as ca. 250 mm/day (0.6 m^2/pe) in contrast with the conventional values of 30 mm/day (3-5 m^2/pe) used in constructed wetlands operated under horizontal subsurface flow rate (García et al., 2003). Indeed, such design values are in the same range of METland® units already constructed for treating urban wastewater (iMETland European H2020).

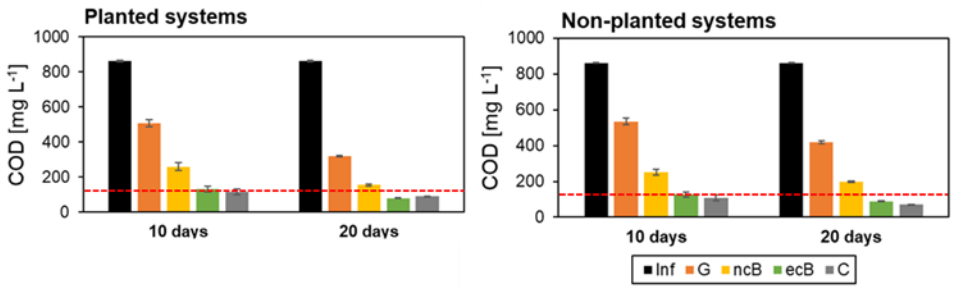

Figure 2.3. COD concentration at the influent (black) and effluent of every biofilter: gravel (orange), nc-biochar (yellow), ec-biochar (green) and ec-coke (grey), operating up flow during 0-10 days and 10-20 days, in the planted systems (up) and non-planted systems (down). Red line: European discharge limit = 125 mg/L (Council Directive 2000/60/EC of 23 October 2000).

To gain further insight into the different performance of the different biofilters, we proceed to analyse the composition of the microbial communities colonizing all bed materials (Fig. 2.4). Once the biofilters were operated under steady-state regime, the gravel (control biofilter) was mainly colonized by bacteria from genus *Clostridium*. Such strictly anaerobic *Clostridium* populations were likely responsible for the rapid fermentation of carbohydrates from wastewater. In contrast, in all our carbon-based biofilters systems, the most abundant genus was *Trichococcus,* an aerotolerant genus that was reported as electrode colonizer elsewhere (Saheb-alam and Persson, 2019; Zhao et al., 2012). Furthermore, species of this genus were described to perform direct or hydrochar-mediated EET inside anaerobic digesters (Baek et al., 2015; Ren et al., 2020). *Trichococcus* typically exhibits a fermentative metabolism, capable to convert sugars and polysaccharides into acetate. Interestingly, acetate is the main electron donor for bacteria from the genus *Geobacter*, the model microorganism in electromicrobiology (Busalmen and Esteve-Núñez, 2017; Lovley and Walker, 2019), also detected in our electroconductive biofilters but not in the inert gravel systems. Finally, it should be noted that *Pseudomonas* were detected in the upper locations of the systems, especially those made of biochar-based materials. Some species of this genus have been described as

electroactive, such as *Pseudomonas aeruginosa*, *Pseudomonas alcaliphila* and *Pseudomonas fluorescens* (Table S2.13). In ours assays the most abundant species were *Pseudomonas xanthomarina* and *Pseudomonas guangdongensis,* also detected in an electroactive biofilm as organic acids oxidizer (Yang et al., 2013).

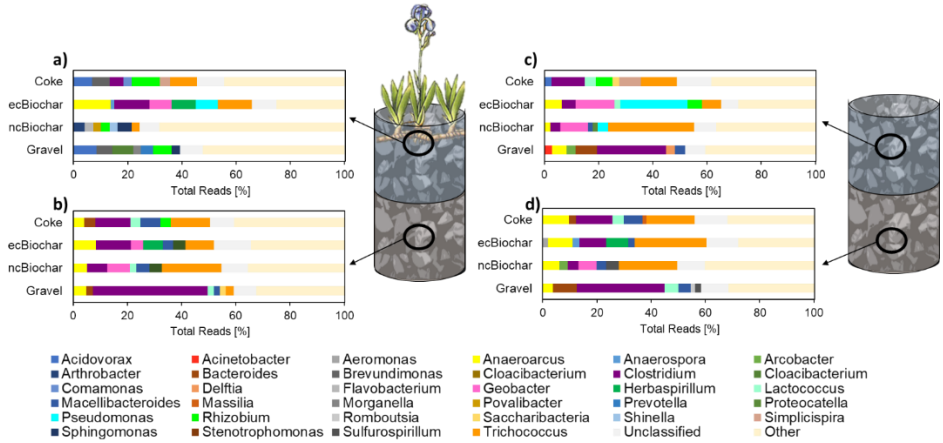

Figure 2.4. The bar graph shows the relative abundance at genus-level. The figure shows the most important genera in each region of each system: a) upper layer of planted systems, b) lower layer of planted systems, c) upper layer of non-planted systems and d) lower layer of non-planted systems.

2.4.2.2 Removal of nitrogen

All systems were fed with urban wastewater free of either nitrate or nitrite but with a constant concentration of ammonium (65 mg/l). Ammonium removal was vastly affected by the bed material and, to a lesser extent, by the growth of plants from *Iris sibirica*. During the starting up period, all biochar-based biofilters already supported ammonium removal as high as 78 %, in contrast with gravel, that showed a very poor response if any at all. However, once the system reached the steady state, all planted systems exhibited ammonium removal efficiency in a range from 40-80 % (Fig. 2.5). Furthermore, the presence of plants led to increase the efficiency exhibited by non-planted systems by 10-20 %. Interestingly, in terms of the material, ammonium removal was the highest in planted biochar-based biofilters (>80 %).

Ammonium removal from effluents can occur via microbial assimilation or nitrification. The last is a typically (but not exclusive) oxygen-based two-step process, where ammonium is first converted to nitrite by ammonia oxidizing bacteria (AOB) from Nitrosomonadales order. Then, the nitrite is converted into nitrate by nitrite-oxidizing bacteria (NOB) (Aguirre-Sierra et al., 2020). The high-throughput sequencing analysis for microbial biodiversity (Table S2.4) revealed that AOB reads were high enough in all systems to support the existence of ammonium oxidation. However, the number of AOB reads was slightly higher in gravel, what correlates with a greater impact of vegetation regarding ammonium removal. This could be related with the fact that plants adapted to flooded conditions present the ability to supply oxygen from the atmosphere to their roots providing a terminal electron acceptor (TEA) for nitrification. In absence of plants, such a TEA role could be played by carbonaceous material, like ec-coke, ec-biochar and nc-biochar biofilters in a similar way that annamox bacteria oxidize ammonium in absence of oxygen. Indeed, some anammox bacteria seem to couple NH_4^+ oxidation to the reduction of carbon-based insoluble extracellular electron acceptors (Shaw et al., 2020; Yang et al., 2012). In this context, Planctomycetes was an anammox bacteria detected in our carbon-based biofilters, representing in all cases a significant increase compared to the influent. Species of this order, such as those from genera *Brocadia, Kuenenia, Jettenia* and *Anammoxoglobus* are able to anaerobically oxidize ammonium, using NO_2^- or NO as intracellular electron acceptor (Hu et al., 2019; Kartal et al., 2011). METlands®, made of electroconductive coke or ec-biochar, could be good environments for the development of such microbial populations. Actually, EET-dependent anammox process may outperform conventional anammox process by avoiding the production of greenhouse gas like N_2O. The actual role of such annamox communities in our ec-biochar for enhancing anaerobic ammonium removal is being currently investigated.

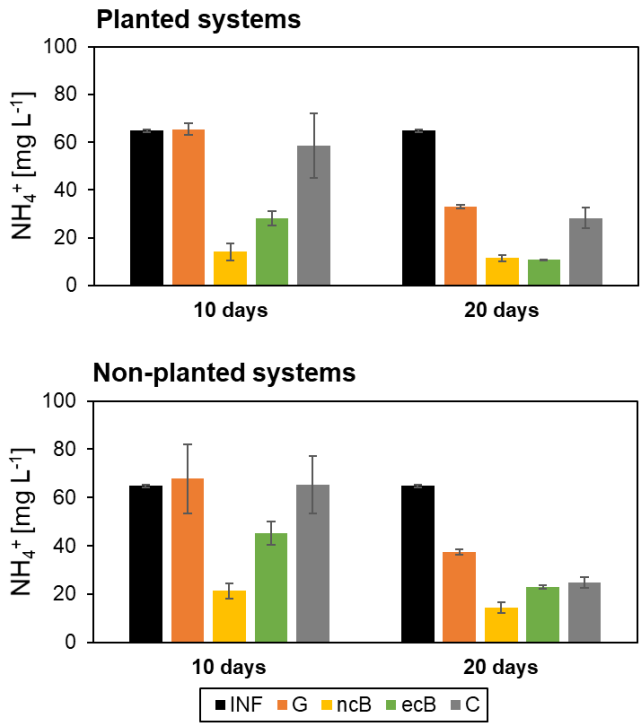

Figure 2.5. NH_4^+ concentration at the influent (black) and effluent of every biofilter: gravel (orange), nc-biochar (yellow), ec-biochar (green) and ec-coke (grey), operating up flow during 0-10 days and 10-20 days, in the planted systems (up) and non-planted systems (down).

Denitrification is the second stage of the elimination of nitrogen in wastewater, which typically occurs under anoxic conditions by denitrifying bacteria (DNB). Interestingly, neither nitrate nor nitrite were detected in the effluent from our biofilters, suggesting that it was effectively consumed by DNB associated to the electroactive biofilm. The number of readings for these bacteria was always higher in biofilters made of carbon-based materials, at least twice as compared to the gravel system (Table S2.4). Dissimilatory nitrate reduction to ammonium (DNRA) is also possible in a two steps process via nitrite without intermediates (Pandey et al., 2021). The read numbers of DNRA bacteria were significantly higher in gravel systems and ec-coke system, what could correlate well with the lower removal of total nitrogen in such systems.

2.4.2.3 Performance in planted and non-planted biofilters

Iris sibirica acclimatized and grew well in presence of wastewater with all different materials as substrate. Gas transport from the air sections of the plant into the rhizome fine roots is driven by specific areas of tissue known as aerenchyma. The release of oxygen in the roots causes the formation of an oxidative protective film directly on the root surface with a thickness between 1-4 mm (Armstrong et al., 1994; Vartapetian and Jackson, 1997). This constant release of oxygen in the rhizosphere led to a great diversity at the very top of the biofilters, with the nitrogen fixing genera *Rhizobium* and *Herbaspirillum as* the most abundant (Fig. S2.13). Although the plant roots supplied oxygen, it was quickly consumed by the aerobic rhizosphere microorganisms, so oxygen was not detected along the depth of the systems and the water column was naturally kept under anoxic conditions. Thus, at the bottom location of every biofilter no major differences between the planted and non-planted systems were detected in terms of biodiversity (Fig. 2.4). This is consistent with the fact that rhizosphere did not reach the deep layers, so the differences in the microorganisms populations will be just a consequence of the effect of the bed material.

2.4.3 Electrochemical characterization of biofilter beds in lab-scale METlands®

2.4.3.1 Electric potentials depth profiles

The up-flow operation of a conventional biofilter made of an inert material (gravel) typically leads to a microbial metabolism limited by the availability of a terminal electron acceptor. In this system, oxidation of pollutants and reduction of terminal electron acceptors are coupled both temporally and spatially (Prado et al., 2020). In contrast, our METland® design overcomes these limitations by means of an electrically conductive material capable of transferring electrons from deeper layers, where the oxidation of organic pollutants mainly occurs (anodic reactions), towards the uppermost layers, where reduction reactions predominate (cathodic reactions). METland® under up-flow configuration operates as single electrode (snorkel mode) so, due to the absence of an external circuit, electrical current cannot be directly measured in contrast with standard microbial electrochemical systems (Prado et al., 2020). However, we

measured the flux of electrons through the biofilter materials by monitoring the electric potential profiles (Damgaard et al., 2014; Prado et al., 2020; Ramírez-Vargas et al., 2019) along the bed (Figure 2.6).

The in-depth EP profiles were also correlated with microbial activity. The EP profile in the very early stage of operation (time 0) was negligible (the electrode potential was roughly zero), even for electroconductive systems (see the results abiotic in Figure 2.6). Initially, these bed materials were abiotic so biofilm was still not developed around the bed granules. Without electroactive communities capable of oxidizing organic compounds and donate electrons to the material, hence, there was no flux of electrons (Figure 2.6).

Over time, however, EP profiles became wider because of the electroactive biofilm development. Thus, once the steady state was reached (20 days), the microbial oxidation of organic pollutants was high enough to support a vertical flux of electrons towards the uppermost layers. At that time, EP profiles showed differences between the tested systems (Fig. 2.6), indicating the impact of the bed material on the flux of ions, and consequently on the flux of electrons. Biofilters made of inert material like gravel cannot support electron flux along the bed, so the EP depth profile showed no variations at all. In a similar way, the EP depth profiles for nc-biochar system were flat, due to the high ohmic resistance of this material. This suggests that this material cannot act as a geoconductor, disabling the transfer of electrons directly to/from the carbon matrix. However, the lack of conductivity did not prevent it from playing a role as geobattery, a mechanism based on the hydroquinone-quinone (HQ/Q) reversible redox reaction able to stimulate microbial activity (Prado et al., 2019; Sun et al., 2017). In contrast, biofilters made of electrically conductive materials, ec-biochar and ec-coke, showed a remarkable EP response with depth, confirming an electron transfer in the vertical axis (Fig. 2.6). The electrons produced by the EAB migrated to the uppermost material because of the redox gradient. The electrically conductive materials resistance also affected the EP profiles. The lower material resistance (ec-coke system, system with less ohmic drop), the greater flux of electrons. Interestingly, the biofilter made of ec-biochar showed a miscellaneous behavior: geoconductor and geobattery. An EP

depth profile could be observed due to some electroconductivity of the material (geoconductor mechanism), but flatter than the ec-coke EP profile. Interestingly, as a consequence of the electrical resistance of the material, the bottom section showed an ohmic drop impact greater than the one from redox gradient, which makes geobattery processes predominate, promoting the presence of electroactive microorganisms with mediated electron transfer. Those electrons donated to carbon-bound mediators, such as quinones and humic-like material, will not migrate directly through the material to the upper layers of the bed and, therefore, will not contribute to the EP profile slope.

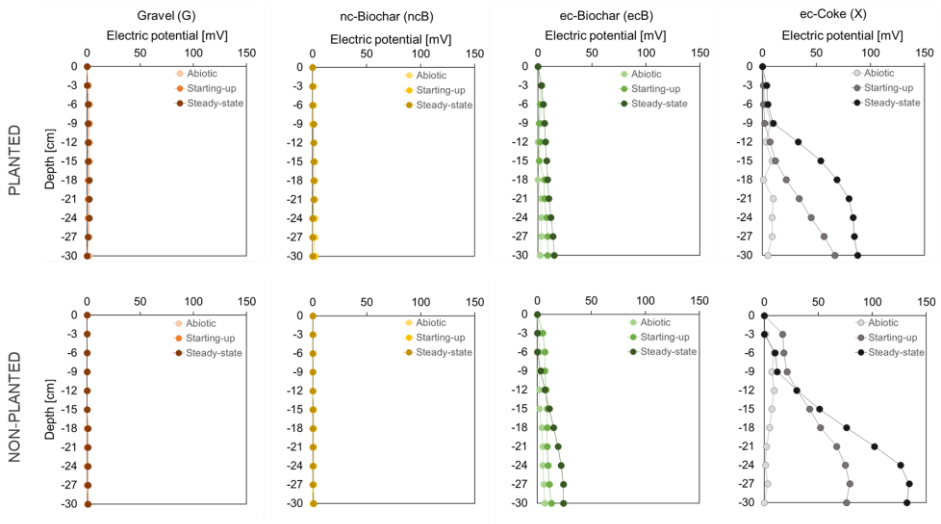

Figure 2.6. Electric potential (EP) depth profiles of tested biofilters along depth at each time (abiotic, 10 days and 20 days) of gravel (orange), nc-biochar (yellow), ec-biochar (green) and ec-coke (grey) bed, in planted (up) and non-planted (down) systems. EP profiles were measured with a shielded Ag/AgCl electric potential electrode.

The use of vegetation (Fig. 2.6 up) should generate a greater vertical redox gradient since the roots were supplying oxygen into the system. However, we did not observe such an effect. A possible reason may be that this oxygen would be directly consumed by rhizosphere-associated communities in presence of organic compounds from root exudates (Scholz et al., 2020, 2019). If so, oxygen would not be really available for cathodophilic bacteria associated to the uppermost layer of the electroconductive material. This was confirmed by the

highest concentration of bacteria of the genus *Rhizobium* found in the upper layer of the planted systems (Fig. S2.14).

2.4.3.2 Cyclic voltammetry of single granules

Cyclic voltammetry (CV) is a standard electrochemical tool to characterize electron transfer between microorganisms or biofilms and electrodes (Fricke et al., 2008; Rodrigo Quejigo et al., 2018), through direct detection of redox signals and electrochemical reactions (Esteve-Núñez et al., 2011). To investigate the evolution of the biofilm and determine the electrochemical activity of the electrode materials, single granules CVs were performed at different stages of biofilm formation (day 0, starting-up and steady-state) from different bed locations (upper and bottom layer). CVs were recorded during non-turnover (NTO), conditions in absence of electron donor. Application of certain potentials can disrupt biofilms either by producing hydrogen (Gião et al., 2005) or by inducing unfolding/ oxidation of adsorbed proteins at oxidizing potentials (Perez-Roa et al., 2006), so we just performed the analyses at a scan rate of 10 mV/s from 0.6 V to -0.6V vs. Ag/AgCl.

Independent granules were taken from the system just before the electrochemical analysis, and their electrical resistivity was measured. A first round of CV was performed on granules from ec-coke (2 Ω/cm), ec-biochar (20 Ω/cm) and nc-biochar (200 Ω/cm) at time 0 to identify redox signals in biofilm-free material. The slope of the voltammogram was directly proportional to the ohmic resistance of the material (Fig. S7, 8, 9). Despite the resistance of the materials, no redox peaks were observed before microbial colonization.

In the case of nc-biochar no redox peaks were observed in material at the start-up and steady-state stages. This is consistent with the poor conductive nature of the material. However, after 20 days of operation (steady-state) the slope of the voltammograms increased with time, as well as the capacitive current recorded in all the granules (Fig. S2.7). This could be explained, because the biofilm growth may have clogged the micro and mesopores, reducing the flow of ions and, therefore, increasing the resistance due to ohmic drop.

In the case of ec-biochar granules (Fig. S2.8), an evolution of the voltammograms was observed over time. During the start-up process, an increase in capacity was observed. Furthermore, the capacitive current of the voltammograms after 20 days together with the electric resistance of the material, might mask the presence of small faradaic currents from microbial nature. Slow reactions may not be detected because due to the fast potential shifts caused by the scan rate. Thus, as the scan rate increases, the kinetics of interfacial electron transfer between redox proteins and electrodes strongly affects the voltametric response, even hiding the kinetics of continuous enzymatic turnover. The fact that no clear CV shape was observed for ec-biochar granules could also suggest that such material was originally colonized by mediator-based electroactive community and, unfortunately soluble redox mediator cannot be detected when a single granule was analysed in an independent electrochemical cell.

Finally, the CVs curves of the ec-coke systems under non-turnover condition (Fig. 2.7) revealed that formal potentials from all voltammograms were similar and in accordance with literature data typical for wastewater-derived biofilm and the oxidation and reduction peaks evidenced the presence of redox-active species (Katuri et al., 2012; Zhuang et al., 2012). In contrast with the biochar-based analysis, the CVs of the ec-coke granules (Fig. S2.9) showed the greatest evolution over time. From a very flat voltammogram in biofilm-free granules, the material evolved to eventually show a capacitive current and slight oxidation after 10 days of operation. Once steady-state was reached, such features became more remarkable and the capacitive current was considerably higher than the bioelectrocatalytic current densities. This capacitive current was due to a non-catalytic activity, because the presence of both redox-active microbiological moiety and exo-polysaccharide matrix. To calculate the formal potential of the oxidation-reduction pair that appeared in the upper planted and lower non-planted ec-coke systems the first derivative of such CVs (steady-state) was performed (Fig. S2.10). The formal potential value for the redox pairs that appeared, E_0 = -220 mV (vs. the Ag / AgCl), was in accordance with the literature data for non-turnover CVs of biofilms enriched from primary

wastewater (Carmona-Martínez et al., 2013; Pierra et al., 2015). On the other hand, the voltagram recorded on the granule of the non-planted bottom ec-coke system (Fig. 2.7) showed a redox couple. The formal potential was -201 mV (vs. the Ag / AgCl). Similar responses have been previously reported for the oxidation of acetate by biofilms of single culture *Geobacter sulfurreducens* (Marsili et al., 2008; Torres et al., 2009). The currents densities reached under steady-state were probably the result of a higher cell density at the electrode surface or higher expression of membrane-bound electron transfer proteins (Fricke et al., 2008). This is confirmed by the presence of to the microbial community results (Table. S2.5) since in the ec-coke systems, electroactive community with direct electron transfer were more abundant than the mediated electron transfer, while the second was the most common in biochar materials.

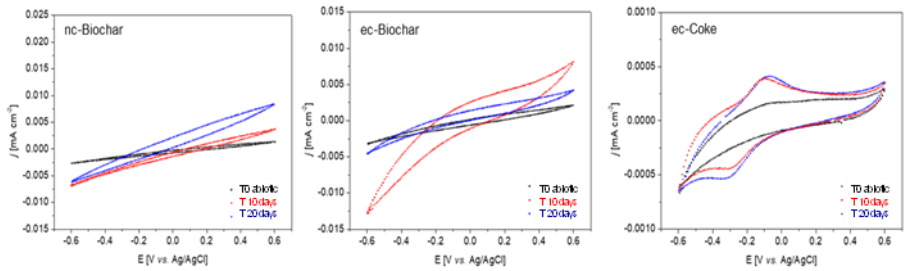

Figure 2.7. Cyclic voltammograms of a single granule of nc-biochar, ec-biochar and ec-coke from the non-planted bottom system at different stages (biofilm-free (black), 10 days (red) and 20 days (blue)). Scan rate 10 mV/s; phosphate buffer 100mM, acetate 10mM.

2.4.4 Geobacter as key actor in electrochemical syntrophies

Microbial Extracellular electron transfer, either in form of DIET (Direct Interspecies Electron Transfer) or CIET (Conductive-particle-mediated Interspecies Electron Transfer) is currently trending topic in environmental biotechnology field (Shi et al., 2016). Thus, such kind of syntrophies have a key role in engineering applications for treating brewery wastewater in anaerobic digestors (Morita et al., 2011) or microbial electrochemical fluidized bed reactors (Asensio et al., 2021; Tejedor-Sanz et al., 2020, 2017). In this context, the nature of the material determines how extracellular electron transfer can be stimulated. In our case, electrically conductive minerals, such as ec-coke,

promote the transfer of electrons through electronic channels and depends on the electrically conductivity of the material. In biochar materials, humic-like substances are also present acting as electron acceptors for microbial respiration (Chen et al., 2014; Lovley et al., 1996, 1998).

In such syntrophic interactions, electroactive microorganism like those from genus *Geobacter* play a key role (Rotaru et al., 2021; Shrestha and Rotaru, 2014). So, we evaluated its relative abundance in our biofilters, both at genus and species level (Fig. 2.8).

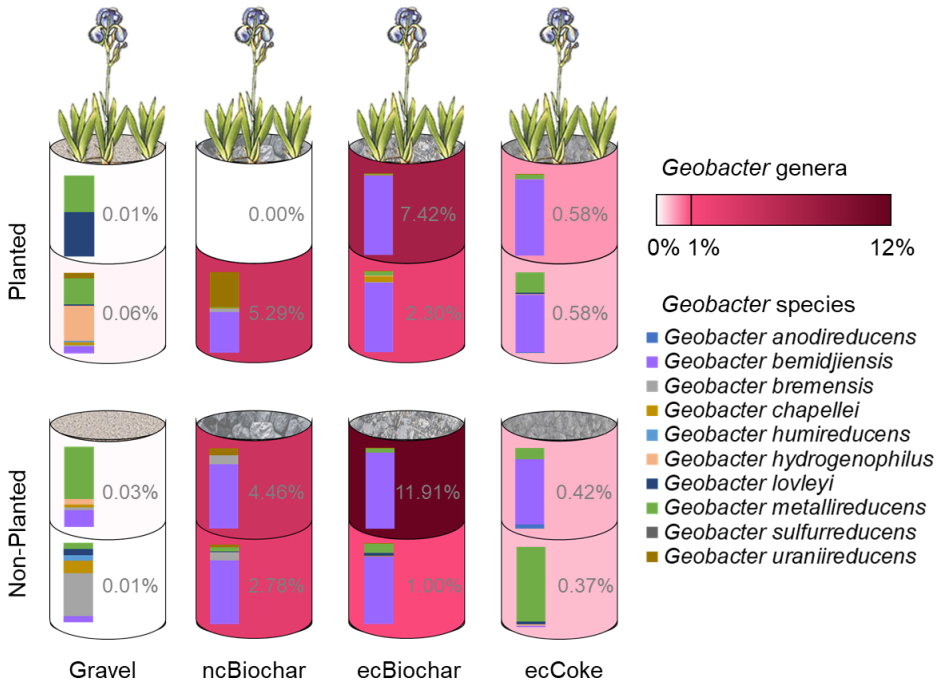

Figure 2.8. Relative abundance of *Geobacter* (represented with pink colour intensity) at different locations from biofilters made of a) gravel, b) nc-biochar, c) ec-biochar and d) ec-coke. In bar graph: percentage of each *Geobacter* species of the total registered for each location.

The highest presence of *Geobacter* occurred in the carbonaceous materials, especially in the electrically conductive biochar (12 %); probably due to the presence of quinone-like groups on the surface (Lovley, 2006). In the carbonaceous materials, *Geobacter bemidjiensis* seem to predominate among all *Geobacter* genus detected. Interestingly, this specie can couple not just

acetate oxidation but also end-products (butanol, ethanol, formate, lactate) from fermenters to the reduction of EET respiration (Koch and Harnisch, 2016; Nevin et al., 2005). In contrast, the percentage of *Geobacter* found in the gravel bed was no more than 0.05 %, with no clear dominance of a specific species.

2.5. Conclusions

In conclusion, the use of electroconductive carbon-based materials for the construction of biofilters like METland® are capable of stimulating electroactive microbial communities to perform an efficient extracellular electron transfer and, eventually, greatly enhance pollutants removal in wastewater. The low resistance of materials like electroconductive coke allow to operate METland® following a pure geoconductor mechanism. However, the fact that sustainable materials like biochar exhibit phenolic and carbonyl/quinone groups able to support electron transfer opens an interesting field for exploring new concepts in wastewater treatment. Indeed, the existence of such a geobattery mechanism suggests that electroconductivity of the material is not necessarily the only feature for selecting a material to grow electroactive microbial communities like *Geobacter*. Ideally, we should deeply investigate those materials able to couple, even spatially distant, microbial redox reactions and accordingly carry out specific syntrophic and/or cooperative metabolisms to maximize pollutant biodegradation.

2.6. References

Aguirre-Sierra, A., 2017. Integrating microbial electrochemical systems in constructed wetlands, a new paradigm for treating wastewater in small communities. Universidad de Alcalá, Spain.

Aguirre-Sierra, A., Bacchetti-De Gregoris, T., Berná, A., Salas, J.J., Aragón, C., Esteve-Núñez, A., 2016. Microbial electrochemical systems outperform fixed-bed biofilters in cleaning up urban wastewater. Environ. Sci. Water Res. Technol. 2, 984–993. https://doi.org/10.1039/c6ew00172f

Aguirre-Sierra, A., Bacchetti-De Gregoris, T., Salas, J.J., De Deus, A., Esteve-Núñez, A., 2020. A new concept in constructed wetlands: Assessment of aerobic electroconductive biofilters. Environ. Sci. Water Res. Technol. 6, 1312–1323. https://doi.org/10.1039/c9ew00696f

APHA/AWWA/WEF, 2012. Standard Methods for the Examination of Water and Wastewater, Standard Methods. https://doi.org/ISBN 9780875532356

Armstrong, W., Brandle, R., M.B., J., 1994. Mechanism of Flood Tolerance Plants. Acta Bot. Neerl 43, 307–358.

Asensio, Y., Tejedor-Sanz, S., Llorente, M., Fern, P., Ortiz, J.M., Ciriza, J.F., Monsalvo, V., Rogalla, F., Esteve-Núñez, A., 2021. Upgrading fluidized bed bioelectrochemical reactors for treating brewery wastewater by using a fluid-like electrode 406. https://doi.org/10.1016/j.cej.2020.127103

Baek, G., Kim, J., Cho, K., Bae, H., Lee, C., 2015. The biostimulation of anaerobic digestion with (semi)conductive ferric oxides: their potential for enhanced biomethanation. Appl. Microbiol. Biotechnol. 99, 10355–10366. https://doi.org/10.1007/s00253-015-6900-y

Brix, H., 1994. Constructed wetlands for municipal wastewater treatment in Europe. In: Mitsch, W.J. (Ed.), Global Wetlands: Old World and New 325–334. https://doi.org/ISBN 13: 9780444814784

Brix, H., Koottatep, T., Laugesen, C.H., 2007. Wastewater treatment in tsunami affected areas of Thailand by constructed wetlands 69–74. https://doi.org/10.2166/wst.2007.528

Busalmen, J.P., Esteve-Núñez, A., 2017. C - Type Cytochromes Wire Electricity - Producing Bacteria to Electrodes C-Type Cytochromes Wire Electricity-Producing Bacteria to Electrodes ** 4952–4955. https://doi.org/10.1002/ange.200801310

Carmona-Martínez, A.A., Harnisch, F., Kuhlicke, U., Neu, T.R., Schröder, U., 2013. Electron transfer and biofilm formation of Shewanella putrefaciens as function of anode potential. Bioelectrochemistry 93, 23–29. https://doi.org/10.1016/j.bioelechem.2012.05.002

Chen, S., Rotaru, A.E., Shrestha, P.M., Malvankar, N.S., Liu, F., Fan, W., Nevin, K.P., Lovley, D.R., 2014. Promoting interspecies electron transfer with biochar. Sci. Rep. 4. https://doi.org/10.1038/srep05019

Corbella, C., Guivernau, M., Viñas, M., Puigagut, J., 2015. Operational, design and microbial aspects related to power production with microbial fuel cells implemented in constructed wetlands. Water Res. 84, 232–242. https://doi.org/10.1016/j.watres.2015.06.005

Corbella, C., Puigagut, J., 2015. Microbial fuel cells implemented in constructed

wetlands: Fundamentals, current research and future perspectives. Contrib. to Sci. 11, 113–120. https://doi.org/10.2436/20.7010.01.220

Damgaard, L.R., Risgaard-Petersen, N., Nielsen, L.P., 2014. Electric potential microelectrode for studies of electrobiogeophysics. J. Geophys. Res. Biogeosciences 119, 1906–1917. https://doi.org/10.1002/2014JG002665

Doherty, L., Zhao, Y., Zhao, X., Hu, Y., Hao, X., Xu, L., Liu, R., 2015a. A review of a recently emerged technology: Constructed wetland – microbial fuel cells. Water Res. https://doi.org/10.1016/j.watres.2015.08.016

Doherty, L., Zhao, Y., Zhao, X., Wang, W., 2015b. Nutrient and organics removal from swine slurry with simultaneous electricity generation in an alum sludge-based constructed wetland incorporating microbial fuel cell technology. Chem. Eng. J. 266, 74–81. https://doi.org/10.1016/j.cej.2014.12.063

Erable, B., Etcheverry, L., Bergel, A., 2011. From microbial fuel cell (MFC) to microbial electrochemical snorkel (MES): maximizing chemical oxygen demand (COD) removal from wastewater. Biofouling 27, 319–326. https://doi.org/10.1080/08927014.2011.564615

Esteve-Núñez, A., Busalmen, J.P., Berná, A., Gutiérrez-Garrán, C., Feliu, J.M., 2011. Opportunities behind the unusual ability of geobacter sulfurreducens for exocellular respiration and electricity production. Energy Environ. Sci. 4, 2066–2069. https://doi.org/10.1039/c1ee01067k

Faivre, N., Fritz, M., Freitas, T., de Boissezon, B., Vandewoestijne, S., 2017. Nature-Based Solutions in the EU: Innovating with nature to address social, economic and environmental challenges. Environ. Res. 159, 509–518. https://doi.org/10.1016/j.envres.2017.08.032

Figueiredo, J.L., Pereira, M.F.R., Freitas, M.M.A., Orfao, J.J.M., 1999. Modification of the surface chemistry of activated carbons. Carbon N. Y. 37, 1379–1389.

Fox, J., 2005. Getting startedwith the R commander: a basic-statistics graphical user interface to R. J Stat Softw 14, 1–42. https://doi.org/https://doi.org/10.18637/jss.v014.i09.

Fricke, K., Harnisch, F., Schro, U., 2008. On the use of cyclic voltammetry for the study of anodic electron transfer in microbial fuel cells 144–147. https://doi.org/10.1039/b802363h

García, J., Vivar, J., Aromir, M., Mujeriego, R., 2003. Role of hydraulic retention time and granular medium in microbial removal in tertiary treatment reed beds. Water

Res. 37, 2645–2653. https://doi.org/10.1016/S0043-1354(03)00066-6

Gião, M.S., Montenegro, M.I., Vieira, M.J., 2005. The influence of hydrogen bubble formation on the removal of Pseudomonas fluorescens biofilms from platinum electrode surfaces. Process Biochem. 40, 1815–1821. https://doi.org/10.1016/j.procbio.2004.06.068

Hu, Z., Wessels, H.J.C.T., van Alen, T., Jetten, M.S.M., Kartal, B., 2019. Nitric oxide-dependent anaerobic ammonium oxidation. Nat. Commun. 10. https://doi.org/10.1038/s41467-019-09268-w

iMETland European H2020 project. [WWW Document], n.d. URL http://imetland.eu/

Kadlec, R., Wallace, S., 2009. Ttreatment wetlands, in: Vasa. p. 1048.

Kartal, B., Maalcke, W.J., De Almeida, N.M., Cirpus, I., Gloerich, J., Geerts, W., Op Den Camp, H.J.M., Harhangi, H.R., Janssen-Megens, E.M., Francoijs, K.J., Stunnenberg, H.G., Keltjens, J.T., Jetten, M.S.M., Strous, M., 2011. Molecular mechanism of anaerobic ammonium oxidation. Nature 479, 127–130. https://doi.org/10.1038/nature10453

Katuri, K.P., Enright, A.M., O'Flaherty, V., Leech, D., 2012. Microbial analysis of anodic biofilm in a microbial fuel cell using slaughterhouse wastewater. Bioelectrochemistry 87, 164–171. https://doi.org/10.1016/j.bioelechem.2011.12.002

Klindworth, A., Pruesse, E., Schweer, T., Peplies, J., Quast, C., Horn, M., Glöckner, F.O., 2013. Evaluation of general 16S ribosomal RNA gene PCR primers for classical and next-generation sequencing-based diversity studies. Nucleic Acids Res. 41, 1–11. https://doi.org/10.1093/nar/gks808

Koch, C., Harnisch, F., 2016. Is there a Specific Ecological Niche for Electroactive Microorganisms? ChemElectroChem 3, 1282–1295. https://doi.org/10.1002/celc.201600079

Koottatep, T., Polprasert, C., 1997. Role of plant uptake on nitrogen removal in constructed wetlands located in the tropics. Water Sci. Technol. 36, 1 LP – 8.

Lemus-Yegres, L.J., Such-Basáñez, I., Román-Martínez, M.C., De Lecea, C.S.-M., 2007. Catalytic properties of a Rh–diamine complex anchored on activated carbon: effect of different surface oxygen groups. Appl. Catal. A Gen. 331, 26–33.

Lovley, D.R., 2006. Bug juice: harvesting electricity with microorganisms. Nat. Rev. Microbiol. 4, 497–508. https://doi.org/10.1038/nrmicro1442

Lovley, D.R., Coates, J.D., Blunt-Harris, E.L., Phillips, E.J.P., Woodward, J.C., 1996. Humic

substances as electron acceptors for microbial respiration. Nature. https://doi.org/10.1038/382445a0

Lovley, D.R., Walker, D.J.F., 2019. Geobacter Protein Nanowires . Front. Microbiol. .

Lovley, D R, Fraga, J L, Blunt-Harris, E L, Hayes, L A, Phillips, E J P, Coates, J D, Lovley, Derek R, Fraga, Jocelyn L, Blunt-Harris, Elizabeth L, Hayes, Lory A, Phillips, Elizabeth J P, Coates, John D, 1998. Humic Substances as a Mediator for Microbially Catalyzed Metal Reduction Huminstoffe als Vermittler bei der mikrobiell katalysierten Metallreduktion. Acta Hydrochim. hydrobiol 26.

Lowell, S., Shields, J.E., Thomas, M.A., Thommes, M., 2012. Characterization of porous solids and powders: surface area, pore size and density. Springer Science & Business Media.

Marsili, E., Rollefson, J.B., Baron, D.B., Hozalski, R.M., Bond, D.R., 2008. Microbial biofilm voltammetry: Direct electrochemical characterization of catalytic electrode-attached biofilms. Appl. Environ. Microbiol. 74, 7329–7337. https://doi.org/10.1128/AEM.00177-08

Miccoli, I., Edler, F., Pfnür, H., Tegenkamp, C., 2015. The 100th anniversary of the four-point probe technique: the role of probe geometries in isotropic and anisotropic systems. J. Phys. Condens. Matter 27, 223201.

Morita, M., Malvankar, N.S., Franks, A.E., Summers, Z.M., Giloteaux, L., Rotaru, A.E., Rotaru, C., Lovley, D.R., 2011. Potential for Direct Interspecies Electron Transfer in Methanogenic Wastewater Digester Aggregates. MBio 2, e00159-11. https://doi.org/10.1128/mBio.00159-11

Nevin, K.P., Holmes, D.E., Woodard, T.L., Hinlein, E.S., Ostendorf, D.W., Lovley, D.R., 2005. Geobacter bemidjiensis sp. nov. and Geobacter psychrophilus sp. nov., two novel Fe(III)-reducing subsurface isolates. Int. J. Syst. Evol. Microbiol. 55, 1667–1674. https://doi.org/10.1099/ijs.0.63417-0

Pandey, A., Suter, H., He, J.Z., Hu, H.W., Chen, D., 2021. Dissimilatory nitrate ammonification and N2 fixation helps maintain nitrogen nutrition in resource-limited rice paddies. Biol. Fertil. Soils 57, 107–115. https://doi.org/10.1007/s00374-020-01508-2

Peñacoba-Antona, L., Senán-Salinas, J., Aguirre-Sierra, A., Letón, P., Salas, J.J., García-Calvo, E., Esteve-Núñez, A., 2021. Assessing METland® design and performance through LCA: techno-environmental study with multifunctional unit perspective. Front. Microbiol. In press.

Perez-Roa, R.E., Tompkins, D.T., Paulose, M., Grimes, C.A., Anderson, M.A., Noguera, D.R., 2006. Effects of localised, low-voltage pulsed electric fields on the development and inhibition of Pseudomonas aeruginosa biofilms. Biofouling 22, 383–390. https://doi.org/10.1080/08927010601053541

Pierra, M., Carmona-Martínez, A.A., Trably, E., Godon, J.J., Bernet, N., 2015. Microbial characterization of anode-respiring bacteria within biofilms developed from cultures previously enriched in dissimilatory metal-reducing bacteria. Bioresour. Technol. 195, 283–287. https://doi.org/10.1016/j.biortech.2015.07.010

Prado, A., Berenguer, R., Berná, A., Esteve-Núñez, A., 2020. Simultaneous characterization of porous and non-porous electrodes in microbial electrochemical systems. MethodsX 7. https://doi.org/10.1016/j.mex.2020.101021

Prado, A., Berenguer, R., Esteve-Núñez, A., 2019. Electroactive biochar outperforms highly conductive carbon materials for biodegrading pollutants by enhancing microbial extracellular electron transfer. Carbon N. Y. 146. https://doi.org/10.1016/j.carbon.2019.02.038

Prado, Amanda, Ramírez-Vargas, C.A., Arias, C.A., Esteve-Núñez, A., 2020. Novel bioelectrochemical strategies for domesticating the electron flow in constructed wetlands. Sci. Total Environ. 735, 139522. https://doi.org/10.1016/j.scitotenv.2020.139522

Pun, Á., Boltes, K., Letón, P., Esteve-nuñez, A., 2019. Bioresource Technology Reports Detoxification of wastewater containing pharmaceuticals using horizontal flow bioelectrochemical filter. Bioresour. Technol. Reports 7, 100296. https://doi.org/10.1016/j.biteb.2019.100296

Ramírez-vargas, C.A., Arias, C.A., Carvalho, P., Zhang, L., Esteve-núñez, A., Brix, H., 2019. Science of the Total Environment Electroactive bio fi lm-based constructed wetland (EABB-CW): A mesocosm-scale test of an innovative setup for wastewater treatment. Sci. Total Environ. 659, 796–806. https://doi.org/10.1016/j.scitotenv.2018.12.432

Ramírez-Vargas, C.A., Arias, C.A., Carvalho, P., Zhang, L., Esteve-Núñez, A., Brix, H., 2019. Electroactive biofilm-based constructed wetland (EABB-CW): A mesocosm-scale test of an innovative setup for wastewater treatment. Sci. Total Environ. 659, 796–806. https://doi.org/10.1016/j.scitotenv.2018.12.432

Ramírez-Vargas, C.A., Prado, A., Arias, C.A., Carvalho, P.N., Esteve-Núñez, A., Brix, H., 2018. Microbial electrochemical technologies for wastewater treatment:

Principles and evolution from microbial fuel cells to bioelectrochemical-based constructed wetlands. Water (Switzerland) 10. https://doi.org/10.3390/w10091128

Ren, S., Usman, M., Tsang, D.C.W., Sompong, O., Angelidaki, I., Zhu, X., Zhang, S., Luo, G., 2020. Energy and Climate Hydrochar-facilitated anaerobic digestion : Evidence for direct interspecies electron transfer mediated through surface oxygen-containing functional groups. https://doi.org/10.1021/acs.est.0c00112

Rios-Del Toro, E.E., Valenzuela, E.I., Ramírez, J.E., López-Lozano, N.E., Cervantes, F.J., 2018. Anaerobic Ammonium Oxidation Linked to Microbial Reduction of Natural Organic Matter in Marine Sediments. Environ. Sci. Technol. Lett. 5, 571–577. https://doi.org/10.1021/acs.estlett.8b00330

Rodrigo Quejigo, J., Rosa, L.F.M., Harnisch, F., 2018. Electrochemical characterization of bed electrodes using voltammetry of single granules. Electrochem. commun. 90, 78–82. https://doi.org/10.1016/j.elecom.2018.04.009

Rotaru, A.E., Yee, M.O., Musat, F., 2021. Microbes trading electricity in consortia of environmental and biotechnological significance. Curr. Opin. Biotechnol. 67, 119–129. https://doi.org/10.1016/j.copbio.2021.01.014

Saheb-alam, S., Persson, F., 2019. Response to starvation and microbial community composition in microbial fuel cells enriched on different electron donors. https://doi.org/10.1111/1751-7915.13449

Scholz, V. V., Meckenstock, R.U., Nielsen, L.P., Risgaard-Petersen, N., 2020. Cable bacteria reduce methane emissions from rice-vegetated soils. Nat. Commun. 11, 1–5. https://doi.org/10.1038/s41467-020-15812-w

Scholz, V. V., Müller, H., Koren, K., Nielsen, L.P., Meckenstock, R.U., 2019. The rhizosphere of aquatic plants is a habitat for cable bacteria. FEMS Microbiol. Ecol. 95. https://doi.org/10.1093/femsec/fiz062

Shaw, D.R., Ali, M., Katuri, K.P., Gralnick, J.A., Reimann, J., Mesman, R., van Niftrik, L., Jetten, M.S.M., Saikaly, P.E., 2020. Extracellular electron transfer-dependent anaerobic oxidation of ammonium by anammox bacteria. Nat. Commun. 11, 1–12. https://doi.org/10.1038/s41467-020-16016-y

Shi, L., Dong, H., Reguera, G., Beyenal, H., Lu, A., Liu, J., Yu, H.Q., Fredrickson, J.K., 2016. Extracellular electron transfer mechanisms between microorganisms and minerals. Nat. Rev. Microbiol. 14, 651–662. https://doi.org/10.1038/nrmicro.2016.93

Shrestha, P.M., Rotaru, A.E., 2014. Plugging in or going wireless: Strategies for interspecies electron transfer. Front. Microbiol. 5, 1–9.

https://doi.org/10.3389/fmicb.2014.00237

Sun, T., Levin, B.D.A., Guzman, J.J.L., Enders, A., Muller, D.A., Angenent, L.T., Lehmann, J., 2017. Rapid electron transfer by the carbon matrix in natural pyrogenic carbon. Nat. Commun. 8, 1–12. https://doi.org/10.1038/ncomms14873

Tang, C., Zhao, Y., Kang, C., Yang, Y., Morgan, D., Xu, L., 2019. Towards concurrent pollutants removal and high energy harvesting in a pilot-scale CW-MFC: Insight into the cathode conditions and electrodes connection. Chem. Eng. J. 373, 150–160. https://doi.org/10.1016/j.cej.2019.05.035

Tejedor-Sanz, S., Fernández-Labrador, P., Hart, S., Torres, C.I., Esteve-Núñez, A., 2018. Geobacter Dominates the Inner Layers of a Stratified Biofilm on a Fluidized Anode During Brewery Wastewater Treatment . Front. Microbiol. .

Tejedor-Sanz, S., Fernández-Labrador, P., Manchón, C., Esteve-Núñez, A., 2020. Fluidized bed cathodes as suitable electron donors for bacteria to remove nitrogen and produce biohydrogen. Electrochem. commun. 116, 106759. https://doi.org/10.1016/j.elecom.2020.106759

Tejedor-Sanz, S., Quejigo, J.R., Berná, A., Esteve-Núñez, A., 2017. The Planktonic Relationship Between Fluid-Like Electrodes and Bacteria: Wiring in Motion. ChemSusChem 10, 693–700. https://doi.org/10.1002/cssc.201601329

Torres, C.I., Krajmalnik-Brown, R., Parameswaran, P., Marcus, A.K., Wanger, G., Gorby, Y.A., Rittmann, B.E., 2009. Selecting anode-respiring bacteria based on anode potential: Phylogenetic, electrochemical, and microscopic characterization. Environ. Sci. Technol. 43, 9519–9524. https://doi.org/10.1021/es902165y

Vartapetian, B.B., Jackson, M.B., 1997. Plant adaptations to anaerobic stress. Ann. Bot. 79, 3–20. https://doi.org/10.1006/anbo.1996.0295

Vymazal, J., 2008. The use constructed wetlands with horizontal sub-surface flow for various types of wastewater 5, 1–17. https://doi.org/10.1016/j.ecoleng.2008.08.016

Wang, X., Aulenta, F., Puig, S., Esteve-Núñez, A., He, Y., Mu, Y., Rabaey, K., 2020. Microbial electrochemistry for bioremediation. Environ. Sci. Ecotechnology 1, 100013. https://doi.org/10.1016/j.ese.2020.100013

Xu, F., Cao, F. qian, Kong, Q., Zhou, L. lu, Yuan, Q., Zhu, Y. jie, Wang, Q., Du, Y. da, Wang, Z. de, 2018. Electricity production and evolution of microbial community in the constructed wetland-microbial fuel cell. Chem. Eng. J. 339, 479–486. https://doi.org/10.1016/j.cej.2018.02.003

Yadav, A.K., Dash, P., Mohanty, A., Abbassi, R., Mishra, B.K., 2012. Performance

assessment of innovative constructed wetland-microbial fuel cell for electricity production and dye removal. Ecol. Eng. 47, 126–131. https://doi.org/10.1016/j.ecoleng.2012.06.029

Yang, G., Han, L., Wen, J., Zhou, S., 2013. Pseudomonas guangdongensis sp. nov., isolated from an electroactive biofilm, and emended description of the genus Pseudomonas Migula 1894. Int. J. Syst. Evol. Microbiol. 63, 4599–4605. https://doi.org/10.1099/ijs.0.054676-0

Yang, W.H., Weber, K.A., Silver, W.L., 2012. Nitrogen loss from soil through anaerobic ammonium oxidation coupled to iron reduction. Nat. Geosci. 5, 538–541. https://doi.org/10.1038/ngeo1530

Yuan, Y., Bolan, N., Prévoteau, A., Vithanage, M., Biswas, J.K., Ok, Y.S., Wang, H., 2017. Applications of biochar in redox-mediated reactions. Bioresour. Technol. 246, 271–281. https://doi.org/10.1016/j.biortech.2017.06.154

Zhang, L., Lyu, T., Ramírez Vargas, C.A., Arias, C.A., Carvalho, P.N., Brix, H., 2018. New insights into the effects of support matrix on the removal of organic micro-pollutants and the microbial community in constructed wetlands. Environ. Pollut. 240, 699–708. https://doi.org/10.1016/j.envpol.2018.05.028

Zhao, G., Ma, F., Wei, L., Chua, H., Chang, C., Zhang, X., 2012. Electricity generation from cattle dung using microbial fuel cell technology during anaerobic acidogenesis and the development of microbial populations. Waste Manag. 32, 1651–1658. https://doi.org/10.1016/j.wasman.2012.04.013

Zhuang, L., Zheng, Y., Zhou, S., Yuan, Y., Yuan, H., Chen, Y., 2012. Scalable microbial fuel cell (MFC) stack for continuous real wastewater treatment. Bioresour. Technol. 106, 82–8. https://doi.org/10.1016/j.biortech.2011.11.019

2.7. Supplementary Information

Table S2.1. Physiochemical characteristics of bed materials.

	ec- Coke (C)	ec-Biochar (ecB)	nc-Biochar (nc-B)	Gravel (G)
Density (g/cm^3)	2.2533	1.7767	1.4272	2.6909
S_{BET} (m^2/g)	1.2	306	1.3	< 1
$V_{0.995}$ (cm^3/g)	0.006	0.177	0.006	0.000
$V_{DR}(N_2)$ (cm^3/g)	0.000	0.117	0.000	0.000
V_{meso} (cm^3/g)	0.006	0.059	0.006	0.000
$A_{DR}(CO_2)$ (m^2/g)	3	627	393	---
$V_{DR}(CO_2)$ (cm^3/g)	0.001	0.213	0.169	---
$V_{INTRUDED}$(Hg) (cm^3/g)	0.2941	0.2205	0.0909	0.0124
Porosity (%)	45.95	36.81	53.07	1.61
CO_2 (µmol/g)	70	605	1950	---
CO_2 (µmol/g)	40	995	2725	---
O (µmol/g)	180	2200	6630	---
Conductivity [S/cm]	10.42	5.84*10-4	2.55*10-9	---
Granulometry [cm]	1.5-3	1.5-3	1.5-3	1.5-3

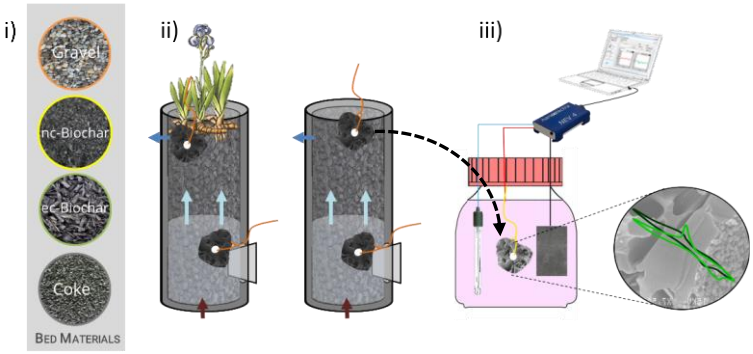

Figure S2.1. Scheme of how the cyclic voltammetries of single granules were carried out. From left to right: (i) materials used as a bed, (ii) locations of selected granules, (iii) single chamber to performed CVs.

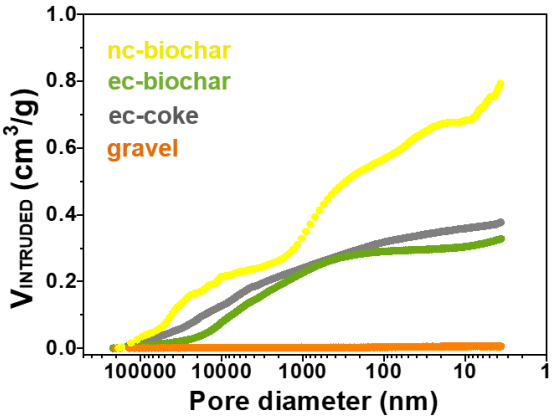

Figure S2.2. Hg intrusion curves of the different biofilter materials.

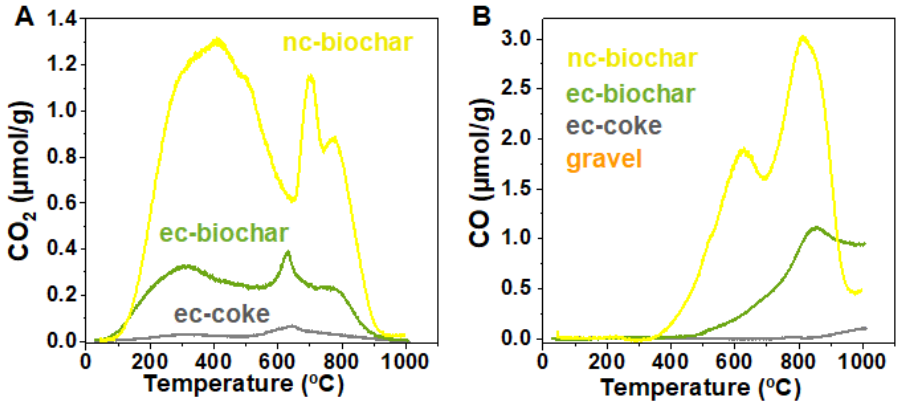

Figure S2.3. CO2- and (d) CO-evolution from TPD experiments for the different carbonaceous biofilter materials.

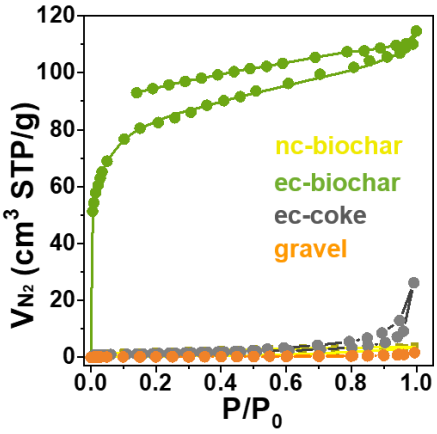

Figure S2.4. N_2 adsorption-desorption isotherms at -196 °C of the different biofilter materials.

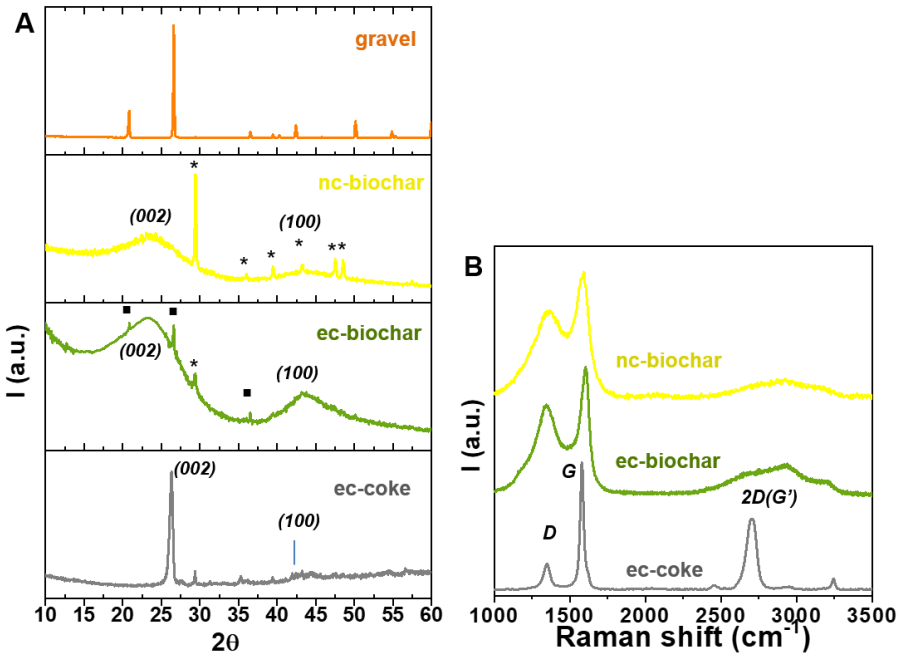

Figure S2.5. X-ray diffractograms (A) and Raman spectra (B) of the different biofilter materials. The * and ■ symbols in the diffractograms showed the presence of adventitious CaCO3 and SiO2, respectively.

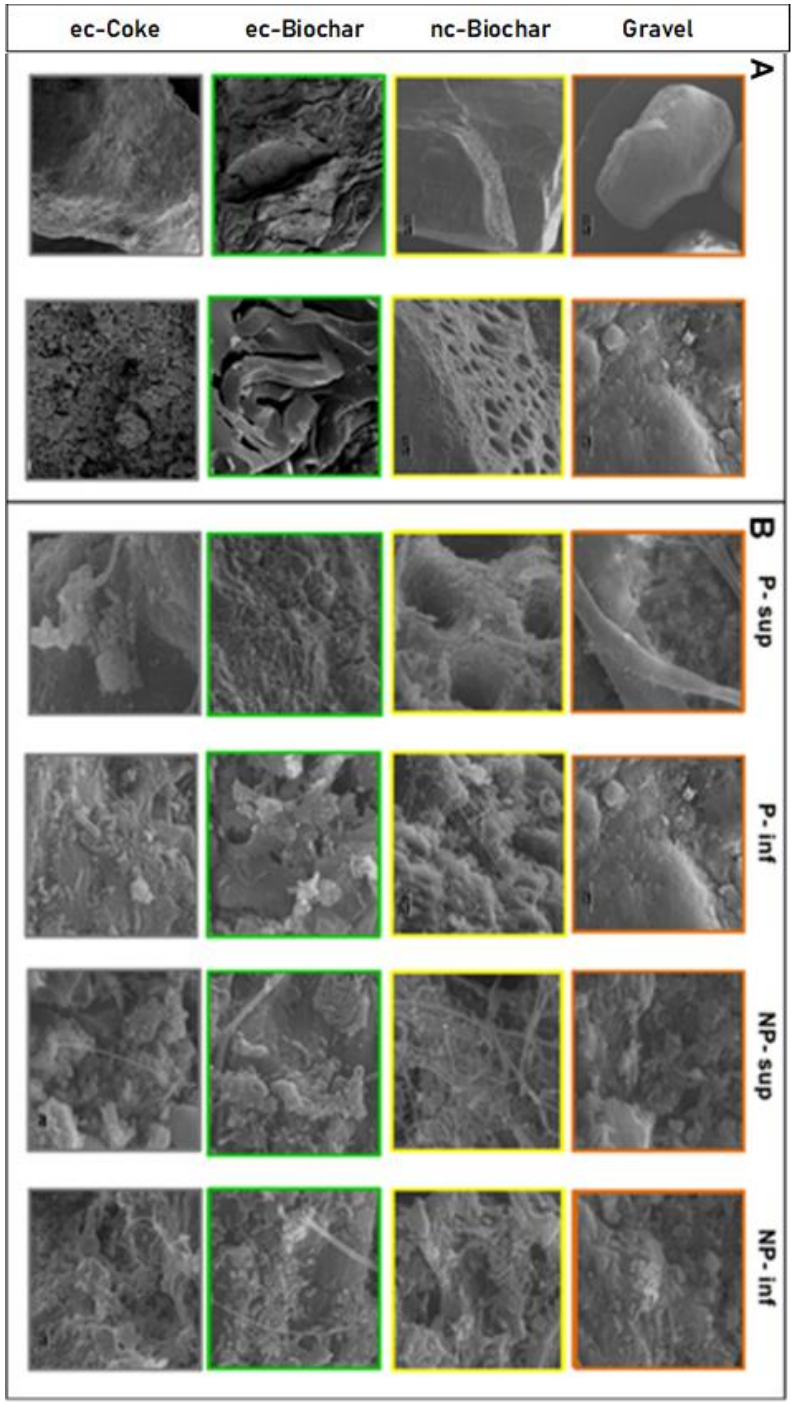

Figure S2.6. SEM micrographs of granules from the eight systems (four material (G, ncB, ecB andec C) and planted (P) and unplanted (NP)) at upper (sup) and bottom (inf) layer. The granules were abiotic (A) and materials at day 20 (B).

Table S2.2. Influent and effluent COD concentration, removal rate and efficiency for the different systems during 0-10 days and 10-20 days.

		COD Concentration [mg L^{-1}]					COD Removal rate [g/m3 day]				COD Efficiency [%]			
	Biofilter	Influent	G	ncB	ecB	ecC	G	ncB	ecB	ecC	G	ncB	ecB	ecC
0-10 days	Planted	862.0±3	508.0±20	259.3±22	130.7±17	114.0±17	80.45±4	136.9±6	166.2±3	170.0±3	41.1±2	69.9±3	84.9±2	86.8±2
	Non-planted	862.0±3	535.0±17	251.0±18	127.3±15	107.7±15	74.3±3	138.9±3	166.9±3	171.4±3	37.9±2	70.9±2	85.2±2	87.5±2
10-20 days	Planted	862.0±3	319.3±4	153.7±4	79.3±2	88.0±3	123.3±1	160.9±1	177.9±1	175.9±1	63.0±1	82.2±1	90.8±1	89.8±1
	Non-plantd	862.0±3	418.3±8	196.0±4	89.3±3	69.3±4	100.8±2	151.4±1	175.6±1	180.2±1	51.5±1	77.3±1	89.6±1	92.0±1

Table S2.3. Influent and effluent NH_4^+ concentration and efficiency for the different systems during 0-10 days and 10-20 days.

		NH_4^+ Concentration [mg L^{-1}]					NH_4^+ Efficiency [%]			
	Biofilter	Influent	G	ncB	ecB	ecC	G	ncB	ecB	ecC
0-10 days	Planted	64.7±0.5	65.4±2	14.0±4	28.0±3	58.5±13	0	78.4±5.3	56.7±4.8	9.3±3.3
	Non-planted	64.7±0.5	67.8±14	21.3±3	45.3±5	65.3±12	0	67.2±4.7	29.9±7.6	0
10-20days	Planted	64.7±0.5	33.0±1	11.4±1	10.7±1	28.3±4	49.1±1	82.3±2	83.4±1	56.2±7
	Non-planted	64.7±0.5	37.3±1	14.5±3	22.9±1	24.7±2	42.3±4	77.7±3	64.6±1	61.8±4

Table S2.4. Functional microbes in the eight reactors (four materials (G, ncB, ecB and ecC) and planted (P) and unplanted (NP))

Name of bacteria		INF	G-P	G-NP	ncB-P	NcB-NP	ecB-P	ecB-NP	ecC-P	ecC-NP
EAB	total	268	1447	3223	6184	7869	21898	15808	2391	1787
AOB	Nitrosomonadales	19	120	113	85	29	32	37	60	21
NOB	Nitrospirales	3	27	47	23	49	7	15	63	22
DNB	*Bacillus*	208	73	62	229	459	2163	379	229	139
	Thauera	13	76	38	23	50	160	70	34	47
	total	221	149	100	252	509	2323	449	263	186
DNRA	*Desulfovibrio*	416	1258	2802	516	724	738	942	1137	1197
Anam.	Planctomycetaceae	1	5186	5430	860	4224	4411	1924	825	1759

EAB: electro active bacteria
AOB: ammonia oxidizing bacteria
NOB: nitrite-oxidizing bacteria
DNB: denitrifiying bacteria
DNRA: dissimilatory nitrate reduction to ammonium
Anammox

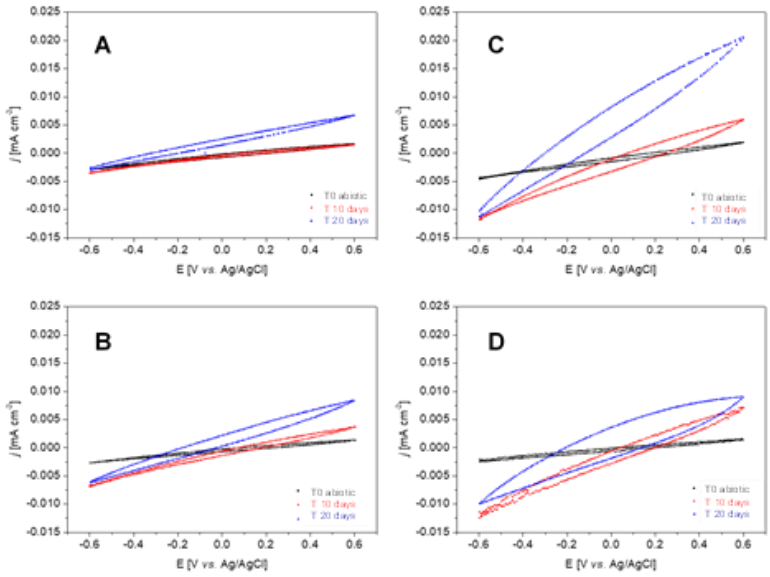

Figure S2.7. Cyclic voltammograms of a single granule of nc-biochar from the planted system (A: upper layer, B bottom layer) and non-planted system (C: upper layer, D: bottom layer) at different stages (biofilm-free (black), 10 days (red) and 20 days (blue)). Scan rate 10 mV/s; phosphate buffer 100mM, acetate 10mM.

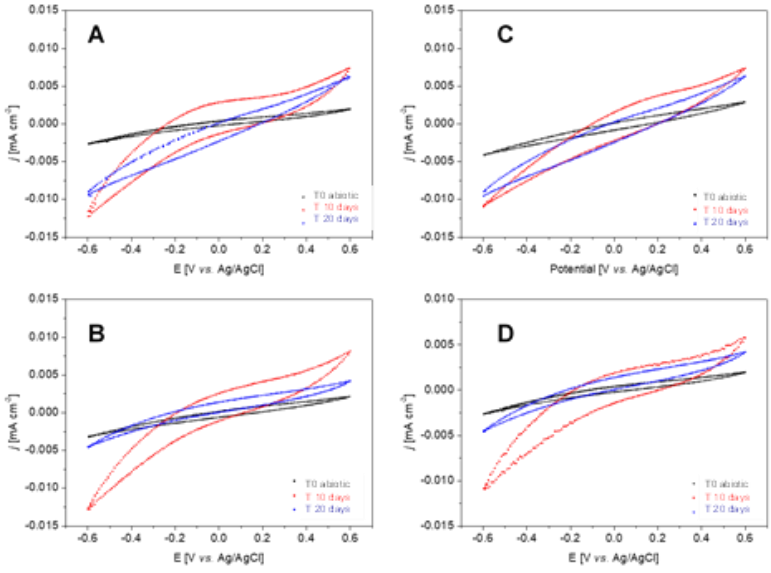

Figure S2.8. Cyclic voltammograms of a single granule of ec-biochar from the planted system (A: upper layer, B bottom layer) and non-planted system (C: upper layer, D: bottom layer) at different times (abiotic (black), 10 days (red) and 20 days (blue)). Scan rate 10 mV/s; phosphate buffer 100mM, acetate 10mM.

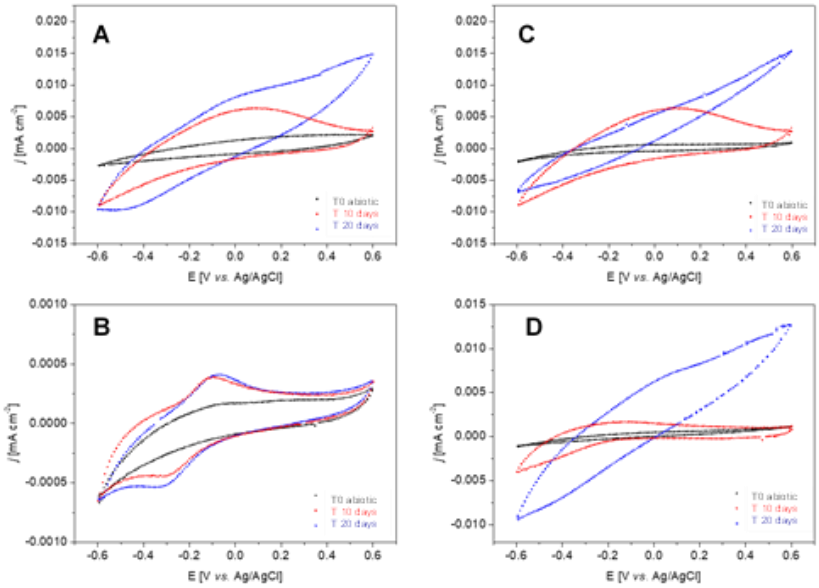

Figure S2.9. Cyclic voltammograms of a single granule of ec-coke from the planted system (A: upper layer, B bottom layer) and non-planted system (C: upper layer, D: bottom layer) at different times (abiotic (black), 10 days (red) and 20 days (blue)). Scan rate 10 mV/s; phosphate buffer 100mM, acetate 10mM.

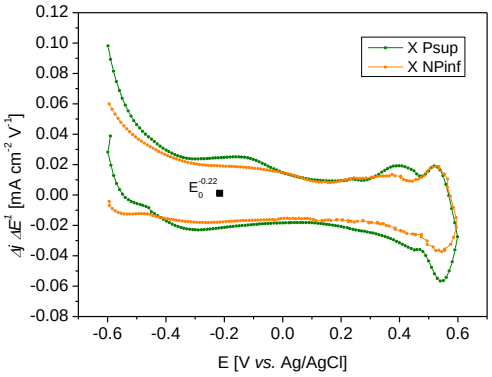

Figure S2.10. First derivative of the 20 days CVs of the coke granules, from the ecC-Psup (green) and ecC-NPinf (orange) systems. Value of the formal potential for the redox pairs.

Table S2.5. Richness indices of microbial community composition in the reactors.

Sample	Reads numbers	Species (obs)	Simpson's inverse	Simpson's index	Shannon's index	CHAO1 Index	ACE index
0 Inf	114318	1838	16.49	0.94	3.035	2584.81	2906.79
1 G-Psup	1325522	1969	49.75	0.98	3.754	2771.28	3131.22
2 G-Pinf	124664	1920	8.12	0.88	2.556	2744.87	3031.43
3 G-NPsup	114930	1771	16.34	0.94	2.924	2661.87	2881.92
4 G-NPinf	105297	1848	11.85	0.92	2.807	2660.50	2916.31
5 ncB-Psup	117288	2728	117.91	0.99	4.151	3651.46	4053.76
6 ncB-Pinf	105286	2291	15.88	0.94	2.338	3207.34	3521.51
7 ncB-NPsup	94391	2201	9.05	0.89	2.818	2931.47	3279.36
8 ncB-NPinf	108053	2276	16.80	0.94	2.946	3059.93	3481.89
9 ecB-Psup	164642	2001	17.08	0.94	3.169	2916.80	3152.98
10 ecB-Pinf	163641	1801	23.88	0.96	2.857	2476.85	2773.96
11 ecB-NPsup	149400	1884	16.61	0.94	2.831	2796.37	3062.26
12 ecB-NPinf	148659	1782	10.67	0.91	2.885	2610.78	2877.02
13 C-Psup	115627	2158	36.50	0.97	3.200	3073.41	3428.59
14 C-Pinf	124777	2217	24.71	0.96	3.031	3087.04	3400.19
15 C-NPsup	5044	594	24.78	0.96	2.816	1049.27	1115.88
16 C-NPinf	101998	2048	16.74	0.94	2.612	2862.44	3188.58

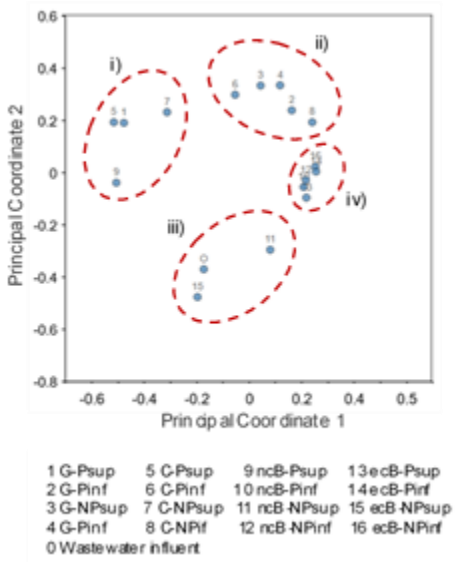

Figure S2.11. This scatterplot shows a Principal Coordinate Analysis (PCoA) of the normalized relative abundance of all the seventeen samples. The PCoA measures differences in the distribution of taxonomic classifications between samples at specie level.

Table S2.6. List of the electro active bacteria (EAB) and its main characteristics.

Level	Species	Electrode	Electron transfer	Resp.	Spore forming	Metabolism	EA	ED
Bacilli	*Bacillus subtilis*	A & C	(S) MET	AN F	yes	Mon	Sol	Sol
	Geobacillus sp. S2E	A	MET	AN F	yes	Mon	Sol	Sol
	Lactobacillus plantarum	A	MET	AN F	yes	Mon	Sol	Sol
	Staphylococcus carnosus	C		AN F	yes	Mon	Sol	Sol
	Streptococcus lactis	A	(S) MET	AN F	yes	Mon	Sol	Sol
Clostridium	*Clostridium aceticum*	C		AN	yes	Org. Ac and CO2	Sol	Flex
	Clostridium acetobutylicum	A & C	MET	AN	yes	Org. Ac	Sol	Sol
	Clostridium butyricum	A		AN	yes	Org. Ac	Flex	Sol
	Clostridium ljungdahlii	C		AN	yes	Org. Ac	Sol	Flex
	Clostridium pasteurianum	C	DET	AN	yes	Org. Ac	Sol	Flex
	Clostridium propionicum	A	MET	AN	yes	Org. Ac	Sol	Sol
	Clostridium tyrobutyricum	C	MET	AN	yes	Org. Ac	Sol	Sol
Desulfovibrio	*Desulfovibrio desulfuricans*	A	MET	AN	no	Mon	Sol	Sol
Geobacteraceae	*Geobacter anodireducens*	A	DET	AN	no	Org. Ac	Flex	Sol
	Geobacter bemidjiensis	A	DET	AN	no	Org. Ac	Flex	Sol
	Geobacter bremensis	A	DET	AN	no	Org. Ac	Flex	Sol
	Geobacter chapellei	A	DET	AN	no	Org. Ac	Flex	Sol
	Geobacter humireducens	A	DET	AN	no	Org. Ac	Flex	Sol
	Geobacter hydrogenophilus	A	DET	AN	no	Org. Ac	Flex	Sol
	Geobacter lovleyi	A & C	DET	AN	no	Org. Ac	Flex	Flex
	Geobacter metallireducens	A & C	DET	AN	no	Org. Ac	Flex	Flex
	Geobacter sulfurreducens	A & C	DET	AN	no	Org. Ac	Flex	Flex
	Geobacter uraniireducens	A	DET	AN	no	Org. Ac	Flex	Sol
	Geopsychrobacter electrodiphilus	A	DET	AN	no	Org. Ac	Flex	Sol
Euryarchaeota	*Methanobacterium palustre*	C	DET	AN	no	Org. Ac and CO2 f	Sol	Flex
	Methanococcus maripaludis	C	MET	AN	no	Org. Ac and CO2 f	Sol	Sol
Pseudomona	*Pseudomonas aeruginosa*	A & C	(S) MET	AN F	no	Mon	Sol	Sol
	Pseudomonas alcaliphila	A & C	(S) MET	AN F	no	Mon	Sol	Sol
	Pseudomonas fluorescens	A & C	MET	AN F	no	Mon	Sol	Sol
Rhodobacter	*Rhodobacter capsulatus*	A	DET	AN F	no	Mon and CO" fix.	Flex	Sol
	Rhodobacter sphaeroides	A	MET	AN F	no	Mon and CO" fix.	Sol	Sol
Rhizobiales	*Rhodopseudomonas palustris*	A & C	DET	AN F	no	Org. Ac	Flex	Flex sol
Shewanellaceae	*Shewanella amazonensis*	A & C		AN F	no	Mon	Flex	Sol
	Shewanella decolorationis	A		AN F	no	Mon	Sol	Sol
	Shewanella electrodiphila	A		AN F	no	Mon	Flex	Sol
	Shewanella frigidimarina	A	(S) MET DET	AN F	no	Mon	Sol	Sol
	Shewanella japonica	A	(S)MET	AN F	no	Mon	Flex	Sol
	Shewanella loihica	A & C	DET	AN F	no	Mon	Flex	Sol
	Shewanella marisflavi	A	DET	AN F	no	Mon	Sol	Sol
	Shewanella oneidensis	A & C	(S)MET	AN F	no	Mon	Flex	Sol
	Shewanella putrefaciens	A & C	DET	AN F	no	Mon	Flex	Sol
	Shewanella sp. ANA-3	A & C		AN F	no	Mon	Flex	Sol
	Shewanella sp. HN-41	A	(S) MET	AN F	no	Mon	Flex	Sol
Negativicutes	*Sporomusa ovata*	C		AN	yes	Org. Ac	Sol	Flex
	Sporomusa silvacetica	C		AN	yes	Org. Ac	Sol	Flex
	Sporomusa sphaeroides	C		AN	yes	Org. Ac	Sol	Flex

Electrode activity
A: anodic
C: cathodic

Electron transfer
DET: direct electron transfer
MET: mediated electron transfer
SMET: self-synthesized mediator

Respiration
AN: anaerobic
F: facultative anaerobes

Metabolism
Mon: monosaccharides
Org. Ac: organic acids
CO2 fixation

EA: electron acceptor
EA: electron donor
Sol: soluble
Flex: flexible

Table S2.7. Number of reads of each EAB species found in each region of each system.

Species	Inf	G Psup	G Pinf	G NPsup	G NPinf	ncB Psup	ncB Pinf	ncB NPsup	ncB NPinf	ecB Psup	ecB Pinf	ecB NPsup	ecB NPinf	C Psup	C Pinf	C NPsup	C NPinf
Bacillus subtilis	0	0	0	0	0	0	0	0	0	0	0	0	0	0	0	0	0
Geobacillus sp. S2E	4	4	1	0	0	0	2	4	7	2	10	1	16	3	2	1	2
Lactobacillus plantarum	0	0	0	0	0	0	0	0	0	0	0	0	0	0	0	0	0
Staphylococcus carnosus	0	0	0	0	0	0	0	0	0	0	0	0	0	0	0	0	0
Streptococcus lactis	0	0	0	0	0	0	0	0	0	0	0	0	0	0	0	0	0
Clostridium aceticum	0	0	0	0	0	0	0	0	0	0	0	0	0	0	0	0	0
Clostridium acetobutylicum	0	0	0	0	0	0	0	0	0	0	0	0	0	0	0	0	0
Clostridium butyricum	2	4	82	45	44	1	11	4	6	35	31	16	37	4	29	1	43
Clostridium ljungdahlii	0	0	4	1	6	0	3	1	0	1	0	0	1	0	0	0	0
Clostridium pasteurianum	0	0	0	0	0	0	0	0	0	0	0	0	0	0	0	0	0
Clostridium propionicum	0	0	42	19	3	3	169	51	82	127	48	60	114	44	131	2	387
Clostridium tyrobutyricum	0	1	18	2	16	0	0	0	1	0	0	0	0	33	117	0	0
Desulfovibrio desulfuricans	242	251	781	2272	761	67	346	173	293	307	360	199	274	217	544	15	903
Geobacter anodireducens	1	0	0	0	0	0	0	0	0	0	2	0	0	0	3	1	0
Geobacter bemidjiensis	2	0	6	7	1	0	2817	3361	2414	10916	3251	18524	1242	634	355	17	5
Geobacter bremensis	0	0	1	1	7	0	224	466	299	2	4	21	1	2	0	0	0
Geobacter chapellei	0	0	3	1	2	0	37	17	10	81	290	53	7	0	3	0	1
Geobacter humireducens	0	0	1	0	1	0	0	0	0	0	0	0	0	0	0	0	0
Geobacter hydrogenophilus	1	0	32	2	0	0	0	0	3	2	17	20	3	0	5	0	6
Geobacter lovleyi	10	8	1	0	1	0	5	6	11	3	4	10	53		6	0	12
Geobacter metallireducens	1	7	24	22	1	0	52	6	171	47	193	961	170	36	127	3	350
Geobacter sulfurreducens	0	0	0	0	0	0			1	0	0	0	0	0	0	0	0
Geobacter uraniireducens	0	0	5	0	0	0	2436	352	97	39	5	25	14	1	0	0	0
Geopsychrobacter electrodiphilus	0	0	0	1	0	0	1	0	1	3	0	1	0	1	0	0	0
Methanobacterium palustre	0	2	0	0	0	0	0	0	1	0	3	1	0	2	5	0	0
Methanococcus maripaludis	0	0	0	0	0	0	0	0	0	0	0	0	0	0	0	0	0
Pseudomonas aeruginosa	1	1	0	1	0	0	0	0	0	3	2	10	0	1	1	6	0
Pseudomonas alcaliphila	0	0	0	0	0	0	0	0	0	0	0	0	0	0	0	0	0
Pseudomonas fluorescens	0	0	1	0	0	1	0	0	0	3	1	0	0	0	0	0	0
Rhodobacter capsulatus	0	147	11	0	3	0	0	1	0	0	0	1	0	0	3	0	3
Rhodobacter sphaeroides	0	0	0	0	0	0	0	26	0	0	0	0	0	0	0	0	1
Rhodopseudomonas palustris	0	1	0	0	0	0	0	0	0	0	0	0	0	0	1	0	0
Shewanella amazonensis	0	1	1	0	0	0	0	0	0	0	0	3	1	0	0	0	1
Shewanella decolorationis	0	0	0	0	0	0	0	0	0	0	0	0	0	0	0	0	0
Shewanella electrodiphila	0	0	0	0	0	0	0	0	0	0	0	0	0	0	0	0	0
Shewanella frigidimarina	0	0	0	0	0	0	0	0	0	0	0	0	0	0	0	0	0
Shewanella japonica	0	0	0	0	0	0	0	0	0	0	0	0	0	0	0	0	0
Shewanella loihica	0	0	0	0	0	0	0	0	0	0	0	0	0	0	0	0	0
Shewanella marisflavi	0	0	0	0	0	0	0	0	0	0	0	0	0	0	0	0	0
Shewanella oneidensis	0	0	0	0	0	0	0	0	0	0	0	0	1	0	0	0	0
Shewanella putrefaciens	0	2	0	0	0	0	0	0	0	0	1	0	11	0	0	0	0
Shewanella sp. ANA-	0	0	0	0	1	0	0	0	0	0	0	0	0	0	0	0	27
Shewanella sp. HN-41	0	0	0	0	0	0	0	0	0	0	0	0	0	0	0	0	0
Sporomusa ovata	4	2	1	2	0	0	6	2	2	4	8	42	4	15	60	0	0
Sporomusa silvacetica	0	0	1	0	0	0	3	0	0	0	3	1	0	0	6	0	0
Sporomusa sphaeroides	0	0	0	0	0	0	0	0	0	0	0	0	0	0	0	0	0

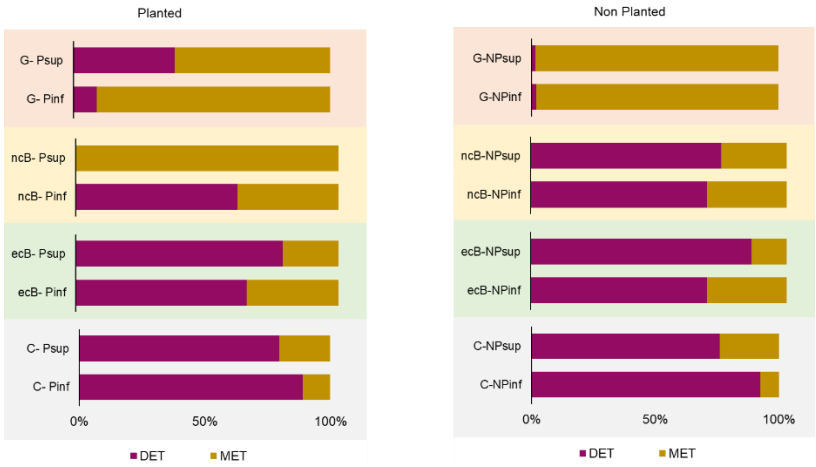

Figure S2.12. Microbial community composition of the eight reactors (four materials (G, ncB, ecB and ecC), planted (P) and unplanted (NP), and upper (sup) and bottom (inf) layer) at phylum (A) and class (B) level.

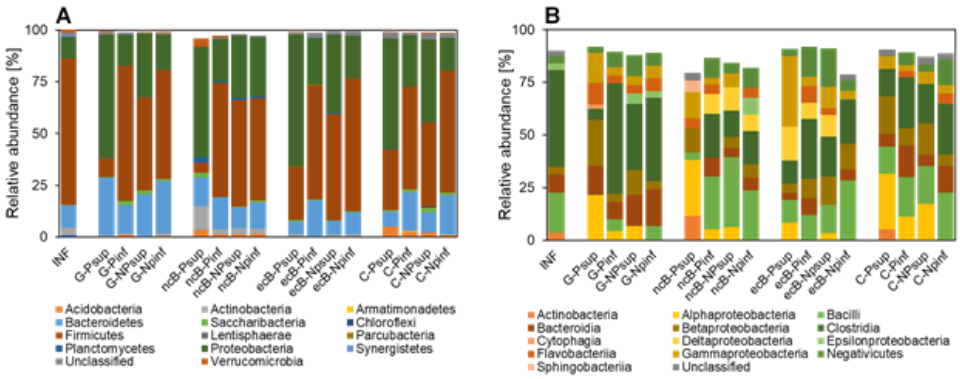

Figure S2.13. Microbial community composition of the eight reactors (four materials (G, ncB, ecB and ecC), planted (P) and unplanted (NP), and upper (sup) and bottom (inf) layer) at phylum (A) and class (B) level.

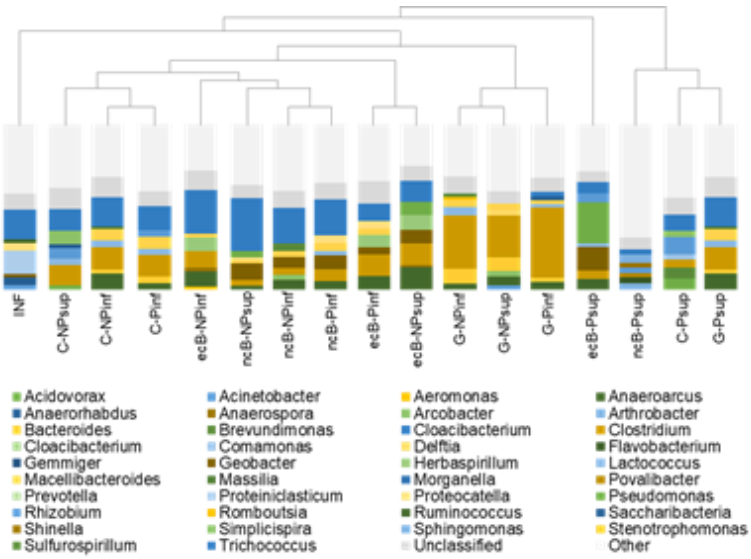

Figure S2.14. This dendrogram shows a hierarchical clustering of samples based on genus-level classifications. The barchart beneath each sample show the relative abundance of its genus-level classifications.

CHAPTER 3:

EC-BIOCHAR OUTPERFORMS HIGHLY CONDUCTIVE CARBON MATERIALS FOR BIODEGRADING POLLUTANTS BY ENHANCING MICROBIAL EET

This section has been redrafted after:

Amanda Prado de Nicolás[a,b] , Raúl Berenguer[b,c], Abraham Esteve-Núñez[a,b]. 2019. *Electroactive biochar outperforms highly conductive carbon materials for biodegrading pollutants by enhancing microbial extracellular electron transfer*. Carbon, 146, 597-609.

A Prado[a,b], R Berenguer[b,c], A Berná[a,b], A Esteve-Núñez[a,b]. 2020. *Simultaneous characterization of porous and non-porous electrodes in microbial electrochemical systems. MethodsX, 7, 101021.*

[a] Department of Analytical Chemistry, Physical Chemistry and Chemical Engineering, University of Alcalá, Alcalá de Henares, Spain
[b] IMDEA Water Institute, Alcalá de Henares, Madrid, Spain
[c] Instituto Universitario de Materiales, Departamento Química Física, Universidad de Alicante, Alicante, Spain

500 10kV WD12
OH
O
CO_2
e⁻
15KV X4,000 1PW WD
OH
O
CO_2
e⁻
cycle
1264 15KV
OH
O
CO_2
e⁻

Electroactive biochar outperforms highly conductive carbon materials for biodegrading pollutants by enhancing microbial extracellular electron transfer

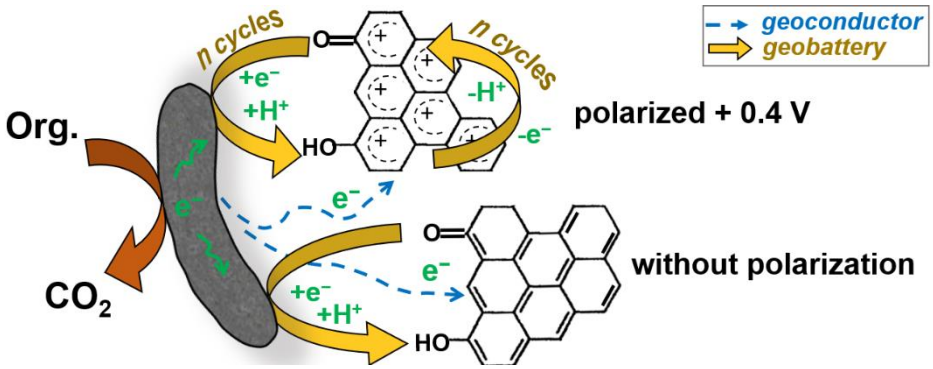

3.1. Abstract

The development and full-scale application of microbial electrochemical technologies (METs) for wastewater treatment demand massive amounts of electroconductive carbon materials to promote extracellular electron transfer (EET) and biodegradation. While the potential capability of these materials and their properties to design efficient systems is still in their infancy, the state-of-the-art METs are based on highly-conductive fossil-derived carbons. In this work we evaluate the performance of different electroconductive carbon materials (graphite, coke, biochar) for supporting microbial EET and treating urban wastewater. Our results reveal that the electroconductive biochar was the most efficient biofilter-material, enabling to stimulate bioremediation at anodic potential as high as 0.6 V (maximum removal efficiency (92%) and degradation rate (185 gCOD $m^{-3}d^{-1}$), and to fulfil the discharge limits under conditions where the other materials failed. A deep materials characterization suggests that, despite electroconductivity is necessary, the optimal EET on biochar can be mainly assigned to its large number of electroactive surface oxygen functionalities, which can reversibly exchange electrons through the geobattery mechanism. We propose the modulation of quinone-like e-acceptors by anodic polarization to promote the biodegradation capability of carbon

materials. Because of its great efficiency and sustainability, electroactive biochar will greatly expand the applicability of METs at large scale.

3.2. Introduction

Microbial Electrochemical Technologies (METs) (Logan et al., 2012, Wang et al., 2013) constitute a plethora of emerging technologies based in the fascinating capacity of some microorganisms, so-called electroactive, for establishing a direct redox interaction with electrically conductive materials. Electrons produced by the metabolism of electroactive bacteria can be transferred to an electrode, which acts as terminal electron acceptor as any other natural acceptor like oxygen, nitrate or Fe(III)-oxides (Caccavo et al., 1994, Speers et al., 2012). The clear advantage of exploiting electro-stimulated communities is that electrodes can boost microbial metabolism in anaerobic systems that are typically electron acceptor limited. Electroconductive material may represent an inexhaustible source of electron acceptors, hosting the additional advantage of providing a more easily modulated redox potential compared to standard, low-reducing redox species that generally drive these systems (Aguirre-Sierra et al., 2016). The redox potential of the electrode depends on the chemistry and bioelectrochemistry around the electrode. Moreover, the electrochemical characteristics of those microbial-assisted devices can be simply controlled by altering their configuration. Thus, they can be operated in different configurations, such as i) short-circuit Cell, with no resistors between electrodes (Aguirre-Sierra et al., 2016, Aulenta et al., 2013, Quejigo et al., 2018, Domínguez-Garay et al., 2018); ii) Microbial Electrochemical Cell (MFC), able to harvest energy in the presence of a resistor (Logan et al., 2012, Wang et al., 2013); and iii) Microbial Electrolysis Cell (MEC) by poising a certain electrode potential through a potentiostat or a power source (Logan et al., 2012, Wang et al., 2013). Regardless the configuration, one of the main application of MET is the wastewater treatment, a process based on oxidizing organic and inorganic matter coupled to a harvested microbial electrical current (Logan et al., 2012, Wang et al., 2013).

In spite of the limiting number of MET-based technologies with potential to reach full scale applications, there is at least one proved to be successful. Such application was originally inspired by the biofilter concept in constructed wetlands, a natural system for treating wastewater using inert material (Kaldec and Wallace, 2009). The integration of METs in the concept of a constructed wetland resulted in the so-called METland®, a new hybrid technology for treating urban wastewater in decentralized systems in a sustainable way with no energy cost (iMETland.eu). The newborn configuration (Aguirre-Sierra et al., 2016) was reported for the first time by constructing subsurface flow biofilters made of electroconductive coke able to clean-up urban effluents at rates higher that standard biofilters made of inert materials, like gravel. Such an enhancement was exclusively attributed to a positive effect of the electroconductivity of coke without any evidence of clogging classically associated to biofilter systems (Aguirre-Sierra et al., 2016).

In this context, full scale applications of METland® using large carbon biofilters (> 50 m3), are under construction at present (iMETland.eu). The nature and properties of the carbon material may determine not only the performance of the biofilter, but also the cost and sustainability of this technology. However, the capabilities of different carbon materials have not been explored yet. Thus, while the best candidates and/or the required properties that enable the optimization of these systems are still uncertain, the potential impact of METland® cannot be estimated. In addition, little can be deduced from literature so far because the studies about electroactive bacteria and materials properties are still in their infancy. First, the nature of bacteria extracellular electron transfer (EET) mechanisms involved in METs is still controversial (Patil et al., 2012). Second, despite numerous bacteria-electrode interactions have been described in METs (Lovly et al., 2012, Xie et al., 2015, Lu et al., 2015, Sonawane et al., 2017, Hindatu et al., 2017, Tejedor-Sanz et al, 2017), little is undoubtedly known about the performance-determining electrode properties. This must be due to the complex nature of carbon materials, showing a wide range of intercorrelated properties, and the lack of systematic studies analyzing the effect of only a given electrode property, configuration, etc. In this sense, whereas some authors point

out that the electroconductivity may be crucial for effective direct electron transfer (e-transfer) from bacteria to carbon (graphitic) matrices (Sun et al., 2017), what has been referred to as "geoconductor" mechanism, others suggest that this reaction primarily needs the mediation of electroactive oxygen surface groups (Yuan et al., 2017). Because the transferred electrons can be stored (on carbon basal planes or chemical bonds) and reversibly exchanged in biogeochemical processes, both e-transfer mechanisms have been associated to the so-called "geocapacitor" and "geobattery" behaviors, respectively (Sun et al., 2017). Finally, most of the studies deal with MFCs (Xie et al., 2015, Lu et al., 2015, Sonawane et al., 2017, Hindatu et al., 2017), aiming at generating electrical power, so it is generally believed that the conductivity is the desired property of electrodes to optimize the microbial activity in METs (Xie et al., 2015, Lu et al., 2015, Sonawane et al., 2017, Hindatu et al., 2017). Hence, systematic studies on the influence of the carbon material and its properties in METland® and other METs are necessary.

On the other hand, environmental concerns arise from the utilization of large amounts of carbon materials in full-scale METland® and other METs. In this context, the replacement of highly conductive carbon materials obtained from fossil resources, by those derived from renewable wastes, biomass and natural polymers, constitutes a hot topic of circular economy and big challenge among the scientific community (Qian et al., 2015, Titirici et al., 2012, Jiang et al., 2013Huggins et al., 2014, Sennu et al., 2016, Kaetzl et al., 2018).

Given the lack of fundamental knowledge on the influence of carbon properties in METs performance and e-transfer mechanisms; and the need of more sustainable biofilter materials for large-scale applications, in this work, the potential application of distinct carbon materials for wastewater treatment in METland® was investigated for the first time. Special attention was paid on the physicochemical and electrochemical characterization of these materials to find out properties-performance correlations and more meaningful conclusions. We demonstrate that the electrical conductivity is not the property determining optimal EET and biodegradation performance, but it governs the current production in these microbial electrochemical systems. Interestingly,

electroconductive biochar, exhibiting a large number of electro-active functional groups, revealed itself as the most efficient and sustainable biocompatible material for promoting microbial EET. Furthermore, we first propose the continuous regeneration of electroactive e-accepting quinone functionalities on biochar by anodic polarization to promote or modulate the biodegradation performance of carbon biofilters. All these results are considered to greatly progress the understanding of the e-transfer mechanisms on carbon surfaces through the geoconductor and geobattery mechanisms.

3.3. Material and methods

3.3.1 Bed materials

The graphite (G) and the coke (C) were provided by METfilter SL. (Spain) The biochar (QB) was produced from Quercus wood by Piroeco Bioenergy S.L. A siliceous gravel (Azulejos Manchegos S.L., Spain) was used as a non-conductive material (NC). All the materials had a granular structure with a particle size ranging between 6 to 12 mm.

3.3.2 Characterization of bed materials

The surface morphology of the materials was studied by scanning electron microscopy (SEM), using a JSM-840 JEOL microscope working at 15 kV. X-ray diffraction (XRD) measurements were performed in a KRISTALLOFLEX K 760–80F diffractometer (Bruker D8-Advance) by using a Ni-filtered Cu Kα radiation (λ = 1.5416 Å) generated at 40 kV and 40 mA. Diffraction data points were recorded stepwise within 2θ = 10-60° at a scan rate of 0.56 or 0.83°/min, for the biochar or the rest of samples, respectively, with a scan step of 0.05° in 2θ. The crystallite dimensions (Lc or La), were calculated from the full width at half maximum (FWHM) of (002) and (10) reflections, respectively, by using the Scherrer's equation (Klung et al., 1974). Raman spectra were recorded on a Jasco NRS-5100 dispersive system using a frequency-doubled Nd:YAG 532 nm laser, with a maximal spectral resolution of 1 cm^{-1}, and a Peltier cooled CCD detector. Electrical conductivity measurements were carried out by using a Lucas Lab resistivity equipment with four probes in-line. The samples were

dried under vacuum for 24 h and shaped into pellets of 0.013 m diameter by applying a pressure of $7.4 \cdot 10^8$ Pa.

The porous texture was characterized by N_2 adsorption-desorption at -196 °C and by CO_2 adsorption at 0 °C (in the case of microporous samples), using a Quadrasorb-Kr/MP (Quantrachrome Corporation) apparatus. Samples were previously outgassed for 6 h at 150 °C under vacuum. From the N_2 adsorption/desorption isotherm, the specific surface area (S_{BET}) was calculated using the BET equation (Lozano-Castelló et al., 2010). The micropore volume (Vt) and the external surface area (At) were determined using the t-method. The mesopore volume (V_{mes}) was calculated as the difference between total pore volume ($V_{0.995}$, volume at relative pressure of 0.995) and micropore volume (Lozano-Castelló et al., 2010). The narrow micropore volume (V_{CO2}) and the narrow micropore surface area (S_{CO2}) were estimated for the biochar by applying the Dubinin-Radushkevich equation to the CO_2 adsorption isotherm (Lozano-Castelló et al., 2010). The pore volume and dimensions were further characterized by Hg intrusion-extrusion porosimetry, using a PoreMaster 60-GT porosimeter (Quantachrome Instruments) with applied pressures from 6.84 to 408330 kPa. The Washburn equation was utilized to relate the applied pressure with the pore diameter Lowell et al., 2004.

The surface chemistry of the carbon materials was analyzed by X-ray photoelectron spectroscopy (XPS) in a K-Alpha spectrometer (Thermo-Scientific) with MgKα radiation (1253.6 eV). For the analysis of the XPS peaks, the C 1s peak position was set at 284.5 eV and used as reference to stablish the binding energy of the other peaks. The amount and nature of oxygen surface groups present on the carbon materials were studied by temperature-programmed desorption (TPD) experiments in a simultaneous TGA/DSC 2 equipment (Mettler-Toledo) coupled to a mass spectrometer (ThermoStar GSD 301 T, Pfeiffer Vacuum). In these experiments, around 20 mg of the carbon sample were heated up to 1000 °C at 20 °C/min under a He flow rate of 100 mL/min. Upon heating, surface oxygen groups on carbon materials decompose producing CO and CO_2 at different temperatures as a function of their thermal stability (Figueiredo et al., 1999). The quantification of the evolved CO and CO_2

groups was done by using a calcium oxalate monohydrate calibration and considering the CO disproportionation.

The microbial electrochemical response was studied by cyclic voltammetry in a H-type cell. Three different granules (one of each conductive materials) of ca. 1 cm^2 were externally connected and used as working electrodes in the same anodic chamber. The electrode potentials were referred against an Ag/AgCl/Cl^-(sat.) electrode immersed in the chamber. This contained 200 mL of fresh water medium with 20 mM acetate as electron donor. Cyclic voltammetry of each granule was sequentially performed, at 10 mV/s, just after inoculation (t = 0) with 20 mL of Geobacter sulfurreducens pure culture (OD = 0.6); and after polarization of the granules at 0.2 V for 7 days (t = 7). Further details can be found in the Supplementary Data (SD) file (Fig. S3.1).

3.3.3 Design and construction of biofilters

Eight laboratory-scale up-flow biofilters were constructed to determine the influence of the bed materials in the treatment of urban wastewaters. Four of the systems were constructed with a single material/electrode and operated as a snorkel configuration (see Fig. S3.2A in the SD). This configuration did not allow the conversion of microbial metabolism into electrical current to be monitored, since the anode and cathode were not differentiated. The dimensions of the snorkel biofilters were 24 cm high and 3 cm internal diameter, with a total bed volume of 170 cm^3 and a hydraulic volume of 100 mL. Each biofilter outlet for the effluent was located at the top, which maintained the water level below the bed's surface.

On the other hand, the other systems were assembled with a three-electrode configuration, allowing to harvest electrochemical information about the process (see Fig. S3.2B in the SD). These hybrid biofilters hosted one of the electroconductive materials as anode of 78 cm^3 (working electrode); a bed of 58 cm^3 of pyrolyzed coke used as cathode (counter electrode); and a Ag/AgCl/Cl^- (sat.) reference electrode buried in the anodic bed for its polarization at a given potential. In each system, the anode and the cathode were separated with 14 cm^3 of inert gravel; and they were externally connected through buried graphite rods

(1.5 cm × Ø 0.2 cm, Sofacel) used as current collectors. In the case of the anode, two buried graphite rods were used to ensure homogenous polarization of the particles bed. This condition was confirmed by the constant potential of various granules, registered in different parts of the bed, against the reference electrode. Both, the anode potential and electrical current were monitored by using different NEV-4 potentiostats (Nanoelectra S.L., Spain). Finally, a similar system, but without current collectors and reference electrode, was constructed as a control with the gravel material.

3.3.4 Operation of the biofilters

The different systems were operated in parallel to study the influence of several parameters, including the bed material, the nature of wastewater (synthetic vs. real urban wastewater), the hydraulic retention time and the polarization of bed material at different potentials. In the case of synthetic wastewater, biofilters were operated under batch and continuous mode (pulse fed, HRT = 3.3 days) under snorkel configuration. On the other hand, for real urban wastewater the biofilters were operated in continuous mode, fed by pulses, with (i) two different organic loading rates (OLR= 170 mg/L and 890 mg/L), (ii) two different hydraulic retention times (HRT = 4 and 2 days) and (iii) three different anode potentials (short circuit (non-polarized), 0.4 V and 0.6 V vs. Ag/AgCl/Cl^- (sat.)). In this mode, the measurements started (time of experiment = 0 days) after the systems were stabilized, i.e. when the pollutant concentration at the outlet remained steady (error < 5 %) for 3 subsequent days. This condition was accomplished by subsequently passing and replacing three different aliquots of the different wastewater, enabling adsorption equilibriums to be reached. Therefore, adsorption effects on the reported results can be neglected. The real urban wastewater was pretreated in an Imhoff tank, in the WWTP of Carrión de los Céspedes (Sevilla, Spain), the chemical characterization appears in Table S1. The biofilters were operated under continuous mode for 84 days (12 weeks). In all cases, the temperature was maintained at 30 °C in a temperature-controlled room.

3.3.5 Physical, chemical and statistical analyses

Samples were taken daily at the inlet and the outlet of the biofilters. Acetate concentrations were determined by HPLC coupled to a diode array detector (Varian). The chemical oxygen demand (COD) was analyzed following a standard method (APHA/AWWA/WEF). The theoretical oxygen demand (ThOD) of acetate solutions was determined assuming the complete oxidation of carbon atoms, according to the following stoichiometric equation:

$$C_2H_4O_2 + 2O_2 \rightarrow 2CO_2 + 2H_2O$$

Removal efficiencies were calculated as percentage of the inlets. Removal rates were obtained from the inlet-outet difference as mol or grams per cubic meter of bed material per day. The data provided in the bar graphs (see Fig. 3.4 and 3.5) correspond to the average value of 5 measurements taken, during 5 successive days, after a steady response was reached. In order to discern the true effect of the bed materials for each operation condition, statistical procedures were conducted with these 5 measurements using R software (R Core Team 2013) and R-comander package (Fox 2005). The standard deviation of these measurements is included in these bar graphs. Variance analyses (ANOVAs) were used to determine statistical significance (p-value < 0.05) in the performance differences among the different bed materials.

3.4. Results and discussion

3.4.1 Characterization of biofilter materials: physico-chemical properties, electroconductivity and EET

The textural properties of the materials may play a key role on the microbial activity and/or colonization, so they were characterized by SEM, Hg porosimetry and gas adsorption. The non-electroconductive (NC) siliceous gravel showed a smooth surface from milli- and micro-scale (Fig. 3.1A) to nano-scale, what was confirmed by the negligible volume of Hg intruded (Fig. 3.1E and Table 3.1) or N_2 adsorbed (Table 3.1) in this material. These features are in line with the geological origin of this type of rocks, which were formed by weathering and erosion.

By contrast, all the carbonaceous materials presented a differently rough and porous surface. The graphite shows a heterogeneous surface (Fig. 3.1B), combining relatively smooth with ridged regions of wrinkled sheets and cracks of ca. 1-10 µm. The coke granules present a very abrupt morphology with large crater holes (Fig. 3.1C). Finally, the biochar exhibits a developed porous structure (Fig. 3.1D), with regular pores of cylindrical morphology and different dimensions. In particular, a series of big channels of 50-100 µm, surrounded by several pores of around 1-5 µm (Fig. 3.1D1), prevail at this scale in the biochar. In addition, the magnification of the inner walls at the bigger channels revealed the presence of a large amount of well-arranged and defined transverse pores of ca. 1-2 µm (Fig. 3.1D2), that seem to interconnect the channels. This extraordinary pore structure comes from the distinct channels and/or vascular cells present in the original plant (Jiang et al., 2013).

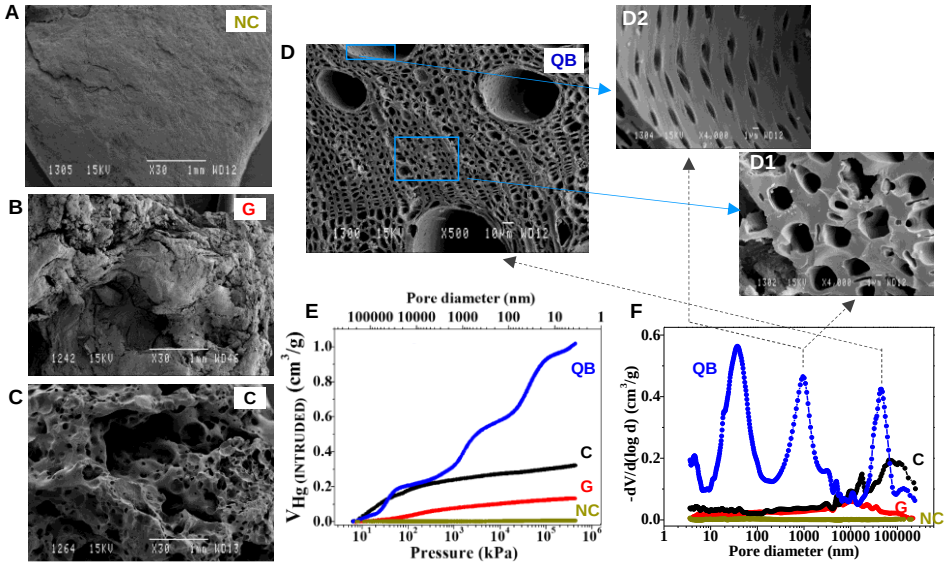

Figure 3.1. A-D) SEM micrographs; E) Hg intrusion porosimetry and F) the derived pore size distribution of the bed materials before being used as electrogenic biofilters. NC, non-conductive gravel; G, graphite; C, coke; QB, Quercus electroconductive biochar.

The porosity analysis by cumulative Hg intrusion curves (Fig. 3.1E) clearly indicates that the Quercus biochar can intrude a considerably larger volume of Hg than the other materials. As shown in Table 1, the calculated total pore volume (V_{Hg}) of the materials remarkably increases in the order NC << G < C < QB

up to ca. 1 cm^3/g, whereas their density increases in the opposite order from about 1.6 to 2.7 g/cm.

From the derived pore size distributions (Fig. 3.1F), it can be inferred that the graphite presents macropores (pore diameter (d) > 50 nm) with a wide spectrum of dimensions and the coke material mainly contains pores above 10 µm. Moreover, these materials contain no micropores (Vt) (d < 2 nm) and mesopores (Vmes) (2 < d < 50 nm) (see N_2 isotherms-Fig. S3.3 in the SD), thus, showing a very low specific surface area (S_{BET}) that is comparable to that of gravel (Table 3.1). By stark contrast, the pore size distribution of the electroconductive biochar revealed three defined peaks, with maximums at ca. 37 nm, 950 nm and 44.5 µm (Fig. 3.1F). This porosity well agrees with the features found by SEM (Figures 3.1D, 3.1D1 and 3.1D2). In addition, this material presents a large volume of micropores (Vt) and, mostly, of narrow micropores (V_{CO2}) (ultramicropores, d < 0.7 nm), leading to a specific surface area (ca. 550 m^2/g) much larger than the other carbon materials (Table 3.1). Furthermore, the N_2 isotherm also revealed the presence of some mesopores in this sample (Table 3.1), what is in line with Hg porosimetry (Fig. 3.1E). Hence, the electroconductive biochar exhibits a unique hierarchical pore architecture gathering ultramicro-, micro-, meso- and macro-pores.

Table 3.1. Textural, structural and chemical parameters of graphite (G), coke (C) and -Quercus electroconductive biochar (QB) before and after being used, polarized at 0.6 V, as electrogenic biofilter beds.

	N_2 isotherms				CO_2 isotherms		Hg porosimetry		XRD		Raman		TPD		
Biofilter	S_{BET} [a]	$V_{0.995}$ [b]	Vt [c]	V_{mes} [d]	S_{CO2} [e]	V_{CO2} [f]	V_{Hg} [g]	ρ [h]	0 0 2 [i]	L_c/L_a [j]	ν_G [k]	$\Delta\nu_G$ [l]	CO_2 [m]	CO [n]	O [o]
G	< 1	0.001	0.000	0.000	---	---	0.133	2.153	26.577	628/653	1579	21.3	45	19	109
G 0.6	< 1	0.004	0.000	0.000	---	---	0.135						---	---	---
C	< 1	0.001	0.000	0.001	---	---	0.322	1.781	25.404	22/43	1599	57.5	49	38	178
C 0.6	< 1	0.002	0.000	0.001	---	---	0.306						---	---	---
QB	250	0.135	0.120	0.010	550	0.187	1.019	1.610	23.520	10/20	1587	77.2	683	1230	2596
QB 0.6	210	0.117	0.098	0.012	526	0.179	0.794						---	---	---

[a] Specific surface area from BET model. [b] Total pore volume at P/P^o = 0.995. [c] Micropore volume from *t*-method. [d] Mesopore volume. [e] Specific surface area and [f] Ultra-micropore volume from Dubinin-Radushkevich. [g] Total Hg intrusion volume. [h] Material density. [i] Position of the 002 peak. [j] Calculated crystallite dimensions of the graphite crystalline structure. [k] Position and [l] width of the G band. [m] Integrated CO_2- and [n] CO-evolving oxygen surface groups from TPD. [o] Total surface oxygen O = CO + 2 CO_2.

The structure of the bed materials was analyzed by XRD and Raman. A detailed compilation of all the spectral parameters can be found in the SD (Tables S3.2 and S3.3), but most important ones are included in Table 3.1. The X-ray diffractograms of the gravel (see Fig. S3.4) indicated that this material is mainly formed of α-quartz (SiO_2) microcrystallites. In the case of the carbon materials, two characteristic diffraction peaks appear centered at around 2θ = 23 - 27° and 42 - 44° (Fig. 3.2A). The first peak is related to the vertical ordering/stacking of graphene sheets aligned along the (002) plane in graphite; whereas the second one is associated to the horizontal arrangement of these sheets along the (100) plane (Coutinho et al., 2000, Rodríguez-Mirasol et al., 1996). In the case of the graphite, the center (2θ) of these peaks greatly approaches that found for highly-ordered pyrolytic graphite (HOPG) at 26.53° and 42.44°, respectively (see Tables 3.1 and S3.2). This involves that the lattice parameters (d-spacings along with *c/a* axis) of this sample are close to those expected for graphite crystals, thus, reflecting its superior structural order. As observed in the inlet of Fig. 3.2A and Table 3.1, the diffraction peaks for the coke and, in more extent, the biochar separate from those of the graphite. On the other hand, the narrower these peaks are, the larger the *Lc/La* dimensions of these crystals. The size of crystallites in the graphite were calculated to be ca. 630-650 Å, and greatly decreased to 20-40 Å and 10-20 Å for coke and biochar, respectively (Table 3.1).

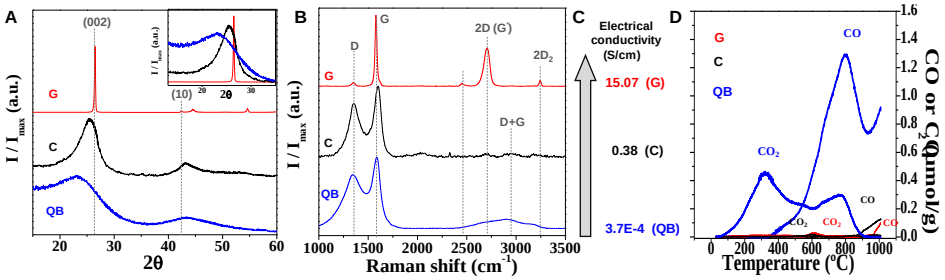

Figure 3.2. Normalized X-ray diffractograms (A) and Raman spectra (B); the electrical conductivity from 4 probe measurements (C); and TPD (D) of the carbon materials used as electrogenic biofilters. NC, non-conductive gravel; G, graphite; C, coke; QB, Quercus electroconductive biochar.

Respect to Raman characterization, the observed two main bands of the first-order spectrum of the carbon materials (Fig. 3.2B), called the D-band (~1340-1360 cm^{-1}) and the G-band (~1579-1599 cm^{-1}), provide information on the structural defects or graphitic order, respectively, related to the degree of two-dimensional orientation of the crystalline units. On the other hand, the overtone of the D band in the second order spectrum, called the 2D-band (~2700 cm^{-1}), has been associated to the degree of three-dimensionally graphitic orientation (Rodríguez-Mirasol et al., 1996). In the case of graphite, the G-band position and width, comparable to the values found for HOPG (νG = 1578-1582 cm^{-1} and $\Delta\nu G$ = 17-20 cm^{-1}) (Wang et al., 1990, Cuesta et al., 1994), the relative low-intensity and narrow D-band, and the high relative intensity of the 2D-band are all characteristic of a graphitic material (Table S3.3). On the contrary, the wider D, G- and 2D-bands, obtained for coke and Quercus biochar reflect their more defective structure, which is exacerbated for the later. All these results point out the poorer crystallinity (structural order) of the coke and, specially, the biochar, and can be well correlated with their electrical conductivity (Fig. 3.2C). Thus, the studied graphite shows a high conductivity of around 15 S/cm, which is in the order of these structurally ordered materials (Cuesta et al., 1994). Interestingly, this conductivity is ca. 40 and more than 40000 times higher than those of coke and biochar, respectively.

The surface oxygen content of the carbonaceous samples, from XPS analysis, was found to be 1.7; 6.5 and 16.7 wt.% for the graphite, coke and biochar,

respectively (Table S3.4). This trend is in line with the quantified evolving groups during TPD experiments (Table 3.1). From the TPD profiles (Fig. 3.2D), it can be clearly deduced that the electroconductive biochar presents a remarkably richer surface chemistry. Particularly, this material is by far characterized by a large CO evolution from 500 °C, with a hump and a maximum at ca. 700 and 800 °C, respectively, which have been assigned to phenol and quinone/carbonyl functionalities in carbon materials (Figueiredo et al., 1999). These oxygen groups have been found to be electroactive (Itoi et al., 2014). Moreover, it contains a considerable amount of oxygen surface groups evolving as CO_2 between 150-400 °C, attributed to carboxylic-like functionalities, and some other groups, like anhydrides and lactones, at higher temperatures (Figueiredo et al., 1999). To summarize, whereas the graphite and coke exhibit a higher conductivity because of their superior crystalline structure (mainly in the former case); the electroconductive biochar displays a higher surface area, a hierarchical pore architecture and a richer surface chemistry, including a large amount of electroactive oxygen functionalities.

The microbial EET capability of the different materials was studied by cyclic voltammetry. Figure 3.3 compares the voltammetric profiles of a single granule of each material before inoculation and after 7 days of promoted (potentiostatic) biofilm growth. Just after inoculation (grey lines), the CV revealed how the different materials display a redox couple attributed to surface e-transfer (acetate - carbon electrode) mediated by cytochrome C of bacteria (Richter et al., 2009). In all cases, the current density and/or charge involved in this EET increased after biofilm growth (colored lines). However, evident differences can be observed among the tested materials. First, the voltammograms obtained from electroconductive biochar (Fig. 3.3C) were comparatively more tilted than those from graphite and coke (Fig. 3.3A-B); a response that can be related to the inherent lower electroconductivity of the former material (Fig. 3.2C). Second, the shape and current density of these electrochemical processes, including its relative increase after biofilm growth, depended on the nature of the biofilter material. Specifically, the coke and the graphite show quite similar straight voltammograms with broad peaks and

relative increments of e-transfer capability after biofilm growth (Fig. 3.3A-B). Nevertheless, the current density of graphite is one order of magnitude higher.

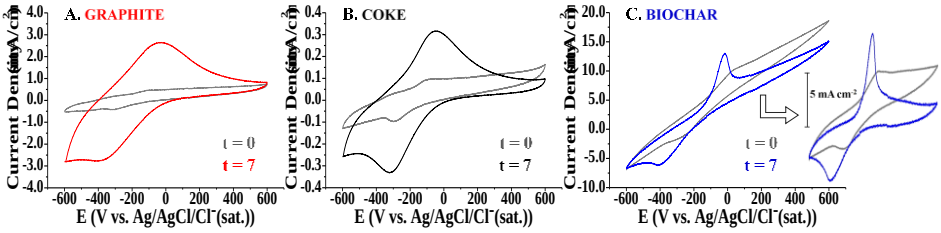

Figure 3.3. Steady-state cyclic voltammograms of a single granule of the different biofilter materials just after inoculation (Geobacter sulfurreducens) (t = 0) and after polarization at 0.2 V (vs. Ag/AgCl/Cl⁻(sat.)) for 7 days (t = 7) to promote biofilm growth; scan rate = 10 mV/s; fresh water medium, 20 mM acetate.

On the other hand, the electroconductive biochar (Fig. 3.3C) exhibited much higher voltammetric currents throughout all the analyzed potential window in comparison with the rest of tested materials, even just after inoculation. This is assigned to the higher specific surface area of electroconductive biochar (Table 3.1). In this case, however, the relative increase in current density after biofilm growth seemed to affect to a narrower potential window, leading to more intense and define peaks. As a result, the charge associated to the e-transfer on the biochar was considerably larger than in the case of graphite and coke. This may be due to a property unlike conductivity.

3.4.2 Biofilters performance for treating wastewater using different electroconductive bed materials

The mere presence of electroconductive material has been shown to stimulate microbial biodegradation of pollutants in a number of studies [5-8]. Thus, we decided to explore such a response using the different materials (graphite, coke, electroconductive biochar and gravel as non-conductive control material) for constructing the biofiltering bed.

3.4.2.1 Biofilter performance for treating synthetic wastewater

The four biofilters were independently operated up-flow with acetate-based synthetic wastewater under batch or continuous mode. The initial

concentrations of acetate were different depending on the operational mode. In batch mode, the initial concentration of acetate was 40 mM, showing a ThOD of 1279.4 mg/L. When the biofilters were operated in continuous mode, the initial acetate concentration was 20 mM (ThOD = 639.7 mg/L), to mimic the organic compound content of a standard urban wastewater. Regardless the operating mode, the residual concentration of acetate in the effluent was lower in those biofilters whose bed was made of electroconductive material (Figure 3.4). Nevertheless, despite its lower conductivity, the electroconductive biochar was the most efficient material for biodegrading acetate under any operating mode. Particularly, in batch operation (Fig. 3.4A) it removed 100 % of the acetate in 2 days (4.14 mol acetate $m^{-3}d^{-1}$), working at double rate than the other tested conductive materials; in contrast, biofilter made of inert gravel only removed 25 % of acetate during the same period.

When operated under continuous mode (Fig. 3.4B), the electroconductive biochar biofilter showed also removal efficiencies close to 100 % after 2 days, implying removal rates of 2.79 mol acetate $m^{-3}d^{-1}$. In this case, however, the other two electroconductive materials were not able to remove more than ca. 70 % of the acetate even after 4 days of treatment (1.0-1.2. mol acetate $m^{-3}d^{-1}$) and the gravel was totally inefficient under these conditions.

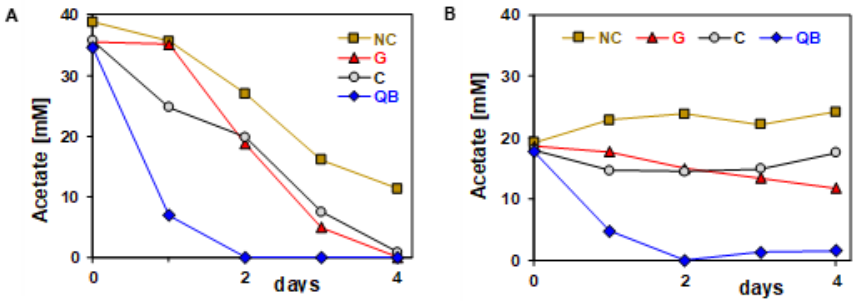

Figure 3.4. Evolution of acetate concentration in the biofilters operating in (A) batch and (B) continuous (HRT = 3.3 days) mode. NC, non-conductive gravel; G, graphite; C, coke; QB, Quercus electroconductive biochar.

3.4.2.2 Biofilter performance for treating real urban wastewater

In order to evaluate the performance of the biofilters under a more real scenario, they were fed with a real urban wastewater under a continuous mode. Moreover, in real scenarios the HRT and the OLR are critical parameters, so their influences were analyzed. Statistical test revealed significant differences ($p < 0.05$) in the COD from effluents at all OLRs and HRTs tested.

Respect to the effect of HRT, as expected, the effluent COD discharges decreased, and the removal efficiencies increased, with the HRT; i.e. by extending the biofilter-wastewater contact time. In the case of a 170 mg/L COD influent, for example, the performances of both the coke and graphite biofilters were within the limits of discharge of the European Directive 91/271/CEE (91/271/CEE) at a HRT of 4 days. In contrast, biofilters made of gravel required an HRT above 4 days to fulfill the limits. Interestingly, only the electroconductive biochar biofilter fulfilled the requirements of the directive for COD at HRT as low as 2 days. Considering the more practical benefits of minimizing the HRT, the following studies exploring both the influence of the OLR or the material polarization were carried out at a HRT of 2 days.

Regarding the influent concentration (OLR), real urban wastewaters typically show a variable nature according to human activity along the day. To quantify the robustness of the system to variations in the organic load, the biofilters were fed with influents showing 5-fold differences in COD levels: 170 and 890 mg/L (Figure 3.5). As mentioned above, when the influent COD was 170 mg/L the only system that fulfilled the requirements of the directive for COD discharge was the electroconductive biochar biofilter, which actually removed COD at ca. 31 g $m^{-3}d^{-1}$.

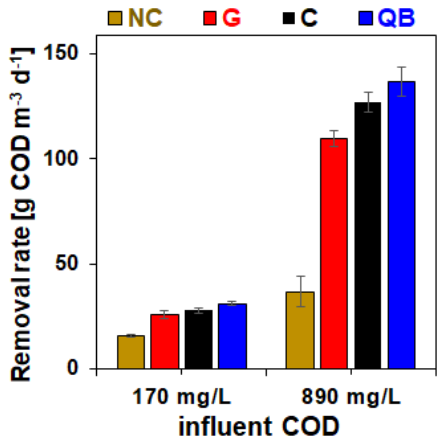

Figure 3.5. Average COD removal rate including ± standard errors in each biofilter without polarization, referred to HRT = 2 days and two different OLRs in urban wastewater. NC, non-conductive gravel; G, graphite; C, coke; QB, Quercus electroconductive biochar.

Under higher COD loads (890 mg/L), the electroconductive biochar was also the biofilter with the best performance (Fig. 3.5). Moreover, the removal rate was increased more than 4-fold in the different electroconductive biofilters, specially up to 137 g $m^{-3}d^{-1}$ for the biochar, while the gravel biofilter did not remove more than ca. 37 g $m^{-3}d^{-1}$. Interestingly, in spite of the high electroconductive nature of the graphite, its performance was worse than that of coke. Hence, a remarkable conclusion is that the conductive character of the carbon biofilters seems to be responsible of the their much better performance than gravel, but something different to conductivity may govern the performance among the carbon biofilters to explain the greater response of the poorly conductive biochar.

3.4.2.3 Biofilter performance for treating real urban wastewater using polarized beds

With the aim of exploring the role of the electroconductive bed for accepting electrons from microbial metabolism, we constructed three independent biofilters with anodic beds subjected to electrochemical control by polarizing them at either 0.4 V or 0.6 V (vs. Ag/AgCl/Cl^- (sat.)) and the produced current was monitored. For comparison purposes, the biofilters were also

operated without polarization (NP) under short circuit mode. The systems worked under continuous mode (HTR = 2 days), fed by pulses, with a high COD load influent (ca. 800 mg/L). Figure 3.6 compilates the results in terms of biodegradation and current production of the different wastewater treatments.

First, in respect of the biodegradation performance, the analysis of variance (ANOVA) revealed significant differences ($p < 0.05$) among the tested materials. As a general response, without polarization (NP bars in Fig. 3.6A), none of the studied biofilters was able to fulfill the discharge limits at such high organic load. On the other hand, the anodic polarization of the electroconductive biofilters (0.4 or 0.6 V) remarkably enhanced their COD removal capacity (Fig. 3.6A). In contrast, the gravel biofilter performance was not affected by polarization, what is assigned to its non-electroconductive nature. Hence, electroconductivity was found a necessary property to optimize the microbial activity of the biofilters by external polarization.

Particularly, the polarized electroconductive biochar was the most effective biofilter for cleaning-up wastewater among all the tested materials and conditions (Fig. 3.6). At 0.4 V, the polarization of the electroconductive biochar bed reduced (by 3.5-fold) the COD level at the effluent down to 100 ppm (Fig. 3.6A), fulfilling the regulative policy. In this case the COD removal efficiency greatly increased from 56 to 87 % (average value in Fig. 3.6C) and the removal rate from 112 to 176 g $m^{-3}d^{-1}$ (Fig. 3.6B). For the other two conductive biofilters, made of coke and graphite, the removal efficiency just increased in 6.1 and 19.4 % (up to 53 and 58 %, average values in Fig. 3.6C), respectively; what was not enough, however, to fulfill the requirements of the directive for COD levels (Fig. 3.6A).

A further increase in the electrode potential up to 0.6 V resulted in a better performance of the conductive biofilters by increasing the COD removal rates (Fig. 3.6B). In this case, however, the most electroconductive biofilters (made of coke and graphite) experienced the largest relative increments in COD removal efficiency, 27 % and 18 %, respectively (vs the efficiency at 0.4 V). Nevertheless, the removal efficiency of the biochar (92 % average, Fig. 6D) was still considerably higher than those of coke and graphite (80 and 75 % average,

respectively, Fig. 3.6D). These effects were also observed for the removal rates (Fig. 3.6B), reaching a maximum degradation rate of 185 g $m^{-3}d^{-1}$ in the case of electroconductive biochar. As a result of these different performances, the effluent from the biochar biofilter (64.13 ± 5.3 mg/L COD) was again the only one not exceeding the discharge limits (Fig. 3.6A). Hence, by simple modulation of the potential, the electroconductive biochar can clean up urban wastewaters even with influents load as high of ca. 800 mg/L COD. Interestingly, such a higher biodegradation performance of the electroconductive biochar biofilter suggests some kind of EET process that was experimentally confirmed by the e-transfer capability between bacteria from genus Geobacter and this material (Fig. 3.3).

Second, production of significant electrical current was detected and monitored during the polarization assays (Fig. 3.6C-D). Interestingly, the progressive addition of new inlet media caused an immediate increase in the electrical current production due to the microbial response. This current-production profile was similar for all systems regardless the material used for the bed. Thus, using the polarized materials as electron acceptors confirmed the conversion of the microbial metabolism into transferable electrons.

In particular, by polarizing at 0.4 V the monitored average currents were 0.78, 3.65 and 6.13 mA for the biochar, coke and graphite biofilters, respectively (Fig. 3.6C). This trend in current production seems to agree with the increasing conductivity of these materials (Fig. 3.2C). With an increment of the electrode potential to 0.6 V, the average current in coke and graphite biofilters slightly increased to 3.74 and 6.69 mA, respectively, in contrast with the practically unaffected current from biochar (Fig. 3.6D). From all these results, it can be concluded that the raise in the electrode potential at higher values (at least from 0.4 to 0.6 V) to increase the COD removal capability and the current production was less effective for biochar, the least conductive carbon biofilter. Another important conclusion is that the current production in these polarized bed-like biofilters is not directly correlated to COD removal, which generally increases in the opposite order, this is graphite < coke < biochar, (Fig. 3.5-3.6).

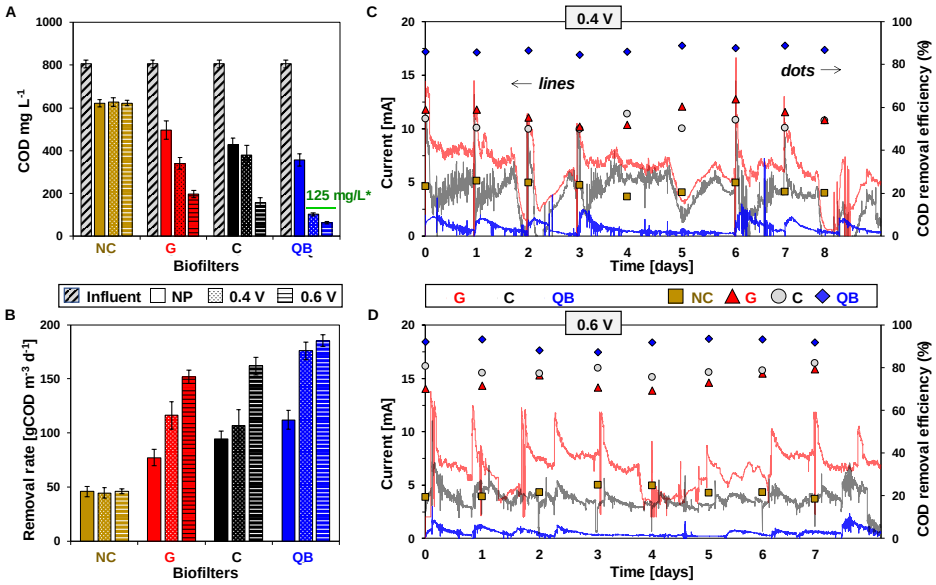

Figure 3.6. (A) Average effluent COD (showing discharge limit*); and (B) COD removal rate, including ± standard errors, in each biofilter submitted to different polarization conditions (NP = non-polarized, in which the open circuit potentials were: -420 mV, -427 mV and -429 mV for the graphite, coke and biochar, respectively). (C-D) Evolution of the COD removal efficiency (dots) and the microbial electrical current (lines) while treating real urban wastewater using electroconductive biofilters anodically polarized at (C) 0.4 V and (D) 0.6 V (vs. Ag/AgCl/Cl^- (sat.)). Influent COD = 800 mg/L; HRT = 2 days. NC, non-conductive gravel; G, graphite; C, coke; QB, Quercus electroconductive biochar.

Regarding that the soluble electron donor (organic matter) present in wastewater is not a limiting factor, this fact could be explained by different reasons. Firstly, previous reports suggested the presence of alternative biodegradation pathways, using methanogens (Liu et al., 2012, García et al., 2010) or sulfate-reducing bacteria (García et al., 2010), which do not contribute to current production (Rabaey et al., 2005). Secondly, part of these "lost" electrons could be utilized in the promotion of syntrophic metabolism by biochar-mediated Interspecies Electron Transfer (Chen et al., 2014, Zhao et al., 2015, Zhao et al., 2016). Thus, Chen et al. (2014) proposed that the electrons can migrate from electron-donating to electron-accepting cells by inducing intrinsic charge differences between sections of biochar (Chen et al., 2014). This intra-particle

electron migration, however, cannot be measured as current. In this sense, the harvested current must be exclusively associated to the capability of the bed of carbon particles to move and extract the electrons from their surface to other particles and, finally, the current collector, i.e. to the inter-particle electron migration. Such ability must be directly related to the intrinsic conductivity of the material and its shape and conformation in the biofilter, i.e. the conductivity of the particles bed. This is line with Sun et al. (2017) (Sun et al. (2017)), who suggested that the electrical conductivity may lead to a relatively longer-distance transport of electrons through carbon matrices. Hence, the most reasonable explanation could be a higher electrical resistance of the biochar particles bed. This agrees with the lower conductivity of the biochar respect to that of the coke and graphite (Fig. 3.2C), together with the insignificant effects on biodegradation by rising the potential of biochar biofilter from 0.4 to 0.6 V (Fig. 3.6).

On the other hand, although both galvanostatic (Fig. 3.6C-D) and voltammetric (Fig. 3.3) measurements reflect a greater microbial activity on biochar, they seem to diverge in the relative capability of the different materials for current production. It must be considered, however, that the experimental conditions in these measurements were substantially different. First, in the case of galvanostatic experiment, the nature of the e-donor (real urban wastewater) was much more complex, showing lower coulombic efficiencies (CE ca.10 % or below depending on the influent COD) (Aguirre-Sierra et al., 2016) than the acetate-based medium (CE ca. 95 %) (Bond et al., 2003) used in voltammetry. Second, while the galvanostatic experiment was performed over a bed of granules, a single granule was used for voltammetric analysis. The fact that greater currents are registered on biochar when using a single granule, and that the opposite occurs in the bed-like configuration, strongly supports the occurrence of higher current losses (resistance) among the particles of the biochar.

3.4.3. Giving insight into the extracellular electron transfer to electroconductive carbon materials

To understand the previous results, the nature of microbial electrochemical processes should be considered. Although the involved mechanisms are not fully understood, the e-transfer capability of carbon materials (e-acceptors) with bacteria has been generally attributed to their electroconductivity (Sun et al., 2017) and/or the presence and mediation of electroactive hydroquinone-quinone (HQ/Q) surface moieties (Yuan et al., 2017). See a proposed scheme of these processes in Figure 3.7.

On the one hand, the electroconductivity-based mechanism, recently referred to as the geoconductor behavior (Sun et al., 2017) involves a direct e-transfer to/from the carbon matrix (aromatic structure) and has been reported for carbons prepared at higher temperatures, i.e. minimizing the contribution of surface oxygen surface groups (Sun et al., 2017, Xu et al., 2013) Nevertheless, the promotion of direct interspecies electron transfer (DIET) for different syntrophic associations of microorganisms in soils has been assigned to the electrical conductivity in both low-conductive carbons, like biochar (Chen et al., 2014, Zhao et al., 2015, Zhao et al., 2016), and more conductive materials, like graphite (Zhao et al., 2016). Indeed, not only the conductivity but also the capability of the conjugated π-electron system of the condensed aromatic rings in carbon materials to accept/donate electrons (redox character) (Montes-Morán 2004) may contribute in this mechanism.

On the other hand, the mechanism based on the HQ/Q reversible redox reaction was proposed to explain how biochars promote interspecies e-transfer in soils (Yuan et al., 2017) acting as rechargeable reservoirs of bioavailable electrons, i.e. the so-called geobattery behavior(Saquing et al., 2016). However, these specific (HQ and Q) functionalities were not experimentally observed or quantified in most of these previous works. On the contrary, the TPD technique has been used in this work to quantify the amount of these groups (Itoi et al., 2016). Most of the CO-evolving groups in Fig. 2D, around 1000-1100 μmol/g, correspond to these types of functionalities. Then, it is reasonably to propose

that the considerably greater e-transfer capability (Fig. 3.3) and higher biodegradation efficiency (Figures 3.4-3.6) observed for the much poorly conductive biochar is assigned to the larger amount of electroactive oxygen functionalities. Similarly, the slightly better performance of the coke compared to graphite, could be also explained by this mechanism (see the amount of CO-evolving groups in Table 1). Then, the bioelectrochemical response of the studied biofilters seems to be governed by the geobattery mechanism.

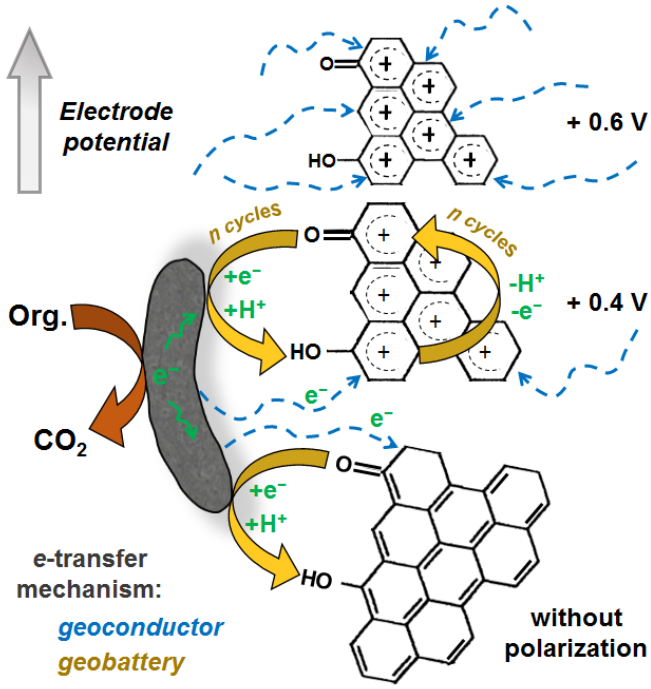

Figure 3.7. Scheme of the proposed geoconductor and geobattery e-transfer mechanisms between bacteria and carbon materials, emphasizing their possible modulation, externally, by polarization.

Concerning the kinetics of the process, it was reported that the direct e-transfer (geoconductor behavior) through carbon matrixes is three times faster than through HQ/Q processes (Sun et al., 2017). However, this study did not consider the effect of the different material's electroconductivity on the reaction kinetics and, additionally it was carried out under abiotic conditions, by analyzing the electron exchange between carbon electrodes and dissolved species (Sun

et al., 2017). In contrast, both the higher acetate and COD removal-rates (Figures 3.4-3.6) obtained in biochar-made biofilters in this work suggest that e-transfer between carbon materials and bacteria is faster when mediated by HQ/Q functionalities

The enhancement in removal efficiency upon polarization observed for these electroconductive biofilters, together with the significant increase in the COD removal rates (Fig. 3.6B), is assigned to a stimulation of the biodegradation rate of microorganisms on these systems. It has to be considered that a polarization at 0.4 - 0.6 V (vs. Ag/AgCl/Cl^-) is remarkable, since the typical environment in anaerobic biofilters reach a very negative redox potential (ca. -350 mV vs. Ag/AgCl/Cl^-). Interestingly, our polarized biofilters may support bacterial growth able to exchange electrons with the material substrate at oxidative potentials as high as 0.6 V, a value which is not far from the value exhibited by oxygen (0.8 V vs. Ag/AgCl/Cl^-) in typical aerobic biological systems. As a result, by providing an electron acceptor with a high potential using electrochemical tools we may optimize the oxidation of the pollutants while avoiding the cost of supplying oxygen into the liquid phase.

This modulation of the e-accepting capability of the biofilter supports the occurrence of the geoconductor mechanism. Thus, the anodic polarization causes a depletion of π-electrons from aromatic rings that may favor their e-accepting capability from bacteria (see Fig. 3.7). Despite such electron extraction is expected to be easier at higher conductivity, the obtained results point out that the polarization at 0.4 V causes a much greater biodegradation promotion on the biochar (Fig. 3.6A and 3.6B). This effect could be explained by the electrochemistry of HQ/Q couple. In fact, several works on the electrochemistry of biomass-derived carbon materials report that 0.4 V (vs. Ag/AgCl/Cl^-) is a high-enough electrode potential to oxidize hydroquinone (HQ) groups into quinone (Q) ones (Berenguer et al., 2015, Berenguer et al., 2016). Considering that these Q groups are the e-acceptors in the geobattery mechanism, the polarization at 0.4 V greatly augments the number of e-acceptors on the biochar and, therefore, its biodegradation ability. Furthermore, the HQ/Q is a well-known reversible redox couple, so that, once the bacteria transfer the electrons to the

Q groups, and reduce them into HQ ones, the effect of the anodic polarization may restore again the quinone functionalities (as schematized in Fig. 3.7). From the experimental results, this cyclical regeneration of quinone e-acceptors by polarization is proposed to remarkably enhance the biodegradation rate and efficiency of the carbon material. Moreover, this e-transfer from bacteria to the continuously recycled quinones (geobattery mechanism) seems to be favored against the e-transfer towards the e-accepting aromatic rings (geoconductor mechanism). As a consequence, these results suggest that external polarization enables the modulation of the e-accepting capability of carbon materials not only through the aromatic rings (geoconductor mechanism), but also by adjusting the ratio of HQ/Q groups (geobattery mechanism).

Nevertheless, the ca. 1000-times larger amount of CO-evolving groups (those potentially electroactive) on the biochar (Table 3.1) cannot explain why the removal efficiencies and rates of this material are "only" less than double those of the conductive carbon materials (Fig. 3.6). This effect could be reasonably explained by considering two facts. First, from this total amount of oxygen groups, only those accessible to electroactive bacteria and/or possible redox mediators may participate in e-transfer. Thus, XPS may provide a more realistic estimation of the (most accessible) surface oxygen functionalities. As it can be seen in Table S3.4, the proportion (%) of surface oxygen in the electroconductive biochar is "only" 2-10 times higher than in the other materials. Second, in a more amorphous and poorly conductive material like the biochar, the anodic polarization must be necessarily less efficient, so that a great part of its carbonaceous structure, including a large amount of potentially electroactive Q groups, may remain electrically disconnected and unaffected by polarization.

Finally, the proposed modulation of e-accepting Q groups and the electrical disconnection on poorly conductive biochar were confirmed when they were polarized at 0.6 V. Thus, compared to 0.4 V, at 0.6 V the conductive materials (coke and graphite) experienced a 20-30 % increment in COD removal efficiency, whereas the biochar only a 5 % (Fig. 3.6). If most of HQ groups on the biochar were oxidized at 0.4 V (as hypothesized), then a further increment of the electrode potential up to 0.6 V may lead to a lesser significant effect on the

generation of Q groups and on the biodegradation. In addition, if the structure of this material is partly disconnected (as hypothesized), the e-accepting capability of aromatic rings (geoconductor mechanism) may be not so influenced by a higher potential than in the case of the high conductive materials. Consequently, a further increase in the electrode potential mainly increases the biodegradation capability of the most conductive carbon materials through the geoconductor mechanism. In other words, despite being globally less important than the geobattery phenomenon, the geoconductor mechanism becomes more significant with the electroconductivity of the carbon materials when they are polarized at higher potentials.

3.4.4. Characterization of the bed materials after microbial colonization

The bed materials were physico-chemically characterized also after being used as polarized working electrodes at 0.6 V to study the biofilm formation. The structural properties of the materials (XRD and Raman) were found to be practically unaffected, whereas their surface-related features changed after the wastewater treatment. The used gravel showed a surface morphology very similar to that before usage and individual bacteria were not discerned (Fig. S3.5). Nevertheless, the parallel decrease and slightly increase in the relative intensity of the Si(2p) and C(1s) XPS core-level signals, respectively (Table S3.4), suggested the formation of some biofilm.

On the contrary, more or less uniform biofilms were clearly observed on the different carbon materials (Figure 3.8). On the graphite, individual bacteria were identified only on some smooth regions (Fig. 3.8A-B), so that most of the wrinkled graphite sheets were covered by a roughened biofilm (Fig. 3.8C). As observed in this figure, this biofilm closely imitated the surface morphology of the pristine material, leaving the cracks and void regions unaffected. Accordingly, the Hg intrusion curves of this material and the derived textural parameters (Table 3.1) were practically identical before and after usage (Fig. 3.9A).

In the case of coke, the surface was totally covered by a biofilm (Fig. 3.8D), and some individual bacteria were difficult to discern (Fig. 3.8E). The biofilm was

so dense (Fig. 3.8F) that it seemed to soften the crater-like holes of this material (compare Fig. 3.8D with Fig. 3.1C) and it even suffered from delamination in some zones (inset of Fig. 3.8F). Thus, unlike graphite, the biofilm slightly reduced the porosity of this material (Table 3.1), mainly affecting pores in the range of 20-10 μm (Fig. 3.9A).

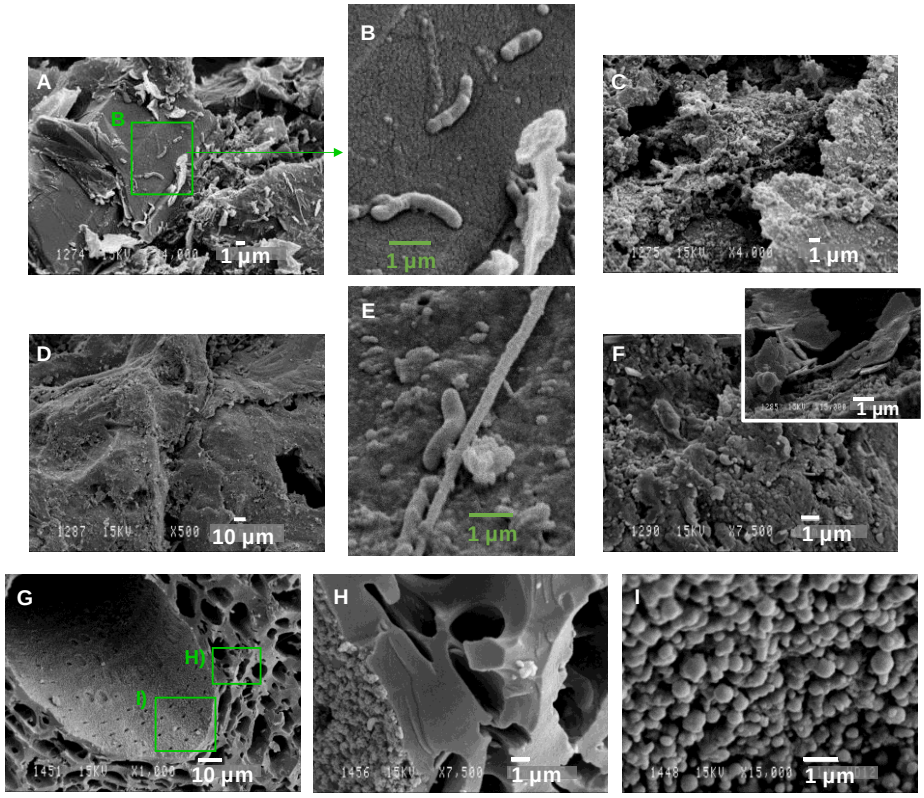

Figure 3.8. SEM micrographs of the carbonaceous bed materials after being used as polarized (0.6 V) electrogenic biofilters: (A-C) graphite; (D-F) coke; and (G-I) Quercus-derived biochar.

The biofilm formed on the biochar was quite different (Fig. 3.8G-I). The magnified images of the biochar (Fig. 3.8G) show that only the inner walls of the larger channels were colonized by microorganisms (Fig. 3.8H). This reflects certain selectivity of the bacteria for zones with, up to now, unknown particular features (dimensions, accessibility, etc.). Further magnification of these images reveals that the biofilm presents a spherical morphology (Fig. 3.8I). In addition, it can be observed that, despite forming a continuous film, they do not

cover/block the pores of 1-2 µm in the inner walls of the large channels (see the Fig. 3.8G). Hence, the biofilm was found to affect mainly the pores of d < 300 nm (Fig. 3.9A and 3.9B), including the micropores (Vt) and ultramicropores (V_{CO2}), reducing the specific surface area of this material (Table 3.1). The comparison of surface chemical composition of the graphite and coke materials before and after usage as biofilters shows a relative decrease in surface C wt% probably related with the increase in O wt%, other heteroatoms (N, P, S) and metal impurities, mainly Fe (Table S4). The same trend was observed for the biochar, but in this case the O wt% was practically unaffected.

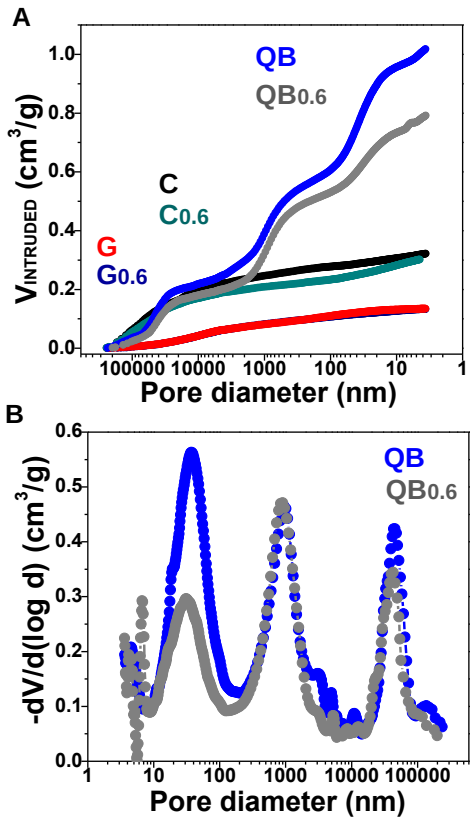

Figure 3.9. Hg Intrusion curves of the different carbon materials (A) and the pore size distribution of the Quercus-derived biochar, before and after being used as biofilters polarized at 0.6 V. G, graphite; C, coke; QB, Quercus electroconductive biochar.

It is well-known that these elements O, N, P, S and Fe are essential macro- and micro-nutrients for all organisms. Thus, although the original

carbon materials contain some of these elements and although some adsorption from the contaminated water could occur, this more heterogeneous and complex surface of the used materials is attributed to the presence of the biofilm or its assimilated elements. In this sense, as a general trend, the biochar is the material showing the largest gain in Fe, N and S nutrients.

3.4.5 Electroconductive biochar: a sustainable material for constructing microbial electrochemical systems

The development of full-scale applications of METs for treating urban wastewater (ca. 150 L/habitant) will demand enormous amounts of carbon materials. In this context, the potential replacement of conductive carbon materials produced from fossil resources, like coke and graphite, by electroconductive biochars constitutes an attractive and sustainable strategy based on circular economy. In addition, the high COD removal efficiencies of the biochar will lead to such a remarkable reduction of biofilter dimensions and/or area requirements to treat a given volume of water. Furthermore, considering that the electroconductive biochar shows the lowest density among the studied materials (Table 3.1), it can be easily deduced that a considerably lower mass of this material will be necessary for treating a given volume of wastewater. Finally, after its service life, the spent electroconductive biochar can be reutilized as soil amendment for giving a second life to this material.

Respect to cost, at present the production of biochar is in the same price range (400-600 euros/Tm) that cokes and graphites, which are obtained from large chemical industries or mining and subjected to market changes. However, the energy (thermal treatment) needed to prepare biochar is by far lower than that used to obtain mineral conductive materials. Consequently, electroconductive biochar production shows a lower CO_2 fingerprint, in addition to its "carbon negative" feature for taking more carbon out of the atmosphere than it puts back into it.

On the other hand, when polarized at 0.4 V and 0.6 V the biochar biodegradation rates lead to effluents with 4.2- and 6.6-fold lower residual COD values, respectively, than those produced by classical biofilter made of inert

gravel. Hence, the results of this work allow to expand the up-to-now estimated potentiality of biofilter-based systems like the so-called METland® [5]. Even more important, our results may help to discern which are the best properties of a carbon material to optimize its performance for enhancing COD removal and/or for current production in METs. Among these properties, the presence of e-accepting quinone surface groups seems to be the essential to achieve higher biodegradations efficiencies, whereas the conductivity is probably the property determining the current-production. However, other typical properties of carbon materials, not considered until now, could also participate in the promotion of the biodegradation, so their study and understanding could lead to further optimization of METs.

In this sense, the present investigation demonstrates that the biochar exhibits various interesting features that cannot be found in the coke or graphite. For example, the high micropore volume and the presence of mesopores and small macropores (d < 300 nm) is exclusive of the biochar (Table 3.1). On the one hand, it is well known that the micropores are essential for the biochar (and other carbons) to storage electrons on the electrical double layer for energy storage (Chacón et al., 2017). The accumulation of a large number of electrons from bacteria, effectively compensated by the adsorption of ions on the micropores of the biochar, is likely to happen because of the low conductivity of this material. This could contribute to explain why all electrons released by bacteria are not "measured" as electrical current in our polarization assays (Fig. 3.6C-D). This agrees with the geobattery mechanism, in which biochars can storage and reversibly exchange electrons (Saquing et al., 2016). On the other hand, it has been reported that small pores or other oxygen functionalities, like the carboxylic ones, could act as physical or chemical anchoring sites, respectively, to attach specific proteins or other functional parts of bacteria (Vijayaraj et al., 2010). In addition, bigger pores may be necessary to host bacteria and biofilms. Consequently, apart from the proposed e-transfer mechanisms, the promotion of bioelectrochemical processes in METs could be also determined by the capability of the carbon materials to host bacteria, biofilms and/or electrons.

3.5. Conclusions

In this work, the performance of two fossil-derived and highly-conductive carbon materials (coke and graphite) for stimulating electroactive bacteria was compared with the one exhibited by biochar with lower electroconductivity but presenting a large volume of different pores and a rich variety of oxygen functionalities. Our studies revealed enhanced microbial EET and higher biodegradation rates when biochar was used as bed material for constructing biofilters under a wide range of operating conditions from non-polarized to polarized conditions. This optimal biodegradation performance has been mainly attributed to the electroactive oxygen functionalities on biochar, whereas the electroconductivity of the material and that of the biofilter bed determine the current production in these systems. Furthermore, we propose the modulation and promotion of its e-accepting capability by polarization, not only through the geoconductor mechanism, but also through the continuous regeneration of quinone-like functionalities (geobattery mechanism). The higher biodegradation efficiency showed by the electroconductive biochar (up to 6.6-fold higher than inert gravel) and the sustainability associated to its production (using renewable natural precursors at remarkably lower temperatures), will satisfy all circular economy criteria to expand the applicability of METs to biofilter-based systems like METland®.

3.6. References

B. E. Logan, K. Rabaey, Conversion of Wastes into Bioelectricity and Chemicals by Using Microbial Electrochemical Technologies, *Science*, 2012, 337, 686-690.

H. Wang, Z. J. Ren, A comprehensive review of microbial electrochemical systems as a platform technology, *Biotechnol. Adv.*, 2013, 31, 1796-1807.

F. Caccavo, D. J. Lonergan, D. R. Lovley, M. Davis, Geobacter sulfurreducens sp. nov., a hydrogen- and acetate-oxidizing dissimilatory metal-reducing microorganism, *Microbiology*, 1994, 60, 3752-3759.

A. M. Speers, G. Reguera, Electron Donors Supporting Growth and Electroactivity of Geobacter sulfurreducens Anode Biofilms, *Appl. Environ. Microbiol.*, 2012, 78, 437-444.

A. Aguirre-Sierra, T. Bacchetti-De Gregoris, A. Berná, J. J. Salas, C. Aragón, A. Esteve-Núñez, Microbial electrochemical systems outperform fixed-bed biofilters in cleaning up urban wastewater, *Environ. Sci. Water Res. Technol.*, 2016, 2, 984-993.

F. Aulenta, R. Verdini, M. Zeppilli, G. Zanaroli, F. Fava, S. Rossetti, M. Majone, Electrochemical stimulation of microbial cis-dichloroethene (cis-DCE) oxidation by an ethene-assimilating culture, *New Biotechnol.*, 2013, 30, 749-755.

J. Rodrigo Quejigo, A. Domínguez-Garay, U. Dörfler, R. Schroll, A. Esteve-Núñez, Anodic shifting of the microbial community profile to enhance oxidative metabolism in soil, *Soil Biol. Biochem.*, 2018, 116, 131-138.

A. Domínguez-Garay, J. R. Quejigo, U. Dörfler, R. Schroll, A. Esteve-Núñez, Bioelectroventing: an electrochemical-assisted bioremediation strategy for cleaning-up atrazine-polluted soils, *Microb. Biotechnol.*, 2018, 11, 50-62.

R. Kadlec, S. Wallace, in Treatment Wetlands, 2nd Edition, CRC Press, Boca Raton, 2009.

METland European H2020 project. http://imetland.eu/

S. A. Patil, C. Hägerhäll, L. Gorton, Electron transfer mechanisms between microorganisms and electrodes in bioelectrochemical systems, *Bioanal. Rev.*, 2012, 4, 159-192.

D. R. Lovley, Happy together: microbial communities that hook up to swap electrons, *ISME J.* 2017, 11, 327-336.

X. Xie, C. Criddle, Y. Cui, Design and fabrication of bioelectrodes for microbial bioelectrochemical systems, *Energy Environ. Sci.*, 2015, 8, 3418-3441.

M. Lu, Y. Qian, L. Huang, X. Xie, W. Huang, Improving the Performance of Microbial Fuel Cells, through Anode Manipulation, *ChemPlusChem*, 2015, 80, 1216-1225.

J. M. Sonawane, A. Yadav, P. C. Ghosh, S. B. Adeloju, Recent advances in the development and utilization of modern anode materials for high performance microbial fuel cells, *Biosens. Bioelectron.*, 2017, 90, 558-576.

Y. Hindatu, M. S. M. Annuar, A. M. Gumel, Mini-review: Anode modification for improved performance of microbial fuel cell, *Renew. Sust. Energ. Rev.*, 2017, 73, 236-248.

S. Tejedor-Sanz, J. R. Quejigo, A. Berná, A. Esteve-Núñez, The planktonic relationship between fluid-like electrodes and bacteria: wiring in motion, *ChemSusChem*, 2017, 10, 693-700.

T. Sun, B. D. Levin, J. J. Guzman, A. Enders, D. A. Muller, L. T. Angenent, J. Lehmann, Rapid electron transfer by the carbon matrix in natural pyrogenic carbon, *Nature Comm.*, 2017, 8, 14873.

Y. Yuan, N. Bolan, A. Prévoteau, M. Vithanage, J. K. Biswas, Y. S. Ok, H. Wang, Applications of biochar in redox-mediated reactions, *Bioresour. Technol.*, 2017, 246, 271-281.

K. Qian, A. Kumar, H. Zhang, D. Bellmer, R. Huhnke, Recent advances in utilization of biochar, *Renew. Sust. Energ. Rev.*, 2015, 42, 1055-1064.

M.-M. Titirici, R. J. White, C. Falco, M. Sevilla, Black perspectives for a green future: hydrothermal carbons for environment protection and energy storage, *Energy Environ. Sci.*, 2012, 5, 6796-6822.

J. Jiang, L. Zhang, X. Wang, N. Holm, K. Rajagopalan, F. Chen, S. Ma, Highly ordered macroporous woody biochar with ultra-high carbon content as supercapacitor electrodes, *Electrochim. Acta*, 2013, 113, 481-489.

T. Huggins, H. Wang, J. Kearns, P. Jenkins, Z.J. Ren, Biochar as a Sustainable Electrode Material for Electricity Production in Microbial Fuel Cells, *Bioresour. Technol.*, 2014, 157, 114-119.

P. Sennu, V. Aravindan, M. Ganesan, Y.-G. Lee, Y.-S. Lee, Biomass-Derived Electrode for Next Generation Lithium-Ion Capacitors, *ChemSusChem*, 2016, 9, 849-854.

K. Kaetzl, M. Lübken, T. Gehring, M. Wichern, Efficient Low-Cost Anaerobic Treatment of Wastewater Using Biochar and Woodchip Filters, *Water*, 2018, 10, 818.

H. P. Klug, L. E. Alexander in X-Ray Diffraction Procedures: For Polycrystalline and Amorphous Materials, 2nd Edition, Wiley-VCH, Weinheim, 1974.

D. Lozano-Castelló, F. Suárez-García, D. Cazorla-Amorós, Á. Linares-Solano, in Carbons for Electrochemical Energy Storage and Conversion Systems, ed. F. Beguin, E. Frackowiak), CRC press, Boca Ratón, 2010, pp. 115-162.

S. Lowell, J. A. Shields, M. A. Thomas, M. Thommes, in Characterization of Porous Solids and Powders: Surface Area, Pore Size and Density, Kluwer Academic Publishers, Dordrecht, 2004.

APHA/AWWA/WEF, Standard Methods for the Examination of Water and Wastewater, 2012.

A. R. Coutinho, J. D. Rocha, C. A. Luengo, Preparing and characterizing biocarbon electrodes, *Fuel Process. Technol.*, 2000, 67, 93-102.

J. Rodríguez-Mirasol, T. Cordero, J.J. Rodríguez, High temperatura carbons from Kraft lignin, *Carbon*, 1996, 34, 43-52.

Y. Wang, D. C. Alsmeyer, R. L. McCreery, Raman Spectroscopy of Carbon Materials: Structural Basis of Observed Spectra, *Chem. Mater.*, 1990, 2, 557-563.

A. Cuesta, P. Dhamelincourt, J. Laureyns, A. Martínez-Alonso, J. M. D. Tascón, Raman microprobe studies on carbon materials, *Carbon*, 1994, 32, 1523-1532.

N. Deprez, D. S. McLachlan, The analysis of the electrical conductivity of graphite conductivity of graphite powders during compaction, *J. Phys. D: Appl. Phys.* 1988, 21, 101-107.

J. L. Figueiredo, M. F. R. Pereira, M. M. A. Freitas, J. J. M. Órfão, Modification of the surface chemistry of activated carbons, *Carbon*, 1999, 37, 1379-1389.

H. Itoi, H. Nishihara, T. Ishii, K. Nueangnoraj, R. Berenguer, T. Kyotani, Large Pseudocapacitance in Quinone-Functionalized Zeolite-Templated Carbon, *Bull. Chem. Soc. Jpn.*, 2014, 87, 250-257.

H. Richter, K. P. Nevin, H. Jia, D. A. Lowy, D. R. Lovley, L. M. Tender, Cyclic voltammetry of biofilms of wild type and mutant *Geobacter sulfurreducens* on fuel cell anodes indicates possible roles of OmcB, OmcZ, type IV pili, and protons in extracellular electron transfer, *Energy Environ. Sci.*, 2009, 2, 506-516.

Council Directive 91/271/EEC of 21 May 1991 concerning urban waste-water treatment.

F. Liu, A. E. Rotaru, P. M. Shrestha, N. S. Malvankar, K. P. Nevin, D. R. Lovley, Promoting direct interspecies electron transfer with activated carbon, *Energy Environ. Sci.*, 2012, 5, 8982–8989.

J. García, D. P. L. Rousseau, J. Morató, E. Lesage, V. Matamoros, J. M. Bayona, Contaminant Removal Processes in Subsurface-Flow Constructed Wetlands: A Review, *Crit. Rev. Environ. Sci. Technol.*, 2010, 40, 561-661

K. Rabaey, P. Clauwaert, P. Aelterman and W. Verstraete, *Environ. Sci. Technol.*, 2005, 39, 8077-8082.

S. Chen, A. -E. Rotaru, P. M. Shrestha, N. S. Malvankar, F. Liu, W. Fan, K. P. Nevin, D. R. Lovley, Promoting Interspecies Electron Transfer with Biochar, *Sci. Rep.,* 2014, 4, 5019

Z. Zhao, Y. Zhang, T. L. Woodard, K. P. Nevin, D. R. Lovley, Enhancing syntrophic metabolism in up-flow anaerobic sludge blanket reactors with conductive carbon materials, *Bioresour. Technol.*, 2015, 191, 140-145.

Z. Zhao, Y. Zhang, D. E. Holmes, Y. Dang, T. L. Woodard, K. P. Nevin, D. R. Lovley, Potential enhancement of direct interspecies electron transfer for syntrophic metabolism of propionate and butyrate with biochar in up-flow anaerobic sludge blanket reactors, *Bioresour. Technol.*, 2016, 209, 148-156.

D. R. Bond, D. R. Lovley, Electricity Production by *Geobacter sulfurreducens* Attached to Electrodes, *Microbiology*, 2003, 69, 1548-1555.

W. Xu, J. J. Pignatello, W. A. Mitch, Role of Black Carbon Electrical Conductivity in Mediating Hexahydro-1,3,5-trinitro-1,3,5-triazine (RDX) Transformation on Carbon Surfaces by Sulfides, *Environ. Sci. Technol.*, 2013, 47, 7129-7136.

M. A. Montes-Morán, D. Suárez, A. Menéndez, E. Fuente, On the nature of basic sites on carbon surfaces: An overview, *Carbon*, 2004, 42, 1219-1224.

J. M. Saquing, Y. -H. Yu, P. C. Chiu, Wood-Derived Black Carbon (Biochar) as a Microbial Electron Donor and Acceptor, *Environ. Sci. Technol. Lett.*, 2016, 3, 62-66.

R. Berenguer, R. Ruiz-Rosas, A. Gallardo, D. Cazorla-Amorós, E. Morallón, H. Nishihara, T. Kyotani, J. Rodríguez-Mirasol, T. Cordero, Enhanced electro-oxidation resistance of carbon electrodes induced by phosphorus surface groups, *Carbon*, 2015, 95, 681-689.

R. Berenguer, F. J. García-Mateos, R. Ruiz-Rosas, D. Cazorla-Amorós, E. Morallón, J. Rodríguez-Mirasol, T. Cordero, Biomass-derived binderless fibrous carbon electrodes for ultrafast energy storage, *Green Chem.*, 2016, 18, 1506-1515.

F. J. Chacón, M. L. Cayuela, A. Roig, M. A. Sánchez-Monedero, Understanding, measuring and tuning the electrochemical properties of biochar for environmental applications, *Rev. Environ. Sci. Biotechnol.*, 2017, 16, 695-715.

M. Vijayaraj, R. Gadiou, K. Anselme, C. Ghimbeu, C. Vix-Guterl, H. Orikasa, T. Kyotani, S. Ittisanronnachai, The Influence of Surface Chemistry and Pore Size on the Adsorption of Proteins on Nanostructured Carbon Materials, *Adv. Funct. Mater.*, 2010, 20, 2489-2499.

3.7. Supplementary material

Cyclic voltammetry analysis

The characterization by cyclic voltammetry was carried out in an H-type electrochemical cell (Fig. S3.5). The anodic and cathodic chambers were separated by a proton exchange membrane (Nafion). Single granules of the three different conductive materials (G, C and BQ) were used as working electrodes, all in the same anodic chamber (under similar environment). The granules of each material (of ca. 1 cm^2) were attached to a wire for external connection. An Ag/AgCl/Cl-(sat.) reference electrode was also placed in this chamber. A graphite plate (3.0 x 1.5 cm) was used as a counter electrode.

The anodic chamber had a volume of 200 mL of Fresh Water Medium (FWM) with 20 mM acetate as electron donor. This medium was inoculated with 20 mL of Geobacter sulfurreducens pure culture with an OD=0.6. Immediately after inoculation, a cyclic voltammetry of each of the granules was made (experiment referred to as t=0). Next, the granules were simultaneously polarized at 0.2 V (vs. Ag/AgCl/Cl-) for 7 days to promote biofilm growth. After this time, a cyclic voltammetry of each of the granules was made again (experiment referred to as t=7).

The voltammetric analysis of the granules was performed sequentially, one by one, using a potentiostat (Nanoelectra NEV-4). The scan rate was 10 mV/s and the potential range -0.6V - +0.6V (vs Ag/AgCl/Cl-). For the potentiostatic polarization, the three conductive granules were simultaneously connected to the same potentiostat. Despite the different electrical resistances of the different materials, the successful polarization (at the same potential) of each granule was confirmed by using a multichannel multimeter (Keithley 2700) connected in series between each granule and the reference electrode.

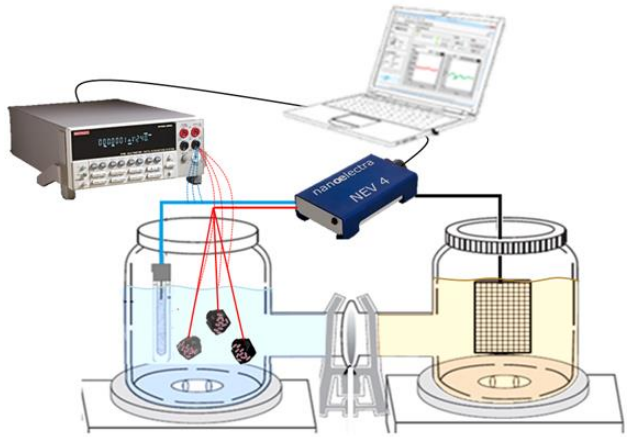

Figure S3.1. Scheme of the used H-type cell and experimental set-up to carry out the voltammetric characterization of single granules of the different conductive materials and the potentiostatic treatment to promote biofilm growth.

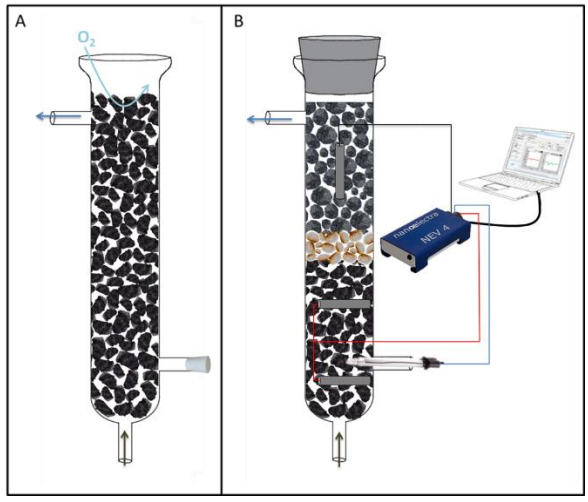

Figure S3.2. Scheme of the used laboratory-scale upflow electroconductive biofilters: A. single-electrode (snorkel) configuration; B. three-electrode configuration, with the anode (down), the counter-electrode (up), and the reference electrode (buried in the anode).

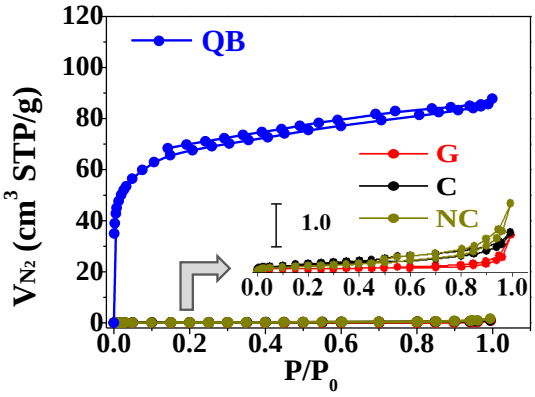

Figure S3.3. N_2 adsorption-desorption isotherms at -196 ° C of the bed materials before being used as electrogenic biofilters: G = graphite; C = coke; QB = Quercus biochar; NC = gravel.

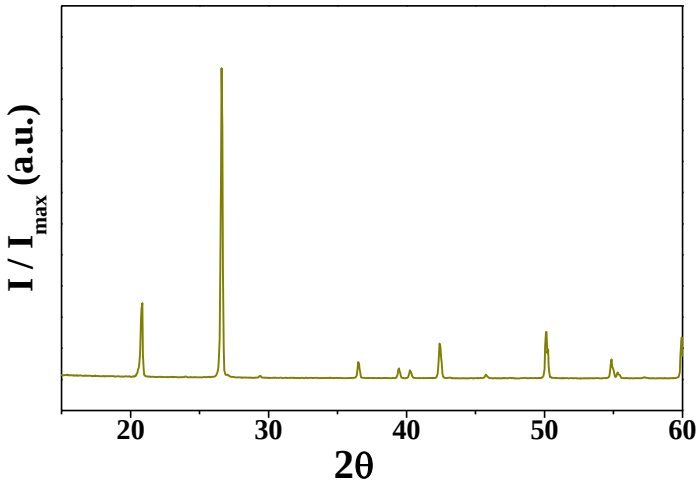

Figure S3.4. X-ray diffractogram of the gravel (NC).

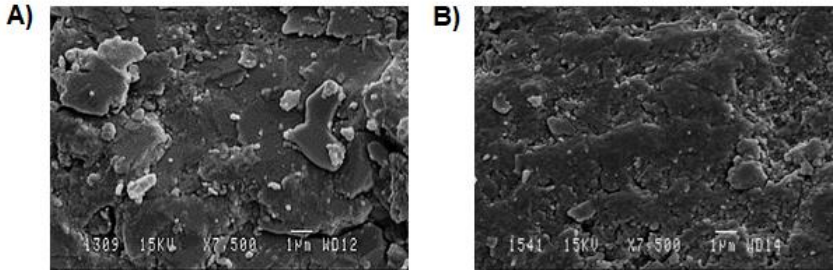

Figure S3.5. SEM micrographs of gravel before (A) and after (B) be used as material for biofilter operation.

Table S3.1. Width (FWHM) and position as well as the calculated interlayer spacing and crystallite dimensions for the characteristic diffraction peaks of the graphite crystalline structure for graphite (G), coke (C) and biochar (QB) materials.

Sample	h k l [a]	FWHM[b] °2θ	Peak pos.[c] °2θ	d-spacing[d] (c/a) Å	Crystallite size[e] (Lc/La) Å
G	0 0 2	0.180	26.577	3.35343	628
C	0 0 2	3.768	25.404	3.50554	22
QB	0 0 2	8.392	23.520	3.78191	10
G	1 0 0	0.309	42.404	2.13130	653
C	1 0 0	3.846	43.207	2.09353	43
QB	1 0 0	8.050	43.810	2.06611	20

a Crystallographic planes (Miller indices) of graphite.
b Full Width at Half Maximum.
c Position of the peaks corrected from the position of the standard Si.
d Distance between the planes of the crystalline lattice calculated from the angle of Bragg by the law of Bragg
e Vertical (Lc) or horizontal (LA) microcrystal size calculated from the width of the peaks (002) or (10), respectively, by the Scherrer equation.

Table S3.2. Spectral parameters from the most important Raman bands; and quantified CO_2- and CO-evolving oxygen surface groups (O = CO + $2CO_2$) of graphite (G), coke (C) and biochar (QB) materials.

Sample	D		G			2D		TPD		
	ν_D cm^{-1}	$\Delta\nu_D$ cm^{-1}	ν_G cm^{-1}	$\Delta\nu_G$ cm^{-1}	I_D/I_D+I_G %	ν_{2D} cm^{-1}	$\Delta\nu_{2D}$ cm^{-1}	CO_2 µmol g^{-1}	CO µmol g^{-1}	O µmol g^{-1}
G	1350.2	41.1	1579.5	21.3	5.0	2705.6	57.7	45	19	109
C	1359.0	127.3	1598.7	57.5	42.7	2695.5	130.0	49	38	178
QB	1343.5	182.0	1587.4	77.2	44.4	2694.5	283.0	683	1230	2596

Table S3.3. Surface chemical composition according to XPS analysis for graphite (G), coke (C) and biochar (QB), before and after being used as polarized electrogenic biofilter bed at 0.6 V.

Sample	Mass surface composition (%)								
	C	O	P	S	N	Fe	ΔO	ΔN	ΔFe
G	98.3	1.7	0.0	0.0	0.0	0.0			
G0.6	87.6	7.5	2.3	0.6	0.8	1.2	5.8	0.8	1.2
C	88.1	10.0	0.0	1.1	0.8	0.0			
C0.6	85.4	11.3	0.0	1.5	1.1	0.7	1.3	0.3	0.7
QB	81.0	16.7	0.9	0.4	0.9	0.0			
QB0.6	77.6	15.5	1.9	1.0	1.7	2.4	---	1.2	2.4

Table S3.4. Characteristics of influent real urban wastewater after the Inhoff tank (average ± SD)

Parameter	Value	Units
pH	7.2 ± 0.4	---
Conductivity	1335 ± 307	µS/cm
Dissolved oxygen	1.0 ± 0.6	mg/l
Redox potential (ORP)	-175 ± 55	mV
Total suspended solids (TSS)	166 ± 111	mg/l
Volatile suspended solids (VSS)	117 ± 58	mg/l
BOD_5	238 ± 134	mg/l
COD	805 ± 98	mg/l
Total nitrogen (TN)	51.7 ± 13.4	mg N/l
Ammonium nitrogen (NH_4N)	41.4 ± 15.5	mg N/l
Nitrate nitrogen (NO_3N)	2.0 ± 4.8	mg N/l
Total phosphorous (TP)	7.1 ± 3.0	mg P/l

Simultaneous characterization of porous and non-porous electrodes in microbial electrochemical systems

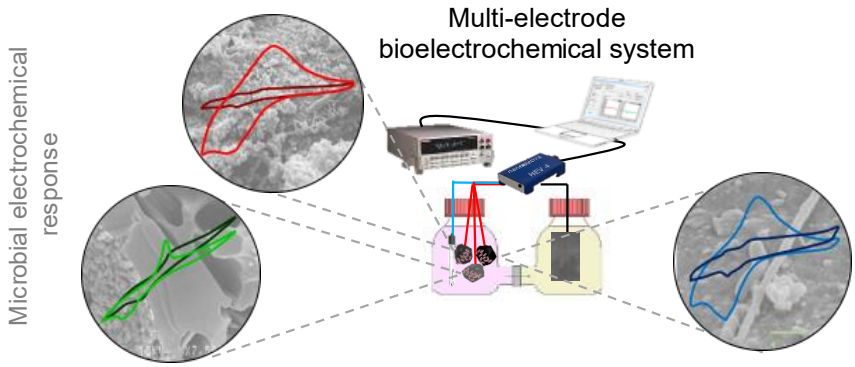

3.8 Abstract

Adequate electrochemical characterization of electrode material/biofilms is crucial for a comprehensive understanding and comparative performance of bioelectrochemical systems (BES). However, their responses are greatly affected by the metabolic activity and growth of these living entities and/or the interference of electrode wiring that can act as an electroactive surface for growth or constitute a source of contamination by corrosion. This restricts the meaningful comparison of the performance of distinct electrode materials in BES. This work describes a methodology for simultaneous electrochemical control and measurement of the microbial response on different electrode materials under the same physicochemical and biological conditions. The method is based on the use of a single channel potentiostat and one counter and reference electrodes to simultaneously polarize several electrode materials in a sole bioelectrochemical cell. Furthermore, various strategies to minimize wiring corrosion are proposed. The proposed methodology, then, will enable a more rigorous characterization of microbial electrochemical responses for comparisons purposes.

3.9 Method details

Electroactive biofilms are of vital importance in the context of fundamental research questions and for their potential exploitation in engineering systems, such as bioelectrochemical systems (BES) (Harnisch et al., 2012). Various electrochemical techniques, like chronoamperometry (CA) and cyclic voltammetry (CV), are powerful tools for the study of extracellular electron transfer (EET) of electroactive bacteria (Feng et al., 2009). Direct correlation between the biofilm development and sustained electricity generation along time (Sharma et al., 2014) could be established from analyzing changes in CA and CV response and biofilm coverage for a given electrode. Indeed, the electrode material has a crucial role on the growth of electroactive biofilms and their EET and bioelectricity production capabilities (Yasri et al., 2019).

In order to perform CA and CV analysis for studying the electrode-bacteria interaction, it is required to set-up a three-electrode with: a working electrode (WE), a reference electrode (RE), and a counter electrode (CE). With this set-up, polarization curves can be recorded by using a potentiostat, where 1) the potential difference between WE and RE is controlled, and 2) the electrical current flow between WE and CE is measured (Bard et al., 2001). This three-electrode system is called Microbial Electrolytic Cell (MEC).

MECs are constructed using a wide variety of electrode materials and in an ever-increasing diversity of configurations. These systems are operated under several physicochemical conditions that include differences in temperature, pH, final electron acceptor, electrode surface area, reactor size, and operation timescale. In order to compare the results from electrochemical analysis, it is necessary to take into account different parameters such as reference states, internal resistance or power densities derived from polarization curves. Such data have been generally obtained using different experimental conditions, materials and/or configurations, making the interpretation and comparison of results among these systems difficult (Logan et al., 2006).

The characterization of the microbial electrochemical response of electrode material/biofilms presents various important problems. First, in contrast to inorganic catalytic systems, microbes are living entities and thus may change over time in their composition (variable microbial population) and activity. Therefore, the physiological state, growth phase, and "history" of the microorganisms should be taken into consideration. In addition, planktonic bacteria also play an important role on the bioelectrocatalytic reaction (Katja et al., 2008). Hence, it is very difficult to replicate exactly the same biological conditions, like number of bacteria, metabolic activity and growth phase. This fact remarkably hampers the reproducibility of the results of a given MEC and makes it practically impossible to compare the performance of different materials that either have been characterized in different cells or in the same cell but under different operation conditions.

Secondly, a deoxygenated solution is necessary in biological chamber, to keep anaerobic microorganisms viable and to avoid oxygen-related reduction currents/peaks in CVs that could hinder the identification of bioelectrochemical processes. Electrochemical characterization of electrode materials requires them to be immersed in an oxygen-free aqueous electrolyte, so all external connection by using wires or, alternatively, wire-material connectors (like conductive adhesives) are inevitably exposed to water. In other cases, although direct exposure of wire-material junction is avoided, the electrolyte can penetrate through the pores of the material to reach the junction. This contact with the medium usually causes the corrosion of wires and/or connectors, thus, releasing redox active and/or non-biocompatible species that can interfere the bioelectrochemical response of the bacteria. Moreover, corrosion may enhance the electric resistance of these elements, affecting the measurements. Consequently, the recorded electrochemical response for an electrode material/biofilm system might be remarkably affected by corrosion of connecting elements, again hampering the reproducibility and comparability of the electrochemical behavior of materials and systems.

To face these problems, this work presents a new method for the meaningful and comparative characterization of the microbial electrochemical

response of different electrode materials (Prado et al., 2019). The method is based on the simultaneous electrochemical control and characterization of various distinct material/electroactive bacteria systems in the same reactor, under identical physicochemical and biological conditions, and minimizing wiring-derived corrosion effects.

The method essentially requires the use of a (i) single-channel potentiostat, (ii) one counter electrode and (iii) one reference electrode and (iv) several working electrodes connected by (v) a suitable wiring. All the electrodes are immersed in (vi) a sole bioelectrochemical cell with (vii) bacterial growth in a deoxygenated medium, and their respective electric signals (current, potential, resistance, etc.) are registered by (viii) proper measuring equipment. These elements are schematized in Figure 1 and operate as a conventional MEC capable to perform classical electroanalytical techniques (Brad et al., 2001).

(i)-(iv) The single-channel potentiostat is used to impose a fixed or varying potential, enabling to register the overall produced electrical current. Apart from the multiple target working electrodes, a blank electrode showing a well-known characteristic response is also recommended to validate the measurements. The wires connecting each of the working electrode are all merged with the working terminal of the potentiostat. In contrast, the counter and reference electrodes are individually connected to their corresponding pins. During electrochemical measurements, the potentiostat displays the potential difference between the working terminal and the reference electrode. Indeed, the electrical current recorded by the potentiostat adds up all the individual currents passing through each working electrode; hence, such value does not correspond to the real single value for each of the working-reference electrode potential systems.

(v) Wiring the electrode materials entails the creation of conductive, mechanically stable and corrosion-resistant wire-material junctions. The type of wire-material connection will depend on the nature and properties of both the wire and the material, emphasizing their corrosion susceptibility and porosity, respectively. The porosity of the material may play a role, by facilitating the penetration and accessibility of the electrolyte to the wire or junction, and/or

by adsorbing and concentrating the released corroded redox-active species on the surface of the electrode. Overall, to avoid corrosion interferences in the presented method, we propose the following two-step strategy for wiring: promotion and subsequent protection of electrical contacts at wire-material junctions. The promotion of electrical contacts can be achieved physically (insert the wire in a drilled hole, tying the wire, etc.), by the aid of conductive adhesives (glues, tapes, etc.), and/or by interposing an additional conductive material which can be better connected to the wire. On the other hand, the protection/isolation of junctions from the electrolyte is generally addressed by coating/sealing with non-corroding resin-like adhesives.

(vi) Different configurations of bioelectrochemical cell can be used. Figure 1 describes two typical set-ups enabling to work at laboratory scale. The *single-chamber configuration* (Fig. 3.10A) consists of a unique cell/chamber containing the working electrodes together with the counter and reference electrodes immersed in the same electrolyte. In the *two-chamber configuration* (Fig. 3.10B), the working and reference electrodes are physically separated from the counter electrode by using two different compartments (the so-called main and auxiliary chambers, respectively) that are ionically interconnected through a suitable polymeric membrane. This last configuration is preferred when the electrochemical processes occurring at the counter electrode can interfere in the characterization of the working electrodes. The cells are usually isolated to keep deoxygenated conditions by hermetic sealing.

Both configurations allow to have all the working electrodes under the same conditions. Physicochemical parameters, such as temperature, pH, solar radiation, presence of gases, concentration of electron donors and salts would be the same, so the bacterial culture inoculum, and its initial metabolic activity, will be the same for all working electrodes. The differences observed in the responses of each of the working electrodes will only be the consequence of the interaction electrode material/bacteria. In this way, possible external factors that may lead to erroneous interpretations are minimized.

(vii) The bacterial growth medium must include the following compounds: salts to assure bacterial viability and to maintain osmotic balance. Furthermore,

such salts include pH buffering species. Vitamins and minerals, required in small amounts and necessary for metabolic reactions. Finally, oxidizing and reducing species are necessary. The reducing specie is the carbon source that e microorganisms oxidize. In this particular case, no soluble electron acceptor was added, since the electrode performed this role. This medium must be deoxygenated by flushing N_2 or Ar, and alternatively, N_2:CO_2 in case of using bicarbonate buffer. It is also recommended to keep the medium in continuous agitation with a magnetic stirrer. In this sense, a laminar agitation allows a faster biofilm formation while a turbulent agitation may increase the homogeneity of the medium.

(viii) Measuring equipment, involving various single multimeters or a multichannel multimeter to register the individual currents produced by each of the working electrodes. Some multichannel measuring devices cannot record electrical current signals, and only measuring potential differences is available. In this case, resistors of a well-known value and negligible compared to the whole internal resistance of the system are required, in order to be the measured value for the potential difference corresponding to an electrical current value equal to the real value in absence of that resistor, the so-called shunt resistor. The resistor was placed in series on each working electrode, and potential drop was measured in the shunt resistor. The value of the current produced by each of the working electrodes was calculated using Ohm's Law.

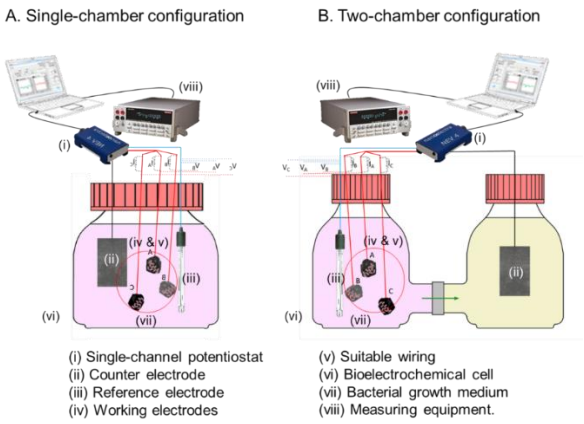

Figure 3.10. Diagram of the MEC and the connections with the potentiostat and the multimeter.

3.10 Method validation

To validate the method, two different measurements were proposed. On the one hand, the prevention of wiring corrosion was validated by using abiotic electrochemical measurements, e.g. cyclic voltammetry. Under these conditions, the absence of microbial electrochemical processes enabled to better discern corrosion-derived currents. On the other hand, the success of using a multielectrode analysis together with a single potentiostat was validated by means of a chronoamperometric experiment in presence of microbial electrochemical processes.

Strategies for avoiding corrosion in wiring: a CV diagnosis

The corrosion phenomena in the working electrodes is an important phenomenon since a bad wiring would be reporting artefacts, that could be erroneously attributed to the electroactive bacteria activity. This confusion could occur, for example, since the cyclic voltammetry (CV) of a model electroactive bacterium like *Geobacter sulfurreducens* (Fig. 3.11) (Estevez-Canales 2005), presents oxidation and reduction peaks in a potential range very close to those shown occurring with the copper wire CV (Fig. 3.12A). Therefore, it is important to consider the nature of both the wire and the working electrode material, for deciding how the attachment is made. In this sense, the corrosion of wires and/or wire-material junctions can be easily evidenced by an abiotic voltammetric characterization of the wired electrode materials.

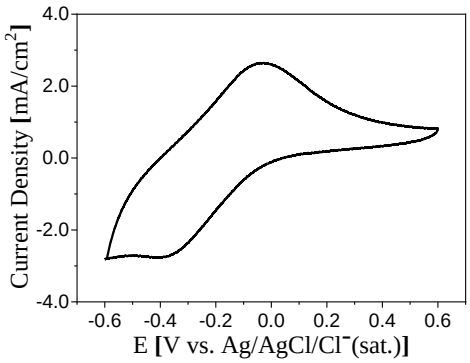

Figure 3.11. Cyclic voltammogram at 10 mV/s of a graphite electrode after promoted biofilm growth in fresh water medium.

In this context, we validated some strategies to prevent the corrosion of wires and wire-material junctions involving both porous and nonporous materials by using abiotic CV as diagnosis methodology. The CV experiments were carried out in a conventional three-electrodes cell at 10 mV/s in a potential range between -0.6 V and 0.6 V (vs. Ag/AgCl/Cl^-(sat.)). A HANNA HI-5311 glass body Ag/AgCl/Cl^-(sat.) electrode with ceramic junction was used as reference electrode, whereas a 2x3 cm Ti/Pt mesh, attached to a copper wire protected by heat shrink tubing, acted as a counter electrode. All the electrodes were immersed in phosphate buffer 100 mM deoxygenated with N_2.

Wires and connections

To construct the working electrodes, gold and copper were chosen as wire material for their different corrosion susceptibility, while carbonaceous materials were used as electrode materials due to their suitable response in microbial electrochemical systems (Prado et al., 2019). We validated the material-wire connection for each electrode according to their voltammetric response (Fig. 3.12).

A) Wires. The oxidation and reduction processes of the wire material were studied. In the case of gold wire (Fig. 3.12A-a.3), the CV did not show any peak in the selected potential window demonstrating the absence of oxidation-reduction processes in the potential window explored. In contrast, copper wire showed oxidation-reduction peaks (Fig. 3.12A-a.1), which could be mistaken as signals provided by electroactive microorganisms. Therefore, this type of wire cannot be used directly with porous carbonaceous materials. To solve this problem, the copper wire should be coated and effectively isolated from the electrolyte with a conductive adhesive, such as PELCOR® Conductive Carbon Glue, avoiding the oxide-reduction processes (Fig. 3.12A-a.2).

Wire-material connections: In most practical cases the wires are susceptible of corrosion, so the proposed general strategy should be to isolate wires (are exposed at wire-material junctions) from the electrolyte but keeping intact electrical contact. Hence, a wire-material contact must be

properly established, physically or assisted by a conductive adhesive, and eventually protected from the electrolyte. The protection is recommended to be extended also to the conductive adhesive in case it might undergo any kind of electrochemical process (interference). However, the type of wire-working electrode connection will depend on the porous or non-porous nature of the carbonaceous material.

B) Connecting wires with non-porous carbonaceous materials. The material used for validation was isostatic Graphite grade 2114-45 provided by Mersen. Due to the non-porous nature of the material, the isolation of connections can be addressed at any point of the electrode surface, independently of whether the junction was on the outer surface or just inserted inside the material. Both two possibilities were tested (Fig. 3.12B).

b.1) A 1 mm diameter orifice was drilled in one of the sides of the isostatic graphite plate and a copper wire was inserted for a proper physical contact. Then, the connection was isolated and reinforced on the outer surface of the material in contact with the electrolyte by using Araldit® epoxy.

b.2) Another possibility was to glue the copper wire to the surface of the isostatic graphite using conductive copper adhesive tape, finally this junction will be covered and isolated with Araldit® epoxy. The response of copper wire-isostatic graphite connections was studied. Our studies revealed that both connections (Fig. 3.12B) were valid for the construction of working electrodes. Indeed, in spite of the resistance and capacity of the electrode, no oxidation-reduction peaks were observed in the range of selected potentials, so the electrochemical response is truly having a biological origin in the interaction between electroactive microorganisms and electrode surface.

C) Connecting wires with porous carbonaceous materials. The material used for validation was Graphite grade 6506, provided by Mersen.

The porous nature of the material enables the electrolyte to permeate through, so the isolation of connections can be exclusively faced just on the junctions (Fig. 3.12C): c.1) In the case of using non-corroding wires, e.g. gold, a simple physical junction could be made to safely avoid any corrosion interference. In contrast, if corroding materials are used as wires, e.g. copper or nickel, the following connections are suggested:

C.2) The wire should be connected with PELCOR® Conductive Carbon Glue, so the copper wire would be directly attached to the porous carbonaceous material while isolated from the electrolyte. This junction should be coated with Araldit® epoxy to seal and strengthen the connection.

c.3) An alternative actin would b is to stick the porous carbonaceous material to a current collector (for example, isostatic graphite) with PELCOR® Conductive Carbon Glue, and coat the junction with Araldit® epoxy to isolate and reinforce the connection. Interestingly, the use of appropriated connections revealed the absence of oxidation-reduction peaks and the CV response was pure capacitive (Fig. 3.12C).

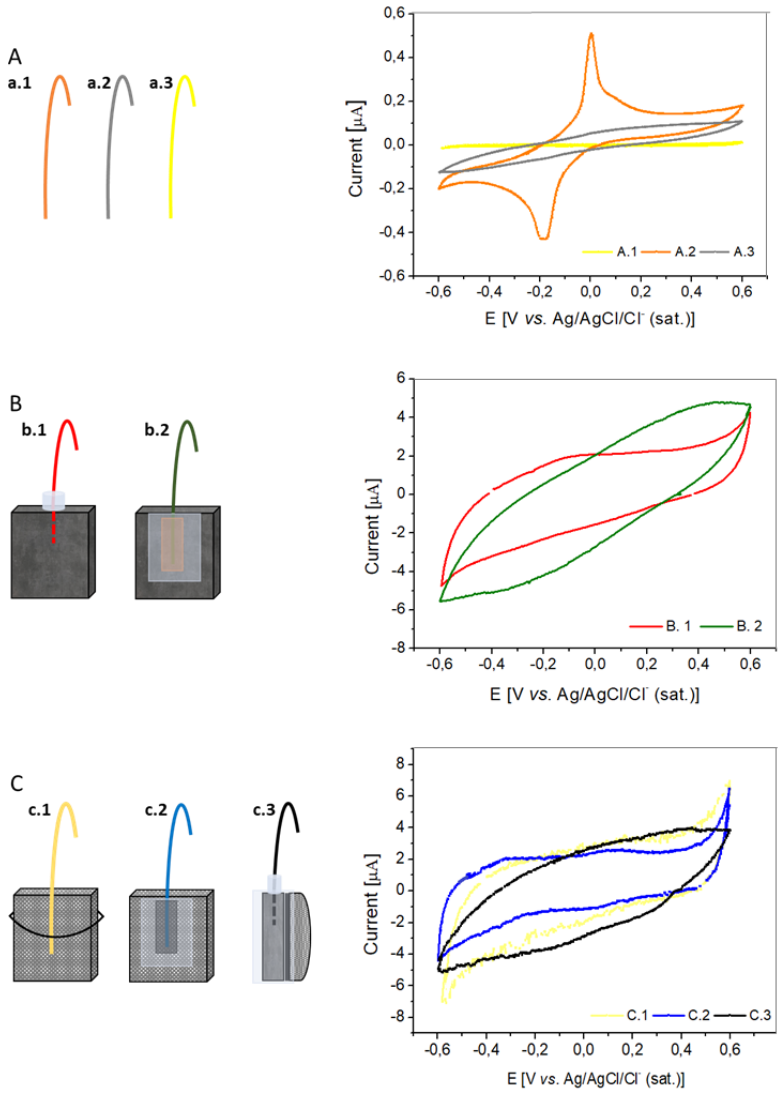

Figure 3.12. A) Left: Wires used for working electrode connections: (a.1), copper wire, (a.2) copper wire coated with carbon glue and (a.3) gold wire. Right: cyclic voltammograms corresponding to left configurations; scan rate = 10 mV s-1; 100 mM buffer phosphate. B) Left: Isostatic graphite connected to copper wire and (b.1) sealed with epoxy resin or (b.2) glued with adhesive copper tape and insulated with epoxy resin. Right: cyclic voltammograms corresponding to left configurations; scan rate = 10 mV s-1; 100 mM buffer phosphate. C) Left: Porous graphite connected to (c.1) gold wire, (c.2) to copper wire through isolation with carbon glue and epoxy resin, or (c.3) to copper wire through isostatic graphite, carbon glue and epoxy resin. Right: cyclic voltammograms corresponding to left configurations; scan rate = 10 mV s-1; 100 mM buffer phosphate.

Method for performing a multielectrode analysis using a single potentiostat

Chronoamperometry is one of the most important characterization techniques of microbial electrochemical systems, so it was used to validate our simultaneous multielectrode analysis. Three different porous carbonaceous materials were used as working electrodes (WE) in a single chamber cell. These materials differed in electrical conductivity (WE1, WE2 and WE3, from lowest to highest electrical conductivity). The wiring was done as described in section one (Fig. 3.12C-c.2). The counter electrode and reference electrode were identical to those described in section one. The cell had a volume of 500 mL, the electrolyte used was Fresh Water Medium (FWM). FWM contained the following mineral salts (per liter): 2.2 g of Na_2HPO_4, 1.18 g of NaH_2PO_4, 0.64 g of NH_4Cl, 0.26 g of KCl and 0.024 g of $C_6H_5FeO_7$ (ferric citrate). Moreover, it includes a mix of vitamins and trace minerals [10]. Acetate (20 mM) was supplied as the sole carbon and electron donor. Anaerobic conditions were achieved by flushing the culture media with N_2 to remove oxygen and a phosphate buffer was used to keep a pH of 7. This medium was inoculated with 20 mL of *Geobacter sulfurreducens* pure culture with an OD_{600} = 0.6.

Each working electrode was polarized to +0.2 V (*vs.* Ag/AgCl(sat.)) with a Nanoelectra NEV-4 potentiostat, which allows to monitor the overall electrical current passing through the system. The real potential difference WE-RE and individual current at each working electrode were continuously recorded with a Keithley 2700 multichannel multimeter. The basic model of this family of multimeters has only 2 channels to measure current and 20 channels for recording potential differences. Alternatively, a resistor of known value, shunt resistor can be incorporated to potential-measuring channels for registering the potential drop across it the it is related to the electrical current through Ohm's Law. This resistor is usually called shunt-resistor in electronic field.

Nevertheless, to follow the same measurement strategy (for a better comparability), three resistors were used to measure the current of the three working electrodes. The resistor values should be selected according to the expected currents and the accuracy of the measuring equipment. The resistors

were connected in series between each working electrode and in parallel with respect to the multimeter. In addition, another channel of the multimeter was connected in parallel between the working and reference electrodes, to know the real polarization potential for each working electrode. Thus, although the resistance of each material that is acting as working electrode is different, it can be checked if electrodes are polarized at the right potential. Finally, to verify that the current produced by the system is being correctly monitored, one of the multimeter current channels was connected, in series, to the counter electrode. The sum of the current generated by each working electrode should be equal to both the current registered at the counter electrode and the current registered by the potentiostat.

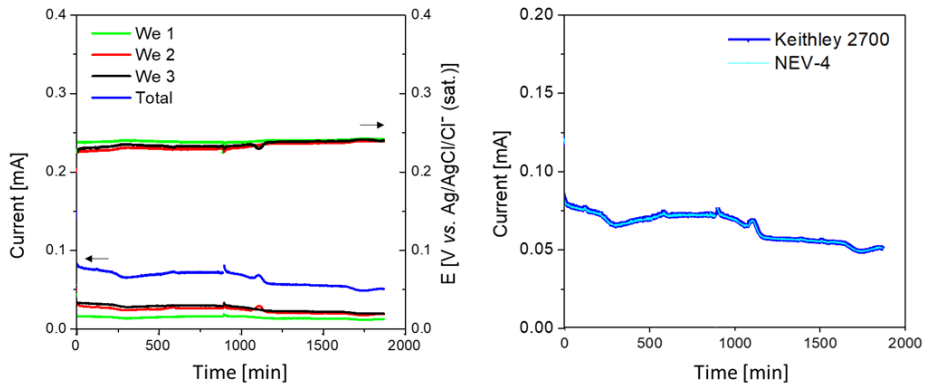

Figure 3.13. (left) Current intensity and polarization potential associated to the 3 working electrodes of the MEC including the summation of all currents. (right) Comparison of the total current recorded by both the multimeter and the potentiostat.

Fig. 3.13A shows the calculated values of current produced by each of the three working electrodes, the bigger electrical current value corresponds to the electrode material with lower electrical resistance. These values were calculated through the instantaneous potential difference measured in each working electrode and the value of the resistor used in the external circuit (1 KΩ). The total sum of the currents produced by each working electrode measured by the aid of the Keithley multimeter (blue line in Fig. 3.13A) was the same as the one recorded by the NEV-4 potentiostat (see fitting in Fig. 4B). Furthermore, the real potential of each working electrode remained constant

around 0.23 V over time for the different electrodes (Fig. 3.13A). The difference of 30 mV between the set and measured potentials is assigned to the inevitable circuit and connections resistances, but this small value supports that the electrochemical characterization based on the proposed method has been carried out successfully.

3.11 References

F. Harnisch, S. Freguia. A basic tutorial on cyclic voltammetry for the investigation of electroactive microbial biofilms, Chemistry–An Asian Journal, 7(3) (2012) 466-475.

Z. Feng, R. Slade, J. R. Varcoe. Techniques for the study and development of microbial fuel cells: an electrochemical perspective. Chemical Society Reviews 38(7) (2009) 1926-1939.

M. Sharma, S. Bajracharya, S. Gildemyn, S. A. Patil, Y. Alvarez Gallego, D. Pant, K. Rabaey, X. Dominguez-Benetton. A critical revisit of the key parameters used to describe microbial electrochemical systems, Electrochim. Acta 140 (2014) 191–208.

Yasri, N., Roberts, E. P., & Gunasekaran, S., The electrochemical perspective of bioelectrocatalytic activities in microbial electrolysis and microbial fuel cells. Energy Reports, 5 (2019) 1116-1136.

A. J. Bard, L. R. Faulkner. Electrochemical Methods: Fundamentals and Applicati-ons, 2nd ed.; John Wiley & Sons: New York, 2001.

B. E. Logan, B. Hamelers, R. Rozendal, U. Schroder, J. Keller, S. Freguia, et al, Microbial fuel cells: methodology and technology, Environ Sci Technol. 40 (2006) 5181–92.

F. Katja, F. Harnisch, U. Schröder. On the use of cyclic voltammetry for the study of anodic electron transfer in microbial fuel cells, Energy & Environmental Science 1(1) (2008) 144-147.

A. Prado, R. Berenguer, A. Esteve-Núñez, Electroactive biochar outperforms highly conductive carbon materials for biodegrading pollutants by enhancing microbial extracellular electron transfer, Carbon 146 (2019) 597-609.

M. Estevez-Canales, A. Berná, Z. Borjas, & A. Esteve-Núñez. Screen-printed electrodes: new tools for developing microbial electrochemistry at microscale level, Energies 8(11) (2015) 13211-13221.

A. Esteve-Núñez, M. Rothermich, M. Sharma, D. Lovley. Growth of Geobacter sulfurreducens under nutrient-limiting conditions in continuous culture, Environ Microbiol 7(5) (2005) 641-648.

CHAPTER 4:

NOVEL BIOELECTROCHEMICAL STRATEGIES FOR DOMESTICATING THE E-FLOW IN CONSTRUCTED WETLANDS

This section has been redrafted after:

International Patent application under PCT program. App number: PCT/ES2017/070160.

Amanda Prado de Nicolás[a,b], Carlos A. Ramírez-Vargas[c,d], Carlos A. Arias[c,d], Abraham Esteve-Núñez[a,b]. 2019. *Novel bioelectrochemical strategies for domesticating the electron flow in constructed wetlands*. Science of The Total Environment, 735, 139522

[a] Chemical Engineering Department, Universidad de Alcalá, Alcalá de Henares, Spain

[b] Bioe Group, IMDEA Agua, Parque Tecnológico de la Universidad de Alcalá, 28805, Alcalá de Henares, Spain

[c] Department of Bioscience, Aarhus University, Ole Worms Allé 1, 8000 Aarhus C, Denmark

[d] WATEC, Aarhus University, Ny Munkegade 120, 8000 Aarhus C, Denmark

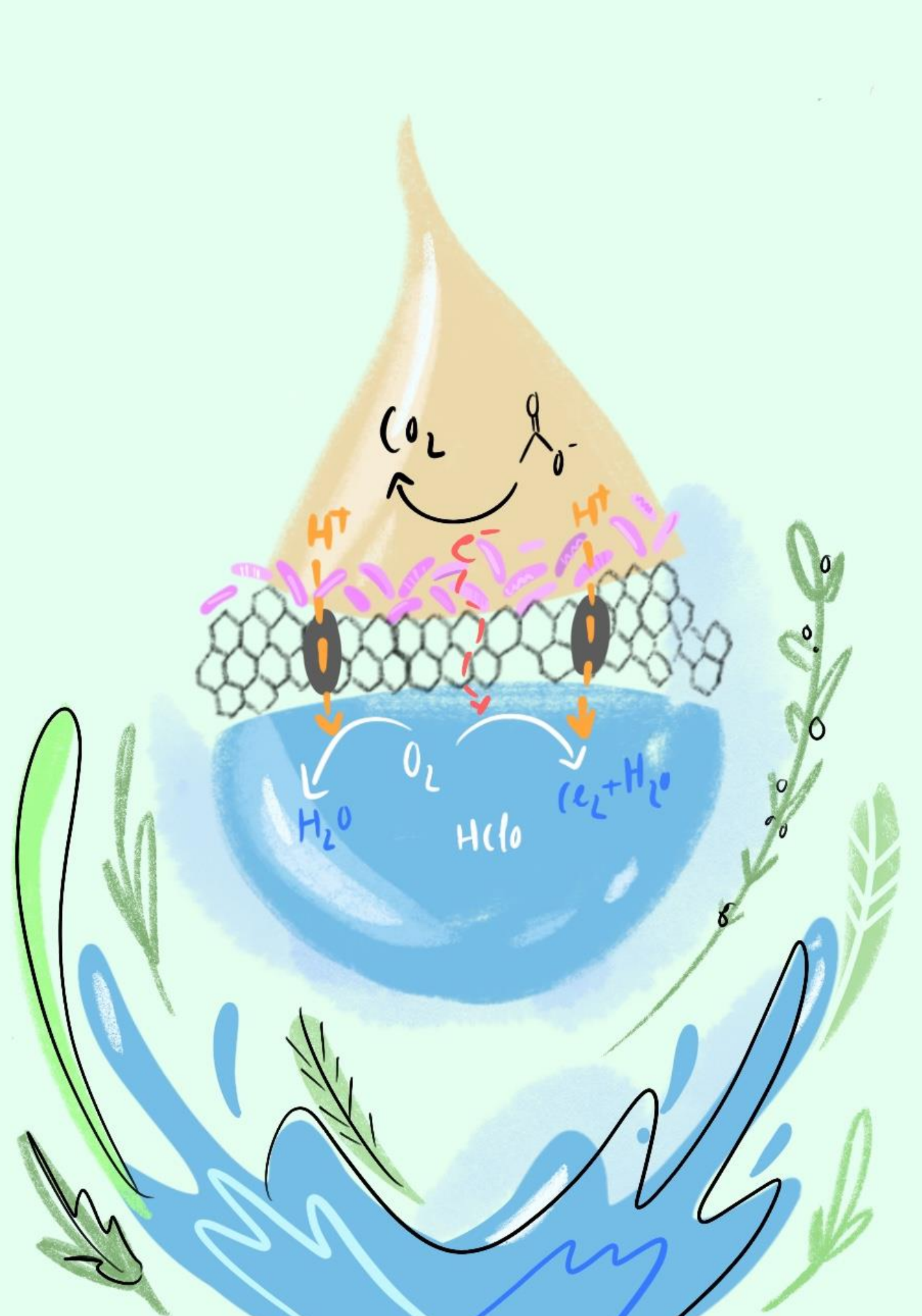
CO_2
H^+
H^+
O_2
H_2O
HClO
Cl_2+H_2O

Novel bioelectrochemical strategies for domesticating the electron flow in constructed wetlands

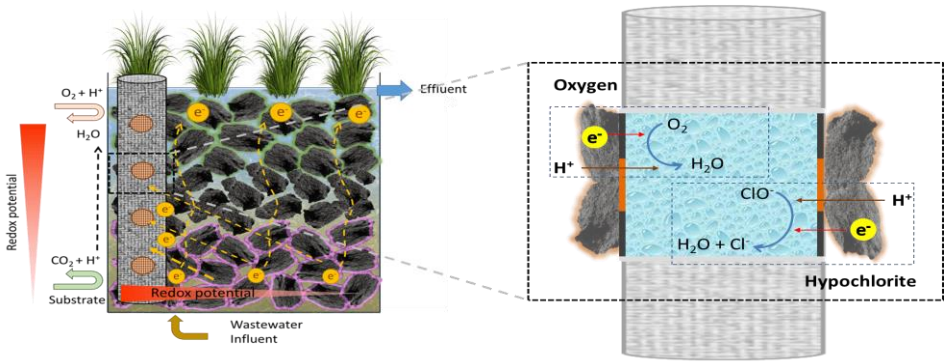

4.1. Abstract

Constructed wetlands are an effective biofilter-based technology for treating wastewater in a sustainable way; however, their main disadvantage is a large area footprint. To cope with this limitation a new generation of constructed wetlands, the METlands®, have been recently reported. METlands® replace gravel with a granular electrically conductive material to enhance the oxidative metabolisms of electroactive bacteria by facilitating the flux of electron through the material and, consequently, increase bioremediation rates. In this work we evaluated the performance of a new electron sink (e-sink) device with the purpose of controlling and enhancing the electrochemical consumption of electrons from microbial metabolism without energy consumption. The e-sink device was integrated inside the biofilter bed and was tested using different electron acceptors with high redox potentials, like oxygen and hypochlorite. Interestingly, the presence of the e-sink allowed novel redox gradients to form inside the METland® and, consequently, a new electron flow was demonstrated by measuring both the electric potential and current density profiles of the bed. Three independent biofilters were constructed and operated under flooded conditions. Ec-coke and electroconductive biochar (ec-biochar) were used as electrically conductive bed materials, while gravel was used as an inert control. Furthermore, e-sink integration inside the electrically conductive bed outperformed METlands® for removing pollutants, already much

more efficient than standard gravel biofilters. COD removal was increased from 90% in METland® to 95% in the e-sink METland® as compared to 75% for the control, while total nitrogen removal was enhanced from 64% in METland® to 71% in e-sink METland® as compared to 55% for the control. Our results indicate that increasing the electrochemical availability of electron acceptors by using the e-sink will be a suitable method for controlling the electron flow inside the filter bed and can be integrated in full scale METlands® for achieving high removal rates.

4.2 Introduction

Constructed wetlands (CW) are biological wastewater treatment systems that mimic the physical, chemical, and biological degradation processes taking place in natural wetlands. This technology emerged several decades ago (Brix, 1994) as a robust, eco-friendly, and cost-effective decentralized treatment system that requires low operational and maintenance costs (Brix et al., 2007; Dotro et al., 2017; Vymazal, 2008; H. Wu et al., 2014). CWs can be used to treat a wide range of water pollutants such as domestic wastewater (García et al., 2010), industrial wastewater (Vymazal, 2014), mine drainage (Isosaari P. & Sillanpää M. , 2016), agricultural runoff (Roley et al., 2012) and urban storm runoff (Carleton et al., 2000). However, when compared to conventional biological wastewater treatments CWs main disadvantages are the large footprint of land required and certain limitations for nutrient removal (Kadlec and Wallace, 2009).

Therefore, to reduce the surface area requirements, constructed wetlands have been evolving from passive into intensified systems (Wu S. et al., 2014) by supplying oxygen to enhance oxidative metabolism. More recently, the new-born discipline of microbial electrochemistry has been applied to constructed wetlands in the name of intensification (Ramírez-Vargas et al., 2018). Redox gradient profiles along the depth of a CW are produced as it transitions from aerobic zones at the top to anoxic zones at the bottom. This scenario lends to the application of a microbial electrochemical system where pollutants can be converted into electrical current by the metabolic activity of

the electroactive bacteria and form a new gradient to increase removal efficiency (Corbella et al., 2014; Aguirre-Sierra et al., 2016; Wang et al., 2017).

The integration of microbial electrochemical technologies (MET) into constructed wetlands is illustrated by the many different configurations used (Ramírez-Vargas et al., 2018). The microbial fuel cell (MFC) is able to harvest energy from the wetland using an anode located in the anaerobic zone (bottom) and a cathode located in the aerobic zone (top). These are separated by a layer of inert material (gravel) and connected through an external circuit (Zhao et al., 2013; Corbella et al., 2014). Microbial electrolysis cells (MEC) are integrated into the wetland in a similar manner as the MFC but the electrodes are polarized through a potentiostat or a power source (Aguirre-Sierra et al., 2016; Srivastava et al., 2018). Microbial electrochemical snorkels (MES) are the most basic configuration, simply a conductive bed that forms a redox gradient according to the chemical environment around the material. Anodic and cathodic reactions are not occurring under different electrodes but in different locations of a unique conductive body. This situation is ideal when the objective is to raise electrochemical reaction rates that do not require a strict control of redox potential. In contrast with standard two-electrode systems, the microbial metabolism cannot be converted into electric power (Aguirre-Sierra et al., 2016; Ramírez-Vargas et al., 2019) (Fig. 1S).

Despite their good performance at the laboratory scale, full scale implementation of the CW-MFC is under development due to a number of challenges. Mainly, internal resistance in the CW–MFC is dependent on both the resistance of the electrolyte and the material-based electrical resistance between the electrodes. This resistance increases linearly as the size and distance between electrodes increases (Doherty et al., 2015).

The METland® (Aguirre-Sierra et al., 2016) is an alternative configuration based on a continuous bed of electrically conductive material, also known as a MES. This material promotes the metabolism of electroactive bacteria by acting as an inexhaustible connector with the distant terminal electron acceptors (TEAs), like surface oxygen. The concept has been successfully tested under flooded conditions such as those found in conventional horizontal subsurface

flow (HSSF) wetlands (Aguirre-Sierra et al., 2016; Prado et al., 2019; Ramírez-Vargas et al., 2019) COD removal rates were as high as 400 g/m3day with real urban wastewater fed at ca. 0.5 m3/m2day (Aguirre-Sierra, 2017). Interestingly, the system outperformed classical gravel-based HSSF CW reaching a ratio of 0.4 m2/pe. The METland® can also outperform conventional CW in their ability to remove emergent pollutants in the form of pharmaceuticals (Pun et al., 2019). Many different carbon-based electroconductive materials have been tested for use in the METland® system (Aguirre-Sierra et al., 2016; Ramírez-Vargas et al., 2019), electrically conductive biochar, from the high-temperature pyrolysis of various Quercus biomass, showed the best performance (Prado et al., 2019; Schievano et al., 2019).

Unlike typical bioelectrochemical systems, METlands® do not have two differentiated electrodes but host anodic and cathodic reactions on the surface of a single electrode bed exposed to different redox environments. Thus, in METlands® the major anodic and cathodic processes follow a gradient across the depth of the bed. The main cathodic process, like the reduction of oxygen, happen at the upper bed layers whereas the anodic oxidation of organic matter occurs in the anoxic bottom layers; (Ramírez-Vargas et al., 2018). The vertical separation of the anodic and cathodic reactions promotes a local charge imbalance that generates an electric field and an increased electric potential with depth. The electric field can be used to estimate the electric current generated by the electroactive bacteria, a method already followed to measure the electric current generated by cable bacteria in marine sediments (Risgaard-Petersen et al., 2014).

In this context, the electron flow generated inside METland® systems are a direct consequence of the electroactive bacteria's metabolism. They use a mechanism similar to the one reported in natural electric current generators like geobatteries or biogeobatteries (Nielsen and Risgaard-Petersen, 2014), in which a conductive material crosses two different redox domains, like that found in the transition between sediment and the water column in a pond or lake. The electrically conductive material allows the transport of electrons from the anodic oxidation reactions in the sediment to the cathodic reduction reactions

near the water's surface (Nielsen et al., 2010). Furthermore the sediment acts as an electrolytic conductor allowing ion migration to complete the electric circuit and maintain charge balance (Sato and Mooney, 1960). Interestingly, ion migration in the METland® is taking place in the pore water and generates a typical electric potential profile that is absent in gravel-based CW (Ramírez-Vargas et al., 2019). The long-distance separation (30-40 cm) between cathodic and anodic processes by electrically conductive material represents a change in the paradigm of biological wastewater treatment where the conventional thinking was that both electron donors and acceptors for a metabolic process need to be in the same living cell, or at least within a few micrometers of each other. In METlands®, bacteria can directly use electrically conductive material as an electron mediator, these electrons can flux to cathodic areas where TEAs, such as oxygen or nitrate, can be reduced to further drive the formation of a redox gradient.

Unlike most MET applications which require an anaerobic environment, METlands® can operate as an aerobic vertical subsurface downflow (VSSF) biofilter (Aguirre-Sierra et al., 2020). The presence of oxygen enhances nitrifying conditions over gravel-based systems and unexpectedly it promoted the presence of electroactive bacteria from *Geobacter* genus typical of anoxic environments (Aguirre-Sierra et al., 2020). Thus, operational modes in METland® allow for additional control of redox gradients and electron transfer along bed, this is nearly impossible in standard CWs.

This work aims to integrate the new concept of the e-sink into METlands® to artificially create new redox gradients to promote both electron transfer and biodegradation of pollutants in wastewater. This novel device will allow for the "domestication" of the flux of electrons from microbial metabolism and allowing for their distal consumption in environments different from their original biological niche.

4.3 Material and methods

4.3.1 Construction of the e-sink device

The electron sink (e-sink) device was built using electrically conductive carbon fiber tube (20 cm long x 2 cm diameter) sealed at the bottom with a silicone stopper. This created a cylindrical chamber capable of housing a solution. The tube was further drilled to produce 0.5 cm holes every two centimeters (Fig. 4.1). All holes where sealed with a cation exchange membrane (Nafion®) to keep the tube impermeable to water but allowing for the flow of protons into the interior of the e-sink. Direct contact with the bed granules allows for a flux of electrons passed through the carbon fiber tube and interact with the solution inside the e-sink. The e-sink devices were installed inside beds of either gravel, ec-coke, or ec-biochar and different catholytes were tested in the e-sink (Fig. 2S):

i) Oxygenated water $O_2 + 4e^- + 4H^+ \rightarrow 2H_2O$

ii) Hypochlorite 80 mM solution $HClO + 2e^- + H^+ \rightarrow Cl^- + H_2O$

4.3.2 Biofilters construction and operation

Three biofilters were built with three bed materials: ec-coke (C), ec-biochar (ecB) and gravel (G). The ec-coke and ec-biochar are electrically conductive and carbonaceous while the third, gravel, was an inert control (Table 4.1). Each biofilter consisted of a 5.4 L polyvinylchloride (PVC) cylinder (diameter: 25 cm, height: 15 cm), with an outlet at a height of 11 cm to maintain the water level, and a perforated pipe inlet in the bottom of the system. Each biofilter was filled with the materials previously stated, the pore volume was approximately 50% of total volume.

An e-sink device was placed next to the inner wall of each biofilter. In addition, three perforated pipes for sampling were placed inside the biofilter at different distances (0, 6, 12 cm) from the e-sink device (Fig. 4.1), these pipes were the sample points SP1, SP2, and SP3 respectively.

Table 4.1. Physiochemical characteristics of bed materials.

	EC- Coke (C)	EC-Biochar (ecB)	Gravel (G)
Density [g/cm^3]	0.5	0.5	0,6
Resistance [Ω]	1	15	-
Porosity [%]	48	52	43
Granulometry [cm]	1.5-3	2-3	1.5-3

The biofilters were housed outdoors with natural temperature variations (ranging from 13°C to 34°C) but protected from rain. The systems were fed with urban wastewater containing 625 mg/L COD, 320 mg/L BOD_5, 45 mg/L total nitrogen (TN). The columns were operated in a continuous up-flow mode with a hydraulic loading rate of 0.6 L/d and COD loading rate 88 g COD/m^{3}d for 45 days, using a peristaltic pump (LongerPump®).

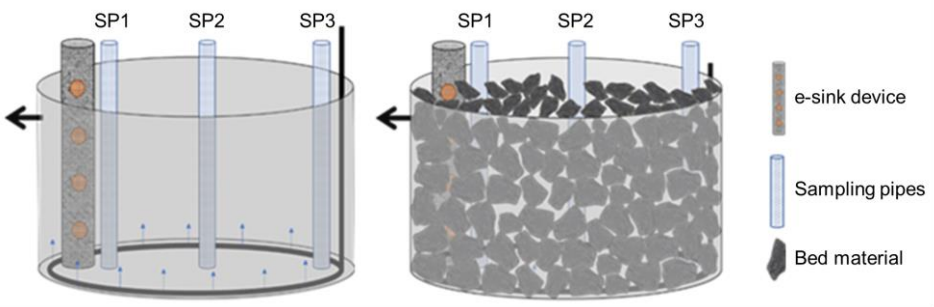

Figure 4.1. Biofilter scheme without (left) and with (right) bed material.

4.3.3. Sampling and laboratory analysis

Steady state conditions for the biofilters were reached after three weeks of an initial acclimation period. Steady state was defined as constant removal efficiencies for each of the biofilters. Then, to study the COD and nutrient removal efficiency, three conditions were tested based on the electron acceptor used in the e-sink device: (1) control: empty e-sink device, so removal efficiency was just depending on the bed material, (2) oxygen saturated water, and (3) an 80mM hypochlorite solution. Each condition was operated for a week before sampling. For each experimental condition three samples were taken. The samples were taken every 48 h. Influent and effluent samples were analyzed for

the presence of COD, and N species. COD analysis was carried out by photometric evaluation (Hach LCK cuvette test + DR 3900 spectrophotometer). BOD_5 analysis was performed using respirometric method (WTW OxiTOP®). NH_4^+ and NO_3^- was measured with photometric evaluation (Hach APC and LCK cuvette test + DR 3900 spectrophotometer).

4.3.4 Electric potential measurements

To measure the electric potential (EP), a custom-made shielded silver/silver chloride EP sensor was developed (height: 60 cm; diameter: 0.12 cm) (Ramírez-Vargas et al., 2019). These EP electrodes were built to be insensitive to redox-active compounds (Damgaard et al., 2014). The EP sensor was coupled to an Ag/AgCl reference electrode placed on the surface of the biofilter below the surface water. Both electrodes were connected to a digital voltmeter. The electric potential was measured in each sample point (SP1, SP2, SP3) in steps of 1cm against Ag/AgCl reference electrode positioned in the top water column. Profiles were measured to 11 cm depth in the biofilters (Fig. 4.3S). Each profile point was measured for 30 sec, recording one data point per second. For all profiles, the signal value in the overlying water was subtracted from all the values in the profile, resulting in profiles of electric potential relative to that of the overlying water, which was used as a reference potential for normalized the EP values.

The METland® represents a complete electric circuit in which charges are carried as i) electron currents within the electrically conductive material and ii) as ionic currents in the pore water. At steady state, these currents are equal in magnitude but opposite in direction (Sato and Mooney, 1960). The ion current density running through the bed obeys Ohm's law (Risgaard-Petersen et al., 2014) can, consequently. be quantified from the EP and the conductivity of the water *(σ)*, which, with a homogenous distribution of electroactive bacteria, implies that the quantity of electrons running in the biofilter bed per second through a unit area, i.e., the electron current density *(J)*, can be estimated as (Risgaard-Petersen et al., 2014):

$$J = -\sigma \cdot \frac{d\varphi}{dz} \qquad (Eq.\,1)$$

Where J [A m^{-2}] is the electron current density, σ [S m^{-1}] is the electrical conductivity of water in the column and $\frac{d\varphi}{dz}$ [V m^{-1}] is the EP gradient, the rate of increasing EP with respect to decreasing depth.

The electric current is the result of anodic and cathodic reactions occurring in the METland®. Therefore, the analysis of electric fields recorded in an EP profile, could be used to estimate the areas acting as electron sources and electron sinks along biofilter profile (Damgaard et al., 2014). The electron transfer rate (*R*) can be estimated (adapted from Risgaard-Petersen et al., 2014):

$$R = -\frac{dJ}{dz} \cdot \frac{1}{F} \qquad (Eq.\ 2)$$

Where R is the rate of electron transfer from reactions per unit volume [μmol m^{-3} s^{-1}], $\frac{dJ}{dz}$ is the gradient of electron current density [A m^{-2} m], and F is the Faraday constant [9.65 x 104 C mol^{-1}].

4.3.5 Statistical analysis

Removal efficiencies were calculated as a percentage of the total inlet concentration of pollutants. Removal rates were obtained from the inlet-outlet difference as grams per cubic meter of bed per day. The data in the bar graphs corresponds to the average value of 3 measurements taken once steady state conditions was reached. In order to discern the true effect of the bed materials for each operation condition, statistical procedures were conducted with these 3 measurements using R software (R Core Team 2013) and R-commander package (Fox 2005). The standard error of the mean of these measurements is included in the error bars.

4.4 Results and discussion

4.1 Electric potential profiles and electron currents

In order to verify this new redox gradient concept, we monitored the electric potential profiles along the bed. Since the METland® operates as single electrode this methodology is key; without an external circuit electrical current cannot be directly measured as typically occurs with standard microbial electrochemical systems (Borjas et al., 2017). This elegant method of measuring

electric potential (EP) to estimate derived ionic current densities was performed previously to calculate current density (*J*) along the METland® bed and the rate of electrons transfer from reactions per unit volume (*R*) (Ramírez-Vargas et al., 2019). Furthermore, it has also been shown that the electrical potential profile is not affected by pH or the redox gradient (Damgaard et al., 2014).

EP profiles were analysed for the three biofilters (gravel (G), ec-coke (C) and ec-biochar (ecB)) at three independent sampling points (Fig. 4.2) when the systems reached steady state. In addition, the systems were operated under snorkel configuration with an e-sink inside the bed. The e-sink was operated under three conditions: (i) empty as a control, (ii) with aerated water and (iii) with hypochlorite (80 mM). The EP profile showed differences between the tested systems (Fig. 4.2), indicating the impact of electrochemical electron acceptors on the flow of ions, and consequently on the flux of electrons. This behaviour was correlated with the microbial activity, in terms of the removal efficiency of pollutants for each treatment.

The up flow operation of a conventional biofilter, made of inert material like gravel, typically leads to microbial metabolism being limited by the availability of an electron acceptor. Electrons cannot travel along the inert bed so the EP depth profile of this system showed no variations at all between sampling points. In this system, oxidation and reduction reactions leading to pollutant removal are coupled both temporally and spatially (Ramírez-Vargas et al., 2019). We confirmed such behaviour in our gravel-based biofilters (Fig. 4.2) which acted as control, free of a vertical redox gradient. In contrast, systems made of electroconductive bed showed variations of the EP with depth due to the transfer of electrons from the microbial oxidation of pollutants. (Fig. 4.2). The electric potential generated by this microbial electron transfer triggered a flux of ions in the liquid phase with the same value and magnitude but in the opposite direction of the electrons thereby closing the electric circuit.

The implementation of e-sink devices hosting different electrochemical electrons acceptors generated a new redox gradient in the horizontal axis, this provides a new dimension for the EP profiles. As expected, the sampling point closest to the e-sink device (SP1), was the one most affected. The electrons

generated at the bottom layers of the bed migrated towards the e-sink device instead of towards the upper top layer where oxygen is present. For this reason, the EP vertical profile in SP1 (Fig. 4.2) showed a lower slope, therefore behaving similarly to gravel system. In contrast, for the sampling point farthest away (SP3) from the e-sink device, showed less influence and an EP vertical profile was similar to e-sink free systems.

The electrochemical electron acceptor used in the e-sink device significantly affected the EP vertical profiles. When the redox potential of the electron acceptor was more positive, it corresponded to a higher reduction rate of the acceptor, a higher flux of electrons, and a greater radius of influence by the e-sink device. Operating a METland® with e-sink increased the net volume of TEA available. The electron flux was then also established along the horizontal direction and, consequently, the electron flux towards the oxygen at the uppermost surface was reduced. Such differences can be observed in the EP vertical profiles when oxygen or hypochlorite were the TEA tested the e-sink device (Fig. 4.2). So, the higher the TEA redox potential the lower the slope for the EP vertical profile. This is consistent with the fact that hypochlorite from e-sink consume more electrons than just oxygen, so it shows higher impact in its EP vertical profile (Fig. 4.2). Furthermore, the impact of e-sink in EP vertical profile was stronger in those sampling points (SP1) closer to the e-sink, and weaker in those located far away (SP3). Finally, the electrically conductive material's resistance also affected the EP profiles. The lower the material's resistance, the greater the influence from the e-sink device. This increases the flux of electrons that will be diverted to the e-sink instead of the uppermost surface, what eventually increased the efficiency of the biofilters.

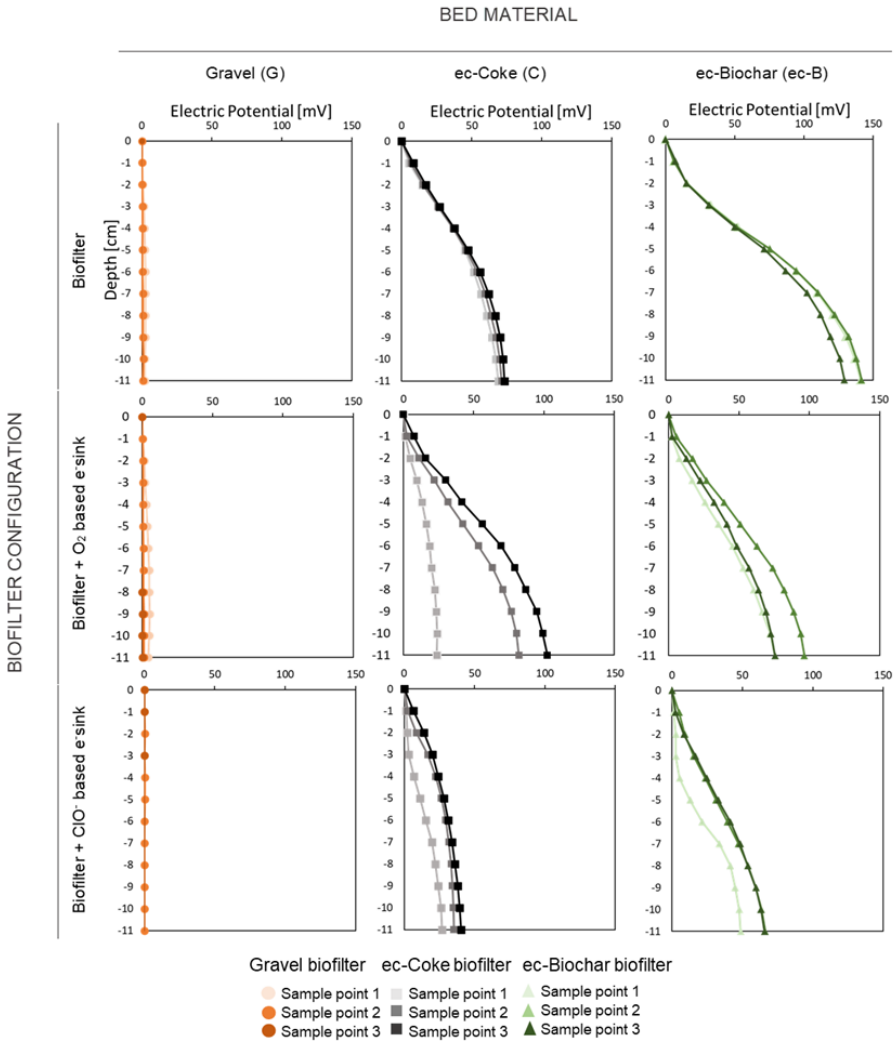

Figure 4.2. Electric vertical potential (EP) profiles of tested biofilters along depth at each sampling point (SP1, SP2 and SP3) of gravel (orange), ec-coke (grey) and ec-biochar (green) bed operating as biofilter, biofilter + O_2 based e-sink and biofilter + ClO^- based e-sink. EP profiles were measured with a shielded Ag/AgCl electric potential electrode.

Our study shows that connecting microorganisms through an electrically conductive bed allows the problems associated with limited electron acceptor availability to be overcome, by coupling the metabolism between disparate communities performing pollutant oxidation and the electrochemical reduction of electron acceptors inside the e-sink device.

As described before, METlands® represents a complete electric circuit in which charges, resulting from the organic matter oxidation by electroactive bacteria are carried as a flux of electrons through the electrically conductive bed and as ion flows through currents in the water. At steady state, these currents are equal in magnitude but opposite in direction (Damgaard et al., 2014). The ion current density *(J)* through the electrically conductive material was calculated along depth, at 1 cm interval, for each sample point (Fig. 4.3) in ec-coke and ec-biochar biofilters. For these calculations the *Eq. 2* was used, the values of the water conductivity are provided in Table 4.11S. In the gravel biofilter, it was not possible to calculate the current density since the EP at all points was not significant.

In the systems operating as standard METlands® , without an e-sink device (Fig. 4.3A and 4.3C), the profiled current density was the same at all sample points and followed the same trend in both the ec-biochar and ec-coke biofilter. The current density was increasing from the bottom layers (J= 20 mA/m^2 for ec-coke and J= 40 mA/m^2 for ec-biochar) toward the upper layers until reaching an inflection point. This point was located at 5 cm from the surface for the ec-biochar biofilter (J= 280 mA/m^2) and 3 cm from the surface for the ec-coke biofilter (J= 135 mA/cm^2). The current density decreased after the inflection. This inflection point indicated when cathodic versus anodic reactions were predominant, and may be caused by an increase in the concentration of electron acceptor or by a decrease in the electron donor (organic pollutants) at the upper layers of the biofilter.

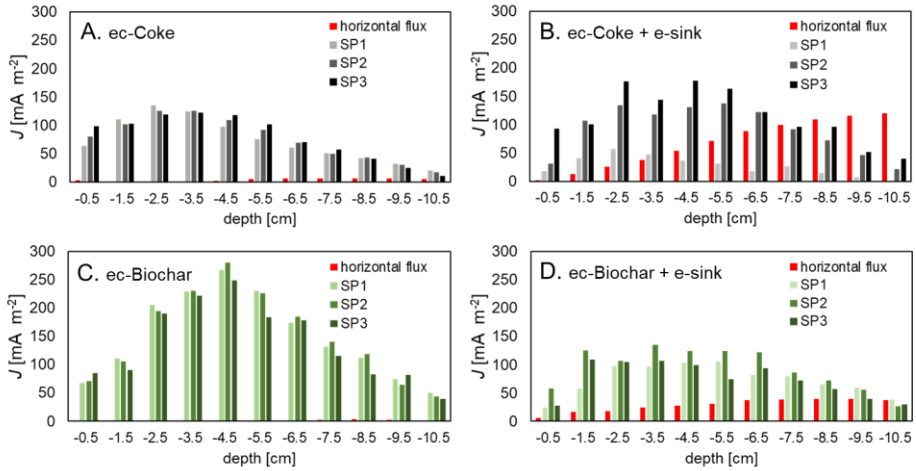

Figure 4.3. Current density (*J*) values of the up-flow biofilters made of ec-coke (grey) and ec-biochar (green) in each sampling point (SP1, SP2, SP3). The systems were operated with an empty e-sink (A and C) and with an e-sink hosting oxygen saturated water (B, D). In presence of e-sink, the current density has two directions: i) vertical (grey and green bars) towards the top surface, and horizontal (red bars) towards the e-sink.

By incorporating the e-sinks into the biofilters bed the current density profile was shifted from vertical to horizontal direction (Fig. 4.4S). In absence of e-sink, the highest availability of TEAs was in the upper layers of the biofilter (atmospheric oxygen), so behaviour at all sample points was governed by the vertical distribution of oxygen. On the contrary, the use of a e-sink in the bed (see location in Fig. 4.1) add an additional redox gradient driving the flux of electrons horizontally into the e-sink. This change of direction in the flux of electrons will affect the distribution of the current density (Fig. 4.3B and 4.3D) inside the bed, including at each sampling point. The sampling point that was most affected in both ec-biofilters was SP1, as the distance between the e-sink and the SP increased, the current density was less affected. In this way, the current density profile in SP3 of both biofilters did not change (dark bars in Fig. 4.3B and 4.3D) compared to biofilters without an e-sink, which means that the entire electron flux at this sample point it went towards the uppermost surface of the biofilter. This indicates that SP3 was outside the field of influence of the e-sink. However, in SP1 (light bars in Fig. 4.3B and 4.3D), the value of *J* falls

drastically compared to the values presented in the biofilters without an e-sink (Fig. 4.3A and 4.3C). Around SP1, the flux of electrons was more towards the e-sink (horizontal flux). To know the value of this horizontal distribution of current density (*Eq.2*) was applied to calculate *J* between SP1 and SP3 (12 cm of horizontal sampling distance). Such new distribution of fluxes (red bars in Fig. 3B and 3C) revealed how the current density towards the e-sink (horizontal flux) was higher at the bottom layers in both biofilters, at -11cm for both the ec-coke (120 mA / m^2) and the ec-biochar (40 mA / m^2). As the distance between the e-sink TEA and the surface TEA becomes similar, the current density towards the e-sink decreases (red bars in Fig. 4.3B and 4.3C) and the current density towards the surface increases (light bars in Fig. 4.3B and 4.3C). The situation in SP2 is an intermediate state between SP1 and SP3. Beyond the physical distance to the TEA, the electrical resistance of the material exerts a major influence on the distribution of the potential along the bed and therefore the current density. The greater electrical conductivity of the ec-coke in comparison with ec -biochar allowed a higher electronic transfer rate of the electrons towards the e-sink. Therefore, the differences between current density in SP2 and SP3 were greater in the ec-coke biofilter (Fig. 4.3B). This three-dimensional study of the current density inside a biofilter reveals how the spatial location of the TEA affects the flow of charges. Still, more detailed maps are required to more specifically determine the radius of influence of the e-sink.

The electron transfer rates (*R*) (Fig. 4.4) revealed the presence of electron transfer between electron donors and acceptors located in different environments. Positive values signify electron transfer from an electron donor (anodic reaction), while negative values signify electron transfer to an electron acceptor (cathodic reaction). When the biofilters operate free of e-sink (Fig. 4.4) the main electron acceptor will be the oxygen present in the upper layers and the main electron donor is the organic pollutants supplied from the bottom. Thus, in the bottom layers the electron transfer rate was positive and corresponded to areas where anodic reactions predominate, like the oxidation of organic pollutants. Negative values of *R* indicate that cathodic reactions dominate over anodic reactions. The reason for that could be a higher availability

of TEAs, such as nitrate or oxygen, or because there is less organic pollutant that can be potentially oxidized. This will also be a consequence of the amount of electrons generated as a result of the oxidation processes that occurred in the bottom layers, the more oxidation, the more electron flux and more electron acceptor is required. In the absence of an electron acceptor, oxidation reactions and therefore the removal of the organic matter will be limited. According to the electron transfer rates (*R*) (Fig. 4.4), the cathodic area in the ec-biochar biofilter reaches deeper environments, up to -4 cm in absence of e-sink, while in the ec-coke biofilter it was located just two centimeters closer to the surface.

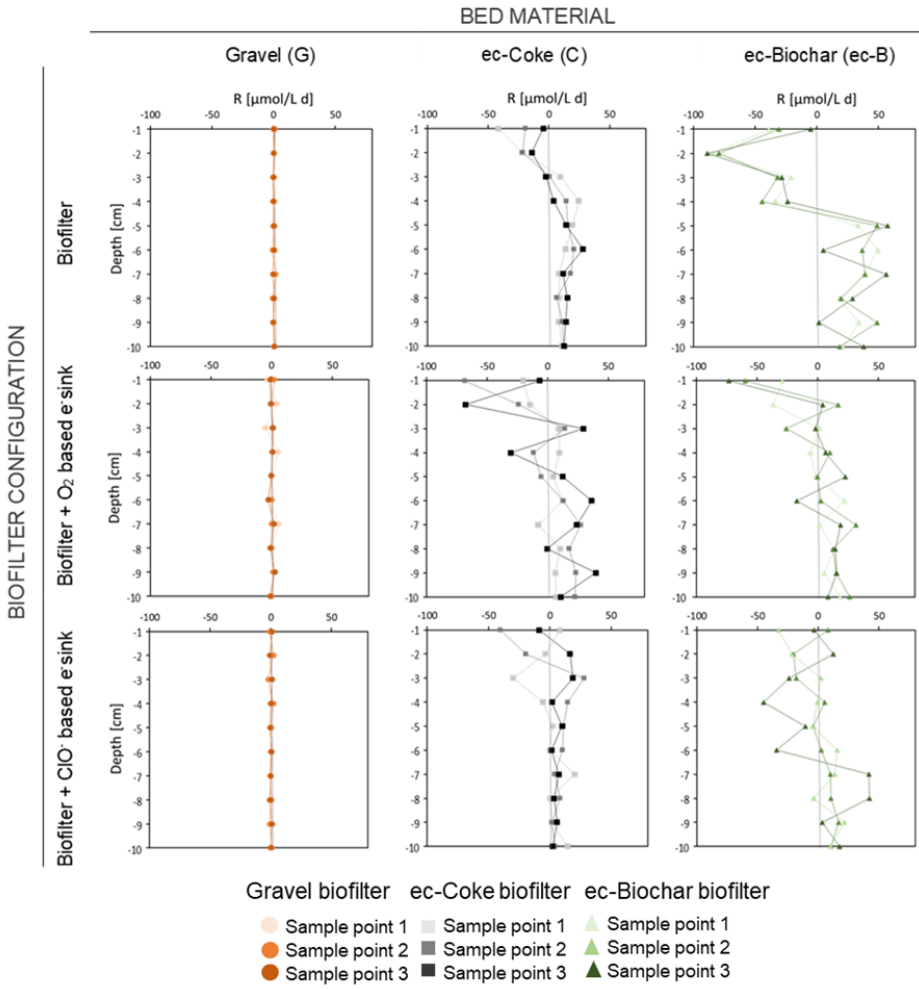

Figure 4.4. Vertical distribution of electron transfer rates (*R*) for the three biofilters, gravel (orange), ec-coke (grey) and ec-biochar (green), operating without e-sink, O_2

based e-sink and ClO^- based e-sink. Positive values signify electron transfer from an electron donor (anodic reactions), while negative values signify electron transfer to an electron acceptor (cathodic reactions).

4.4.2 Pollutants removal rates and electron flux

The impact of our e-sink device was evaluated with different bed materials by measuring the COD removal efficiency and the flux of electrons. The organic matter removal rates revealed different responses to reach treatment (Fig. 4.5).

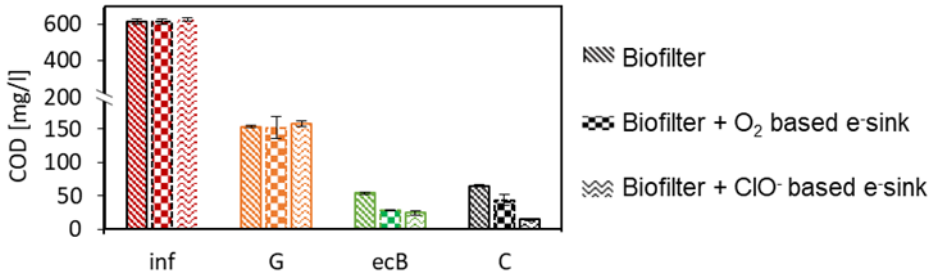

Figure 4.5. COD concentration at the influent (red) and effluent of each biofilters: gravel (orange), ec-biochar (green) and ec-coke (grey), operating up flow with e-sink either in absence of electron acceptor or in presence of oxygen (O_2) and hypochlorite (ClO^-).

Table 4.2. Influent and effluent COD concentration, removal rate and efficiency for the different systems.

	COD Concentration [mg L^{-1}]				COD Removal rate [g/m^3 day]			COD Efficiency [%]		
Biofilter	Influent	G	ecB	C	G	ecB	C	G	ecB	C
+ e^-sink free	613.0 ± 14	153.0 ± 2	54.2 ± 2	65.1 ± 2	110.4 ± 3	134.2 ± 3	131.6 ± 4	75.0 ± 1	91.0 ± 1	89.0 ± 1
+ e^-sink (O_2)	615.0 ± 17	15.8 ± 16	28.3 ± 1	43.8 ± 8	111.0 ± 8	140.9 ± 4	137.2 ± 6	74.0 ± 3	95.0 ± 1	93.0 ± 2
+ e^-sink (ClO^-)	627.0± 10	157.0 ± 4	24.4 ± 4	14.6 ± 2	112.8 ± 3	144.7 ± 2	147.1 ± 3	74.0 ± 1	96.0 ± 1	98.0 ± 1

When biofilters without e-sinks were operated in the up flow configuration, the electron acceptor in the medium was mostly oxygen present at the surface and nitrate, resulting from the nitrification. In the case of the

gravel biofilter, the oxidation processes of organic matter are very limited because the majority electron acceptors are only available at the top layer. Due to this limit in TEAs, our gravel biofilter did not have a COD removal efficiency higher than 75%. Taking into account that the influent COD was around 600 mg/L (Table 4.2), and the effluent COD was 150 mg/L, then the standard system did not fulfil the discharge limit (Dir. 00/60 / EC of 23 Oct 2000) for treated urban wastewater. Although the TEA concentration was increased with the e-sink, the efficiency of the gravel biofilter did not increase since these TEAs were not dissolved in the bed and could not be reduced intracellularly. Therefore, the removal efficiency remained constant around 75% operating under the three conditions (Table 4.2). In METlands®, electroactive bacteria can transfer electrons directly to the electrically conductive bed material therefore the flux of electrons was to the surface areas with higher redox potential. In this way, the organic matter oxidation processes will not be slowed down despite the low availability of electron acceptor dissolved in the bed. In the ec-coke bed METland®, the COD removal efficiency was 89%. This efficiency was increased with the e-sink in the bed by increasing the effective quantity of TEA available through extracellular electron transfer and a conductive bed. Using an e-sink with oxygen saturated water, the COD removal efficiency increased to maximum of 93% and when the redox potential of the TEA is greater with hypochlorite inside the e-sink, the removal efficiency became 98% (Table 4.2). The effluent COD from this system is always below the discharge limit regardless of the operating condition. It should be noted that when the ec-coke METland® operates with an e-sink with hypochlorite, the COD value in the effluent is only 15 mg L^{-1} compared to 65 mg L^{-1} when it operated without an e-sink (Fig. 4.5). In this way, the influence of the e-sink is demonstrated in biofilters where there is an electrically conductive bed with a low internal resistance.

According to previous studies (Prado et al., 2019), the presence of carbonaceous electrically conductive materials based on pyrolyzed biomass can stimulate microbial oxidative activity more than in ec-coke beds. The ec-biochar METland® without an e-sink had a removal efficiency of 91% (Table 4.2). The efficiency of the system increases with an e-sink in the bed, but in this case the

redox potential of the TEA did not have much influence. The effluent COD values from the ec-biochar METland® drop from 54 mg L^{-1} (without e-sink) to 28 mg L^{-1} for the e-sink with oxygen and 24 mg L^{-1}, with hypochlorite. Although the effluent COD is slightly higher than in METland® ec-coke, it always remains below the discharge limit.

These results indicate that high electron acceptor availability, whether that be direct or indirect, is a requirement for achieving higher removal rates in METlands®. The high removal of COD under a high loading rate reveals the benefits of using an electrically conductive material combined with the high availability of TEAs inside the e-sink device.

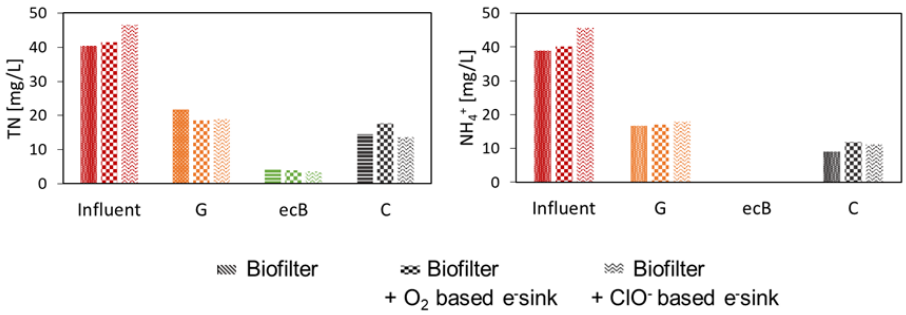

Figure 4.6. NH_4^+-N (left) and TN (right) concentration for the three biofilters, gravel (orange), ec-coke (grey) and ec-biochar (green), operating up flow with e-sink either in absence of electron acceptor or in presence of oxygen (O_2) and hypochlorite (ClO^-).

Table 4.3. Influent and effluent NH_4^+-N and TN concentration for the different systems.

	NH4+-N Efficiency [%]			TN Efficiency [%]		
Biofilter	G	ecB	C	G	ecB	C
+ e-sink free	57 ± 1	100 ± 1	76 ± 1	54 ± 1	89 ± 1	64 ± 1
+ e-sink (O_2)	58 ± 1	100 ± 2	70 ± 1	55 ± 1	90 ± 2	57 ± 1
+ e-sink (ClO^-)	61 ± 1	99 ± 1	76 ± 1	69 ± 1	92 ± 1	71 ± 1

Nitrogen removal was studied in the three biofilters under the different e-sink conditions (Fig. 4.6). Statistical analysis revealed significant reduction in ammonia and TN residual concentrations in the effluent between gravel and

electrically conductive bed biofilters. In the gravel biofilter the ammonia removal efficiency was 60% and due to its non-conductive nature, such performance was not affected even in the presence of the e-sink. In the ec-coke biofilter, the ammonia removal efficiency was 76%, and even 100% when ec-biochar was the bed material. However, in spite of increasing the COD removal, the use of the e-sink in the biofilter bed did not increase the ammonia removal rate (Table 4.3 and Fig. 4.6). Such little impact of e-sink on ammonium oxidation could be due to the anoxic conditions of our biological treatment in contrast with the aerobic nature of typical nitrifying bacteria. In spite of the optimal ammonium removal, not all nitrate was denitrified due to the competitive role of the ec-bed for accepting the electrons and to the low availiability of COD at the upper layers (outlet) of the biofilter.

4.5 Conclusions

Our new strategy to directed the flux of electrons inside the an electroconductive bed by using an e-sink device was successful because the highest performance efficiency was achieved by the TEA solution in the e-sink with highest redox potential (Jadhav et al., 2014) (e.g., hypochlorite 1.3 V in comparison with oxygen 0.8 V). Furthermore, that the resistance of the bed material great influenced the availability of TEAs. Interestingly, the fact that the gravel bed did not exhibit any removal enhancement (Fig. 4.5) supports our e-sink theory that the TEAs in the e-sink remained unavailable due to the inert nature of the bed.

With this technology's great promise, there are several issues that should be further explored. For example, when scaling up what is the effective area of e-sink influence, and the cost to benefit analysis of the e-sink. Therefore, we are currently designing and integrating the e-sink into pilot and full scale METlands® to further understand their efficacy.

4.6 References

Aguirre-Sierra, A., 2017. Integrating Microbial Electrochemical Systems in constructed wetlands, a new paradigm for treating wastewater in small comunities. Alcalá University, Madrid, Spain.

Aguirre-Sierra, A., Bacchetti-De Gregoris, T., Berná, A., Salas, J.J., Aragón, C., Esteve-Núñez, A., 2016. Microbial electrochemical systems outperform fixed-bed biofilters in cleaning up urban wastewater. Environ. Sci. Water Res. Technol. 2, 984–993.

https://doi.org/10.1039/C6EW00172F

Aguirre-Sierra, A., Bacchetti, T., Salas, J.J., de Deus, A., Esteve-Núñez, A., 2020. A new concept in constructed wetlands: assessment of aerobic electroconductive biofilters. Environ. Sci. Water Res. Technol. 2, 984–993. https://doi.org/10.1039/c9ew00696f

Borjas, Z., Manuel, J., Esteve-Núñez, A., 2017. Strategies for merging microbial fuel cell technologies in water desalination processes: Start-up protocol and desalination efficiency assessment 1–10. https://doi.org/10.1016/j.jpowsour.2017.02.052

Brix, H., 1994. Constructed wetlands for municipal wastewater treatment in Europe. In: Mitsch, W.J. (Ed.), Global Wetlands: Old World and New 325–334. ISBN 13: 9780444814784

Brix, H., Koottatep, T., Laugesen, C.H., 2007. Wastewater treatment in tsunami affected areas of Thailand by constructed wetlands 69–74. https://doi.org/10.2166/wst.2007.528

Carleton, J.N., Grizzard, T.J., Godrej, A.N., Post, H.E., Lampe, L., Kenel, P.P., 2000. Performance of a Constructed Wetlands in Treating Urban Stormwater Runoff. Water Environ. Res. 72, 295–304. https://doi.org/https://doi.org/10.2175/106143000X137518

Corbella, C., Garfí, M., Puigagut, J., 2014. Science of the Total Environment Vertical redox pro fi les in treatment wetlands as function of hydraulic regime and macrophytes presence : Surveying the optimal scenario for microbial fuel cell implementation. Sci. Total Environ. 470–471, 754–758. https://doi.org/10.1016/j.scitotenv.2013.09.068

Damgaard, L.R., Risgaard-Petersen, N., Nielsen, L.P., 2014. Electric potential microelectrode for studies of electrobiogeophysics. J. Geophys. Res. Biogeosciences 119, 1906–1917. https://doi.org/10.1002/2014JG002665

Doherty, L., Zhao, Y., Zhao, X., Hu, Y., Hao, X., Xu, L., Liu, R., 2015. A review of a recently emerged technology: Constructed wetland – microbial fuel cells. Water Res., 85, 38-45.

https://doi.org/10.1016/j.watres.2015.08.016

Dotro, G., Molle, P., Nivala, J., Puigagut, J., Stein, O., 2017. Treatment Wetlands. First. ed. IWA Publishing, London.

García, J., Rousseau, D.P.L., Morato, J., Lesage, E., Matamoros, V., Bayona, J.M., 2010. Contaminant removal processes in subsurface-flow constructed wetlands: a review. Critical Reviews in Environ. Science and Technology, 40(7), 561-661.

https://doi.org/10.1080/10643380802471076

Isosaari Pirjo& Sillanpää Mika, 2016. Use of sulphate reducing bioreactors and bioelectrochemical reactors for metal recovery from mine water. Sep. Purif. Rev. 2119.

https://doi.org/10.1080/15422119.2016.1156548

Jadhav, D.A., Ghadge, A.N., Mondal, D., Ghangrekar, M.M., 2014. Comparison of oxygen and hypochlorite as cathodic electron acceptor in microbial fuel cells. Bioresour. Technol. 154, 330–335. https://doi.org/10.1016/j.biortech.2013.12.069

Kadlec, R., Wallace, S., 2009. Ttreatment wetlands, in: Vasa. p. 1048. ISBN 13: 9781566705264

Nielsen, L.P., Risgaard-Petersen, N., 2014. Rethinking Sediment Biogeochemistry After the Discovery of Electric Currents. Ann. Rev. Mar. Sci. 7, 425–442. https://doi.org/10.1146/annurev-marine-010814-015708

Nielsen, L.P., Risgaard-Petersen, N., Fossing, H., Christensen, P.B., Sayama, M., 2010. Electric currents couple spatially separated biogeochemical processes in marine sediment. Nature 463, 1071–1074. https://doi.org/10.1038/nature08790

Prado, A., Berenguer, R., Esteve-Núñez, A., 2019. Electroactive biochar outperforms highly conductive carbon materials for biodegrading pollutants by enhancing microbial extracellular electron transfer. Carbon, 146, 597-609. https://doi.org/10.1016/j.carbon.2019.02.038

Pun, Á., Boltes, K., León, P., Esteve-Nuñez, A., 2019. Bioresource Technology Reports Detoxification of wastewater containing pharmaceuticals using horizontal flow bioelectrochemical filter. Bioresour. Technol. Reports 7, 100296.

https://doi.org/10.1016/j.biteb.2019.100296

R Core Team, 2019. R: A language and environment for statistical computing. R Foundation for Statistical Computing, Vienna, Austria. https://www.R-project.org/.

Ramírez-Vargas, C.A., Arias, C.A., Carvalho, P., Zhang, L., Esteve-Núñez, A., Brix, H., 2019. Electroactive biofilm-based constructed wetland (EABB-CW): A mesocosm-scale test of an innovative setup for wastewater treatment. Sci. Total Environ. 659, 796–806.

https://doi.org/10.1016/j.scitotenv.2018.12.432

Ramírez-Vargas, C.A., Prado, A., Arias, C.A., Carvalho, P.N., Esteve-Núñez, A., Brix, H., 2018. Microbial electrochemical technologies for wastewater treatment: Principles and evolution from microbial fuel cells to bioelectrochemical-based constructed wetlands. Water 10(9). https://doi.org/10.3390/w10091128

Risgaard-Petersen, N., Damgaard, L.R., Revil, A., Nielsen, L.P., 2014. Mapping electron sources and sinks in a marine biogeobattery. J. Geophys. Res. G Biogeosciences 119, 1475–1486. https://doi.org/10.1002/2014JG002673

Roley, S.S., Tank, J.L., Stephen, M.L., Johnson, L.T., Beaulieu, J.J., Witter, J.D., 2012. Floodplain restoration enhances denitrification and reach-scale nitrogen removal in an agricultural stream. Ecol. Appl. 22, 281–297. https://doi.org/10.1890/11-0381.1

Sato, M., Mooney, H.M., 1960. The electrochemical Mechanism of sulfide delf-potentials. Geophysics XXV, 226–249. https://doi.org/https://doi.org/10.1190/1.1438689

Srivastava, P., Yadav, A.K., Abbassi, R., Garaniya, V., Lewis, T., 2018. Denitrification in a low carbon environment of a constructed wetland incorporating a microbial electrolysis cell. Journal of Environ. Chem. Eng., 6(4), 5602-5607. https://doi.org/10.1016/j.jece.2018.08.053

Vymazal, J., 2014. Constructed wetlands for treatment of industrial wastewaters : A review. Ecol. Eng. 73, 724–751. https://doi.org/10.1016/j.ecoleng.2014.09.034

Vymazal, J., 2008. The use constructed wetlands with horizontal sub-surface flow for various types of wastewater. Ecol. Eng., 35, 1–17. https://doi.org/10.1016/j.ecoleng.2008.08.016

Wang, Y., Zhao, Y., Xu, L., Wang, W., Doherty, L., Tang, C., 2017. Constructed wetland integrated microbial fuel cell system: looking back, moving forward. Water Science and Technology, 76(2), 471-477. https://doi.org/10.2166/wst.2017.190

Wu, H., Zhang, J., Hao, H., Guo, W., Hu, Z., Liang, S., Fan, J., 2014. Bioresource Technology A review on the sustainability of constructed wetlands for wastewater treatment: Design and operation. Bioresour. Technol.

https://doi.org/10.1016/j.biortech.2014.10.068

Wu, S., Kuschk, P., Brix, H., Vymazal, J., Dong, R., 2014. ScienceDirect Development of constructed wetlands in performance intensifications for wastewater treatment: A nitrogen and organic matter targeted review. Water Res. 57, 40–55. https://doi.org/10.1016/j.watres.2014.03.020

Zhao, Y., Collum, S., Phelan, M., Goodbody, T., Doherty, L., Hu, Y., 2013. Preliminary investigation of constructed wetland incorporating microbial fuel cell: Batch and continuous flow trials. Chem. Eng. J. 229, 364–370. https://doi.org/10.1016/j.cej.2013.06.023

Schievano, A., Berenguer, R., Goglio, A., Bocchi, S., Marzorati, S., Rago, L., Louro, R.O., Paquete, C. M., Esteve-Núñez, A., 2019. Electroactive Biochar for Large-Scale Environmental Applications of Microbial Electrochemistry. Sustainable Chem. Eng. 7, 22, 18198-18212.

4.7 Supplementary Information

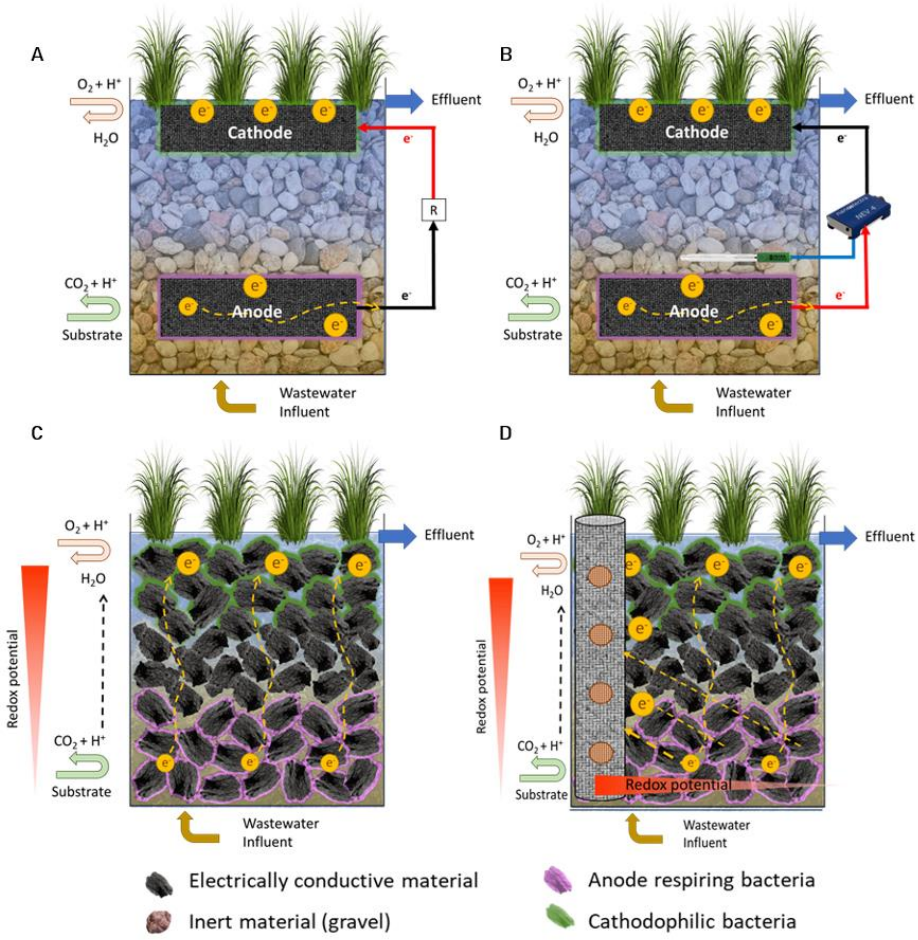

Figure S4.1. The integration of microbial electrochemical technologies (MET) in constructed wetlands (CW): A) microbial fuel cell (MFC) in CW; B) microbial electrolysis cell (MEC) by poising the electrode with a certain potential through a potentiostat or a power source; C) snorkel, a single electrode-based configuration under short circuit with no resistors (METland®) and D) METland® with e-sink.

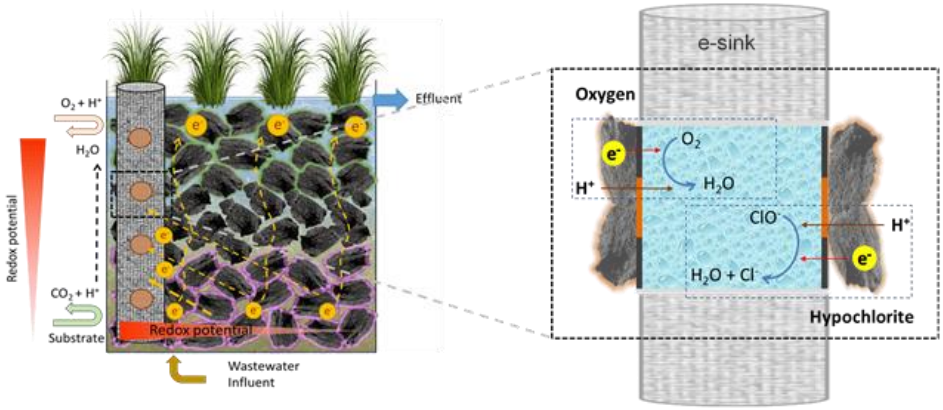

Figure S4.2. Scheme of the e-sink mechanism. Both, electrons, from biodegradation of pollutants, and protons resulting from such metabolism, flux into the e-sink. A catholyte, oxygen or hypochlorite, is reduced inside the e-sink. The flux of electrons is transferred from the electroconductive bed to a tube made of electroconductive carbon fiber. The protons flux is allowed through the cation exchange membrane.

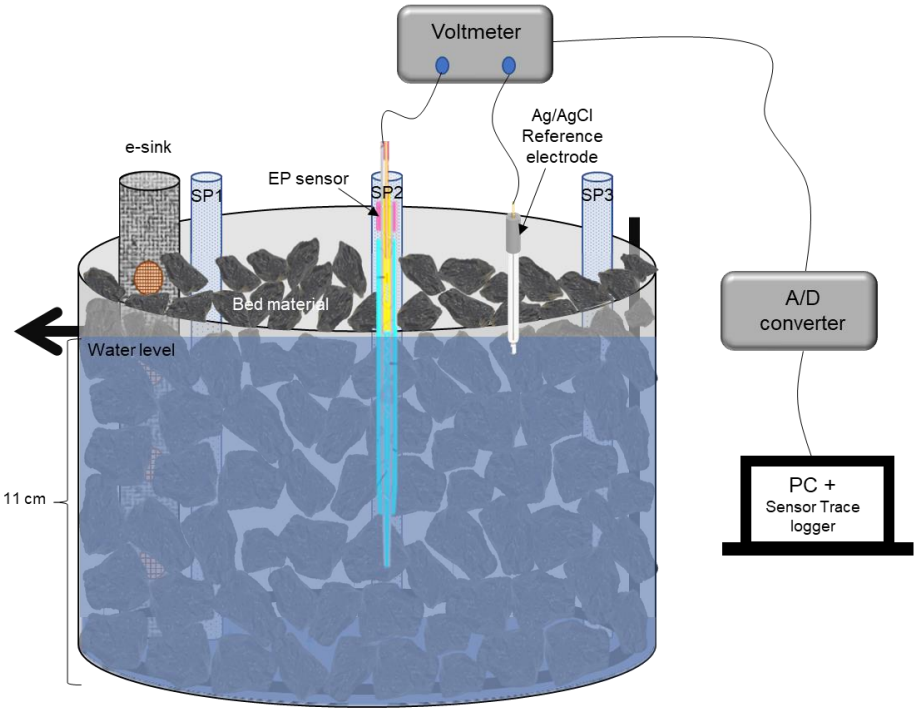

Figure S4.3. Scheme of a biofilter with EP monitoring equipment: Ag/AgCl reference electrode, EP sensor position and sample points (SP1, SP2, and SP3).

Table. S4.1. Water conductivity (σ) in each biofilter operating under each e-sink condition. The conductivity of the water was measured on-site directly with a conductivimeter (Hach sension+ 5060).

Water conductivity [µS/cm]	**Gravel biofilter**	**ec-Coke biofilter**	**ec-Biochar biofilter**
+ e^-sink free	926	1176	1172
+ e^-sink (O_2)	1123	1230	1074
+ e^-sink (ClO^-)	1070	1158	1050

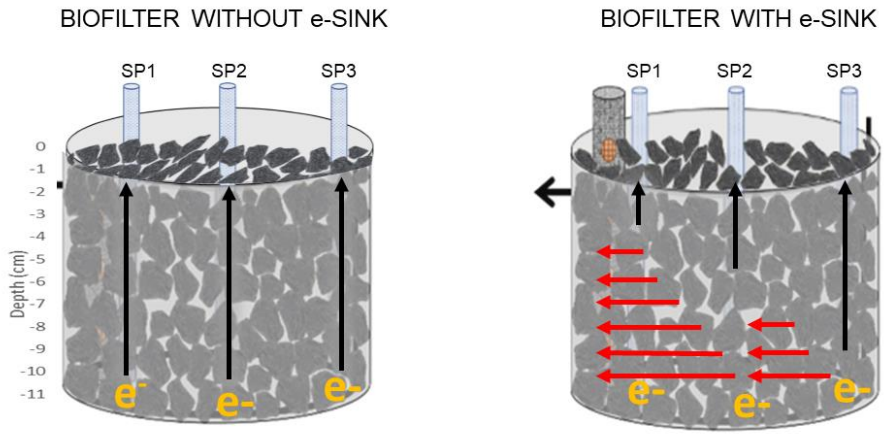

Figure S4.4. Scheme of flux of electrons inside the METlands® without and with e-sink in each sample point (SP1, SP2, and SP3). Black arrows show the flux of electrons to the surface oxygen and red arrows show the flux of electrons horizontally to the e-sink. In deeper layers and closer to the e-sink the horizontal flux (red arrows) is greater than the vertical one, the opposite than in the top layers.

CHAPTER 5:

A METLAND® REAL CASE FOR TREATING MANURE WASTEWATER

This section has been redrafted after:

Amanda Prado de Nicolás[a,b] , A. Ignacio Martín García[c], Abraham Esteve-Núñez [a,b,d] .2021.
A METland real case for treating manure wastewater: from lab-scale to full-scale.

[a] Department of Analytical Chemistry, Physical Chemistry and Chemical Engineering, University of Alcalá, Alcalá de Henares, Spain
[b] IMDEA Water Institute, Alcalá de Henares, Madrid, Spain
[c] Estación Experimental del Zaidín (Consejo Superior de Investigaciones Científicas), Armilla, Granada, Spain
[d] METfilter, Carrión de los Céspedes, Spain. Chemical Engineering Department, Universidad de Alcalá, Alcalá de Henares, Spain

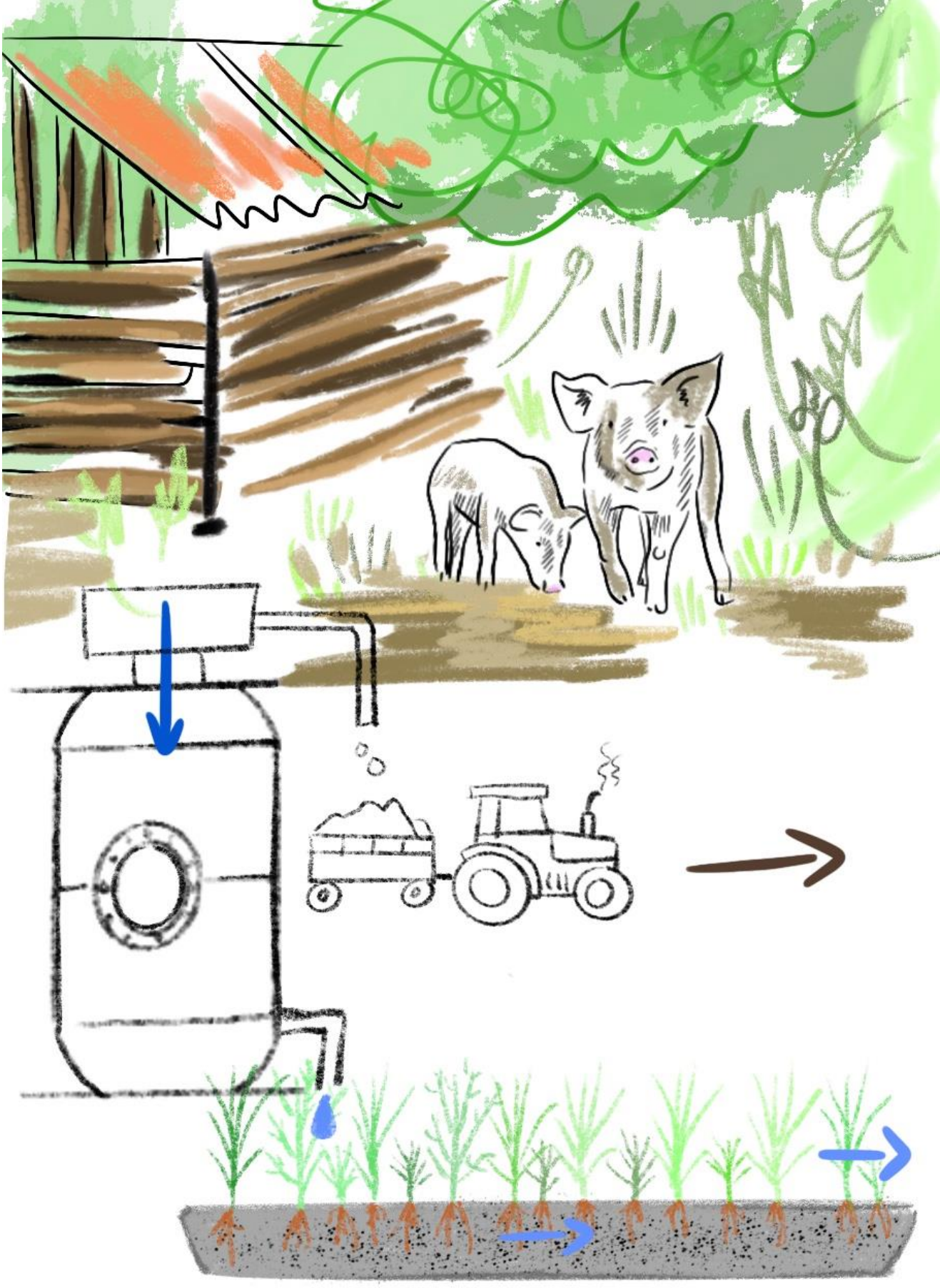

A METland® real case for treating manure wastewater: from lab-scale to full-scale

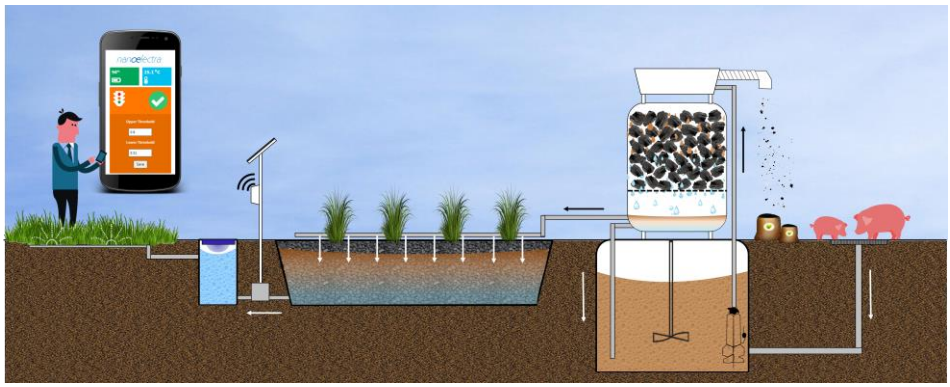

5.1. Abstract

METland constitute a hybrid concept for treating wastewater where microbial electrochemical technologies (MET) are integrated into constructed wetlands (CWs) in order to enhance the pollutant removal performance. In this work, we present the technology scaling process for manure wastewater treatment. To validate this technology, a lab-scale METland base system was operated for one month to define the best design and operational conditions to maximize the removal of wastewater pollutants. The lab-scale system removes 91% of the COD and 96.7% of N-tot. Based on this good performance, we proceed to the implementation of the system on a full scale. As in the laboratory-scale system, i) a tank was built to store the raw water, which also served as an anaerobic digester to promote denitrification; ii) a vertical METland to promote nitrification and iii) an HSSF-METland to facilitate the oxidation processes of organic matter.

Key words: Microbial electrochemistry; constructed wetland; METland®; electroactive bacteria; manure wastewater treatment.

5.2 Introduction

Intensive animal production is located in certain European regions, so we are facing a phenomenon of centralization where more than 50% of the European pig production comes together in only 4 countries: Germany, Belgium, Spain and Italy (Statista, 2016). In those areas, farms are typically very large, with a production of manure wastewater currently reaching 250 million of m^3 each year (EU, 2015, MAGRAMA, 2015). Such swine manure is stored near to the farms in large rafts, which often leak, contaminating the soil and waters of the area (Smith and Frost, 2000). The lack of solutions for the sustainable and cost-effective treatment of agricultural wastewater is a widespread problem (Martinez et al., 2009).

Manure wastewater is made up of a high amount of organic matter and nutrients, like nitrogen and phosphorus. It also contains low concentrations of micronutrients and emerging compounds. Traditionally, the high content of macro- and micro- nutrients in the manure wastewater is a great benefit to farmers as a cheap and effective source of fertilizer (Harrington and Scholz, 2010; Smith and Frost, 2000), watering the fields whit it. However, land availability may be a bottleneck, especially for large farms in nitrate-sensitive zones, where the acceptable nitrogen (N) load is limited to 170 kg ha^{-1} $year^{-1}$ (Luo et al., 2002). An excess of spreading the manure over arable land has resulted in over-fertilization. The excess nutrients seep through the soil, contaminating with nitrate the aquifers that supply water to the population. The result is the deterioration of the environment at all levels: air, release toxic compounds, soil, increasing nutrients and heavy metals accumulation, and water, causing eutrophication of water and contamination aquifers (Kumm, 2003; Martinez et al., 2009; Smith and Frost, 2000).

To prevent environmental impacts, as enforced by the European Nitrate Directive, proper management of manure wastewater is mandatory. The Nitrate Directive (91/676/EEC) limits the amount of nitrogen that can be discharged into the soil. This brings pressure on farmers in the EU to manage their wastewaters effectively. The directive states ‘‘appropriate nitrogen spreading calendars and

sufficient manure storage, for availability only when the crop needs nutrients and good spreading practices" (EEC, 1991) as types of actions that it promotes. To comply with the Nitrates Directive, there is currently no concrete technical solution to reduce or treat manure wastewater. Most treatment plants use very similar methodologies, combining aerobic and anaerobic treatments (Borin et al., 2013; Szogi et al., 1999). Aerobic treatments are very expensive and no added value compound is obtained at the end of the process. Anaerobic treatments are limited in ammonia removal and odour-producing chemicals. Therefore, the development of new technology and more efficient systems in the elimination of organic matter and nitrogen is required (Borin et al., 2013).

Constructed Wetlands (CW) are a Nature-based Solution (NbS) that can provide effective, low-cost, low-maintenance and environmentally beneficial wastewater treatment alternatives to traditional treatment systems (Brito et al., 2008; Brix, 2003; Vymazal, 2008). Modern CWs are engineered systems that have been designed to enhance specific characteristics of wetland ecosystems for improved wastewater treatment capacity under controlled conditions. They mainly act as biofilters, removing solids and pollutants from the water, through physicochemical and biological processes. These systems can be considered as a complex ecosystem in which the main actors are: the substrate, the vegetation and the microorganisms (Kaldec and Wallace, 2008). During the last decades, CWs have been used to treat a wide range of water pollutants such as domestic wastewater (Wu et al., 2015), industrial wastewater (Vymazal, 2014), and urban storm runoff (Carleton et al., 2000). Constructed wetlands have been used to treat agricultural wastewaters high in ammonia, which is toxic to a lot of wetland plants (Brix, 2003; Koottatep and Polprasert, 1997). The loading and flow rates in constructed wetlands vary greatly but according to bibliographic reviews (Tanner et al., 1995) the mean hydraulic loading rate and flow rate were 4.7 cm^3/day and 10 m^3/day, respectively. Most of the systems used for livestock wastewater treatment are of small size with a mean area of only 0.6 ha. Constructed wetlands treating manure wastewater are slightly larger with a mean area of about 1 ha. The most widespread method of enhancing

denitrification is to re-circulate the wastewater or to add partially-nitrified water (Vymazal, 2007; Wang et al., 2019).

More recently, new strategies to make constructed wetlands more efficient systems have been developed (Aguirre-Sierra et al., 2016). For instance, METlands are an eco-friendly technology that can treat different types of wastewaters at zero-energy operation cost, creating a virtuous circle safeguarding the local environment and connecting water, energy and land resources (iMETland). METlands are a hybrid concept where Microbial Electrochemical Technologies (MET) are integrated to Constructed Wetlands (Aguirre-Sierra, 2017; Prado et al., 2020). Microbial Electrochemical Technologies (MET) are based on the electrochemical interaction of electroactive bacteria with electrically conductive materials. These interactions involve extracellular electron transfer (Schröder et al., 2015). Electroactive bacteria (EAB) act as a natural catalyst for oxidizing the organic pollutants present in wastewater, then transferring electrons to the electrically conductive material (Prado et al., 2019).

METlands replace inert bed material like gravel, with electrically conductive (ec) carbonaceous material, ec-coke or ec- biochar. The electrically conductive bed promotes the growth of electroactive bacteria. These bacteria oxidize organic compounds intracellularly and extracellularly transfer electrons to the electrically conductive material. The electrons accepted by the electrically bed material are transferred to the top layers of METland because of the redox gradient, where the atmospheric air acts as a never-ending terminal electron acceptor (Aguirre-Sierra, 2017; Prado et al., 2020; Ramírez-Vargas et al., 2018). Another possibility is that EAB accepts electrons to reduce contaminants like nitrate. This extracellular electron transfer (EET) can be mediated by the conductive bed material itself (Conductive-particle-mediated Interspecies Electron Transfer, CIET) or direct exchange of electrons between microbes (Direct Interspecies Electron Transfer, DIET) (Rotaru et al., 2021).

In this work we are have adapted and validated METland technology for treating manure wastewater. Eventually we designed and constructed a full-

scale system capable of cleaning-up wastewater from livestock in the context of an Animal Research Center.

5.3. Materials and Methods

5.3.1 Site description and manure wastewater sampling

The manure wastewater origin is located in the Animal Nutrition Institute (Zaidín Experimental Station (EEZ) - CSIC) where a variety of cattle heads, including pigs, goats and sheep are used for animal nutrition research. The estimated wastewater production was 2-4m^3 of wastewater per day.

The sampling was carried out both from raw wastewater influent and after pretreatment (rotary screen). Samples were filtered and a completely physical-chemical analysis was performed by the water quality analysis service from Imdea Water (Madrid, Spain) (Table 5.1).

5.3.2 Lab-sale bioelectrochemically-assisted manure wastewater treatment system: design and operating parameters.

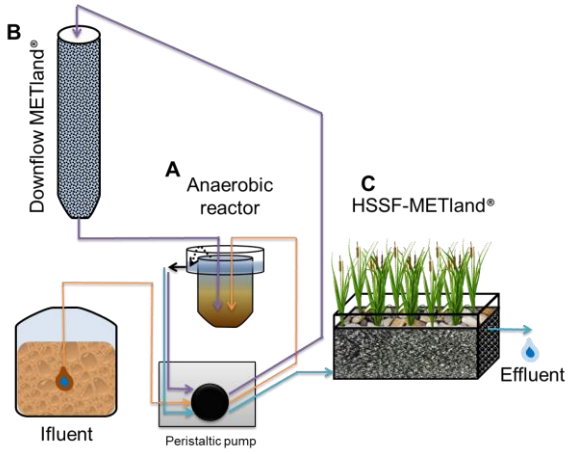

Figure 5.1. Scheme of the lab-sale bioelectrochemically-assisted manure wastewater treatment system.

A laboratory-scale manure wastewater treatment system was built. This system included METland concept as the core of wastewater treatment. For this, electroconductive material, graphitized coke, was used as a biofilter bed material to stimulate the colonization and activity of electroactive bacteria.

The system consisted of three reactors (Fig. 5.1):

A) Anaerobic reactor: cylinder shape (6 cm diameter, 50 cm height and 1.5 L volume). Settling was favoured at the lower part of the system, while in the upper part there is a perimeter spillway to collect the clarified water that overflows from the system. The raw wastewater was fed into the bottom of the reactor with a flow rate of 300 ml/day. From the top of the reactor, 900 ml/day were pumped to the Downflow METland® and 300 ml/day were fed into the HSSF- METland®.

B) Downflow METland®: Tubular reactor (5 cm diameter, 50 cm height and 1 L volume). The oxygen diffuses into the system passively so energy is not consumed. The bed was made of electrically conductive coke granules (1-3 cm size). The flow rate was 900ml/day and the effluent returns to the anaerobic reactor.

C) Horizontal subsurface flow (HSSF) METland®: A fish tank made of glass (10 cm x 10 cm x 25 cm and 2.5 L volume) containing a bed made of electrically conductive coke, with a particle size of 0.5-1 cm. System was operated under horizontal subsurface flow and was fed with 300 ml/day.

5.3.3 Physical, chemical and statistical analyses

To evaluate the efficiency of the lab-scale system, water samples of the influent and effluent from each reactor were taken every two days. The COD was analyzed following a standard method (APHA/AWWA/WEF, 2012) and NH_4^+ and NO_3^- were monitored by ion chromatography using a Metrohm 930 Compact Ion Chromatograph Flex. Removal efficiencies were calculated as a percentage of the respective inlet. Removal rates were obtained from the inlet-outlet difference as grams of COD per cubic meter of bed material per day.

5.4 Results and discussion

A system for treating manure have been designed and constructed by integrating microbial electrochemical concepts into constructed wetland solutions. After validating the technology at lab-scale we used the performance data for constructing a full-scale unit.

5.4.1 Validation of the lab-scale bioelectrochemically-assisted manure wastewater treatment system

The raw manure was analyzed before and after the rotary screen (Table 5.1 and 5.2). The physicochemical characteristics of the raw manure (Table 5.1) indicate a high concentration of nitrogen, in the form of ammonium (NH_4^+> 1000 mg/L) and a COD close to 7000 mg/L. This raw water was pumped to the rotary screen where the suspended solids were separated from the liquid fraction. After this physical process, the COD value dropped ca.50%

Table 5.1. Physicochemical characteristics of the wastewater generated in an Animal Nutrition Center

	Raw wastewater tank	After Rotary screen
Conductivity [µS/cm]	9380	7070
Colour [mg/L Pt-Co]	1112	760
pH	7.90	8.03
Alkalinity [ppm $CaCO_3$]	4120	3361
Hardness [mg $CaCO_3$/L]	949	682
Total P [mg/L]	35.3	29.6
Total N [mg/L]	1000	860
COD [mg/L]	6980	3380

Table 5.2. Ions quantified in the wastewater generated in an Animal Nutrition Center

	Raw wastewater tank	After Rotary screen
ANIONS		
Cl^- [mg/L]	410	346
NO_2^- [mg/L]	2.21	2.39
NO_3^- [mg/L]	2.27	2.55
PO_4^{3-} [mg/L]	188	143
SO_4^{3-} [mg/L]	122	27.6
CATIONS		
Na^+ [mg/L]	198	179
NH_4^+ [mg/L]	1007	1003
K^+ [mg/L]	697	644
Mg^{2+} [mg/L]	209	146
Ca^{2+} [mg/L]	35.5	32.2

Our lab-scale system was fed with liquid phase from real manure, taken after the rotary screen. To keep the same rate as the real system, the organic loading rate (OLR) was 490 mg COD/day. The chemical characteristics of the influent were a COD around 1600 mg/L, ammonium= 500 mg/L and not detected values for nitrates and nitrites.

Downflow METland: COD removal and nitrification

The downflow METland was operated as a vertical subsurface flow constructed wetland; however, the special nature of the bed allowed a much higher hydraulic rate than standard systems. The water treated in the anaerobic reactor was sprayed on the bed before percolating through the bed where it was aerated. The bacteria biofilm grew on the electrically conductive bed granules, where there was a redox and oxygen gradient. Thus, in the inner layers of the biofilm could grow electroactive bacteria. In the outer layers, heterotrophic bacteria could develop. In this way, the direct interspecies electron transfer (DIET) was promoted.

The main process that takes place in this reactor was nitrification, aerobic oxidation of ammonium, but also anaerobic microorganisms could be developed. This was because, in the smallest pores of the electrically conductive material granules, anaerobic conditions arise, where anaerobic electroactive bacteria (EAB) can develop. These EABs accepted part of the electrons resulting from ammonium oxidation while transferring directly to the electrically conductive material. The ammonium concentration in the effluent from this reactor was 15 mg/L (Fig. 5.4). As a consequence of nitrification, there was an increase in nitrate concentration, the highest concentration of which was found in the effluent from the downflow METland (Fig. 5.4). Furthermore, in this reactor a degradation of organic matter was observed, so the average concentration of COD at the outlet was 367 mg/L.

Anaerobic reactor: denitrification

The role of this reactor was to promote denitrification and to separate the sludge through a physical decantation process. At the bottom of this reactor, two independent streams were mixed. One stream was manure wastewater

with high COD and ammonia concentration. The other stream was the effluent of the downflow METland with low concentration of COD and ammonia but high values of nitrate. The COD / N ratio of such mixed streams was 3. In this anaerobic reactor, the anoxic conditions assured those denitrifying bacteria would reduce the nitrate, using the organic matter from the raw wastewater, as electron donor. The COD concentration at the outlet of this anaerobic reactor was 495 mg/L (Fig. 5.2) and the total-N of 85 mg/L (Fig. 5.2).

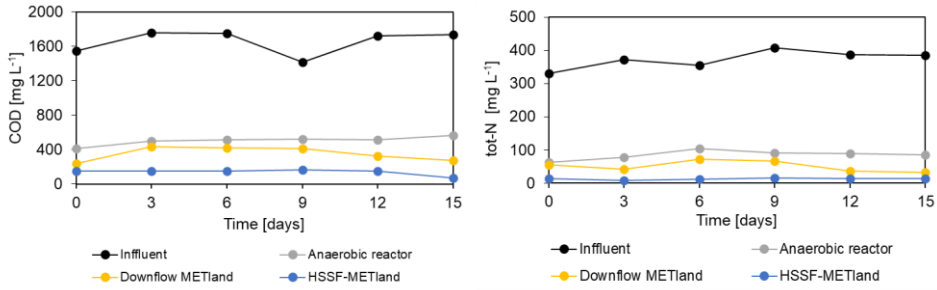

Figure 5.2. COD and total-N concentration at the influent (black) and effluent of every reactor: anaerobic reactor(grey), downflow metland (yellow) and HSSF-METland (blue).

HSSF- METland®: COD removal and denitrification

The *HSSF-* METland® was the last reactor. It consisted of a horizontal subsurface flow anaerobic bioelectrochemically-assisted wetland. The system was fed whit the effluent of the anaerobic digester. There was a redox gradient with the depth because of the presence of atmospheric oxygen at the top water layer. The electrically conductive bed allowed direct extracellular electron transfer; the electroactive bacteria can transfer electrons directly to the graphite coke. These electrons fluxed to the top, where the oxygen can be reduced, or can be used to reduce another terminal electron acceptor like nitrate through the mediated electron transfer mechanism.

In this reactor, the hydraulic retention time was high, which favors the oxidation of the refractory COD, enhanced by the presence of electrically conductive material that allows the extracellular transfer of electrons. The COD at the outlet of the system was 154 mg/L. Nitrogen removal, both ammonium oxidation and nitrate reduction, was also favored, reaching the minimum value of tot-N of 13 mg/L (Fig. 5.2 and 5.3).

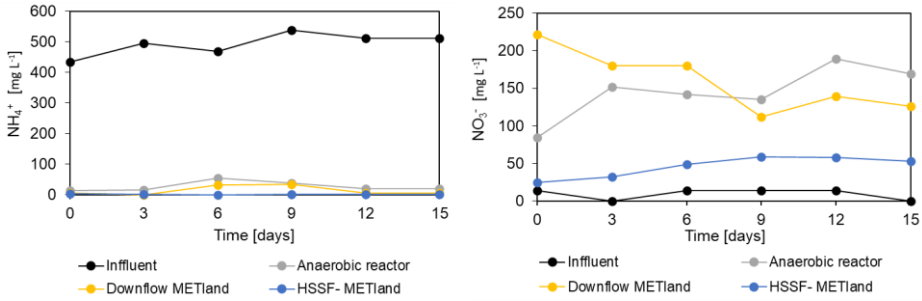

Figure 5.3. NH_4^+ and NO_3^- concentration at the influent (black) and effluent of every reactor: anaerobic digester (grey), aerobic ec-biofilter (yellow) and METland (blue).

Removal efficiency of the lab-scale system

The total efficiency of the system at laboratory scale (Fig. 5.4) was significantly higher than that shown by the conventional manure wastewater treatment system, especially in the removal of nitrogen. Regarding the removal of COD, the influent was 1640 mg/L and the effluent 154 mg/L, which represents a removal rate of 90.6%. Nitrogen removal reached 99% for ammonium removal and 96.6% for total nitrogen removal. It is remarkable that such high efficiency was obtained in absence of external energy consumption.

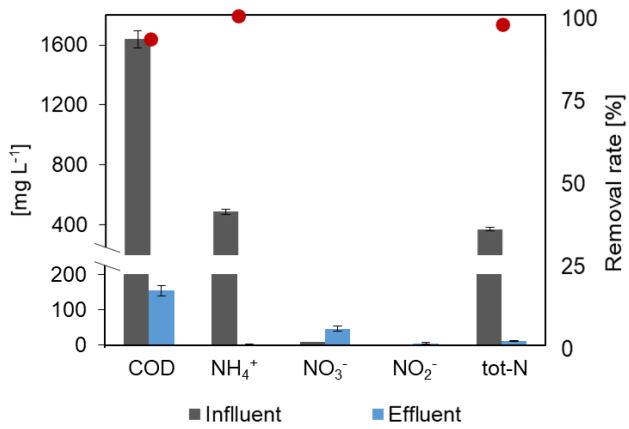

Figure 5.4. COD, NH_4^+, NO_3^-, NO_2^- and tot-N concentration (bar graph, left axe) and removal rate (red dots, right axe) at the influent (grey) and effluent (blue) of the lab-scale bioelectrochemically-assisted manure wastewater treatment system.

5.4.2 Full-scale bioelectrochemically-assisted manure wastewater treatment system

To scale up the bioelectrochemically-assisted manure wastewater treatment system, it was necessary to carry out certain modifications with respect to conventional systems (Fig. 5.5), both in the construction of the reactors and in the mode of operation.

Anaerobic reactor. The anaerobic reactor has a capacity of 23.4 m^3. On average, it received 1$m^3 day^{-1}$ of manure wastewater. This reactor is buried under soil, it can be stirred and host a variable head pump.

Downflow METland. The geometry of our final design consisted of a tubular reactor (3.3 m high and 2.4 m in diameter, 11.4 m^3 of total volume. The influent for this step was wastewater treated in t without suspended solids since at the entrance there was a rotary screen. The material inside the reactor was placed as follows. In the lower third, a grid was installed to create an air chamber to promote passive aeration. On top of it, a 10 cm layer of gravel (3-4 cm granulometry) and a 10 cm layer of graphitized coke (1-3 cm granulometry) were added. The next 2.5 m of the reactor were filled with small graphitized coke (3 -10 mm granulometry). The material volume was 10 m^3.

HSSF- METland®. The dimensions are 7.6 m long, 3.6 m wide and 0.6 m deep, 16.5 m^3 of total volume. The bed material was graphite coke (3-4 cm granulometry) to favor electrogenic processes. The outlet pipes were placed along the entire bottom of the METland. In addition, the inlet pipes were placed along the entire surface layer of the bed in order to create vertical flow and reduce dead zones in the bed. Also, typical wetland plants were planted, such as bamboo and typhus, which have high nitrogen removal rates. The high hydraulic retention time (HRT) in this reactor allows to have a water reservoir that, after tertiary treatment, can be used as irrigation.

Manure wastewater flows suggested in the new full-scale bioelectrochemically-assisted. Raw wastewater is harvested in the anaerobic reactor as first stage of the process. The water should be first pumped to the rotary screen by pulses of 5 min every 20 min with a flow rate of ca. 3 $m^3 day^{-1}$.

The effluent should, by gravity, the downflow METland. At the outlet, there are two solenoid valves to control recirculation. Two-thirds of the effluent from this reactor should be recirculated to the raw wastewater tank and one-third to the HSSF- METland®. So, the HSSF- METland® should be fed by $1m^3day^{-1}$. The total discharge of the system was 1m3, which should be finally treated with UV radiation to eliminate pathogens from the water and be able to reuse the effluent as irrigation.

Smart bioelectrochemically-assisted wastewater treatment system. Finally, some devices based on METs were incorporated in order to remotely monitor water quality in real-time and apply a tertiary treatment to be able to reuse the effluent as irrigation water without problems of eutrophication, contamination or pathogenic bacteria. A UV disinfection chamber was incorporated into the outlet thank, as a tertiary treatment and to eliminate pathogenic bacteria. Also, an IoT biosensing and an autonomous signal transmission system were placed in the outlet pipe. The IoT biosensing, provide by Nanoelectra S.L, is a new MET-based device that transforms bacteria metabolism into an electrical signal. The electrical signal informs of the water quality in real-time such as the organic pollutants or the presence of toxic compounds. Real-time monitoring of the system is accessible via 4G connection through the autonomous signal transmission system (Nanoelectra S.L.).

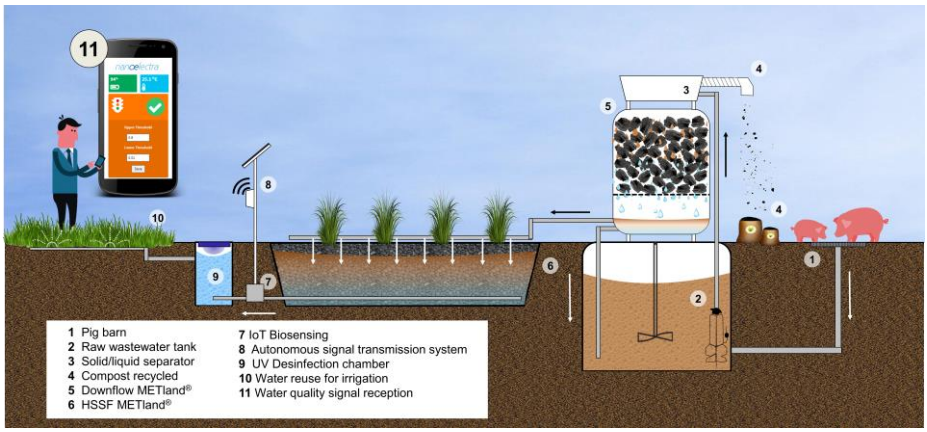

Figure 5.5. Scheme of the Full-scale bioelectrochemically-assisted manure wastewater treatment system installed in the Animal Nutrition Institute (EEZ-CSIC).

5.5 Conclusions

This study demonstrates that a bioelectrochemically-assisted constructed wetland is an efficient technology for the treatment of manure wastewater, showing high rates of removal of COD and nutrients. The COD removal by METland® at laboratory scale (>90%) was higher than the one exhibited by conventional technologies such as the Upflow Anaerobic Sludge Blanket (USAB) (COD elimination = 80%), the Anaerobic Baffled Reactor (ABR) (COD removal = 60%), Sequencing Batch Reactor (SBR) (COD removal = 70%) and Continuous Stirred Reactor (CSTR) (COD removal = 40%) (Chynoweth et al., 1999). Furthermore, our design includes a stage for separating solids that could be used as fertilizer.

The use of METlands could be a convenient strategy for implementing MET for manure wastewater treatment. In this way, an effective treatment of agricultural wastewater could be offered, eliminating the pollutants that cause so many environmental problems. If we also add a tertiary treatment, we obtain safe water for irrigation, giving a second life to the waste produced by the livestock industry.

5.6 References

Aguirre-Sierra, A., 2017. Integrating microbial electrochemical systems in constructed wetlands, a new paradigm for treating wastewater in small communities. Universidad de Alcalá, Spain.

Aguirre-Sierra, A., Bacchetti-De Gregoris, T., Berná, A., Salas, J.J., Aragón, C., Esteve-Núñez, A., 2016. Microbial electrochemical systems outperform fixed-bed biofilters in cleaning up urban wastewater. Environ. Sci. Water Res. Technol. 2, 984–993. https://doi.org/10.1039/C6EW00172F

APHA/AWWA/WEF, 2012. Standard Methods for the Examination of Water and Wastewater, Standard Methods. https://doi.org/ISBN 9780875532356

Borin, M., Politeo, M., De Stefani, G., 2013. Performance of a hybrid constructed wetland treating piggery wastewater. Ecol. Eng. 51, 229–236. https://doi.org/https://doi.org/10.1016/j.ecoleng.2012.12.064

Brito, L.M., Coutinho, J., Smith, S.R., 2008. Methods to improve the composting process of the solid fraction of dairy cattle slurry. Bioresour. Technol. 99, 8955–8960.

Brix, H., 2003. PLANTS USED IN CONSTRUCTED WETLANDS AND THEIR FUNCTIONS. 1 st Int. Semin. USE Aquat. MACROPHYTES WASTEWATER Treat. Constr. Wetl. 2–30.

Carleton, J.N., Grizzard, T.J., Godrej, A.N., Post, H.E., Lampe, L., Kenel, P.P., 2000. Performance of a Constructed Wetlands in Treating Urban Stormwater Runoff. Water Environ. Res. 72, 295–304. https://doi.org/https://doi.org/10.2175/106143000X137518

Chynoweth, D.P., Wilkie, A.C., Owens, J.M., 1999. Anaerobic treatment of piggery slurry-review. Asian-Australasian J. Anim. Sci. 12, 607–628.

EEC, 1991. Council Directive 19/676/EEC of 12 December, 1991 concerning the protection of waters against pollution caused by nitrates from agricultural sources. Official Journal L (375), 1.

Harrington, C., Scholz, M., 2010. Assessment of pre-digested piggery wastewater treatment operations with surface flow integrated constructed wetland systems. Bioresour. Technol. 101, 7713–7723.

iMETland European H2020 project. n.d. URL http://imetland.eu/

Kaldec, R., Wallace, S., 2008. Treatment Wetlands, CRC press.

Koottatep, T., Polprasert, C., 1997. Role of plant uptake on nitrogen removal in constructed wetlands located in the tropics. Water Sci. Technol. 36, 1 LP – 8.

Kumm, K.-I., 2003. Ways to reduce nitrogen pollution from Swedish pork production. Nutr. Cycl. agroecosystems 66, 285–293.

Luo, A., Zhu, J., Ndegwa, P.M., 2002. Removal of carbon, nitrogen, and phosphorus in pig manure by continuous and intermittent aeration at low redox potentials. Biosyst. Eng. 82, 209–216.

MAGRAMA, 2015. Censo y producción: Producción de porcino ibérico

Martinez, J., Dabert, P., Barrington, S., Burton, C., 2009. Livestock waste treatment systems for environmental quality, food safety, and sustainability. Bioresour. Technol. 100, 5527–5536.

Prado, A., Berenguer, R., Esteve-Núñez, A., 2019. Electroactive biochar outperforms highly conductive carbon materials for biodegrading pollutants by enhancing microbial extracellular electron transfer. Carbon N. Y. 146. https://doi.org/10.1016/j.carbon.2019.02.038

Prado, A., Ramírez-Vargas, C.A., Arias, C.A., Esteve-Núñez, A., 2020. Novel bioelectrochemical strategies for domesticating the electron flow in constructed wetlands. Sci. Total Environ. 735, 139522. https://doi.org/10.1016/j.scitotenv.2020.139522

Ramírez-Vargas, C.A., Prado, A., Arias, C.A., Carvalho, P.N., Esteve-Núñez, A., Brix, H., 2018. Microbial electrochemical technologies for wastewater treatment: Principles and evolution from microbial fuel cells to bioelectrochemical-based constructed wetlands. Water (Switzerland) 10. https://doi.org/10.3390/w10091128

Rotaru, A.E., Yee, M.O., Musat, F., 2021. Microbes trading electricity in consortia of environmental and biotechnological significance. Curr. Opin. Biotechnol. 67, 119–129. https://doi.org/10.1016/j.copbio.2021.01.014

Schröder, U., Harnisch, F., Angenent, L.T., 2015. Microbial electrochemistry and technology: Terminology and classification. Energy Environ. Sci. 8, 513–519. https://doi.org/10.1039/c4ee03359k

Smith, K.A., Frost, J.P., 2000. Nitrogen excretion by farm livestock with respect to land spreading requirements and controlling nitrogen losses to ground and surface waters. Part 1: cattle and sheep. Bioresour. Technol. 71, 173–181.

Statista, 2016. Global pork production in 2016, by country [WWW Document]. URL https://www.statista.com/.

Szogi, A.A., Rice, J.M., Humenik, F.J., Hunt, P.G., Stem, G., 1999. Constructed wetlands for confined swine wastewater treatment, in: Proc. 1999 NCS U Animal Waste Management Symp. Cary, NC: North Carolina State University.

Tanner, C.C., Clayton, J.S., Upsdell, M.P., 1995. Effect of loading rate and planting on treatment of dairy farm wastewaters in constructed wetlands—II. Removal of nitrogen and phosphorus. Water Res. 29, 27–34. https://doi.org/https://doi.org/10.1016/0043-1354(94)00140-3

Vymazal, J., 2014. Constructed wetlands for treatment of industrial wastewaters : A review. Ecol. Eng. 73, 724–751. https://doi.org/10.1016/j.ecoleng.2014.09.034

Vymazal, J., 2008. The use constructed wetlands with horizontal sub-surface flow for various types of wastewater 5, 1–17. https://doi.org/10.1016/j.ecoleng.2008.08.016

Vymazal, J., 2007. Removal of nutrients in various types of constructed wetlands. Sci. Total Environ. 380, 48–65. https://doi.org/10.1016/J.SCITOTENV.2006.09.014

Wang, X., Tian, Y., Liu, H., Zhao, X., Wu, Q., 2019. Effects of influent COD/TN ratio on nitrogen removal in integrated constructed wetland-microbial fuel cell systems. Bioresour. Technol. 271, 492–495. https://doi.org/10.1016/j.biortech.2018.09.039

Wu, H., Zhang, J., Ngo, H.H., Guo, W., Hu, Z., Liang, S., Fan, J., Liu, H., 2015. A review on the sustainability of constructed wetlands for wastewater treatment: Design and operation. Bioresour. Technol. 175, 594–601. https://doi.org/10.1016/J.BIORTECH.2014.10.068

CHAPTER 6:

GENERAL DISCUSSION, CONCLUSIONS AND FUTURE WORK

General Discussion, Conclusions and Future Work

The main objective of this thesis was to explore the Nature-based Solution METland® to treat wastewater. We have mainly focused in developing lab scale configurations to outperformance already existing systems for treating urban wastewater. Moreover, we have developed a system for coping with manure wastewater at a relevant environment (TRL6). The work presented in this thesis supports the idea that Microbial Electrochemical Technologies (METs) might present a potential alternative to classical wastewater treatment technologies by incorporating bioelectrochemical designs. A general discussion is presented in question-answer format, followed by a short section on conclusions, recommendations, and future work.

6.1 General discussion

- How does a METland® work?

Our study reveals that METland® technology significantly improves wastewater treatment compared to constructed wetlands (CW) (**Chapter 2, 3** and **4**) through the stimulation of the metabolic activity of electroactive bacteria by the presence of electrically conductive material (Prado et al., 2019).

In contrast with more traditional MET designs (Ramírez-Vargas et al., 2018; Schröder et al., 2015) METlands are not a two-electrode configuration, so the anode potential cannot be electrochemically controlled like in standard microbial electrolysis cells (Rabaey et al., 2007). Moreover, electrical power, typical of microbial fuel cell, cannot be harvested. However, METland® operates as single electrode configuration, so-called snorkel, where a short-circuited system efficiently stimulates extracellular electron transfer (EET). Indeed, this configuration overcome the bottleneck for the flow of electrons, found in standard external circuit (**Chapter 3**). In contrast with standard MET, redox potential from bed material can be controlled by selecting certain hydraulic operation (Aguirre-Sierra et al., 2020, 2016).

In METlands, the fundamental role is played by a unique relationship between material and microorganisms (**Chapter 2**). The presence of electrically

conductive material in the bed promotes the development of Electroactive bacteria (EAB) capable of using it as an inexhaustible Terminal electron acceptor (TEA). As occurs with constructed wetlands (Dotro et al., 2017), we can anticipate two main operation mode for METland: i) flooded conditions where conditions are mainly anoxic, and removal of organic pollutants and nitrate reduction are favoured; and ii) downflow conditions, where oxygen play a double role (respiratory and electrochemical) along the whole bed, and removal organic pollutants and ammonium are favoured. In the context of this thesis, we have mainly focused on flooded configurations (**Chapter 2, 3, 4** and **5**) although downflow configurations were also tested for treating manure wastewater (**Chapter 5**).

If METlands are operated under flooded conditions, the electrons generated by the EAB in anoxic deeper layers of the bed migrate up to the surface following the profile of increasing oxygen (TEA) concentration. This would originate a vertical redox gradient along the bed, from the deeper more negative redox potentials regions, towards the upper more positive redox potential ones, where the electrons are consumed by inexhaustible oxygen or alternative soluble TEAs. This decoupling effect in the microbial oxidation-reduction mechanism allows to physically separate the reduction for the soluble electron acceptor from the location where living cells are catabolizing the pollutants and generating the electrons. This is the actual essence of METland® solution (Amanda Prado et al., 2020).

This flow of electrons inside a METland® was firstly demonstrated by Ramirez et al., (Ramírez-Vargas et al., 2019) by measuring the electric potential profile along the bed. We have followed identical methodology in **Chapters 2** and **4**, for confirming such electron flow among the different material tested.

The other main component in METland® is electroactive bacteria (**Chapter 2**). We have observed how the presence of electrically conductive material stimulates the development of electroactive bacteria and, specifically, of species of the genus *Geobacter.* It has been shown that the stimulation of Direct Interspecies Electron Transfer (DIET) and Conductive-particle-mediated Interspecies Electron Transfer (CIET) (Rotaru et al., 2021) can be accelerated

through electrically conductive materials and carbon-based materials. In electrochemical syntrophic interactions, bacteria from *Geobacter* genus acted as a metabolic mediator, donating or accepting electrons to/from other microorganisms or materials. In this work, we have demonstrated that electroactive activity through cyclic voltammetry in single granules can be measured even under low presence of *Geobacter*, which could indicate the crucial role of *Geobacter* as an electrical connector.

- What elements are key for an optimal METland® performance?

METland® have been already operated almost a decade and we can find a number of cases where its implementation resulted successful (www.imetland.eu). However, now we expect to move one step further, and be able to understand and explain how METland® actually works, exploring each part of this system.

The bed material is a key component of this constructed ecosystem. Its physical and chemical properties are going to determine how electrons are transferred and what microbial communities can be selected (**Chapter 3**). We propose that a proper characterization should be performed at four levels: morphological, textural, structural and chemical. Morphological characterization provides an image of the surface of the material. Textural characterization is important to know the porosity of the material and to be able to relate it to bacterial colonization and ionic flow. To obtain a structural characterization, the most useful techniques are Raman and XRD, thus we will know the size and order of the crystallites of the material's structure that is related to electrical conductivity. Finally, a chemical characterization, through DTP and XPS, offers us an idea of the surface chemical composition of the materials and the concentration of oxygenated groups that can act as quinones. The presence of such functional groups is especially relevant in the case of materials from pyrolyzed vegetal waste (Schievano et al., 2019). Ec-coke presents a very abrupt morphology with large crater holes, ec-biochar presents a large volume of different pores (SEM). Ec-coke is a highly conductive carbon

material, this is due to the order and size of the crystallites in the carbon structure. Ec-coke shows greater structural order, so its electroconductivity will be higher than that of ec-biochar (Raman and XRD). Ec-biochar has richer surface chemistry and shows more oxygen groups on the surface (DTP and XPS), which can act as redox mediators and accept and / or give electrons to the electroactive bacteria.

To understand microbial biodiversity, techniques such as Illumina sequencing (**Chapter 2**) can be applied. Microorganisms are the main actors in the oxidation and reduction processes of wastewater pollutants. It is important to know the bacterial species and their physiology in order to predict biological behaviour. In this way, signals of metabolisms, such as anammox and electroanammox (Shaw et al., 2020), were identified in an operation context where ammonium is oxidized under anaerobic conditions.

Finally, electrochemical techniques offer us information on the response of electroactive microorganisms to the different operating conditions of METLands. The Extracellular electron transfer (EET) is the core of this technology; this can be monitor by electrochemical techniques such as cyclic voltammetry and chronoamperometry (**Chapter 3**) so we can directly measure the bacterium-electrode interaction and be able to quantify the electrons that EABs generate while oxidizing organic matter. Furthermore, as we reported in **Chapters 2** and **4**, the electric potential profiles are key to measure the flow of electrons, including the direction, the sense and the quantity of such flow. These values will allow us to understand what type of electron transfer is taking place, continuous vs. discontinuous, what type of reactions are being favoured, oxidation vs. reduction and can even be correlated with the COD removal rate.

- What can be electrochemically measured in a METland® system?

The main electrochemical techniques that have been applied to microbiology are chronoamperometry and cyclic voltammetry. To perform both, a three-electrode system is required. METland®, acting as a snorkel, has a continuous bed of electrically conductive material that acts as a single

electrode, allowing a continuous flow of electrons but preventing the above techniques from being applied *in situ*.

Therefore, solutions to elucidate the extracellular electron transfer (EET) in bed electrodes have been developed in this work. We have developed a protocol to study the electroactivity of bacterial biofilm in electrically conductive single granules from METland bed through cyclic voltammetry (**Chapter 2**) and we have applied the measurement of electrical potentials (Ramírez-Vargas et al., 2019) to perform EP profiles along the electrically conductive bed (**Chapters 2** and **4**).

To study the electroactivity of a bacterial biofilm growing inside the bed, we performed cyclic voltammetry analysis at single granules, selected and isolated from the bed (A. Prado et al., 2020). Actually, this technique provided valuable information like mass-transfer conditions at the biofilm/ electrode interface and identification of the active sites (Harnisch and Freguia, 2012; Rodrigo Quejigo et al., 2018). Thus, this proof of concept opened the possibility of surveying the electrochemical behaviour of microbial communities on granulated electrodes in general, which up to now was not feasible. The presented results not only contribute to a better understanding of EET fundamentals of METlands, but may serve as a valuable tool to shed light on the relationship between electrochemical parameters, the selection of microbial communities and treatment efficiencies.

Another strategy for obtaining electrochemical info was the use of electrical potential measurements to make profiles along with the depth of the METland bed (Ramírez-Vargas et al., 2019). The flow of electrons produced by the EABs in the anode zones that migrates towards the cathodic zones in favour of the redox gradient was directly measured using electric potential probe. This allows us to i) identify the direction of electrons and, consequently, the anodic and cathodic zones of the system, and i) quantify the flow of electrons, which can be correlated with the amount of organic matter oxidized by electroactive bacteria.

The EP profiles constitute the experimental fact that evidences the effective or inefficient e-transport throughout the bed. In absence of

microorganism and consequently without extracellular electron flux, the EP depth profiles were flat, since there was no vertical electron flux. When the bed material was carbonaceous but not electrically conductive, profiles were not observed, since there was no possibility of flow through the bed granules. However, we have shown that, in presence of microorganism extracellular flow of electrons was recorded through the EP depth profile. The slope of this profile is correlated with the number of electrons that migrate along the bed and the higher values allow to locate the areas (anodic region) where oxidation reactions predominate.

- Can the properties of the material determine the microbial community?

The physical-chemical properties of the material have proven to be decisive in the microbial community that colonizes the bed of the METlands (Aguirre-Sierra et al., 2020, 2016). As a consequence of the electrically conductive carbonaceous material, the growth of electroactive bacteria was stimulated in our assays. This led to a marked difference between the microbial communities that colonize the constructed wetlands and the METlands.

In our hands, the gravel bed systems were enriched in the genus *Clostridium* as predominant. The *Clostridium* populations, a strict anaerobic genus, were likely responsible for the rapid fermentation of carbohydrates and were involved in reduction processes (Liu et al., 2017; Zhang et al., 2011). However, in the electrically conductive bed systems, the most abundant genera were related to species of electroactive bacteria, reaching 11-fold more EAB in an ec-biochar bed than in a gravel bed. Thus, genera like *Trichococcus, Pseudomonas* and *Geobacter* were the main ones in carbonaceous material.

Trichococcus is an aerotolerant genus that exhibits a fermentative metabolism, related with the metabolism of various sugars and polysaccharides. Furthermore, species of this genus were described as electroactive (Baek et al., 2015; Rainey, 2015). Species of the genus *Pseudomonas* are strict aerobics, although in some cases they can use nitrate

as an electron acceptor. Some species of this genus have been described as EAB (Pham et al., 2008; Yang et al., 2013), such as *Pseudomonas aeruginosa*, *Pseudomonas alcaliphila* and *Pseudomonas fluorescens*. Regarding the genus *Geobacter*, it is the model electroactive microorganism (Koch and Harnisch, 2016; Pous et al., 2014). *Geobacter* could enhance COD removal efficiency using acetate as the electron donor and electrically conductive material as the electron acceptor. For this reason, it appeared in a higher concentration in the beds of carbonaceous materials, especially in those made of biochar.

Furthermore, according to the alpha diversity indices, carbonaceous materials stimulate greater diversity of bacterial species. This is due to the physical-chemical properties of the materials since electrically conductive carbonaceous materials can act as extracellular TEA, favouring the growth of EAB. In addition, materials of vegetal origin such as biochar, present oxygenated groups on the surface that can act as quinones and/or extracellular redox mediators, allowing the development of species that present a mediated extracellular electron transfer.

It has also been seen how plants also favour higher diversity since, supplying oxygen in anaerobic layers (Brix, 2003; Stottmeister et al., 2003), allowing the localized development of aerobic microorganisms. At the root-plant interface, the most abundant genera were *Rhizobium* and *Herbaspirillum*. Both are within the rhizobia paraphyletic group since they are atmospheric nitrogen-fixing bacteria.

- What is the impact of using electrically conductive materials for making a fixed bed? Does ec-coke behaves differently than biochar?

In **Chapters 2** and **3** we demonstrated that in a polarized METland® made of highly conductive materials like graphite and ec-coke led to significantly greater electrical currents than a less conductive material, such as ec-biochar. These differences were assigned to the different characteristics of the predominant e-transfer mechanisms on both types of materials.

The geoconductor mechanism, in which the EABs directly donate the electrons to the conducting graphitic network, may prevail in ec-coke and may involve a faster bioelectrochemical process. Furthermore, if we favour a fast intraparticle and interparticle e-flux along the conductive bed of ec-coke, one can envisage a fast and continuous transport of electrons from organic matter to TEAs mediated by the EABs-coke biofilter. We have to consider that, given the negligible microporous system and the low number of oxygen functionalities of this material, the mediated geobattery mechanism in ec-coke must be minor. Then, it may be easy to infer that the fast e-transfer and e-flux during this continuous mechanism may imply a high activity of the EABs.

For the ec-biochar, the e-transfer with EABs must be greatly mediated by its electroactive functionalities through the geobattery mechanism. The reaction rates, in this case, are considerably slower than for the geoconductor behaviour. In addition, the lower electrically conductivity may slow down the e-flux through the bed, in agreement with the less marked EP profile found in our assays. In spite of the minor e-flow, ec-biochar showed a high COD removal efficiency which led to wonder about the electron destiny in such materials. Some of the electrons could be used by other bacteria for N-removal ($NH4^+$ reduction to N_2). Another hypothesis is that part of the electrons might be progressively accumulated in the micropores and functionalities (e-storing entities) of the granules of ec-biochar. This could occur in electrically isolated domains in the granules of this material or when the electrical resistance between contacting granules is so high that the electrons cannot easily go across in the direction of TEAs; or, simply, under an occasional scarcity of TEAs. It is reasonable to think that these situations may lead to the generation of potential differences between contacting granules. Hence, it is hypothesized that, under these scenarios, the storage of electrons becomes of paramount importance for keeping the metabolism of EABs, and that it may persist until the granules of ec-biochar are so charged, i.e. the potential differences become so large, that the electrons can overcome the different resistances to proceed towards either adjacent granules (at different redox potential) and/or TEAs. This release of electrons (discharge) may periodically regenerate the e-accepting capacity of the granules, triggering

the activity of the EABs. Thus, the mechanism of e-flux in ec-biochar biofilters could be discontinuous, with repeated episodes of electron transfer-storing-transport from organic matter to TEAs. This discontinuous biodegradation mechanism, characterized by a slower e-transfer and e-flux, may necessarily involve the granules of ec-biochar acting as individual supercapacitors that are continuously charged and discharged.

From these results and discussion, we could hypothesise that the continuous or discontinuous character of the e-flux in METlands will depend on the e-accepting, e-storing and e-transport capabilities of their biofilters.

- Can the electron flux be controlled in a METland®?

There are several strategies to control the flow of electrons in the bed of a METland (**Chapters 3** and **4**). The main reasons to control e-flux are: i) to drive the flow of electrons towards a TEA, with the aim of increasing the oxidation rate of compounds such as organic matter, and ii) alternatively, consume the electrons via TEA (like nitrate), with the aim of removing the nutrient from the wastewater.

The use of a material with a high electrical conductivity is a simple and effective way to increase e-flux along the bed. In this thesis we have evaluated material hosting such capacity: graphite, ec-coke and ec-biochar. The electrically conductivity of the material enables the movement of electrons among the bed granules. In this scenario, an optimal material packing must be determinant to overcome the electric resistances at granule boundaries. Then, the conductivity of both the material and the bed may determine the e-transport (e-flux) capability of the system.

Another possibility to favour e-flow is to increase the concentration of TEA in contact with the bed material. To do this, we have developed a new device called e-sink. By incorporating this tool into the bed, new electron fluxes appeared and the organic matter was oxidized faster, reaching higher COD removals rates. When oxygen is used as TEA inside the e-sink, the removal efficiency increases up to 95% for the removal of COD. When a TEA with a higher

redox potential is used as a TEA inside the e-sink, such as hypochlorite, the treatment efficiency increases up to 98% of COD removal.

To favour the flow of electrons towards TEAs present in wastewater, such as nitrate, with redox potentials lower than oxygen, we use materials in which a discontinuous electron transfer predominates (via geocapacitor). These materials are based on biochar-like materials, which have a high concentration of oxygen functionalities, like phenol/quinone groups. The accumulation of electrons in biochar could occur in the form of phenol (hydroquinone) groups, by reduction of quinone ones (similar to a pseudocapacitive mechanism driven by EABs), or by electrostatic forces in the micropores (similar to a double-layer capacitive mechanism driven by EABs). Thus, the quinone-like functionalities and micropores may contribute to the e-storing capacity of the material. Nevertheless, it is worthy to mention that not all the quinone groups or micropores might be susceptible to be reduced or polarized by EABs, respectively; and that, for effective storage, certain conductivity and reversibility of the processes may be necessary in both cases. The accepted electrons finally reduce a nearby terminal electron acceptor (TEA).

Taking into account all these materials properties and possibilities, the wastewater treatment by the metabolism of EABs may mainly depend on (i) the number of electrons that can be accepted and/or stored by the biochar granules (ie the e-accepting and e- storing capabilities), and/or (ii) just the possibility of the electrons to find TEAs for renewing these capabilities.

- How robust is METland technology?

In the publications presented, we have worked with METlands systems that have been operated under different conditions. We have designed different reactor configurations, in order to test different materials such as bed, reactor volumes and organic loading rates, among other factors. Lab scale METland® operating flooded in upflow mode (**Chapter 2, 3, 4**) fed with real urban wastewater, revealed a COD removal rate in a range of 140-180 gCOD/ bed·m^3day, capable of supporting footprint as low 0.6 m^2/pe (Aguirre-Sierra et

al., 2016). Regarding the oxidation of ammonia, a higher efficiency (80-99%%) was observed in reactors with biochar as bed material, including 90% of total nitrogen. This data are consistent with previously reported. Furthermore, in **Chapter 4**, we have demonstrated how, by incorporating an extra TEA through the e-sink, the efficiencies in the oxidation of compounds increase reaching values of 98% in urban wastewater (Amanda Prado et al., 2020).

After this study, we can confirm that electrically conductive carbonaceous materials have a positive effect on the elimination of organic pollutants and that, specifically, biochar-based materials promote a higher elimination of ammonia.

- Is the full-scale implementation of METland technology a reality?

In **Chapter 5** we discussed the scaling problem of METland® technology. Although previous studies (Aguirre-Sierra, 2017; Peñacoba-Antona et al., 2021b) have shown that the scaling of METlands for the treatment of urban wastewater (www.imetland.eu) is feasible, here we have i) first, validate a design for treating manure wastewater at lab scale, and ii) scale up the system to be implemented in an Animal Nutrition Research Institute (CSIC, Granada).

Our METland® design is a combination of different stages: a) anaerobic reactor for promoting denitrification; b) downflow METland® to oxidize COD and ammonium, and finally c) flooded METland® to final polishing stage. The whole system showed greater efficiencies in the removal of COD (90%) and total nitrogen (96%). In conventional systems such as the Upflow Anaerobic Sludge Blanket (USAB) the COD elimination is 80%, in the Anaerobic Baffled Reactor (ABR) it is 60% and in the Sequencing Batch Reactor (SBR) it is 70%) (Chynoweth et al., 1999).

In this livestock context, METland® technology is an eco-friendly solution with zero-energy operation cost, landscape beautification and ICT remote control, since the conversion of sewage treatment into the electric current can be used as an output signal to inform users remotely. In addition, it is key to integrate a tertiary treatment to eliminate pathogens from the effluent, obtaining

safe water for irrigation, giving a second life to the waste produced by the livestock industry.

- Intensifying the extensive, have the METlands succeed?

Constructed wetlands are an extensive technology that provides a quick, economical and satisfactory solution to the problem of wastewater treatment in small communities. However, as the name of the technology indicates, they require large areas of land (> 1 m^2/p.e). These high surface requirements for the implementation of extensive technologies constitute one of the main challenges for its expansion in countries where it is not easy to have these surfaces. Another important handicap is the fact that extensive technologies do not have the same capacity as intensive technologies to deal with alterations in operating conditions (such as increases in flow rates and organic loads to be treated).

The objective of integrating METs into CWs was to incorporate those benefits from intensive treatments without missing those of extensive treatments. Indeed, we have managed to overcome this challenge. METland technology, as we have shown, has zero operating cost, low maintenance cost, low production of odors, and a good landscape integration that gives the value from an ecological point of view. On the other hand, we have reached, and exceeded in many cases, the performance of intensive technologies. We have shown that METlands have the ability to cope with variations in volume and quality of the influent (**Chapters 3 and 5**). So, it is feasible to implement this technology in urban locations where wastewater production fluctuates annually (such as in residential vacation areas). In addition, the surface requirements have been reduced by up to 88%. For example, with a constructed wetland (extensive technology) the necessary area for a population of 200 equivalent inhabitants would be around 550-700 m^2: moreover, with an aerated wetland (intensive technology) the necessary area is 125 to 150 m^2, however, with METland technology, this area has been reduced to 80m^2 while maintaining zero energy costs. On top of that, new design of modular METlands using larger

heights of electroconductive beds are treating same pe number in roughly 16 m2.

In conclusion, in this thesis we have validated a robust, efficient and economical technology that can be implemented on a real scale, capable of be used it in a wide range of locations such as green areas, or even on the roofs of residential and service buildings, in isolated communities, eco-neighborhoods, scattered communities and gardens of single-family homes.

6.2 Final conclusions

The general conclusions that can be withdrawn from this thesis are the following:

- The integration of Microbial Electrochemical Technologies (METs) in Constructed Wetlands (CW) is a suitable solution so-called METland capable of efficiently treating wastewater.

- The presence of electrically conductive materials promotes the development of electroactive bacteria (EAB), like species from *Geobacter* genus, generating electrochemical syntrophies, that favour pollutant removal.

- Electrons are generated by EABs in the anodic areas, then transferred by EET to the electrically conductive bed material. The electrons will migrate to cathodic areas, where soluble terminal electron acceptors (TEA) are present. Thus, we have unequivocally demonstrated that the METland acts as a snorkel.

- The bed material will determine the flow of electrons. ec-coke has a low electrical resistance that favours a continuous electron transfer, the so-called geoconductor mechanism. On the other hand, ec-biochar has a lower electrical conductivity but exhibits oxygenated groups (quinones) so a discontinuous electron transfer is favoured, the so-called geobattery mechanism.

- The flow of electrons in a METland can be controlled through a new electrochemical device so-called e-sink. Now, we can bring TEA and setup cathodic areas at any environment inside METland, in order to increase the electron flow and then the pollutant removal.

- METland technology has been validated as a robust and intensive technology, capable of treating different types of wastewaters under different modes of operation. The implementation on a full-scale system in the livestock sector opens the technology to new applications beyond urban wastewater from small communities.

6.3 Recommendations and future work

Recommendations for future research are made based on the results presented in this thesis. The main outcome of this work is that METlands are a versatile, controllable and environmentally sustainable technology to treat wastewater in a wide range of locations. Nevertheless, some limitations should be overcome and optimization of an operational configuration should be addressed. This challenge may need researching efforts in multiple disciplines including biotechnology, geochemistry, material science and electrochemistry.

a) In order to obtain a better understanding of the extracellular electron transfer process occurring between electroactive bacteria and electrically conductive bed, a number of additional assays should be performed:

- In the current work, we have successfully presented a species-level characterization that allowed us to identify the key bacteria. However, a deeper analysis concerning gene expression could provide further information. Proteomic or metabolomic studies would clarify the role and importance of many bacterial species in wastewater treatment since not always the most abundant species are the ones that have the determining role.

- Electric potential profiles have proven to be a useful tool for measuring the electron flow in the METland bed. However, more studies must be performed to correlate with the elimination of COD and clean-up efficiency

of the system. Furthermore, alternative TEAs should be investigated, including the direction, sense and magnitude of the electron flow. It is a tool with potential application *on-site* for quantification of treatment efficiency.

- Another field that requires future study is that of carbonaceous materials. Here we have shown the implications of their physicochemical properties may have on electron transfer and pollutant removal. However, a deeper exploration of their properties, together with their interaction with electroactive bacteria would allow an optimization of the technology, and eventually a customization for every specific case.

- METlands have proven to be a robust technology for COD removal. They are also effective for the removal of nitrogenous compounds under anoxic conditions, but understanding the microbial mechanism involved is key to promote them and develop a complete wastewater treatment. In addition, the elimination of another nutrient that pollutes wastewater, like phosphorus, must be studied.

b) To consolidate this technology as a competitive wastewater treatment in the water market, a number of barriers should be addressed:

- *Back to the future*: the impact of micropollutants present in wastewater is matter of concern and it will be incorporated into water legislation very soon. In this context, METland have been proved to be effective for removing micropollutants from urban wastewater (Pun et al., 2019). However, due to the vast diversity of such chemicals (drugs, cosmetic compounds, flame retardants) it is necessary to investigate such removal capacity with water of different sources, in combination with the most accurate analytical equipment.

- *Sustainability*: is one of the most attractive features behind METland technology, already confirmed by recent life cycle assessments (LCA) (Peñacoba-Antona et al., 2021b). However, we can anticipate in the future new configurations and new materials that will have in LCA the right tool to be evaluated. Production, distribution, use and end of life (reuse,

recycling, recovery and disposal of residues / waste), together with the use of resources ("inputs" such as energy, raw materials, water) and environmental emissions ("outputs" to air, water and soil) should be must be quantified in order to assist stakeholders for accepting METland®.

- *Social acceptance:* METland technology can be implemented on a full scale in various geolocations, but it is necessary to study the factors that determine the optimal locations for METland. In addition to climatic conditions, factors such as land use, distance to rivers and distance to population centres could help to choose the ideal location for the construction of a METland (Peñacoba-Antona et al., 2021a).

6.4 References

Aguirre-Sierra, A., 2017. Integrating microbial electrochemical systems in constructed wetlands, a new paradigm for treating wastewater in small communities. Universidad de Alcalá, Spain.

Aguirre-Sierra, A., Bacchetti-De Gregoris, T., Berná, A., Salas, J.J., Aragón, C., Esteve-Núñez, A., 2016. Microbial electrochemical systems outperform fixed-bed biofilters in cleaning up urban wastewater. Environ. Sci. Water Res. Technol. 2, 984–993. https://doi.org/10.1039/C6EW00172F

Aguirre-Sierra, A., Bacchetti-De Gregoris, T., Salas, J.J., De Deus, A., Esteve-Núñez, A., 2020. A new concept in constructed wetlands: Assessment of aerobic electroconductive biofilters. Environ. Sci. Water Res. Technol. 6, 1312–1323. https://doi.org/10.1039/c9ew00696f

Baek, G., Kim, J., Cho, K., Bae, H., Lee, C., 2015. The biostimulation of anaerobic digestion with (semi)conductive ferric oxides: their potential for enhanced biomethanation. Appl. Microbiol. Biotechnol. 99, 10355–10366. https://doi.org/10.1007/s00253-015-6900-y

Brix, H., 2003. PLANTS USED IN CONSTRUCTED WETLANDS AND THEIR FUNCTIONS. 1 st Int. Semin. USE Aquat. MACROPHYTES WASTEWATER Treat. Constr. Wetl. 2–30.

Chynoweth, D.P., Wilkie, A.C., Owens, J.M., 1999. Anaerobic treatment of piggery slurry-review. Asian-Australasian J. Anim. Sci. 12, 607–628.

Dotro, G., Molle, P., Nivala, J., Puigagut, J., Stein, O., 2017. Treatment Wetlands. First. ed. IWA Publishing, London.

Harnisch, F., Freguia, S., 2012. A basic tutorial on cyclic voltammetry for the investigation of electroactive microbial biofilms. Chem. - An Asian J. 7, 466–475. https://doi.org/10.1002/asia.201100740

Koch, C., Harnisch, F., 2016. Is there a Specific Ecological Niche for Electroactive Microorganisms? ChemElectroChem 3, 1282–1295. https://doi.org/10.1002/celc.201600079

Liu, R., Tursun, H., Hou, X., Odey, F., Li, Y., Wang, X., Xie, T., 2017. Microbial community dynamics in a pilot-scale MFC-AA/O system treating domestic sewage. Bioresour. Technol. 241, 439–447. https://doi.org/10.1016/j.biortech.2017.05.122

Peñacoba-Antona, L., Gómez-Delgado, M., Esteve-Núñez, A., 2021a. Multi-criteria evaluation and sensitivity analysis for the optimal location of constructed wetlands (METland) at oceanic and Mediterranean locations. Int. J. Environ. Res. Public Health.

Peñacoba-Antona, L., Senán-Salinas, J., Aguirre-Sierra, A., Letón, P., Salas, J.J., García-Calvo, E., Esteve-Núñez, A., 2021b. Assessing METland® design and performance through LCA: techno-environmental study with multifunctional unit perspective. Front. Microbiol. In press.

Pham, T.H., Boon, N., Aelterman, P., Clauwaert, P., De Schamphelaire, L., Vanhaecke, L., De Maeyer, K., Höfte, M., Verstraete, W., Rabaey, K., 2008. Metabolites produced by Pseudomonas sp. enable a Gram-positive bacterium to achieve extracellular electron transfer. Appl. Microbiol. Biotechnol. 77, 1119–1129. https://doi.org/10.1007/s00253-007-1248-6

Pous, N., Koch, C., Colprim, J., Puig, S., Harnisch, F., 2014. Extracellular electron transfer of biocathodes: Revealing the potentials for nitrate and nitrite reduction of denitrifying microbiomes dominated by Thiobacillus sp. Electrochem. commun. 49, 93–97.

Prado, A., Berenguer, R., Berná, A., Esteve-Núñez, A., 2020. Simultaneous characterization of porous and non-porous electrodes in microbial electrochemical systems. MethodsX 7. https://doi.org/10.1016/j.mex.2020.101021

Prado, A., Berenguer, R., Esteve-Núñez, A., 2019. Electroactive biochar outperforms

highly conductive carbon materials for biodegrading pollutants by enhancing microbial extracellular electron transfer. Carbon N. Y. 146. https://doi.org/10.1016/j.carbon.2019.02.038

Prado, Amanda, Ramírez-Vargas, C.A., Arias, C.A., Esteve-Núñez, A., 2020. Novel bioelectrochemical strategies for domesticating the electron flow in constructed wetlands. Sci. Total Environ. 735, 139522. https://doi.org/10.1016/j.scitotenv.2020.139522

Pun, Á., Boltes, K., Letón, P., Esteve-nuñez, A., 2019. Bioresource Technology Reports Detoxification of wastewater containing pharmaceuticals using horizontal flow bioelectrochemical filter. Bioresour. Technol. Reports 7, 100296. https://doi.org/10.1016/j.biteb.2019.100296

Rabaey, K., Rodríguez, J., Blackall, L.L., Keller, J., Gross, P., Batstone, D., Verstraete, W., Nealson, K.H., 2007. Microbial ecology meets electrochemistry: electricity-driven and driving communities. ISME J. 1, 9–18. https://doi.org/10.1038/ismej.2007.4

Rainey, F.A., 2015. Trichococcus . Bergey's Man. Syst. Archaea Bact. 1–7. https://doi.org/10.1002/9781118960608.gbm00599

Ramírez-Vargas, C.A., Arias, C.A., Carvalho, P., Zhang, L., Esteve-Núñez, A., Brix, H., 2019. Electroactive biofilm-based constructed wetland (EABB-CW): A mesocosm-scale test of an innovative setup for wastewater treatment. Sci. Total Environ. 659, 796–806. https://doi.org/10.1016/j.scitotenv.2018.12.432

Ramírez-Vargas, C.A., Prado, A., Arias, C.A., Carvalho, P.N., Esteve-Núñez, A., Brix, H., 2018. Microbial electrochemical technologies for wastewater treatment: Principles and evolution from microbial fuel cells to bioelectrochemical-based constructed wetlands. Water (Switzerland) 10. https://doi.org/10.3390/w10091128

Rodrigo Quejigo, J., Rosa, L.F.M., Harnisch, F., 2018. Electrochemical characterization of bed electrodes using voltammetry of single granules. Electrochem. commun. 90, 78–82. https://doi.org/10.1016/j.elecom.2018.04.009

Rotaru, A.-E., Yee, M.O., Musat, F., 2021. Microbes trading electricity in consortia of environmental and biotechnological significance. Curr. Opin. Biotechnol. 67, 119–129. https://doi.org/https://doi.org/10.1016/j.copbio.2021.01.014

Schievano, A., Berenguer, R., Goglio, A., Bocchi, S., Marzorati, S., Rago, L., Louro, R.O., Paquete, C.M., Esteve-Núñez, A., 2019. Electroactive biochar for large-scale

environmental applications of microbial electrochemistry. ACS Sustain. Chem. Eng. 7, 18198–18212.

Schröder, U., Harnisch, F., Angenent, L.T., 2015. Microbial electrochemistry and technology: terminology and classification. Energy Environ. Sci. 8, 513–519. https://doi.org/10.1039/C4EE03359K

Shaw, D.R., Ali, M., Katuri, K.P., Gralnick, J.A., Reimann, J., Mesman, R., van Niftrik, L., Jetten, M.S.M., Saikaly, P.E., 2020. Extracellular electron transfer-dependent anaerobic oxidation of ammonium by anammox bacteria. Nat. Commun. 11, 2058. https://doi.org/10.1038/s41467-020-16016-y

Stottmeister, U., Wießner, A., Kuschk, P., Kappelmeyer, U., Kästner, M., Bederski, O., Müller, R.A., Moormann, H., 2003. Effects of plants and microorganisms in constructed wetlands for wastewater treatment. Biotechnol. Adv. 22, 93–117. https://doi.org/10.1016/J.BIOTECHADV.2003.08.010

Yang, G., Han, L., Wen, J., Zhou, S., 2013. Pseudomonas guangdongensis sp. nov., isolated from an electroactive biofilm, and emended description of the genus Pseudomonas Migula 1894. Int. J. Syst. Evol. Microbiol. 63, 4599–4605. https://doi.org/10.1099/ijs.0.054676-0

Zhang, Y., Min, B., Huang, L., Angelidaki, I., 2011. Electricity generation and microbial community response to substrate changes in microbial fuel cell. Bioresour. Technol. 102, 1166–1173. https://doi.org/10.1016/j.biortech.2010.09.044

ANNEX

ANNEX

List Of Figures

Chapter 1

Figure 1.1: Nature-based Solutions as an umbrella term for ecosystem-related approaches.....20

Figure 1.2: Types of wastewater that can be treated in a METland.....27

Figure 1.3: Basic elements of a free water surface constructed wetland.....37

Figure 1.4: Schematic horizontal subsurface flow constructed wetland.....38

Figure 1.5: Schematic diagrams of respiration: (A) electron transfer to a soluble compound (as oxygen) and (B) microbial extracellular electron transfer.....45

Figure 1.6. A. MEET via secondary metabolites B. DEET to electrodes via membrane bound cytochromes. C. Direct Interspecies electrons transfer (DIET). D. Conductive-particles mediates interspecies electron transfer (CIET)..... 48

Figure 1.7: Cyclic voltammetry where Epa: anodic peak potential; Epc: cathodic peak potential; Ipa: anodic peak current; Ipc: cathodic peak current; E0: standard potential.....53

Figure 1.8: Schematic representation of microbial fuel cell working principle.....55

Figure 1.9: Schematic of a typical Microbial Desalination Cell (MDC) of 3 cameras, without external power supply. The current flow comes from the microbial oxidation at the anode of anode of organic matter and the cathodic reduction reaction is Fe(III)/Fe(II).....56

Figure 1.10 A) Schematic of a typical Microbial electrochemichal fluidized bed reactor (ME-FBR). B) Schematic of a Microbial electroremediating cell (MERC).....60

Figure 1.11: Microbial electrochemical snorkel (MES) concept.....61

Figure 1.12: Bioelectrochemical nitrogen and organic matter removal process in wastewater.....61

Figure 1.13: The integration of microbial electrochemical technologies (MET) in constructed wetlands (CW): left) microbial fuel cell (MFC) in CW; right) snorkel, a single electrode-based configuration under short circuit with no resistors (METland®).....64

Figure 1.14. Constructed METland® implemented at different internal locations.....66

Figure 1.15: Reconstruction of the implementation of a full-scale METland® in a green city.....68

Chapter 2

Figure 2.1. Scheme of electrochemically-assisted biofilters made of four materials: (gravel, nc-biochar, ec-biochar and ec-coke) operating up-flow in absence or presence of plants.....96

Figure 2.2. Main physico-chemical properties of the carbonaceous biofilter materials, including the electrical conductivity (A); morphology (SEM images, B); porosity (BET and ADR(CO_2) specific surface areas and % porosity in C); pore size distribution (D); oyxgen surface groups (CO_2-like and CO-like evolving groups from TPD in E).....101

Figure 2.3. COD concentration at the influent (black) and effluent of every biofilter: gravel (orange), nc-biochar (yellow), ec-biochar (green) and ec-coke (grey), operating up flow during 0-10 days and 10-20 days, in the planted systems (up) and non-planted systems (down). Red line: European discharge limit = 125 mg/L (Council Directive 2000/60/EC of 23 October 2000).....105

Figure 2.4. The bar graph shows the relative abundance at genus-level. The figure shows the most important genera in each region of each system: a) upper layer of planted systems, b) lower layer of planted systems, c) upper layer of non-planted systems and d) lower layer of non-planted systems.....106

Figure 2.5. NH4+ concentration at the influent (black) and effluent of every biofilter: gravel (orange), nc-biochar (yellow), ec-biochar (green) and ec-coke (grey), operating up flow during 0-10 days and 10-20 days, in the planted systems (up) and non-planted systems (down).....108

Figure 2.6. Electric potential (EP) depth profiles of tested biofilters along depth at each time (abiotic, 10 days and 20 days) of gravel (orange), nc-biochar (yellow), ec-biochar (green) and ec-coke (grey) bed, in planted (up) and non-planted (down) systems. EP profiles were measured with a shielded Ag/AgCl electric potential electrode.....111

Figure 2.7. Cyclic voltammograms of a single granule of nc-biochar, ec-biochar and ec-coke from the non-planted bottom system at different stages (biofilm-free (black), 10 days (red) and 20 days (blue)). Scan rate 10 mV/s; phosphate buffer 100mM, acetate 10mM.....114

Figure 2.8. Relative abundance of Geobacter (represented with pink colour intensity) at different locations from biofilters made of a) gravel, b) nc-biochar, c) ec-biochar and d) ec-coke. In bar graph: percentage of each Geobacter species of the total registered for each location.....115

Chapter 3

Figure 3.1. A-D) SEM micrographs; E) Hg intrusion porosimetry and F) the derived pore size distribution of the bed.....150

Figure 3.2. Normalized X-ray diffractograms (A) and Raman spectra (B); the electrical conductivity from 4 probe measurements (C); and TPD (D) of the carbon materials used as electrogenic biofilters. NC, non-conductive gravel; G, graphite; C, coke; QB, Quercus electroconductive biochar.....153

Figure 3.3. Steady-state cyclic voltammograms of a single granule of the different biofilter materials just after inoculation (Geobacter sulfurreducens) (t = 0) and after polarization at 0.2 V (vs. Ag/AgCl/Cl-(sat.)) for 7 days (t = 7) to promote biofilm growth; scan rate = 10 mV/s; fresh water medium, 20 mM acetate.....155

Figure 3.4. Evolution of acetate concentration in the biofilters operating in (A) batch and (B) continuous (HRT = 3.3 days) mode. NC, non-conductive gravel; G, graphite; C, coke; QB, Quercus electroconductive biochar.....156

Figure 3.5. Average COD removal rate including ± standard errors in each biofilter without polarization, referred to HRT = 2 days and two different OLRs in urban wastewater. NC, non-conductive gravel; G, graphite; C, coke; QB, Quercus electroconductive biochar.....158

Figure 3.6. (A) Average effluent COD (showing discharge limit*); and (B) COD removal rate, including ± standard errors, in each biofilter submitted to different polarization conditions (NP = non-polarized, in which the open circuit potentials were: -420 mV, -427 mV and -429 mV for the graphite, coke and biochar, respectively). (C-D) Evolution of the COD removal efficiency (dots) and the microbial electrical current (lines) while treating real urban wastewater using electroconductive biofilters anodically polarized at (C) 0.4 V and (D) 0.6 V (vs. Ag/AgCl/Cl- (sat.)). Influent COD = 800 mg/L; HRT = 2 days. NC, non-conductive gravel; G, graphite; C, coke; QB, Quercus biochar.....161

Figure 3.7. Scheme of the proposed geoconductor and geobattery e-transfer mechanisms between bacteria and carbon materials, emphasizing their possible modulation, externally, by polarization.....164

Figure 3.8. SEM micrographs of the carbonaceous bed materials after being used as polarized (0.6 V) electrogenic biofilters: (A-C) graphite; (D-F) coke; and (G-I) Quercus-derived biochar.....168

Figure. 3.9. Hg Intrusion curves of the different carbon materials (A) and the pore size distribution of the Quercus-derived biochar, before and after being used as biofilters polarized at 0.6 V. G, graphite; C, coke; QB, Quercus biochar.....169

Figure. 3.10. Diagram of the MEC and the connections with the potentiostat and the multimeter.....187

Figure. 3.11. Cyclic voltammogram at 10 mV/s of a graphite electrode after promoted biofilm growth in fresh water medium.....188

Figure. 3.12. A) Left: Wires used for working electrode connections: (a.1), copper wire, (a.2) copper wire coated with carbon glue and (a. 3) gold wire. Right: cyclic voltammograms corresponding to left configurations; scan rate = 10 mV s-1; 100 mM buffer phosphate. B) Left: Isostatic graphite connected to copper wire and (b.1) sealed with epoxy resin or (b.2) glued with adhesive copper tape and insulated with epoxy resin. Right: cyclic voltammograms corresponding to left configurations; scan rate = 10 mV s-1; 100 mM buffer phosphate. C) Left: Porous graphite connected to (c.1) gold wire, (c.2) to copper wire through isolation with carbon glue and epoxy resin, or (c.3) to copper wire through isostatic graphite, carbon glue and epoxy resin. Right: cyclic voltammograms corresponding to left configurations; scan rate = 10 mV s-1; 100 mM buffer phosphate.....192

Figure. 3.13. (left) Current intensity and polarization potential to the 3 working electrodes of the MEC including the summation of all currents. (right) Comparison of the total current recorded by both the multimeter and the potentiostat.....194

Chapter 4

Figure 4.1. Biofilter scheme without (left) and with (right) bed material.....207

Figure 4.2. Electric vertical potential (EP) profiles of tested biofilters along depth at each sampling point (SP1, SP2 and SP3) of gravel (orange), ec-coke (grey) and ec-biochar (green) bed operating as biofilter, biofilter + O_2 based e-sink and biofilter + ClO^- based e-sink. EP profiles were measured with a shielded Ag/AgCl electric potential electrode.....212

Figure 4.3. Current density (J) values of the up-flow biofilters made of ec-coke (grey) and ec-biochar (green) in each sampling point (SP1, SP2, SP3). The systems were operated with an empty e-sink (A and C) and with an e-sink hosting oxygen saturated water (B, D). In presence of e-sink, the current density has two directions: i) vertical (grey and green bars) towards the top surface, and horizontal (red bars) towards the e-sink.....214

Figure 4.4. Vertical distribution of electron transfer rates (R) for the three biofilters, gravel (orange), ec-coke (grey) and ec-biochar (green), operating without e-sink, O2 based e-sink and ClO^- based e-sink. Positive values signify electron transfer from an electron donor (anodic reactions), while negative values signify electron transfer to an electron acceptor (cathodic reactions).....216

Figure 4.5. COD concentration at the influent (red) and effluent of each biofilters: gravel (orange), ec-biochar (green) and ec-coke (grey), operating up flow with e-sink either in absence of electron acceptor or in presence of oxygen (O_2) and hypochlorite (ClO^-).....217

Figure 4.6. NH4+-N (left) and TN (right) concentration for the three biofilters, gravel (orange), ec-coke (grey) and ec-biochar (green), up flow with e-sink in absence of electron acceptor or in presence of oxygen (O_2) and hypochlorite (ClO^-).....219

Chapter 5

Figure 5.1. Scheme of the lab-sale bioelectrochemically-assisted manure wastewater treatment system.....237

Figure 5.2. COD and total-N concentration at the influent (black) and effluent of reactor: anaerobic (grey), downflow metland (yellow) and HSSF-METland (blue).....241

Figure 5.3. NH_4^+ and NO_3^- concentration at the influent (black) and effluent of every reactor: anaerobic (grey), aerobic ec-biofilter (yellow) and METland (blue).....242

Figure 5.4. COD, NH_4^+, NO_3^-, and tot-N concentration (bar graph, left axe) and removal rate (red dots, right axe) at the influent (grey) and effluent (blue) of the lab-scale bioelectrochemically-assisted manure wastewater treatment system.....242

Figure 5.5. Scheme of the Full-scale bioelectrochemically-assisted manure ww treatment system installed in the Animal Nutrition Institute (EEZ-CSIC).....244

List Of Supplementary Figures

Chapter 2

Figure S2.1 Scheme of how the cyclic voltammetries of single granules were carried out. From left to right: (i) materials used as a bed, (ii) locations of selected granules, (iii) single chamber to performed CVs.....125

Figure S2.2. Hg intrusion curves of the different biofilter materials.....126

Figure S2.3. CO2- and (d) CO-evolution from TPD experiments for the different carbonaceous biofilter materials.....126

Figure S2.4. N2 adsorption-desorption isotherms at -196 °C of the different biofilter materials.....127

Figure S2.5. X-ray diffractograms (A) and Raman spectra (B) of the different biofilter materials. The * and ■ symbols in the diffractograms showed the presence of adventitious $CaCO_3$ and SiO_2, respectively.....127

Figure S2.6. SEM micrographs of granules from the eight systems (four material (G, ncB, ecB andec C) and planted (P) and unplanted (NP)) at upper (sup) and bottom (inf) layer. The granules were abiotic (A) and materials at day 20 (B).....128

Figure S2.7. Cyclic voltammograms of a single granule of nc-biochar from the planted system (A: upper layer, B bottom layer) and non-planted system (C: upper layer, D: bottom layer) at different stages (biofilm-free (black), 10 days (red) and 20 days (blue)). Scan rate 10 mV/s; phosphate buffer 100mM, acetate 10mM.....130

Figure S2.8. Cyclic voltammograms of a single granule of ec-biochar from the planted system (A: upper layer, B bottom layer) and non-planted system (C: upper layer, D: bottom layer) at different times (abiotic (black), 10 days (red) and 20 days (blue)). Scan rate 10 mV/s; phosphate buffer 100mM, acetate 10mM.....130

Figure S2.9. Cyclic voltammograms of a single granule of ec-coke from the planted system (A: upper layer, B bottom layer) and non-planted system (C: upper layer, D: bottom layer) at different times (abiotic (black), 10 days (red) and 20 days (blue)). Scan rate 10 mV/s; phosphate buffer 100mM, acetate 10mM.....131

Figure S2.10. First derivative of the 20 days CVs of the coke granules, from the ecC-Psup (green) and ecC-NPinf (orange) systems. Value of the formal potential for the redox pairs.....131

Figure S2.11. This scatterplot shows a Principal Coordinate Analysis (PCoA) of the normalized relative abundance of all the seventeen samples. The PCoA measures differences in the distribution of taxonomic classifications between samples at specie level.....132

Figure S2.12. Microbial community composition of the eight reactors (four materials (G, ncB, ecB and ecC), planted (P) and unplanted (NP), and upper (sup) and bottom (inf) layer) at phylum (A) and class (B) level.....135

Figure S2.13. Microbial community composition of the eight reactors (four materials (G, ncB, ecB and ecC), planted (P) and unplanted (NP), and upper (sup) and bottom (inf) layer) at phylum (A) and class (B) level.....135

Figure S2.14. This dendrogram shows a hierarchical clustering of samples based on genus-level classifications. The barchart beneath each sample show the relative abundance of its genus-level classifications.....136

Chapter 3

Figure S3.1. Scheme of the used H-type cell and experimental set-up to carry out the voltammetric characterization of single granules of the different conductive materials and the potentiostatic treatment to promote biofilm growth.....178

Figure S3.2. Scheme of the used laboratory-scale upflow electroconductive biofilters: A. single-electrode (snorkel) configuration; B. three-electrode configuration, with the anode (down), the counter-electrode (up), and the reference electrode (buried in the anode).....178

Figure S3.3. N_2 adsorption-desorption isotherms at -196 ° C of the bed materials before being used as electrogenic biofilters: G = graphite; C = coke; QB = Quercus biochar; NC = gravel.....179

Figure S3.4. X-ray diffractogram of the gravel (NC).....179

Figure S3.5. SEM micrographs of gravel before (A) and after (B) be used as material for biofilter
operation.....180

Chapter 4

Figure S4.1. The integration of microbial electrochemical technologies (MET) in constructed wetlands (CW): A) microbial fuel cell (MFC) in CW; B) microbial electrolysis cell (MEC) by poising the electrode with a certain potential through a

potentiostat or a power source; C) snorkel, a single electrode-based configuration under short circuit with no resistors (METland®) and D) METland® with e-sink.....225

Figure S4.2. Scheme of the e-sink mechanism. Both, electrons, from biodegradation of pollutants, and protons resulting from such metabolism, flux into the e-sink. A catholyte, oxygen or hypochlorite, is reduced inside the e-sink. The flux of electrons is transferred from the electroconductive bed to a tube made of electroconductive carbon fiber. The H^+ flux is allowed through the cation exchange membrane.....226

Figure S4.3. Scheme of a biofilter with EP monitoring equipment: Ag/AgCl reference electrode, EP sensor position and sample points (SP1, SP2, and SP3).....226

Figure S4.4. Scheme of flux of electrons inside the METlands® without and with e-sink in each sample point (SP1, SP2, and SP3). Black arrows show the flux of electrons to the surface oxygen and red arrows show the flux of electrons horizontally to the e-sink. In deeper layers and closer to the e-sink the horizontal flux (red arrows) is greater than the vertical one, the opposite than in the top layers.....227

List Of Tables

Chapter 1

Table 1.1 parameters are used to measure contamination.....31

Table 1.2. Treatment performance values in subsurface slow constructed wetlands (From Ortega *et al.* 2010).....39

Table 1.3. Summary of those Research and Innovation actions leading to METland® solution from TRL1 to TRL9.....67

Chapter 3

Table 3.1. Textural, structural and chemical parameters of graphite (G), coke (C) and - Quercus electroconductive biochar (QB) before and after being used, polarized at 0.6 V, as electrogenic biofilter beds.....151

Chapter 4

Table 4.1. Physiochemical characteristics of bed materials.....207

Table 4.2. Influent and effluent COD concentration, removal rate and efficiency for the different systems.....217

Table 4.3. Influent and effluent NH_4^+-N and TN concentration for the systems.....219

Chapter 5

Table 5.1. Physicochemical characteristics of the wastewater generated in an Animal Nutrition Center.....239

Table 5.2. Ions quantified in the wastewater generated in an Animal Nutrition Center.....239

ANNEX

List Of Supplementary Tables

Chapter 2

Table S2.1. Physiochemical characteristics of bed materials.....125

Table S2.2. Influent and effluent COD concentration, removal rate and efficiency for the different systems during 0-10 days and 10-20 days.....129

Table S2.3. Influent and effluent NH_4^+ concentration and efficiency for the different systems during 0-10 days and 10-20 days.....129

Table S2.4. Functional microbes in the eight reactors (four materials (G, ncB, ecB and ecC) and planted (P) and unplanted (NP)).....129

Table S2.5. Richness indices of microbial community composition in the reactors.....132

Table S2.6. List of the electro active bacteria (EAB) and its main characteristics.....133

Table S2.7. Number of reads of EAB species found in each region of each system.....134

Chapter 3

Table S3.1. Width (FWHM) and position as well as the calculated interlayer spacing and crystallite dimensions for the characteristic diffraction peaks of the graphite crystalline structure for graphite (G), coke (C) and biochar (QB) materials.....180

Table S3.2. Spectral parameters from the most important Raman bands; and quantified CO2- and CO-evolving oxygen surface groups (O = CO + $2CO_2$) of graphite (G), coke (C) and biochar (QB) materials.....180

Table S3.3. Surface chemical composition according to XPS analysis for graphite (G), coke (C) and biochar (QB), before and after being used as polarized electrogenic biofilter bed at 0.6 V.....181

Table S3.4. Characteristics of influent real urban wastewater after the Inhoff tank (average ± SD).....181

Chapter 4

Table S4.1. Water conductivity (σ) in each biofilter operating under each e-sink condition. The conductivity of the water was measured on-site directly with a conductivimeter (Hach sension+ 5060).....227

Abbreviations

AD	Anaerobic digestion
AEM	Anion exchange membrane
AOB	Ammonium oxidizing bacteria
ARB	Anode-respiring bacteria
BES	Bioelectrochemical system
BET	Specific surface area
BOD	Biological oxygen demand
CA	Chronoamperometry
CE	Coulombic efficiency
CEM	Cation exchange membrane
CIET	Conductive particle-mediated Interspecies e-transfer
COD	Chemical oxygen demand
CV	Cyclic voltammetry
CW	Constructed wetland
CW-MFC	Constructed wetland - microbial fuel cell
DEET	Direct extracellular electron transfer
DF	Down-flow
DIET	Direct interspecies electron transfer
DMRB	Dissimilatory iron-reducing bacteria
DNB	denitrifying bacteria
DNRA	Dissimilatory nitrate reduction to ammonium
DO	Dissolved oxygen
EA	Electron acceptor
EAB	Electroactive bacteria
ec-B	electrically conductive biochar
ec-C	electrically conductive coke
ED	Electron donor
EET	Extracellular electron transfer
EP	Electric potential
EPS	Extracellular polymeric substances
FWHM	Full width at half maximum
FWS	Free water surface
HLR	Hydraulic loading rate
HPLC	High-performance liquid chromatography
HQ/Q	Hydrochinone / Quinone
HRT	Hydraulic retention time

HSSF	Horizontal subsurface flow
IET	Interspecies electron transfer
j	Current density
MBR	Membrane bioreactor
MDC	Microbial desalination cell
ME	Microbial electrochemistry
MEC	Microbial electrolysis cell
MEET	Mediated extracellular electron transfer
ME-FBR	Microbial electrochemical fluidized bed reactor
MERC	Microbial electroremediating cell
MES	Microbial electrochemical snorkel
MES	Microbial electrosynthesis
MET	Microbial electrochemical technology
MFC	Microbial fuel cell
N	Nitrogen
NbS	Nature-based solutions
nc-B	non-electrically conductive biochar
NOB	Nitrite oxidizing bacteria
OCP	Open circuit potential
OD	Optical density
OLR	Organic loading rate
OM	Organic matter
ORR	Organic removal rate
P	Phosphorous
p.e.	Population equivalent
PEM	Proton exange membrane
RE	Reference electrode
RT	Reaction time
SBR	Sequencing batch reactor
SD	Supplementary data
SDG	Sustainable development goals
SEM	Scanning electron microscopy
SF	Surface flow
SMFC	Sedimentary microbial fuel cell
SS	Suspended solids
SSF	Subsurface flow
TDP	Temperature-programmed desorption
TEA	Terminal electron acceptor

ThOD	Theoretical oxygen demand
TN	Total nitrogen
TNLR	Total nitrogen loading rate
TOC	Total organic carbon
TP	Total phosphorous
TSS	Total suspended solids
UF	Up-flow
UNDP	United Nations development programme
VF	Vertical flow
WE	Working electrode
WFD	Water framework directive
WWT	Wastewater treatment
WWTP	Wastewater treatment plant
XPS	X-ray photoelectron spectroscopy
XRD	X-ray diffraction